

**UNDERSTANDING THE STABILITY OF SALTS AND COCRYSTALS
IN A DRUG PRODUCT ENVIRONMENT**

A DISSERTATION

SUBMITTED TO THE FACULTY OF THE

UNIVERSITY OF MINNESOTA

BY

NAVPREET KAUR

IN PARTIAL FULFILLMENT OF THE REQUIREMENTS

FOR THE DEGREE OF

DOCTOR OF PHILOSOPHY

RAJ SURYANARAYANAN (ADVISOR)

JUNE 2021

© 2021
Navpreet Kaur

ACKNOWLEDGEMENTS

I gratefully acknowledge the invaluable contributions of several people who have supported, guided and inspired me during my graduate studies at the University of Minnesota.

I express my deepest gratitude towards my thesis advisor, Dr. Raj Suryanarayanan. I am grateful to him for his mentorship through all these years in the doctoral program. He has taught me the nuances of pharmaceutical materials science and has instilled a lifelong intellectual curiosity in me. I have learnt the importance of meticulous planning, diligence, patience and perseverance through this journey. His guidance, support and encouragement have made the completion of this thesis possible. I am very grateful to Dr. Changquan Calvin Sun, Dr. Ronald Siegel, and Dr. Victor Young for serving on my doctoral committee, and for critically examining my thesis. I also want to thank Dr. Andreas Stein for serving on my oral examination committee, and for his valuable feedback and suggestions. I am extremely grateful to have had amazing mentors, Dr. Noro Andriamanalina and Dr. Esam El-Fakahany, who constantly encouraged me to believe in myself and supported my professional development. I am deeply grateful to my Master's thesis advisor, Dr. Arvind Kumar Bansal. His contributions to my scientific, professional and personal growth are precious.

I will always be thankful to my collaborators Dr. Naga K. Duggirala (Pfizer Inc, Connecticut), Dr. Seema Thakral (University of Minnesota), Dr. Greg Haugstad (University of Minnesota), Dr. Victor Young (University of Minnesota) and Dr. Yongchao Su (Merck Inc, Rahway) for their valuable inputs, helpful suggestions, and countless research discussions on different projects. I also deeply appreciate the valuable scientific discussions and insights provided by Dr. Devalina Law, Dr. Paroma Chakravarty and Dr. Susan Reutzler-Edens. My gratitude also extends to Dr. Andrey Yakovenko, Dr. Saul H. Lapidus and Dr. Wenqian Xu for their help with my synchrotron XRD experiments at the Advanced Photon Source (APS) at Argonne National Laboratory (beamlines 11-BM-B and 17-BM-B). I would like to thank APS for providing top-notch user facilities. The Characterization Facility at the University of Minnesota is acknowledged for providing excellent XRD and microscopy facilities. Financial support from the College of Pharmacy, Rowell graduate fellowship, William and Mildred Peters Endowment fund, David J.W. Grant & Marilyn J. Grant Fellowship in Physical Pharmacy, Ludo Frevel Crystallography Scholarship, IPEC Americas and COGS is gratefully acknowledged.

I would like to thank past and present members of the Sury lab. Special thanks to Dr. Michelle Fung, Mr. Jayesh Sonje, Dr. Kweku Amponsah-Efah, Dr. Bhushan Munjal and Dr. Krishna Kumar for their helpful discussions and scientific inputs. It has also been my pleasure to get to know Mr.

Rahul Lalge and Mr. Jinghan Li. Their presence has upheld the positive lab environment that I greatly value. I greatly appreciate faculty members, staff and my fellow colleagues at the Department of Pharmaceutics for creating an engaging and friendly environment. I would also like to specially thank Surabhi Talele, Amanda Hokanson, Krutika Jain and Dr. Vidhi Khanna for their valuable support and encouragement over the years.

I also extend my heartfelt thanks to my colleagues and mentors at the Council of Graduate Students (COGS), Council of International Graduate Students (CIGS) and Association of Multicultural Scientists (AMS). I would like to thank my friends Pranav Bhandari, Hammad Quddusi, Gurjot Singh, Rhythm Arora and Harmanjeet Kaur for their friendship and wonderful camaraderie.

I feel blessed to have my sister, Dilpreet Kaur, by my side. I will always be indebted to her for her constant care and support throughout my doctoral journey. I thank her for helping me believe in my abilities, bringing out the best in me and loving me unconditionally. My parents, Naib Singh and Veerpal Kaur, deserve special mention for standing by me and supporting me in all my pursuits. They have nurtured my dream of pursuing higher education and supported me in all my endeavors.

Dedicated to my family.

ABSTRACT

Transition of a drug substance to drug product necessitates the use of excipients and often includes several unit operations.¹ A risk associated with processing pharmaceutical solids is their propensity to undergo solid form transformations such as polymorphism and amorphization. Changes in the physical form during drug product manufacture or storage can have an influence on their chemical stability and product performance. The central goal of this thesis work is to mechanistically understand the influence of processing and formulation composition on the stability of pharmaceutical salts and cocrystals.

Processing induced lattice disorder was investigated for caffeine-oxalic acid cocrystals. The unmilled cocrystals were stable in presence of excipient and water. However, very short milling times induced sufficient lattice disorder to induce cocrystal dissociation. Quantification of disorder was performed using X-ray diffractometry (XRD). The lattice disorder was proposed to be predominant on the particle surface experiencing shear and hence served to explain the disproportionate influence that low levels of disorder had on the stability of the cocrystals. Cocrystal dissociation was observed to be a water mediated reaction and was influenced by the pH of the microenvironment. Very low levels of lattice disorder, which cannot be characterized using bulk characterization tools such as XRD and thermal analysis, can induce chemical instability and lead to product failure. Disorder induced during processing was also imaged using atomic force microscopy.

The second part of the thesis focused on understanding the challenges associated with the formulation development of levothyroxine sodium pentahydrate (LSP). The influence of pharmaceutical processing on the hydration state of LSP was investigated using single crystal and synchrotron X-ray diffractometry, and a novel crystal form of the drug was reported when it undergoes partial dehydration to form levothyroxine sodium monohydrate (LSM). LSM has a higher chemical reactivity than the pentahydrate form. The influence of excipients on the physical and chemical stability of LSP was investigated using synchrotron XRD and high performance liquid chromatography (HPLC). Hygroscopic and acidic excipients can induce dehydration and salt disproportionation of LSP, respectively. Microenvironment pH and excipient hygroscopicity were critical determinants of LSP stability.

TABLE OF CONTENTS

List of Figures	ix
List of Tables.....	xviii
List of Schemes.....	xviii
Chapter 1. Introduction	2
1.1 Introduction	2
1.2 Pharmaceutical solids	2
1.2.1 Crystalline and amorphous solids.	2
1.2.2 Pharmaceutical salts.	3
1.2.3 Pharmaceutical cocrystals.....	4
1.2.4 Pharmaceutical hydrates.....	6
1.3 Pharmaceutical processing.....	7
1.3.1 Processing induced lattice disorder.	8
1.4 Model systems	9
1.4.1 Caffeine – oxalic acid (2:1) cocrystals.	9
1.4.2 Levothyroxine sodium pentahydrate.	10
1.5 Motivation and thesis overview.....	27
1.5.1 Chapter 2	27
1.5.2 Chapter 3	28
1.5.3 Chapter 4	29
1.5.4 Chapter 5	30
Chapter 2. The role of lattice disorder in water mediated dissociation of pharmaceutical cocrystal systems.*	32
2.1 Synopsis.....	32
2.2 Introduction	32
2.3 Experimental section	35
2.3.1 Materials.....	35

2.3.2 Preparation of binary mixtures.....	35
2.3.3 Water sorption analysis.	35
2.3.4 Differential scanning calorimetry (DSC).....	35
2.3.5 Thermogravimetric analysis (TGA).	35
2.3.6 Powder X-ray diffractometry (XRD).	36
2.3.7 Cryomilling.....	36
2.3.8 Particle size distribution.	37
2.3.9 Surface area.	37
2.4 Results and discussion	37
2.4.1 Baseline characterization.	37
2.4.2 Lattice disorder.	38
2.4.3 Cocrystal dissociation.....	43
2.4.4 Experimental controls.....	45
2.4.5 Impact of co-processing on cocrystal dissociation.	46
2.4.6 Impact of lattice disorder on cocrystal dissociation.	47
2.5 Significance	49
2.6 Conclusions	50
2.7 Supporting information.....	51
Chapter 3. Use of Atomic Force Microscopy (AFM) to monitor surface crystallization of disordered caffeine-oxalic acid (CAFOXA) cocrystals in real time.....	58
3.1 Synopsis.....	58
3.2 Introduction	58
3.3 Experimental section	60
3.3.1 Materials.	60
3.3.2 Differential scanning calorimetry (DSC).....	60
3.3.3 Thermogravimetric analysis (TGA).	61
3.3.4 Preparation of tablets.....	61
3.3.5 Water sorption analysis.	61
3.3.6 Cryogenic milling.....	61
3.3.7 Atomic force microscopy (AFM).....	62
3.4 Results and discussion	62

3.4.1 Preliminary characterization.....	62
3.4.2 Lattice disorder and cocrystal instability.....	63
3.4.3 Impact of tableting on the crystallinity of caffeine-oxalic acid (CAFOXA) cocrystals.....	64
3.4.4 Surface changes upon exposure to high humidity.....	66
3.4.5 Using <i>in situ</i> AFM to monitor surface crystallization on cocrystal tablets upon exposure to RT/75% RH.....	68
3.5 Significance.....	72
3.6 Conclusions.....	73
3.7 Supporting information.....	74
Chapter 4. Partial dehydration of levothyroxine sodium pentahydrate in a drug product environment: structural insights into stability.*.....	78
4.1 Synopsis.....	78
4.2 Introduction.....	78
4.3 Experimental section.....	80
4.3.1 Materials.....	80
4.3.2 Water sorption and desorption analysis.....	81
4.3.3 Differential scanning calorimetry (DSC).....	81
4.3.4 Karl fischer titrimetry (KFT).....	81
4.3.5 Thermogravimetric analysis (TGA).....	81
4.3.6 Powder X-ray diffractometry (PXRD).....	81
4.3.7 Synchrotron X-ray diffractometry (SXRD).....	82
4.3.8 SXRD of LSP tablet.....	82
4.3.9 Dehydration of levothyroxine in a drug product environment.....	83
4.3.10 Single crystal X-ray diffraction.....	83
4.3.11 Solid-state nuclear magnetic resonance spectroscopy.....	84
4.3.12 Scanning electron microscopy.....	84
4.3.13 High pressure liquid chromatography (HPLC).....	85
4.4 Results and discussion.....	85
4.4.1 Baseline characterization of LSP.....	85
4.4.2 Water sorption analysis.....	86
4.4.3 Synchrotron XRD.....	88
4.4.4 Single crystal XRD.....	90

4.4.5 ssNMR of LSP and the dehydrated samples.....	97
4.4.6 Evaluating the physical stability of LSP in a “drug product” environment.....	101
4.5 Significance.....	103
4.6 Conclusions.....	104
4.7 Supporting information.....	105
Chapter 5. Investigating the influence of excipients on the stability of levothyroxine sodium pentahydrate.	113
5.1 Synopsis.....	113
5.2 Introduction.....	113
5.3 Experimental section.....	116
5.3.1 Materials.....	116
5.3.2 Differential scanning calorimetry (DSC).....	117
5.3.3 Thermogravimetric analysis (TGA).....	117
5.3.4 Powder X-ray diffractometry (PXRD).....	117
5.3.5 Synchrotron X-ray diffractometry (SXR).....	117
5.3.6 High performance liquid chromatography (HPLC).....	117
5.3.7 Dehydration and salt disproportionation of LSP in hermetically sealed chambers.....	118
5.3.8 Stability testing.....	118
5.4 Results and discussion.....	119
5.4.1 Physical stability.....	119
5.4.2 Chemical stability.....	124
5.4.3 Physical transition of LSP in drug products – potential impact on chemical stability.....	127
5.5 Significance.....	132
5.6 Conclusions.....	134
5.7 Supporting information.....	134
Chapter 6. Summary.....	139
Chapter 7. Future work.....	145
Bibliography.....	149

List of Figures

Figure 1.1. Salt and solid form selection. ¹⁶	4
Figure 1.2. Flow chart highlighting the impact of hydration state on the physicochemical and mechanical properties of a drug. ‘A’ represents the surface area of the solid exposed to the dissolution medium, ‘k’ stands for the mass transfer coefficient; ‘Cs’ is the equilibrium solubility of the solid form; ‘C’ is the concentration in solution; ‘J’ represents the intrinsic dissolution rate and ‘dm/dt’ is the dissolution rate. Reproduced from Khankari et al. ³⁷	7
Figure 1.3. Schematic of defects and disorder on a crystalline surface. ³⁸	8
Figure 1.4. (a) Ionization states of thyroxine. Adapted from Virili et al. ²⁰⁰	14
Figure 1.5. (A) pH - solubility profile of levothyroxine sodium at 25°C. Adapted from Won <i>et al.</i> ²⁰² (B) The solubility at selected pH values. Reproduced from Kocic <i>et al.</i> ^{203,204}	14
Figure 1.6. Comparison of levothyroxine sodium stability in the solution (a) and solid (b) states. (a) First order plots of the percent of levothyroxine sodium remaining as a function of time at solution pH values of 2.05 (■), 6.86 (●), 7.96 (▲) and 10.55 (◆) at 80°C. Decomposition occurred via deiodination. (b) First order plot obtained following isothermal storage of levothyroxine sodium at 50 (◆), 60 (▲), 70 (●) and 80°C (■). While the state of hydration of levothyroxine sodium was not mentioned, it is likely to be the pentahydrate since it is the stable form under ambient conditions. Storage in the temperature range of 50 to 80°C is expected to cause rapid dehydration (in a time scale of a few hours). Data from Won <i>et al</i> has been reproduced. ²⁰²	17
Figure 1.7. (a) Overlay of diffraction patterns showing the impact of temperature on the physical form of levothyroxine sodium pentahydrate. The data was collected at 30, 40, 50, 60, 70, 80, 90, 100, 110, 120 and 130°C—top to bottom. (b) Effect of relative humidity and temperature on the chemical stability of levothyroxine sodium in the presence of molecular oxygen. Adapted from Shah et al. ¹⁶³	18
Figure 2.1. X-ray diffraction patterns of (A) milled CAFOXA and (B) comilled mixture of CAFOXA and DCPA (1:1 w/w). The milling times were: (a) 0, (b) 10, (c) 30, (d) 60, and (e) 120 sec.	39

Figure 2.2. (A) Crystallinity (%) as a function of milling time of CAFOXA, DCPA and the comilled mixture of CAFOXA and DCPA. (B) The effect of milling time on the width of a representative diffraction peak of CAFOXA ($2\theta=16.4^\circ$) milled alone and with DCPA (comilled). The peak width is represented as full width at half maximum (FWHM in degrees, 2θ). The lines are drawn to assist in visualization of trends. Error bars represent standard deviation (n=3).....	40
Figure 2.3. Gravimetric water sorption behavior of (a) CAFOXA cocrystals, and (b) DCPA (Mean \pm SD; n=3).	41
Figure 2.4. Gravimetric water sorption of comilled (CAFOXA-DCPA) mixtures (Mean \pm SD; n=3). The inset shows data at $RH \leq 60\%$	42
Figure 2.5. (a) X-ray diffraction patterns of a CAFOXA-DCPA (1:1 w/w) mixture comilled for 10 sec, and stored at RT/75% RH for 24 h. Characteristic peaks of possible decomposition products are highlighted. (b) Proposed mechanism of water mediated CAFOXA cocrystal dissociation in the presence of DCPA at RT/75% RH.	44
Figure 2.6. The effect of storage on the width of a representative diffraction peak of CAFOXA ($2\theta=16.4^\circ$). The peak width is represented as full width at half maximum (FWHM in degrees, 2θ). CAFOXA was milled for 120 sec and stored at RT/75% RH. Error bars represent standard deviation (n=3).	45
Figure 2.7. Dissociation (expressed in %) of CAFOXA following storage at RT/75% RH. A physical mixture of CAFOXA and DCPA (1:1 w/w) was comilled either for 10 (CM 10 sec) or 120 (CM 120 sec) sec. CAFOXA and DCPA were individually milled for 120 sec and mixed (PM 120 sec). Percent dissociation for comilled and physical mixtures maintained at RT/75% RH in an X-ray holder for 10 h. For details on the calculation of percent dissociation, refer to Supporting Information, Figure 2.19.....	46
Figure 2.8. (A) X-ray diffraction patterns of CAFOXA and DCPA, individually milled and then mixed (PM), or comilled (mixed and milled together). The milling time was 120 sec and the mixtures were stored either at RT/50% RH or RT/75% RH for 10 h. The XRD patterns of CAFOXA (reactant) and caffeine hydrate (product) are also provided. (B) Water sorption kinetics of these mixtures at 50 or 75% RH (25°C).	48
Figure 2.9. Flow chart highlighting the role of water, lattice disorder (induced by milling) and inter-particulate contact area on cocrystal dissociation.....	50

Figure 2.10. Experimental and calculated X-ray diffraction patterns of CAFOXA. The calculated pattern was obtained from the CSD database.....	51
Figure 2.11. DSC heating curves of (a) CAFOXA and (b) DCPA. The samples were heated in hermetically sealed pans.....	51
Figure 2.12. TGA and derivative (right y-axis) TGA heating curves of CAFOXA.....	52
Figure 2.13. TGA and derivative (right y-axis) TGA heating curves of DCPA.	52
Figure 2.14. Water sorption and desorption curves of (a) CAFOXA and (b) DCPA at 25°C.	53
Figure 2.15. (A) X-ray diffraction patterns of DCPA samples milled for (a) 0, (b) 10, (c) 30, (d) 60 and (e) 120 sec. (B) The effect of milling time on the width of a representative diffraction peak of DCPA ($2\theta = 26.4^\circ$). The peak width is represented as full width at half maximum (FWHM in degrees, 2θ). Error bars represent standard deviation (n=3).....	53
Figure 2.16. Overlay of X-ray diffraction patterns of comilled CAFOXA cocrystals. The milling times were (a) 0, (b) 10, (c) 30, (d) 60 and (e) 120 sec. The diffraction patterns were offset to assist in visualizing the peak intensities.....	54
Figure 2.17. Mean particle size of unmilled and milled CAFOXA and DCPA (Mean \pm SD; n=3).	54
Figure 2.18. Water sorption data of comilled (CAFOXA-DCPA), and the average of separately milled CAFOXA and DCPA. All samples were milled for 120 sec.	55
Figure 2.19. Plot of the caffeine hydrate peak intensity ($2\theta = 10.6^\circ$) versus its weight fraction in ternary mixtures of caffeine hydrate, CAFOXA and calcium oxalate. The dissociation of cocrystal will result in the formation of caffeine hydrate and calcium oxalate. Therefore, mixtures were prepared with CAFOXA concentration ranging from 97% to 9% w/w. The first sample is the cocrystal before it undergoes any dissociation (there caffeine hydrate content is 0.0% w/w). The last mixture represents 90% cocrystal dissociation (the caffeine hydrate content is 61.5% w/w). This data enabled us to generate a hypothetical “standard curve” of caffeine hydrate peak intensity as a function of % dissociation. Plot (b) was used to determine the % dissociation in the unknown samples (Figure 2.7 in the main manuscript). Error bars represent standard deviations (n=3).....	55

Figure 3.1. Water sorption data for CAFOXA powder and tablet samples at 25°C. The starting material (a highly crystalline powder sample of CAFOXA cocrystals) is referred to as the ‘annealed powder’. The powder was cryomilled for 10 sec and is referred to as the ‘milled sample’ in the figure legend. The behavior of a freshly prepared tablet as well as the tablet sample stored RT/75% RH for 3 weeks (‘annealed tablet’) are also shown.	64
Figure 3.2. Representative 2D- (top) and 3D- (bottom) rendered AFM height images of a tablet surface prepared by compacting CAFOXA cocrystals. Acquired images decrease in size from left to right. (Vertical scale is stretched compared to lateral scale in the 3D renderings.)	65
Figure 3.3. Representative 2D renderings of ambient AFM height images of (a) a freshly prepared tablet of CAFOXA cocrystals, and (b) the same tablet after storing at RT/75% RH for 3 weeks. (c) Radial power spectral density functions computed for images in (a,b).....	67
Figure 3.4. Representative 2D (left) and 3D (right) renderings of <i>in situ</i> AFM height images showing time-dependent surface topography transformation on a milled (10 sec) CAFOXA sample during exposure to RT/80% over 22 h. 2D and 3D renderings are explicitly designated with rectangles around two of the crystals. (Vertical scale is stretched compared to lateral scale in the 3D renderings.)	69
Figure 3.5. Representative AFM height and phase images showing recrystallization of milled (10 sec) CAFOXA sample upon exposure to RT/80% RH. (i) Comparison of the milled sample surface imaged <i>in situ</i> at RT/80%RH at t = 0 and 8 h. White arrows are used as reference markers. (ii) includes smaller, more highly resolved images of the recrystallized regions at 8 h. Crystals with a different morphology were observed in (ii).....	71
Figure 3.6. DSC and TGA heating curves of CAFOXA cocrystals.	74
Figure 3.7. Gravimetric water-desorption behavior of CAFOXA cocrystals at 25°C.....	75
Figure 3.8. Optical microscopy of CAFOXA cocrystals.....	76
Figure 3.9. Optical images of the tablet sample and cantilever.....	76
Figure 4.1. DSC and TGA heating curves of LSP. The DSC profile over the temperature range of 145 to 180 °C has been expanded in the inset.	86

Figure 4.2. Water desorption and sorption behavior of LSP. The inset represents the isothermal water sorption/desorption at 40°C. For each cycle, the sample weight at 90% RH represents LSP (the starting material). The sample weight at other RH values were scaled accordingly. At each temperature, the lower profile was the sorption cycle.....87

Figure 4.3. Diffraction patterns of LSP and samples analyzed following storage of LSP at different temperature/RH conditions for 3 h. The bottom pattern is that of ‘as is’ LSP. While the XRD patterns were obtained using synchrotron radiation (0.45256 Å), they were converted to Cu K α radiation (1.54 Å), so as to enable direct comparison with the reference patterns. The XRD patterns of LSP obtained following long term storage at 40°C/75% RH is presented in the supporting information (Figure 4.14).89

Figure 4.4. XRD patterns of an ‘as is’ LSP tablet stored at 40°C/0% RH for three hours. The experiment was performed using the temperature/humidity controlled chamber placed in the path of synchrotron beam. Selected angular ranges, where some of the characteristic peaks of LSP and LSM are observed, are highlighted. The topmost and bottommost diffraction patterns are the calculated diffraction patterns of LSM and LSP respectively. In an effort to maintain clarity, only diffraction patterns at selected time points are shown.....90

Figure 4.5. XRD patterns of levothyroxine sodium tablet stored at RT/75% RH for three hours. Before this experiment, LSP tablets had been stored at 40°C/0% RH for three hours. The results were presented in Figure 4.4. In a continuing experiment, the storage conditions were changed to RT/75% RH and the XRD patterns were collected. Selected angular ranges, where some of the characteristic peaks of LSP and LSM are observed, are highlighted. The calculated diffraction patterns of LSP and LSM are also provided (Supporting information; Figure 4.15). The experiment was performed using the temperature/humidity controlled chamber placed in the path of synchrotron beam.....91

Figure 4.6. (a) LSP is displayed with anisotropic displacements drawn at 50% probability for all atoms except for water oxygens coordinated to Na₂ which are drawn with isotropic displacements. The minor occupancy of these water molecules are omitted as well as all hydrogen atoms and both solvent water molecules. Atoms shaded in red break the pseudo-inversion symmetry of the two thyroxine molecules. (b) LSM is displayed with anisotropic displacements drawn at 50% probability for all atoms. The minor occupancy sites of the disordered sodium cation as well as all hydrogen atoms are omitted for clarity.²¹⁰94

Figure 4.7. LSM is displayed in a ball and stick drawing to illustrate the non-bonded contacts (Å) found for Na2'. The non-bonding contacts between the two LSM residues above Na2' are also shown. One contact is omitted for clarity that overlaps in the foreground: Na2'... O8 (x, y, z-1) = 2.943 Å. The residue at the bottom illustrates the bonding for the major occupancy for Na2.²¹⁰..95

Figure 4.8. (a) Chemical structure of LSP. (b) 1D ¹H spectra of LSP powder and samples stored under different temperatures at 0% RH for 3 h. ¹H spectra are normalized by aromatic peaks of LSP at approximately 5-10 ppm. Note the gradually decreased intensity of the sharp water peak at ~ 4.55 ppm for samples stored at higher temperatures. (c→e) 1D ¹³C spectra of LSP powder and samples stored under different temperatures (0% RH) for 3 h. (c) Full spectra; and enlarged spectra of C1 (d) and C3 (e). Note the two sets of peaks from the two conformers in the crystalline lattice. The corresponding XRD patterns under these conditions are provided in Figure 4.3.98

Figure 4.9. ¹³C chemical shift differences (Δ) of the two conformers in the crystalline lattice for C1, C3, C5, C7, C10, C13, and C12, C14 in the spectra of LSP powder samples stored at different temperatures (at 0% RH) for 3 h..... 100

Figure 4.10. Overlay of XRD patterns of physical mixtures prepared using LSP and oxalic acid (1:1 w/w), and stored in hermetically sealed pans at 40°C. Dotted lines and solid lines represent characteristic peaks of oxalic acid and oxalic acid dihydrate, respectively. 103

Figure 4.11. HPLC calibration curve for LSP prepared by dissolving LSP in an alkaline methanolic solution (discussed in depth in materials and methods). 105

Figure 4.12. Reported and experimental X-ray diffraction pattern of levothyroxine sodium pentahydrate (LSP).⁴⁶⁵ 105

Figure 4.13. Hot stage microscopy of LSP crystals..... 106

Figure 4.14. Overlay of the XRD patterns of LSP stored at 40°C/75% RH. 106

Figure 4.15. Calculated powder diffraction patterns for LSP and LSM. The powder patterns have been calculated in Mercury using the experimentally generated single crystal files. The pattern of LSP generated from the single crystal file shows an excellent overlap with the powder patterns (reported and experimental) shown in Figure 4.12..... 107

Figure 4.16. Optical and polarized light microscopic images of LSP. 107

Figure 4.17. SEM images of LSP crystallized using methanol.	108
Figure 4.18. ATR-FTIR spectrum of LSP.	108
Figure 4.19. Crystal packing of LSP (a) and LSM (b).	109
Figure 4.20. Representative 2D ^{13}C - ^1H HETCOR spectra of LSP, with 1D ^{13}C and ^1H spectra shown as projections in direct and indirect dimensions, respectively.	110
Figure 5.1. Chemical structure of LSP.	116
Figure 5.2. Two-dimensional XRD patterns of (A) levothyroxine (free acid; unionized levothyroxine) and (B) levothyroxine sodium pentahydrate obtained using synchrotron radiation ($\lambda = 0.45256 \text{ \AA}$). To facilitate visualization, the corresponding one-dimensional XRD patterns have been presented (C) as intensity versus 2θ plots (calculated for Cu $K\alpha$ radiation, $\lambda = 1.54 \text{ \AA}$). The “unique” peaks of levothyroxine free acid and LSP are seen at 3.5° and 5.6° 2θ , respectively... 119	119
Figure 5.3. SXRD patterns of powder mixture of LSP and povidone (1:1 w/w) stored in hermetically sealed pans at 40°C . The highlighted region indicates partial dehydration of LSP to LSM during storage. The decrease in the intensity of the characteristic peak of LSP (peak at 5.6° 2θ) was accompanied by the appearance of the LSM peak at 6.5° 2θ . The reference diffraction patterns of LSP and LSM are also provided.....	120
Figure 5.4. SXRD patterns of powder mixture of LSP and stearic acid (1:1 w/w) stored in hermetically sealed pans at 40°C . After 28 days of storage, salt disproportionation leading to the formation of levothyroxine free acid (peak at 3.5° 2θ) was observed.....	122
Figure 5.5. SXRD patterns of a powder mixture of LSP and oxalic acid (1:5 w/w) stored at $40^\circ\text{C}/75\% \text{ RH}$. Following 28 days of storage, the characteristic peak of LSP at 5.6° 2θ completely disappeared. The appearance and the pronounced intensity of the characteristic diffraction peak of levothyroxine free acid at 3.5° 2θ indicates pronounced and possibly complete disproportionation during storage. The highlighted regions indicate the appearance of the characteristic diffractions peaks of levothyroxine free acid (3.5 and 6.1° 2θ) and sodium oxalate (19.9° 2θ), the products of the disproportionation reaction.....	123
Figure 5.6. LSP remaining as a function of time following storage of binary powder blends of LSP and individual excipients (1:5 w/w). The samples were stored at $40^\circ\text{C}/75\% \text{ RH}$, and quantification	

of LSP was performed using SXRD. The integrated intensity of the diffraction peak at $5.6^\circ 2\theta$ (Cu $K\alpha$) was used for the quantification of LSP in powder blends. The calibration curve is available in the supporting information (Figure 5.12). Mean \pm SD (n=3).	128
Figure 5.7. Concentration of LSP as a function of time following storage of binary powder blends of LSP and individual excipients (1:5 w/w). The samples were stored at $40^\circ\text{C}/75\%$ RH, and quantification of LSP was performed using SXRD. The integrated intensity of the diffraction peak at $5.6^\circ 2\theta$ (Cu $K\alpha$) was used for quantification of LSP in powder blends. The calibration curve is available in the supporting information (Figure 5.12). Results are reported as a mean of three measurements.	129
Figure 5.8. Concentration of levothyroxine sodium as a function of time following storage of binary powder blends of LSP and individual excipients (1:5 w/w). The samples were stored at $40^\circ\text{C}/75\%$ RH, and quantification of levothyroxine sodium was performed using HPLC. Results are reported as a mean of three measurements.	130
Figure 5.9. XRD patterns of physical mixtures of LSP and maleic acid (1:5 w/w) following storage at $40^\circ\text{C}/75\%$ RH for 28 days.	134
Figure 5.10. XRD patterns of physical mixtures of LSP and stearic acid (1:5 w/w) following storage at $40^\circ\text{C}/75\%$ RH for 28 days.	135
Figure 5.11. XRD patterns of physical mixtures of LSP and tartaric acid (1:5 w/w) following storage at $40^\circ\text{C}/75\%$ RH for 28 days.....	136
Figure 5.12. Plot of the integrated intensity of the 15.65 \AA (peak at $5.6^\circ 2\theta$ for Cu $K\alpha$ radiation) line of LSP as a function of LSP content in binary mixtures of LSP and stearic acid. Similar plots were observed for physical mixtures of LS.....	137
Figure 6.1. Schematic of lattice disorder introduced in crystalline materials during pharmaceutical processing, and the impact of lattice disorder on the water mediated dissociation of cocrystals in the presence of excipients.....	140
Figure 6.2. Representative AFM height images (3D) showing surface recrystallization of milled CAFOXA cocrystals upon exposure to RT/80% RH for 10 h.....	141

Figure 6.3. Schematic for partial dehydration of LSP under “modest” and realistic processing and storage conditions to form the more reactive form, LSM. 142

Figure 6.4. Schematic of the potential physical and chemical instability that may be induced in LSP when combined with a range of pharmaceutical tablet excipients. 143

List of Tables

Table 1.1. Crystallographic data for 2:1 caffeine oxalic acid cocrystals reproduced from Trask et al. ⁵⁰	10
Table 1.2. Marketed levothyroxine sodium formulations with the list of excipients in each dosage form. The first section contains oral tablet dosage forms. The formulation details of other oral dosage forms (soft gel, liquid) and injectables are presented in the second section. Their therapeutic equivalence codes (updated by the FDA in March 2020) ²⁹⁷ , if available, have been listed in parenthesis.	23
Table 2.1. Surface area measurements of binary (CAFOXA-DCPA) powder mixtures.....	56
Table 4.1. Crystal data and structure refinement for LSP and LSM.	96
Table 4.2. Conformational perturbations as observed from the different torsional angles (χ) between LSP and LSM.	101
Table 4.3. ¹³ C chemical shifts (CS) of LSP samples stored at RT/0% RH and 85°C/0% RH, and the chemical shift differences (Δ CS) of the two conformers for each carbon.....	111
Table 5.1. Physical properties of selected organic acids.	124
Table 5.2. Physical properties of excipients. ^{381,506}	131

List of Schemes

Scheme 5.1. Influence of excipients on the stability of LSP. SXRD was used to monitor dehydration and disproportionation (both in the solid state), while the chemical decomposition was monitored by HPLC (solution based).	133
---	-----

CHAPTER 1

Chapter 1. Introduction

1.1 Introduction

Recent introduction of combinatorial chemistry and high-throughput screening in drug discovery has promoted the development of numerous new chemical entities (NCE) with poor aqueous solubility. This poses a challenge to oral drug absorption as the drug needs to dissolve in GI fluid to enable absorption. Compounds with solubility limited oral absorption are typically categorized as BCS class II drugs.²⁻⁴ Owing to the prevalence of NCEs with poor water solubility in the discovery pipeline, identification and selection of optimum solid forms is critical from the standpoint of effective drug delivery.

A simple and cost effective strategy to enhance the solubility of ionizable drugs is salt formation. This approach is also used to optimize the physicochemical stability and mechanical properties of active pharmaceutical ingredients (API). For non-ionizable drugs, wherein the ability of salt formation is rather limited, cocrystallization of the API with suitable cofomers is an attractive alternative. While both salts and cocrystals have gained momentum due to the advantageous properties they confer to the API, the stability of these solid forms during drug product development mandates diligent investigations. The API would be combined with a suitable set of excipients and undergo pharmaceutical processing in order to develop a dosage form. The central goal of this thesis research is to understand the influence of pharmaceutical processing and excipients (including storage) on the physical form and chemical stability of model salts and cocrystals. These studies can provide a scientific basis for the design and development of mitigation strategies to circumvent the risk of unintended instability and thereby ensure robust drug products.

1.2 Pharmaceutical solids

1.2.1 Crystalline and amorphous solids.

Pharmaceutical solids exist in either the crystalline or amorphous form. A crystalline solid can be described as one with molecules arranged in a perfectly ordered three dimensional lattice. This is also referred to as long-range order. An amorphous solid, on the other hand, is devoid of long range order. Amorphous solids are often referred to as being in the ‘disordered’ state. From a thermodynamic standpoint, crystalline solids are stable whereas the amorphous counterparts are metastable. Amorphous solids have higher molecular energy and mobility as compared to the crystalline forms.^{5,6}

Differences in the molecular properties of crystalline and amorphous solids lead to distinctive physicochemical and mechanical properties. For instance, amorphous solids, owing to absence of crystal lattice energy, have a higher apparent solubility than the crystalline form. This property is valuable for BCS class 2 compounds. On the other hand, the higher molecular mobility and Gibbs free energy of amorphous solids promote physical and chemical instability.^{5,6}

It is crucial to have a comprehensive understanding of solid form landscape in order to select a solid form suitable for dosage form development. It is also instrumental to understand inadvertent conversions in the solid form during drug product development, such as introduction of disorder into otherwise crystalline solids during milling, mixing, blending and granulation. The unintended disorder can result in undesirable physical and chemical transformations.

1.2.2 Pharmaceutical salts.

1.2.2.a Introduction to pharmaceutical salts.

Salt formation is an attractive avenue to modify the physicochemical and mechanical properties of ionizable drugs such as solubility, physical stability, hygroscopicity and crystallinity. Since most drug substances are weak electrolytes and ionizable, salt formation is a popular strategy to optimize their solid form. Approximately, 50% of all drugs on the market are formulated as salts.^{7,8} The crystal structure and consequently, the physicochemical properties of the salt form are often different from those of the parent compound. By using a range of pharmaceutically acceptable counterions with FDA GRAS (generally regarded as safe) status, the properties can be optimized to meet formulation needs. A schematic for salt and solid form selection has been presented in Figure 1.1. The choice of counterion is based on the nature of the ionizable functional group on the drug molecule. The “rule of 3”, i.e. a $\Delta pK_a \geq 3$ between the ionic groups on the two species, is routinely used to form stable salts.

1.2.2.b Stability of pharmaceutical salts.

If a salt reverts to the corresponding free acid (or base), the reaction is referred to as salt disproportionation. Salt disproportionation reactions are a sub-category of acid-base reactions, and are often considered to be the reverse of salt formation. Numerous investigations have speculated the detrimental influence of salt disproportionation such as dissolution failure⁹, decrease in bioavailability¹⁰ and altered tablet disintegration^{11,12} Salt disproportionation in the solid-state has been reported to be a function of the pH_{max} of the drug and microenvironmental “pH” experienced by the salt.^{13,14} pH_{max} is defined as the pH of maximum solubility (in the solution state) and at pH_{max} , the salt and free acid (or base) co-exist in equilibrium. For salts of weak acids, if the pH of the

microenvironment drops below the pH_{max} of the salt, salt disproportionation will occur (and vice versa for bases). The microenvironmental acidity is the pH of the sorbed water layer formed by dissolution and saturation of the solid on the surface. This pH is believed to be influenced by the temperature, RH and formulation composition (especially excipients), and pH alterations have been implicated in salt disproportionation.¹⁵

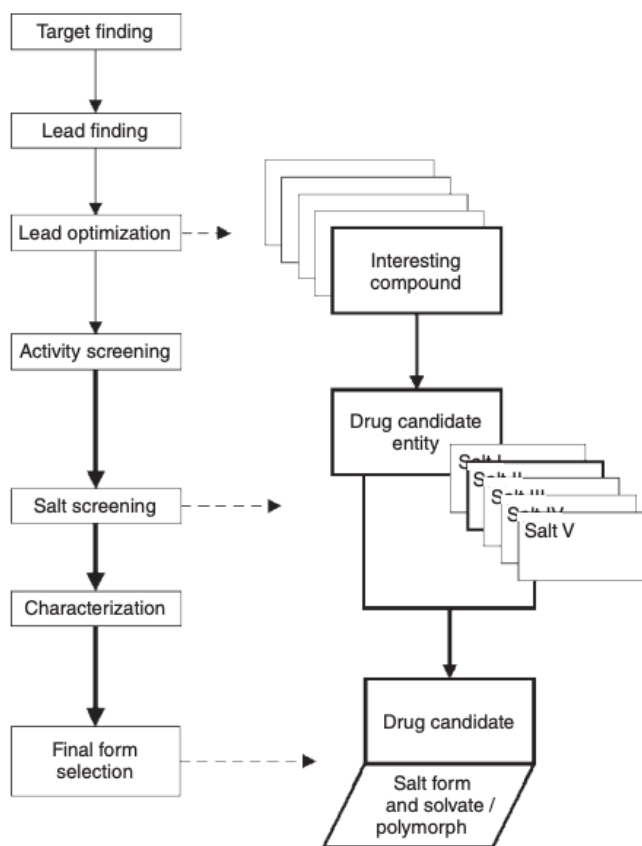


Figure 1.1. Salt and solid form selection.¹⁶

1.2.3 Pharmaceutical cocrystals.

1.2.3.a Introduction to cocrystals. Pharmaceutical cocrystals are multi-component crystalline solids where the active pharmaceutical ingredient (API) and coformer(s) combine stoichiometrically via non-covalent interactions.^{17,18} Cocrystallization has proven to be an effective strategy to selectively modify the physicochemical, mechanical and biopharmaceutical properties of an API without altering its pharmacologic activity. This approach has been used to enhance the aqueous solubility and dissolution rate of several poorly soluble drugs including fluoxetine hydrochloride¹⁹, nevirapine²⁰, danazol²¹ and ibuprofen²². In compounds with a propensity to form

hydrates, for example caffeine and theophylline, cocrystallization provides an avenue to mitigate the risk of hydrate formation and improve physical stability. It is also an effective strategy for altering mechanical properties of the API, thereby aiding formulation development.^{22,23} Finally, cocrystallization has enabled oral bioavailability enhancement. Some of the cocrystal products in the market are Depakote[®] (divalproex sodium or the valproic acid cocrystal of sodium valproate)²⁴, Lexapro (escitalopram oxalate)²⁵, Entresto[®] (valsartan–sacubitril)²⁶, Steglatro[™] (ertugliflozin–L-pyroglyutamic acid cocrystal)²⁷ and Suglat (iproglifozin–L-proline).²⁸

1.2.3.b Stability of cocrystals. Significant progress has been made in the design and synthesis of pharmaceutical cocrystals. However, their stability, specifically the potential to undergo dissociation, has not been extensively investigated. Studies have highlighted the impact of temperature²⁹ and humidity^{30,31} on cocrystal stability. Caffeine³² and theophylline³³ cocrystals were prepared with different dicarboxylic acids, and the effect of water vapor pressure on cocrystal stability was investigated. The aqueous solubility of the cofomer and the propensity of the API to form a hydrate were key determinants of the dissociation propensity. Eddleston *et al*²⁹ also studied the effect of temperature on the dissociation behavior of a 1:1 cocrystal of caffeine with theophylline. The cocrystal stability was a critical interplay of entropy differences between the cofomers, and enthalpic stabilization provided by cocrystal formation. Since pharmaceutical processing can entail elevated temperatures and water vapor pressures, these studies provide insight into potential instabilities during dosage form manufacture. However, the impact of processing induced mechanical stress and lattice disorder has not been investigated for cocrystal systems.

1.2.3.c Formulation challenges. The formulation of a cocrystal as a solid dosage form (for the purpose of this discussion, tablets) necessitates the use of excipients and entails several processing steps. It is therefore important to evaluate the potential impact of both API-excipient interactions and processing on cocrystal stability. Since cocrystals are sustained by non-covalent interactions, they may be susceptible to dissociation. Excipients can promote cocrystal dissociation by bonding (hydrogen bonding or ionic) with the cofomers. Duggirala *et al*³⁴ evaluated the impact of a range of pharmaceutical excipients on the stability of caffeine-oxalic acid (2:1) cocrystals. Binary cocrystal-excipient mixtures were ground with water, using a mortar and pestle, and their stability was assessed. Excipient mediated cocrystal dissociation was observed to be independent of the water sorption behavior of the excipients, and was reported to be a consequence of the reaction between oxalic acid (the cofomer) and ionic excipients. The model cocrystal system, in the absence of excipients, was stable even at elevated water vapor pressures. Recently, Koranne *et al*³⁵ investigated numerous prototype formulation compositions of theophylline-glutaric acid,

reportedly a robust cocrystal. Pronounced dissociation occurred in the presence of excipients with a high water sorption propensity. The solution mediated dissociation was believed to be initiated at the interface of cocrystal and excipient particles, specifically in the regions with lattice disorder. In both API and excipient particles, disorder can be introduced during pharmaceutical processing steps such as milling, mixing, granulation and compression. The disorder introduced on the particle surface is expected to be more pronounced than in the bulk. However, the impact of processing, and by extension disorder, on cocrystal stability has not been systematically investigated. In light of the potential destabilizing effect of excipients, it also becomes important to evaluate the combined effects of lattice disorder and excipients on cocrystal stability.

1.2.4 Pharmaceutical hydrates.

A pharmaceutical hydrate is a solid adduct containing the anhydrous form of the drug (also referred to as the 'parent' compound) and water. The incorporation of water in the crystal lattice of a compound influences its stability and performance. The hydrate form of a pharmaceutical solid can display differences in physicochemical and mechanical properties as compared to the corresponding anhydrous form. Some of these properties include physical stability, chemical stability, crystal structure, solubility, dissolution rate, flow and compaction behavior. The differences in the properties of a solid and its different hydration states can be attributed to the influence of water on the unit cell dimensions and intermolecular interactions, which in turn affects thermodynamic properties such as internal energy and crystal lattice energy (Figure 1.2). Considering the abundance of water in pharmaceutical manufacturing and product storage, it is estimated that approximately 30% of the compounds in the pipeline are capable of existing in different hydration states.³⁶

Based on structural attributes, hydrates can be classified into three categories: isolated site hydrates, channel hydrates and ion-coordinated site hydrates. Hydrates can also be categorized into stoichiometric and non-stoichiometric hydrates. In case of stoichiometric hydrates, the water content is well defined, and typically, the different hydration states have unique crystal structures. On the other hand, non-stoichiometric hydrates entrap water within the void spaces of the crystalline lattice and can have a continuously variable water content based on the relative humidity. Typically, these hydrates do not exhibit drastic changes in the crystal structure following sorption or release of lattice water. Both these kinds of hydrates are routinely encountered in drug product development, thereby mandating a detailed understanding of their influence on the stability and performance of the final dosage form.³⁶

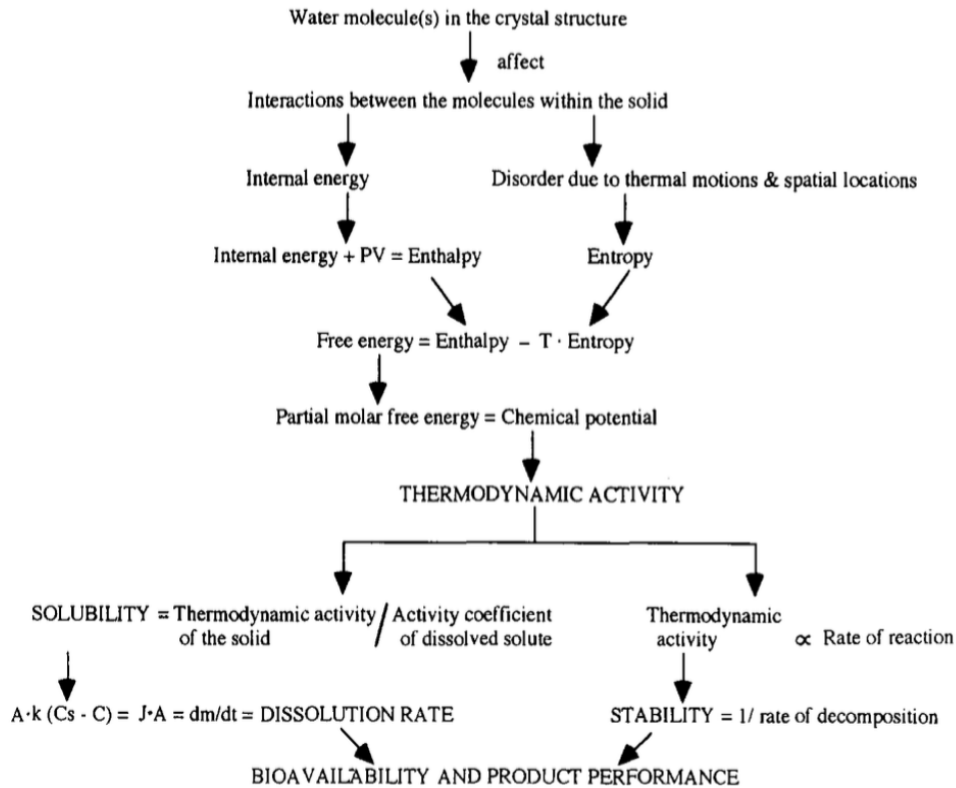


Figure 1.2. Flow chart highlighting the impact of hydration state on the physicochemical and mechanical properties of a drug. ‘A’ represents the surface area of the solid exposed to the dissolution medium, ‘k’ stands for the mass transfer coefficient; ‘Cs’ is the equilibrium solubility of the solid form; ‘C’ is the concentration in solution; ‘J’ represents the intrinsic dissolution rate and ‘dm/dt’ is the dissolution rate. Reproduced from Khankari *et al.*³⁷

1.3 Pharmaceutical processing

Formulating a drug substance into a solid dosage form will likely involve multiple unit operations such as mixing, milling, granulation, and compaction. The mechanical stresses experienced by the API during these processing steps can result in physical form changes that in turn can have an undesirable impact on the biopharmaceutical performance of the dosage form.

During drug product development, there is risk of unintended lattice disorder in the crystalline components (API and excipients). The loss in crystallinity during product development is also referred to as processing induced lattice disorder or mechanical activation. This has been discussed in subsequent sections.

1.3.1 Processing induced lattice disorder.

Lattice disorder refers to a disruption in the long range order of a crystalline solid or reduction in the crystallinity of the substance. Lattice disorder can manifest either as local disorder (lattice defects like vacancies, impurities, dislocations and grain boundaries) or amorphization (Figure 1.3). Disorder generates regions of high energy and molecular mobility, which then lead to physical and chemical instability.

Through the introduction of lattice disorder, there may be a change in the physicochemical and mechanical properties of a compound. This may, in turn, have implications on the chemical stability and shelf life of the API in a dosage form. This phenomenon is of pharmaceutical relevance as routine industrial processing steps such as milling, coating and granulation, have the potential to induce lattice disorder in crystalline actives and excipients. Lattice disorder can be induced in solids as a consequence of numerous factors.

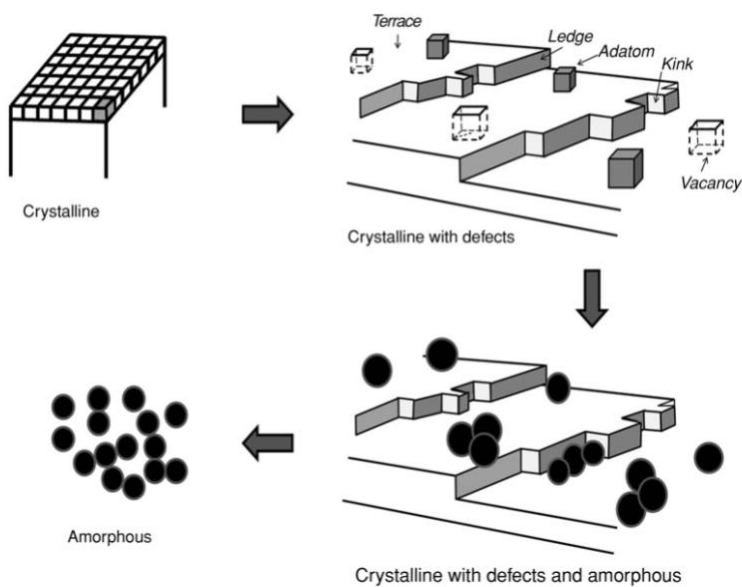


Figure 1.3. Schematic of defects and disorder on a crystalline surface.^{38,39}

1.3.1.a Milling.

Milling is a routinely employed unit operation in chemical and pharmaceutical manufacturing. An obvious and frequent use of milling is for particle size reduction. However, powders are subjected to mechanical stresses during the process, which may induce changes in other physical characteristics of the particles, for example amorphization and polymorphic transformations.⁴⁰⁻⁴² Cryomilling is an alternative to room temperature milling in order to mitigate the risk of phase

transformations inducted by rise in the temperature during milling. However, the risk of amorphization (crystalline → amorphous transition) still persists.⁴³⁻⁴⁵

1.3.1.b Dehydration induced lattice collapse.

Hydrates are the most common of all crystalline solvates encountered amongst pharmaceutical materials and make up roughly 30% of the materials used in the pharmaceutical industry.⁴⁶ Different hydrate forms of a given compound are of importance owing to their ability to modulate the internal energy, enthalpy and entropy, which in turn influence the solubility, dissolution rate, stability, reactivity and bioavailability. Hydration states also have the potential to affect the mechanical properties of solids, hence altering product performance.^{37,38}

Unit operations employed during formulation development of oral solid dosage forms, such as drying, milling, mixing and compression may lead to the dehydration of a crystalline hydrate. The loss of water of crystallization can induce stress on the lattice, often leading to a loss of lattice structure i.e. amorphization.⁴⁷ The consequent increase in molecular mobility of the amorphous form promotes its chemical reactivity. Owing to the influence of hydration state on the physicochemical and mechanical properties of the material, it is imperative to ensure the stability of the pharmaceutical hydrate during the formulation development process.

1.4 Model systems

1.4.1 Caffeine – oxalic acid (2:1) cocrystals.

Caffeine-oxalic acid (CAFOXA; Table 1.1) cocrystals were chosen as the model for studying the influence of processing induced lattice disorder on cocrystal stability. Caffeine (1,3,7-trimethyl-2,6-purinedione) is a central nervous system stimulant and a smooth muscle relaxant. Caffeine exists as a non-stoichiometric crystalline hydrate.^{32,48,49} Cocrystallization of caffeine with oxalic acid provides an avenue to control the solid form of the API. CAFOXA cocrystals have been reported to exhibit robustness against dissociation even at elevated vapor pressures. The cocrystals did not exhibit dissociation even following storage at 98% relative humidity (RH) at room temperature (RT) for 7 weeks. The tendency of disordered CAFOXA cocrystals to recrystallize at elevated RH rendered them an attractive system for our present work, as the recrystallization of the sample serves as an indirect proof of lattice disorder induced during pharmaceutical processing, such as tablet compaction and milling.

Table 1.1. Crystallographic data for 2:1 caffeine oxalic acid cocrystals reproduced from Trask *et al.*⁵⁰

Property	Caffeine/oxalic acid (2:1)
Experimental formula	2(C ₈ H ₁₀ N ₄ O ₂) · C ₂ H ₂ O ₄
Formula weight	478.44
Crystal system	Monoclinic
Space group	P2 ₁ /c
a (Å)	4.41430(10)
b (Å)	14.7701(5)
c (Å)	15.9119(6)
α (degrees)	90
β (degrees)	96.4850(10)
γ (degrees)	90
Z	2

1.4.2 Levothyroxine sodium pentahydrate.

1.4.2.a Hypothyroidism and levothyroxine.

Hypothyroidism is a pathological condition wherein the thyroid gland does not secrete sufficient quantities of thyroid hormones. Levothyroxine is the first line of treatment for patients suffering from hypothyroidism. It is the synthetic form of the physiological hormone, thyroxine (also known as T₄ (3,3',5,5' tetraiodo-*l*-thyronine)). Replacement therapy with levothyroxine is the primary and, in most instances, the only treatment option for hypothyroid patients.⁵¹⁻⁵⁴ At any given time, 5-10% of global human population suffers from hypothyroidism.⁵⁵⁻⁶¹ Thyroid hormones are vital for normal growth and development and also have numerous metabolic, cardiovascular, neurological and calorogenic effects.⁶²⁻⁷¹ In addition to supplementing thyroid levels, levothyroxine is also commonly used for patients with myxedema coma,⁷² non-toxic uninodular or multinodular goitre, and differentiated thyroid cancer in TSH (thyroid stimulating hormone) suppressive doses.⁷³⁻⁷⁷

The first ever thyroid hormone replacement products included desiccated thyroid extracts, thyroid glands and thyroglobulin from bovine and porcine origin. However, there were challenges with respect to the procurement as well as standardization of these products.⁷⁸⁻⁸⁴ The first synthetic substitute, levothyroxine sodium, was introduced into the US market in 1950s. The chemically

synthesized sodium salt is known to have the same therapeutic/physiological effects as the endogenously secreted, T₄.^{55,81,85-92} It is routinely administered orally as tablets, though alternate dosage forms are also available.

Levothyroxine sodium is one of the most prescribed drugs in the United States with over 100 million prescriptions annually.⁹³⁻⁹⁶ It is a low dose (25-300 µg/day) active pharmaceutical ingredient (API) and has a narrow therapeutic index (NTI).⁹⁷⁻⁹⁹ There is less than a two-fold difference between the minimum effective dose and the maximum tolerable dose. Patients requiring levothyroxine can be very sensitive to minor fluctuations in the administered dose.^{55,100-114} Exceeding 20-25% of the therapeutic dose can result in serious side effects, warranting dose titration.¹¹⁵⁻¹²³ The need for precise dose adjustment has resulted in numerous strengths (>10) ranging from 13 to 300 µg.^{124,125} The therapeutic failure may also stem from the chemical instability of the API in drug products and content non-uniformity – reflected by the numerous product recalls.¹²⁶⁻¹²⁸

Thus, in addition to being one of the most prescribed drugs, levothyroxine sodium has a long history of being amongst the most recalled products from the market. The chemical instability during shelf-life is a major reason for the recall.¹²⁹⁻¹⁴⁴ The problem is exacerbated by the low dose (API constitutes 0.04 - 0.5% w/w of the dosage form) and the consequent high excipient burden in levothyroxine formulations. Levothyroxine sodium is sensitive to temperature, light, pH, moisture and oxygen. Due to the potential chemical instability, historically, an overage of up to 20% was added to the drug product.¹⁴⁵⁻¹⁵¹ However, such a practice is questionable in light of its narrow therapeutic index.¹⁴⁷⁻¹⁵¹ Moreover the use of an overage, to compensate for drug degradation during product manufacture or storage, is discouraged by the FDA.¹⁵²

FDA has undertaken several measures to standardize the quality of the marketed products and to reduce variability in stability profile across manufacturers. In 1997, levothyroxine sodium was declared a “new drug”.¹⁵³⁻¹⁵⁵ In 2007, the FDA tightened the assay specifications for marketed products from 100 ± 10% to 100 ± 5% of the labelled amount. In 2008, the US Pharmacopeial convention updated the levothyroxine sodium product monograph to meet the updated FDA specifications.¹⁵⁶⁻¹⁵⁹ There has been a recall of over 100 million tablets between 2012-2015.^{160,161}

The stability of levothyroxine sodium ‘as is’ and in marketed drug products has been the subject of numerous publications. The influence of excipient properties and storage conditions on the physical form and chemical stability of the API were investigated earlier.¹⁶²⁻¹⁶⁷ It is well recognized in the literature that the excipients can govern the formulation performance.¹⁶⁸⁻¹⁷¹ The excipient properties, specifically hygroscopicity and microenvironmental acidity, appeared to be determinants of drug stability.

1.4.2.b History - treatment of hypothyroidism.

The earliest evidence of thyroid supplementation was in the sixth century when sheep thyroid was used to treat cretinism in China.⁸² In 1890, transplantation of animal thyroid glands yielded promising results in patients with myxedema coma.^{78-80,92} Desiccated hormonal products (dried and powdered), prepared from the thyroid glands of domesticated hog, beef or sheep were the preferred form of supplementation from the early 1890s to mid 1970s.^{172,173} The desiccated products contain approximately 80% tetraiodothyronine (T4) and 20% triiodothyronine (T3) along with small fractions of iodinated compounds, such as monoiodotyrosine and diiodotyrosine. The ratio of T4 to T3 in these preparations varied depending on the source (bovine or porcine). Desiccated thyroid extracts of porcine origin are still widely available. However, their use resulted in hypertriiodothyroninemia and thyrotoxicity in some patients, owing to improper dose adjustment and product variability.¹⁷⁴ Treatment with thyroid extracts was time-demanding and expensive. In addition to the concern of content uniformity, these preparations had a short shelf life and were prone to induce allergic reactions owing to the potential immunogenicity of animal derived products.^{52,81,126,175-181}

In 1914, Kendall isolated and crystallized thyroxine (which contained 65.3% w/w iodine) and its chemical structure was elucidated.^{85,90} Following this, Barger and Harington successfully synthesized the unionized (free acid) form of thyroxine in 1927.⁸⁷⁻⁸⁹ They also uncovered the higher potency of the *levo* isomer as compared to the racemic mixture. However, the limited oral absorption of the free acid posed challenges with respect to bioavailability. The sodium salt of thyroxine with acceptable absorption profile was uncovered in 1949. In 1952, liothyronine (T3) was recognized as a more potent thyroid hormone.¹⁸²⁻¹⁸⁵

Subsequently, tetraiodothyronine (T4) and triiodothyronine (T3) were synthesized and became commercially available. They were first marketed in the United States in 1955 but were not FDA approved until 1997. T4 monotherapy is the first line of treatment for hypothyroid patients with dose adjustments to normalize serum TSH.¹⁸⁶⁻¹⁸⁸ However, it might be inadequate in cases with deiodinase polymorphism (i.e. insufficient conversion of T4 to the more potent T3 by 5'-deiodinase), thereby necessitating personalization of the treatment and/or addition of T3 (i.e. combination therapy).^{53,188,189}

1.4.2.c ADME of levothyroxine sodium.

The dose of levothyroxine sodium for each patient has to be “tailored and titrated” and depends on numerous factors including patient’s age, disease state, cardiovascular status, other comorbidities, lean body mass, pregnancy status, coadministered medications and severity of hypothyroidism

(TSH and T4 levels).¹⁹⁰⁻¹⁹⁴ Levothyroxine is absorbed predominantly through the jejunal-ileal section of the gastro-intestinal tract. The absorption is highly variable and incomplete, hence limiting the bioavailability to 40-80%.¹⁹⁵ The absorption of levothyroxine is facilitated by gastric acidity and adversely affected by gastro-intestinal abnormalities.

Levothyroxine is typically administered as immediate release tablets of levothyroxine sodium pentahydrate. It reaches its peak plasma concentration within 2-4 hours following oral administration and has a half-life of 6-8 days.^{125,196-198} Absorption of levothyroxine is affected by food, disease state, age and co-administered drugs. The volume of distribution of levothyroxine is 11-15 L. Levothyroxine has a high plasma protein binding which can be as high as 99.95%. The clearance of levothyroxine in euthyroid patients is 0.055 L/h. The low clearance and high serum half-life of levothyroxine are explained by the high plasma protein binding of the drug. Levothyroxine is eliminated slowly and primarily via sequential deiodination. In addition, thyroid hormones are also metabolized through sulfation and glucuronidation. Levothyroxine is excreted predominantly via kidneys. A fraction of the drug (approximately 20%) undergoes sulfation and glucuronidation followed by enterohepatic recirculation and elimination through feces.^{52,196,197,199-201}

1.4.2.d Physicochemical profile of levothyroxine sodium.

The IUPAC name is sodium (2S)-2-amino-3-[4-(4-hydroxy-3,5-diiodophenoxy)-3,5-diiodophenyl] propanoate. The sodium salt exists as a pentahydrate ($C_{15}H_{10}I_4NNaO_4 \cdot 5H_2O$) under ambient conditions ($RH \geq 15\%$). Levothyroxine has three ionizable functional groups - carboxyl, phenolic hydroxyl and an amino group with pK_a values of 2.4, 6.9 and 10.1, respectively.^{202,203} In addition to the unionized/zwitterionic form, levothyroxine can exist as a cation, anion and dianion (Figure 1.4). The water solubility of levothyroxine sodium decreases as pH increases from 1 to 3, remains constant between 3 and 7 (zwitterionic form) and rises above pH 7 (Figure 1.5).^{203,204}

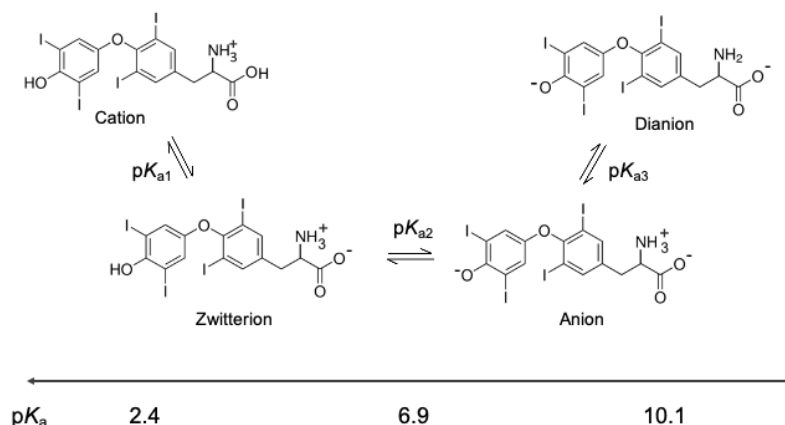


Figure 1.4. (a) Ionization states of thyroxine. Adapted from Virili *et al.*²⁰¹

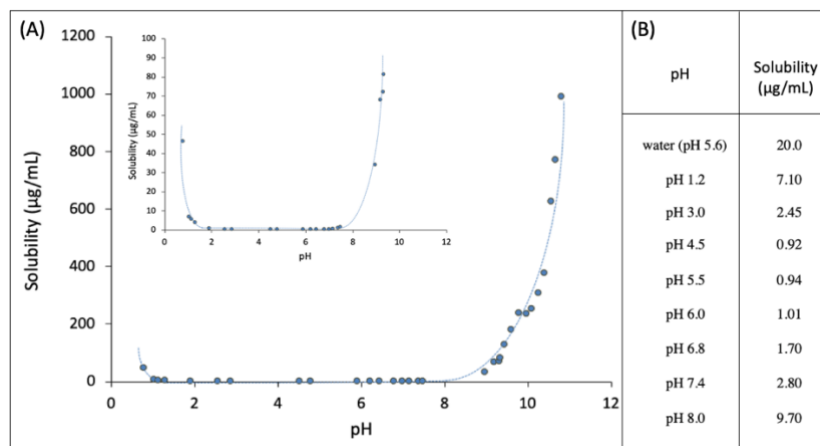


Figure 1.5. (A) pH - solubility profile of levothyroxine sodium at 25°C. Adapted from Won *et al.*²⁰³ (B) The solubility at selected pH values. Reproduced from Kocic *et al.*^{204,205}

1.4.2.e Debate over the BCS class of levothyroxine sodium.

Levothyroxine sodium tablets exhibit erratic bioavailability, ranging from 40 to 80%, thereby necessitating an investigation of the factors affecting its oral absorption.²⁰⁶ There is disagreement in the literature with respect to the BCS (Biopharmaceutical Classification System) categorization of levothyroxine sodium.

According to Kasim *et al.*, levothyroxine sodium is a BCS class I drug.²⁰⁷ It has also been categorized as a BCS class 3 drug i.e. the API has permeability limited oral absorption.^{136,208-210} However, other reports indicate that the API has dissolution limited oral absorption.²⁰⁶ Won *et al.* elucidated the pH solubility profile of levothyroxine and determined the solubility of the unionized form of the API (i.e. levothyroxine) to be approximately 25 µg/mL over the pH range of 4 to 7 (25°C). Levothyroxine is known to aggregate (a zwitterionic molecule; 50-100 nm in diameter) in

aqueous media leading to an increase in the “apparent solubility” values to ≥ 1.5 mg/mL. The solubility increases multiple fold above and below this pH owing to the ionization of the amine and carboxylate group, respectively. However, levothyroxine sodium has an intrinsic dissolution rate (IDR) of 0.0002 mg/min/cm² (for BCS class 1 and 3 drugs, this number is ≥ 0.1 mg/min/cm²) over the physiological pH range. In another study, the dose/ solubility ratios for three different doses of levothyroxine sodium (100, 150 and 500 μ g) were determined at different pH values (i.e. pH 1.2 \rightarrow 7.4). The clinically relevant doses (100 and 150 μ g) failed to meet the criterion for high solubility (< 250 mL) drugs, whereas the 600 μ g dose (which is seldom used) passed the criterion between pH 4.5 and 6.8 only.²¹¹ Based on multiple literature reports, the absorption of levothyroxine sodium seems to be both permeability and dissolution rate limited.^{212,213}

1.4.2.f Dissolution testing.

The appropriate dissolution testing method for levothyroxine sodium tablets has been the subject of debate.²⁰⁶ While the United States Pharmacopeia (USP 43) specifies the use of HCl (0.01 N) with or without SLS (0.2% w/v), the British Pharmacopoeia (BP 2014) specifies distilled water without surfactant.^{214,215} At pH 2.4 (the USP method), the solubility of levothyroxine is very low (~ 2.5 μ g/mL; 25°C). However, the use of sodium lauryl sulfate (SLS), at a concentration of 0.2% w/v, will enhance the dissolution rate by improving wetting.^{204,205,208,216,217}

The USP (USP 43) monograph of levothyroxine sodium tablets have five dissolution tests. They differ in terms of media volume (500 or 900 mL), paddle rotation speed (50 or 75 rpm), tolerance and the presence of SLS (0.2%) in the dissolution medium. The dissolution methods appear to be product specific.

Pabla *et al*²⁰⁸ compared the dissolution profiles of Synthroid tablets (Abbott Laboratories, IL), Tirosint gel capsules (Institut Biochimique, Switzerland) and generic levothyroxine tablets (Sandoz Pharmaceuticals). The testing was performed using a USP II apparatus (75 rpm, 37°C for 3 sec; in the presence and absence of 0.05% w/v sodium lauryl sulfate in seven different buffers with pH ranging from 1.2 to 8.0). In 0.01 N HCl, only a fraction of the levothyroxine (< 25%) was in solution from both Synthroid and generic tablets even at 3 h while $\sim 80\%$ was dissolved from Tirosint capsules. However, the presence of 0.05% SLS considerably accelerated the drug dissolution from tablet formulations with $\sim 75\%$ drug in solution in 30 minutes. Since the SLS concentration is below its critical micellar concentration (0.24% w/v in water at 25°C)^{218,219}, the improved wetting provided by SLS could be one explanation for the observed dissolution behavior. On the other hand, the dissolution profiles from the Tirosint gel capsules appeared to be much less dependent on the presence of surfactant. In the presence of SLS, the dissolution profiles of all the three

formulations were substantially similar at ≥ 60 minutes. However, in the absence of SLS, the dissolution profiles from the three formulations exhibited pronounced differences with incomplete release even after 3 h. Even in the presence of SLS (0.05%), only the Synthroid tablet formulations exhibited pronounced pH dependence (over the pH range of 1.2 to 7.0). In the generic tablets, only $\sim 80\%$ of the drug dissolved at $\text{pH} \geq 4.0$, while complete dissolution occurred at lower pH values. The dissolution profiles from the gel capsules appeared to be pH independent.

Since the USP mandates the use of 0.01 N HCl, we will restrict our conclusions to the results obtained under highly acidic conditions. Based on these limited studies, we can conclude that: (i) the presence of SLS in the dissolution medium drastically influences the dissolution profile, (ii) the gel capsules appear to dissolve more readily than the tablets and (iii) and the dissolution profiles of the generic and Synthroid tablets show pronounced differences in the absence of SLS.

The impact of gastric pH on dissolution is critical. In patients with reduced gastric acidity (for example, due to *H. pylori*, use of antacids or proton pump inhibitors, comorbidities or other concomitant medications), a higher dose of levothyroxine sodium tablets may be required. In these patients, the use of soft gelatin capsules or liquid solution of levothyroxine has been proposed.²²⁰⁻²²⁹ Such an approach will present the drug directly in a solution state and may thereby facilitate oral absorption.

1.4.2.g Chemical degradation pathways for levothyroxine sodium.

In aqueous solutions, levothyroxine sodium undergoes deiodination, first to triiodothyronine (Scheme II; Won *et al.*, 1992)²⁰³ and then to diiodo and monoiodo thyronine. The iodine atoms at the 3' and 5' positions are the first to be removed by electrophilic attack owing to the phenoxide ring resonance which gives them a more cationic character as compared to the iodine atoms on the other ring. The chemical reaction (loss of the first iodine) follows first order kinetics, and is accelerated as the solution pH is lowered (Figure 1.6 a).²⁰³ In the solid state, the API follows complex decomposition pathways with the disappearance of levothyroxine following first order kinetics (Figure 1.6 b).^{203,230} As expected, an increase in temperature accelerated the decomposition reaction.^{147, 231} Recently, the thermal degradation of thyroxine in the solid state was studied in detail using ultrahigh-performance liquid chromatography and high resolution mass spectrometry (UHPLC-HRMS). The predominant decomposition products resulted from oxidation and deiodination. The accurate determination of molecular masses coupled with multi-stage mass spectrometry enabled structure determination of the first and second generation degradation products. By coupling the techniques, the reaction pathways were discerned and enabled an

understanding of the decomposition mechanism in the solid-state.^{232,233} HPLC coupled with ICP-MS enabled separation and identification of levothyroxine degradation products in tablets.²³⁴

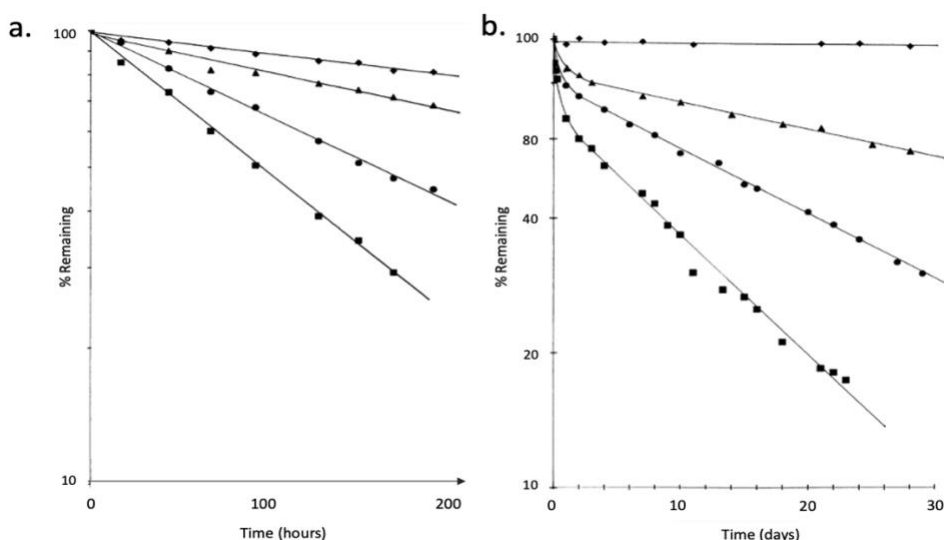


Figure 1.6. Comparison of levothyroxine sodium stability in the solution (a) and solid (b) states. (a) First order plots of the percent of levothyroxine sodium remaining as a function of time at solution pH values of 2.05 (■), 6.86 (●), 7.96 (▲) and 10.55 (◆) at 80°C. Decomposition occurred via deiodination. (b) First order plot obtained following isothermal storage of levothyroxine sodium at 50 (◆), 60 (▲), 70 (●) and 80°C (■). While the state of hydration of levothyroxine sodium was not mentioned, it is likely to be the pentahydrate since it is the stable form under ambient conditions. Storage in the temperature range of 50 to 80°C is expected to cause rapid dehydration (in a time scale of a few hours). Data from Won *et al* has been reproduced.²⁰³

1.4.2.h Physical form and chemical stability.

A correlation between the physical form and chemical stability of levothyroxine sodium has been long speculated.^{47,235-240} In 1951, DL-thyroxine was reported to have a triclinic lattice with $P\bar{1}$ space group.²⁴¹ The crystal structure of the levo form of thyroxine sodium pentahydrate was reported to be triclinic (non-centrosymmetric) with $P1$ space group.²⁴² The authors highlighted the exceptional conformational flexibility of the two non-identical thyroxine anions in a unit cell, enabling easy water movement in and out of the lattice. Of the ten water molecules shared between two levothyroxine sodium molecules in an asymmetric unit, eight are directly coordination bonded to the sodium atoms whereas the other two are independent. The two symmetry independent thyroxine anions form the hydrophobic sheets which enclose the hydrophilic 001 plane containing

the two differently coordinated sodium ions and the non-coordination bonded water molecules. High resolution powder diffraction pattern and H-atom positions were later reported.²⁴³

Based on systematic studies, the ability of lattice water to prevent oxidative decomposition of levothyroxine sodium pentahydrate was pointed out.^{244,245} Their experiments were conducted at two temperatures: room temperature (RT) to simulate realistic pharmaceutical processing conditions, and at 60°C to induce thermal stresses. Levothyroxine sodium pentahydrate underwent no decomposition, either at RT or at 60°C, when stored at 75% RH. However, at 0% RH, there was pronounced chemical decomposition even at RT, which was accelerated at 60°C. Thus the authors believed that the retention of lattice water was necessary for drug stability in the formulation. The use of hygroscopic excipients could lead to levothyroxine dehydration during product storage, and hence must be avoided. The risk of oxidative decomposition could be mitigated with packaging. The use of anti-oxidants could be a second possible approach.

Tablets prepared by direct compression were reported to be more stable than those by wet granulation. In the direct compression process there was no need to dry granules – a processing step, which could induce dehydration of levothyroxine sodium pentahydrate, and consequently accelerate its chemical decomposition in tablets.²⁴⁶

The relation between loss of lattice water in levothyroxine sodium pentahydrate and its oxidative decomposition was investigated.¹⁶⁴ The lattice water existed in ‘channels’ and oxygen occupied the channel sites vacated by dehydration. It then induced oxidative decomposition of levothyroxine sodium. When levothyroxine sodium pentahydrate was subjected to elevated temperatures in an XRD, the complete loss of lattice water was accompanied by a broadening of the X-ray peaks (loss in crystallinity). It was concluded that chemical decomposition was preceded by a change in the physical form of the API (refer to Figure 1.7).¹⁶⁴

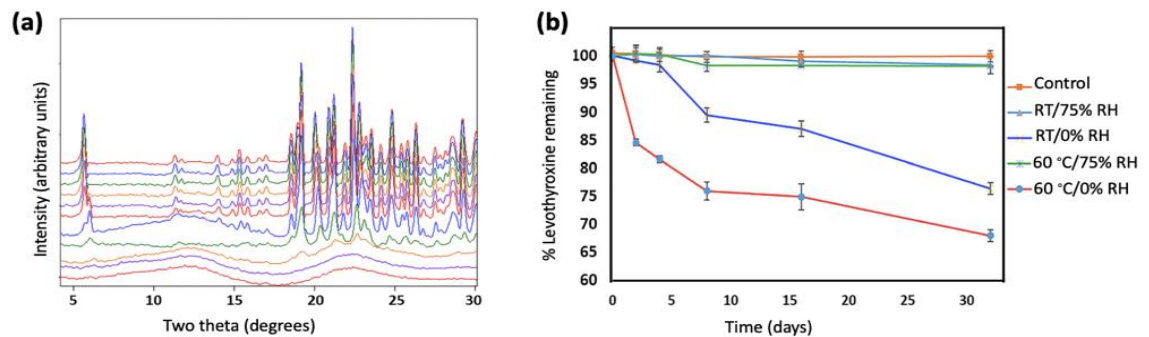


Figure 1.7. (a) Overlay of diffraction patterns showing the impact of temperature on the physical form of levothyroxine sodium pentahydrate. The data was collected at 30, 40, 50, 60, 70, 80, 90, 100, 110, 120 and 130°C—top to bottom. (b) Effect of relative humidity and

temperature on the chemical stability of levothyroxine sodium in the presence of molecular oxygen. Adapted from Shah *et al.*¹⁶⁴

1.4.2.i Drug product analysis.

Since levothyroxine sodium is administered at a very low dose, the excipients constitute a major weight fraction of the dosage form. Thus, any drug-excipient interaction has the potential to disproportionately influence the API stability (in light of its low dose). Moreover levothyroxine is known to be sensitive to light, oxygen, pH, water and to elevated temperatures.^{167,230,233} Interaction with excipients leading to chemical decomposition of levothyroxine sodium has been reported.^{166,247}

There are numerous marketed tablet formulations of levothyroxine sodium (Table 1.2). The narrow therapeutic index has necessitated dose titration in patients, and has also resulted in numerous dosage units, ranging from 25 to 500 µg per tablet. Most manufacturers have marketed formulations with over 10 dosage units, with increments as low as 12 µg. Even over this wide dose range, the major excipients would form a substantial fraction of the dosage form. In light of the very low dose of the API, any API-excipient interaction or incompatibility can result in instability-induced product failure.

As pointed out earlier, there have been numerous instances of recall of levothyroxine formulations, with unacceptable level of chemical decomposition being one of the primary reasons.¹³¹⁻¹⁴⁴ The role of excipients has been investigated. In 1990, a stability indicating HPLC assay was used to analyze multiple tablet batches procured from two different manufacturers.²⁴⁸ While the influence of individual excipients was not evaluated, the excipient(s) in one formulation were identified to be detrimental to levothyroxine stability. Tablets from the same manufacturer also exhibited batch-to-batch variability.

The authors expressed concern with the practice of dispensing a 100-day supply of levothyroxine sodium tablets to patients since the API is susceptible to decomposition upon exposure to light and moisture during the long time period of product usage. While this study was limited, both with respect to the stability testing conditions and identifying the role of individual excipients, it was one of the earliest reports on the subject and paved the way for future investigations on stability testing of levothyroxine sodium in drug products.

The chemical stability of levothyroxine sodium was evaluated in the presence of numerous pharmaceutical excipients including pH modifiers.¹⁶⁶ The influence of lactose anhydrate, microcrystalline cellulose, starch, mannitol and DCPA were individually investigated. When tableted with one of the first three excipients, the formulations failed to meet the USP potency

specification following storage for 3 months at 40°C/75% RH. It should be noted that the tablets were not packaged and were directly exposed to the stipulated conditions. Tablets prepared with either DCPA or mannitol exhibited better stability but exhibited > 10% decomposition following 6 months of storage. Interestingly, the 'as is' API (uncompressed powder) was substantially stable (< 3% decomposition) following storage for 6 months. Thus all of these excipients, when present in a formulation, appeared to facilitate API decomposition.

Aqueous slurries of individual diluents (dicalcium phosphate, microcrystalline cellulose) were prepared, their pH was adjusted between 3 and 11, and the stability of levothyroxine sodium was evaluated following storage at 50°C. Levothyroxine sodium showed more degradation in excipient slurries at pH 3 (assay: 49-68%) than at pH 11 (assay: 89-96%). In excipient slurries with no pH modifications, the assay was intermediate between the two pH extremes (70-87%). The pH of the anion to zwitterion (pK_{a2}) transition is 6.9. For the HPLC assay, the drug is extracted using 0.01 M sodium hydroxide in methanol. Under this condition, all the salt is expected to convert to the free acid. Thus, the assay method is expected to be insensitive to disproportionation of the salt.^{15,249-251}

From Table 1.2, it is evident that lactose is an excipient in numerous levothyroxine drug products on the market. However, being a reducing sugar, it is prone to Maillard condensation reaction with levothyroxine sodium (the primary amino group), resulting in chemical decomposition of the API.²⁵² Levothyroxine sodium has also been observed to be unstable in the presence of other carbohydrates such as sucrose and glucose. The use of polysaccharides such as mannitol, starch and maltodextrin has been claimed to be safe.^{253,254} However, as pointed out earlier, Patel and coworkers had observed unacceptable level of decomposition in presence of mannitol when stored at 40°C/75% RH for six months.¹⁶⁶ Ledeti *et al* observed excipient incompatibility of levothyroxine sodium with mannitol, but only at elevated temperatures. Stability was achieved by combining sucrose and mannitol with an antioxidant (butylated hydroxy anisole).^{255,256} The use of alkaline pH modifiers has also been postulated as a useful strategy to improve formulation stability.^{166,203}

Collier *et al*²⁴⁷ performed comprehensive API-excipient compatibility testing in binary mixtures with API:excipient weight ratio ranging between 1:1 and 1:100 w/w. Excipients with different functionalities were tested. Crospovidone, povidone, and sodium lauryl sulfate (SLS) were deemed unsuitable owing to their hygroscopicity and potential to cause API decomposition. However, it may not be possible to extrapolate the results to actual formulations. The drug-excipient mixtures contained water and were stored at 60°C. Under these conditions, even the control i.e. levothyroxine sodium pentahydrate, exhibited up to 40% decomposition.

Recently, a reformulated version of levothyroxine sodium tablets was introduced by Merck, with a shelf life of three years.²⁵⁷⁻²⁵⁹ The lactose in the original formulation was replaced with mannitol

and citric acid. This was done to mitigate the formation of levothyroxine-2-ketolactose, a decomposition product of Maillard reaction. An additional concern was lactose intolerance, which could also cause levothyroxine malabsorption.²⁶⁰⁻²⁶³

Two marketed levothyroxine sodium formulations were heated up to 500°C in a DSC and in a TGA in ambient atmosphere.²⁶⁴ Similar investigation of the ‘as is’ levothyroxine sodium was also conducted enabling the evaluation of the collective influence of excipients on the thermal behavior of the API. Based on weight loss observed in the TGA, the authors concluded that the API decomposition was initiated at 155°C. This was contrary to other studies, carried out under nitrogen, which report decomposition at 203°C.^{164,247} Thus oxidative decomposition, expected under ambient conditions, seems to occur at a much lower temperature. The excipients in the marketed tablets, by altering its apparent activation energy, were believed to influence the stability of levothyroxine sodium. Thermal analysis enables rapid excipient screening and has the potential to serve as an ‘accelerated stability’ tool. It can be combined with other characterization techniques to gain mechanistic insight into API-excipient interactions. However, the elevated temperatures used (and the reactions observed under these conditions) do not realistically reflect the actual pharmaceutical processing and storage conditions.

The compatibility of levothyroxine, individually with ten commonly used tablet excipients (1:1 w/w binary mixtures; at room temperature), was evaluated by IR spectroscopy. The same mixtures were also subjected to thermal analyses (DSC and TGA).¹⁶³ By combining the results from the two techniques, the authors concluded that levothyroxine sodium was incompatible with sucrose, mannitol and sorbitol.

In a formulation composition, by replacing microcrystalline cellulose with silicified microcrystalline cellulose (SMCC; microcrystalline cellulose combined with colloidal silicon dioxide) there was a pronounced improvement, both in API stability and content uniformity. SMCC is believed to provide a stabilizing matrix while also improving the flow properties.²⁶⁵ The use of anti-oxidants, such as butylated hydroxy anisole (BHA), prevented oxidative decomposition in the solid dosage forms.^{266,267} The use of gelatin and hydroxypropyl methyl cellulose as binders, also improved API stability.¹⁴⁵

1.4.2.j Bioequivalence and clinical interchangeability

Ever since the introduction of Synthroid® tablets to the US market in 1955, numerous issues have been identified with use of levothyroxine sodium tablet formulations. These include impaired absorption,^{55,125,201,268,269} incompatibility with other drugs and excipients,^{263,270-275} chemical instability of the API in marketed formulations,^{53,84,166,248,259,276} and more recently, concerns

associated with product interchangeability, i.e. the interchangeability of commercial levothyroxine product formulations.^{55,92,107,126,178,277-288} If a product switch is necessary, it is followed by careful dose titration and therapeutic drug monitoring.^{287,289} The adequacy and the appropriateness of the current bioequivalence standards are the subject of debate among clinicians. For products considered to be “therapeutically” equivalent, physicians have questioned their clinical interchangeability.^{122,290-296} Despite numerous studies and wide-ranging discussions between academic scientists, regulators and clinicians, no consensus has yet been reached on this issue.²⁹⁷⁻

301

1.4.2.k Alternative oral dosage forms.

While the tablet dosage form of levothyroxine sodium is the most popular, numerous literature reports advocate the use of soft gel capsules and oral solutions. There have been fewer malabsorption issues with these alternate dosage forms.^{227,229,302-312} Since these are solution dosage forms, they are suited for patients with reduced gastric acidity due to a variety of reasons - *H. pylori* infection, concomitant use of proton pump inhibitors or other gastro-intestinal disorders.³¹³⁻³¹⁵ Liquid formulations are easier to administer to newborns and drug absorption is faster than from tablets. Despite these advantages, oral solutions of levothyroxine sodium are not preferred due to their short shelf-life and poor dose control.^{266,316,317} Solid lipid nanoparticles have been developed for oral delivery of levothyroxine sodium but clinical testing is needed to evaluate their safety and efficacy.³¹⁸

Table 1.2. Marketed levothyroxine sodium formulations with the list of excipients in each dosage form. The first section contains oral tablet dosage forms. The formulation details of other oral dosage forms (soft gel, liquid) and injectables are presented in the second section. Their therapeutic equivalence codes (updated by the FDA in March 2020)²⁹⁷, if available, have been listed in parenthesis.

Brand	Manufacturer	Levothyroxine sodium content in each dosage unit	Excipients
Synthroid ^{124,319} (AB2)	Abbvie	25, 50, 75, 88, 100, 112, 125, 137, 150, 175, 200 and 300 µg	Lactose monohydrate, magnesium stearate, povidone, talc, acacia, confectioner's sugar
Levothroid ³²⁰ (AB4)	Forest/ Sanofi Aventis; Alvogen Group Holdings 4 LLC	25, 50, 75, 88, 100, 112, 125, 137, 150, 175, 200 and 300 µg	Calcium phosphate, microcrystalline cellulose, povidone, magnesium stearate, dye
Levoxyl ³²¹ (AB3)	Jones/King Pharmaceuticals; Pfizer	25, 50, 75, 88, 100, 112, 125, 137, 150, 175, 200 and 300 µg	Microcrystalline cellulose, calcium sulfate dihydrate, croscarmellose sodium, magnesium stearate, sodium bicarbonate, dye
Unithroid ³²² (AB1)	Jerome Stevens Pharmaceuticals	25, 50, 75, 88, 100, 112, 125, 150, 175, 200 and 300 µg	Lactose, starch, acacia, magnesium stearate, colloidal silicon dioxide, corn, microcrystalline cellulose, sodium starch glycolate
Levo-T ^{323,324}	Alara	25, 50, 75, 88, 100, 112,	Microcrystalline

		125,137, 150, 175, 200 and 300 µg	cellulose, colloidal silicone dioxide, magnesium stearate, sodium starch glycolate
Euthyrox ³²⁵⁻³²⁷	Merck	25, 50, 75, 88, 100, 112, 125,137, 150, 175 and 200 µg	Mannitol, magnesium stearate, citric acid anhydrous, starch, gelatin, croscarmellose sodium
Eltroxin ^{328,329}	GSK; Aspen Pharma Pvt Ltd	13, 25, 50, 75, 88, 100, 112,125, 137, 150, 175, 200, 300 and 500 µg	Microcrystalline cellulose, pre-gelatinized maize starch, talc, colloidal anhydrous silica, magnesium stearate.
Generic Levothyroxine sodium ³³⁰⁻³³³ (AB4)	Mylan	25, 50, 75, 88, 100, 112, 125, 137, 150, 175, 200 and 300 µg	Butylated hydroxy anisole (BHA), crospovidone, povidone, sucrose, ethanol, colloidal silicon dioxide, magnesium stearate, sodium lauryl sulfate, mannitol, microcrystalline cellulose
Generic Levothyroxine sodium ³³⁰⁻³³³	Lupin Atlantis; Amneal Pharmas LLC	25, 50, 75, 88, 100, 112, 125, 137, 150, 175, 200 and 300 µg	Butylated hydroxy anisole (BHA), crospovidone, povidone, sucrose, ethanol, colloidal silicon dioxide, magnesium stearate, sodium lauryl sulfate, mannitol, microcrystalline cellulose

Oroxine tablets ³³⁴	Aspen Pharma Pvt Ltd	50, 75, 100 and 200 µg	Maize starch, lactose monohydrate, dextrin and magnesium stearate
Soft Gel, Liquid and Injectable Formulations			
Tirosint soft gel capsules ^{335,336}	IBSA	13, 25, 50, 75, 88, 100, 112, 125, 137, 150, 175 and 200 µg	Gelatin, glycerin and water
Tirosint-SOL ³³⁷ (Oral solution)	IBSA	13, 25, 50, 75, 88, 100, 112, 125, 137, 150, 175 and 200 µg/mL	Glycerol, water
*Oroxine Lyophilized powder for injection ³³⁸	APP Pharmaceuticals, LLC	100, 200 and 500 µg	Dibasic sodium phosphate heptahydrate, mannitol and sodium hydroxide
Novothyral Lyophilized powder for injection	Forest Pharmaceuticals, Inc	100, 200, 500 µg	Dibasic sodium phosphate heptahydrate, mannitol, and sodium hydroxide
Thyreocomb N lyophilized powder for injection ^{145,339}	Berlin-Chemie AG, Berlin	100, 200 and 500 µg	Levothyroxine, potassium iodide, potassium hydroxide
Lyophilized powder for injection in	Par sterile	100 µg per vial 200 µg per vial 500 µg per vial	Dibasic sodium phosphate anhydrate, tribasic sodium phosphate, mannitol

single dose vials ³⁴⁰			
Lyophilized powder for injection ³⁴¹⁻³⁴⁴	Fresenius Kabi; Fera pharm; Dr Reddys; Maia Pharms Inc; Piramal Critical	100 µg per vial 500 µg per vial	Dibasic sodium phosphate anhydrate, mannitol

*This compilation focuses on oral levothyroxine sodium formulations. However, for the sake of completeness, the compositions of lyophilized formulations is also given.

1.5 Motivation and thesis overview

The aim of this thesis research is to develop a comprehensive understanding of the impact of excipients, pharmaceutical processing conditions and storage on the physical and chemical stability of a model salt and cocrystal solid drug formulation. Mechanistic insights into these factors would enable rational product development of salts and cocrystals. A detailed investigation into the mechanism of instability (for instance, lattice disorder, microenvironmental acidity and excipient hygroscopicity) would promote rational excipient selection and process optimization for the design and development of robust formulations.

This thesis has been divided into four research chapters. The first two chapters (Chapters 2 and 3) are focused on characterization and understanding of the influence of lattice disorder, induced during routine pharmaceutical processing, on the stability of a model cocrystal system. The next two chapters (Chapters 4 and 5) highlight the challenges associated with the formulation development of a rather popular salt i.e. levothyroxine sodium pentahydrate (LSP). The role of lattice dehydration and excipient properties on the physical and chemical stability of the API have been investigated in these chapters. The conclusions and future directions of this thesis research are discussed in Chapter 6 and 7, respectively. A brief overview of the research chapters has been provided below.

1.5.1 Chapter 2

Cocrystal formation enables modification of the physicochemical and mechanical properties of an active pharmaceutical ingredient (API). Over the past two decades, significant progress has been made in the design and synthesis of pharmaceutical cocrystals.^{23,345-347} However, the challenges associated with the transition of cocrystals from a drug substance to drug product remain poorly understood. The formulation and manufacture of a cocrystal as a solid dosage form (for the purpose of this discussion, tablets) necessitates the use of excipients and often includes several unit operations. It is therefore important to evaluate the potential impact of both API-excipient interactions and processing conditions on cocrystal stability. Cocrystals are typically sustained by non-covalent interactions such as hydrogen bonds. They may be susceptible to dissociation in the presence of competing excipients. While some recent studies have investigated the role of excipients on cocrystal stability, the influence of pharmaceutical processing has not yet been investigated.^{34,35} Lattice disorder can be introduced in the API and excipients during pharmaceutical unit operations steps such as milling, mixing, granulation and compression. In light of the potential destabilizing effect of lattice disorder, it is important to evaluate the combined effects of lattice

disorder and excipients on cocrystal stability.

In this work, we have systematically investigated the impact of processing-induced lattice disorder on cocrystal stability. Lattice disorder was introduced in CAFOXA (the model cocrystal) and DCPA (model excipient) by milling. In an effort to reflect actual pharmaceutical processing, the milling times were short (≤ 2 min). *We hypothesize that even short milling times can induce adequate lattice disorder to render cocrystal system unstable.* The “higher energy” of the disordered regions, both in CAFOXA and DCPA, are believed to be the sites for preferential sorption of water, the medium for the dissociation reaction. In order to study the impact of comilling on cocrystal dissociation, CAFOXA and DCPA were mixed first and then milled together (‘comilled mixture’). Milling together may result in an increase in the inter-particulate contact area. In a separate set of experiments, the cocrystals and DCPA were milled separately and then mixed (‘physical mixtures’). Thus, two processing steps, i.e. milling and mixing, were interchanged to monitor their impact on cocrystal dissociation.

The overall goal of this work was to systematically study the impact of processing-induced lattice disorder on the stability of the model cocrystal system. The specific objectives were (i) to quantify lattice disorder as a function of milling time, (ii) establish the relationship between degree of lattice disorder and extent of cocrystal dissociation, and (iii) understand the influence of co-processing (CAFOXA and DCPA) on lattice disorder and consequently, dissociation.

CAFOXA has been widely reported to be a robust cocrystal. However, transitioning this into a stable solid dosage form requires careful consideration of the processing conditions and formulation composition. In the absence of excipient (DCPA), the cocrystals were robust and withstood routine processing (milling) as well as exposure to elevated water vapor pressures. In the presence of excipient, while the unmilled powder mixtures were stable to elevated RH (75% at RT), lattice disorder induced by milling for just 10 sec resulted in pronounced dissociation. Low levels of lattice disorder induced during routine processing steps, in a drug product environment, can lead to cocrystal instability.

1.5.2 Chapter 3

In this work, atomic force microscopy (AFM) was used to investigate the impact of routinely used pharmaceutical unit operations, i.e. tablet compression and powder milling, on the crystallinity of CAFOXA tablets. Topography and phase imaging were performed on the samples using the ‘tapping mode’ of AFM. Using the technique, we were able to visualize crystallization of the disordered samples upon exposure to elevated water vapor pressure. Low levels of disorder induced during pharmaceutical processing can potentially go undetected when characterized using routine

characterization techniques such as XRD and thermal analysis (which provide the bulk or weighted average of disorder). The determinantal and disproportionate influence of low levels of surface disorder has previously been reported (Chapter 2) thereby underlining the importance of its characterization.

1.5.3 Chapter 4

Levothyroxine sodium pentahydrate (LSP) is the standard treatment option for patients suffering from hypothyroidism. However, there is a limited understanding of the physical and chemical stability of LSP, leading to continued product recalls. The present work evaluated changes in the physical form of LSP under varying conditions of temperature and vapor pressure.

While LSP is used in marketed formulations, the existence of the drug in other states of hydration has been suggested. However, these have not been comprehensively studied and characterized. Our preliminary studies suggested that the dehydration of the pentahydrate resulted in a crystalline monohydrate with a different lattice structure and overall lattice “contraction” upon the loss of the four molecules of water. The potential for an increase in reactivity of levothyroxine, due to a change in its physical form, formed the motivation for this work.

Our work is driven by the following working hypotheses: (i) *The crystal structure of levothyroxine sodium monohydrate (LSM), different from that of the pentahydrate, explains its high reactivity.* (ii) *In a drug product environment, LSP dehydrates to a lower hydrate, possibly LSM.*

We had the following objectives. (i) Identify the conditions of formation and stability of the different hydrates of levothyroxine sodium. (ii) Understand the changes in crystal structure as the pentahydrate is dehydrated, first to the tetrahydrate and then to the monohydrate. (iii) Obtain the crystal structure of LSM. (iv) Use solid state nuclear magnetic resonance (ssNMR) to understand the changes in conformation during and following the solid state pentahydrate to monohydrate transition.

Our X-ray diffraction results indicate a change in the crystal structure of levothyroxine sodium upon dehydration of the pentahydrate salt to the monohydrate form (LSM) at 40°C/0% RH. LSM has a higher chemical reactivity than LSP. The formation of LSM in a drug product is therefore detrimental to its chemical stability. This work underlines the importance of comprehensive physical form characterization in preformulation and formulation development.

1.5.4 Chapter 5

The goal of our work is to systematically investigate and understand the influence of excipients and storage conditions on the physical and chemical stability of LSP in solid oral dosage forms (tablets). The physical stability is discussed in the context of the different hydration states of levothyroxine sodium and its disproportionation to form levothyroxine free acid. Our work is driven by the following working hypothesis: *(i) In presence of routine tableting excipients, LSP can undergo changes in its physical form, such as partial dehydration and salt disproportionation. The physical instability of LSP is governed by excipient properties such as hygroscopicity and surface acidity. (ii) The USP assay method is insensitive to physical instability of LSP in the drug product.*

We had the following objectives: (i) evaluate changes in the physical form of LSP when present as a mixture with excipients, (ii) quantify the chemical stability of LSP under accelerated stability testing conditions using both SXRD and HPLC and finally, (iii) assess the role of excipient properties (hygroscopicity and microenvironmental acidity) on the stability of LSP.

Our X-ray diffraction results indicate partial dehydration and salt disproportionation of LSP when formulated with hygroscopic and acidic excipients, respectively. Chemical stability of LSP in presence of routinely used tablet excipients was also evaluated using XRD and HPLC. LSP is susceptible to chemical decomposition in presence of ‘unbound’ water (hygroscopic excipients), acidic excipients and reducing sugars. Alkaline and hydrophobic excipients provide an avenue to design stable solid oral dosage form of the API. This work underlines the importance of systematic excipient compatibility testing in preformulation and formulation development.

CHAPTER 2

Chapter 2. The role of lattice disorder in water mediated dissociation of pharmaceutical cocrystal systems.*

*Reprinted with permission from Kaur, N., Duggirala, N. K., Thakral, S., & Suryanarayanan, R. (2019). Role of lattice disorder in water-mediated dissociation of pharmaceutical cocrystal systems. *Mol Pharm*, 16 (7), 3167-3177. Copyright (2019) American Chemical Society.

2.1 Synopsis

Our objective is to mechanistically understand the implications of processing-induced lattice disorder on the stability of pharmaceutical cocrystals. Caffeine–oxalic acid (CAFOXA) and dicalcium phosphate anhydrate (DCPA) were the model cocrystal (drug) and excipient, respectively. Cocrystal–excipient mixtures were milled for short times (≤ 2 min) and stored at room temperature (RT)/75% RH. Milling-induced lattice disorder was quantified using powder X-ray diffractometry and gravimetric water sorption. Milling for even 10 s resulted in measurable disorder and an attendant tendency of the solid to sorb water. This was followed by cocrystal–excipient interaction leading to dissociation. The proposed mechanism of cocrystal dissociation entails the following sequence: sorption of water by disordered regions, dissolution of CAFOXA and DCPA in the sorbed water, followed by proton transfer from the coformer (oxalic acid) to DCPA, and the formation of hydrates of caffeine and calcium oxalate. As such, CAFOXA is a robust cocrystal, stable even under elevated humidity conditions (RT/98% RH). However, in a drug product environment, routine pharmaceutical processing steps such as milling and compaction have the potential to induce sufficient disorder to render it unstable.

2.2 Introduction

Cocrystals are defined as “...solids that are crystalline single phase materials composed of two or more different molecular and/or ionic compounds generally in a stoichiometric ratio which are neither solvates nor simple salts. If at least one of the coformers is an API and the other is pharmaceutically acceptable, then it is recognized as a pharmaceutical cocrystal.”^{17,18,348,349}

Cocrystallization enables modification of the physicochemical and mechanical properties of an active pharmaceutical ingredient (API) without altering its pharmacological activity. This approach has improved the aqueous solubility and dissolution rate of several poorly soluble drugs including fluoxetine hydrochloride,¹⁹ nevirapine²⁰ and danazol.²¹ In compounds that may exist both as an anhydrate and as a hydrate (wherein water is incorporated in the crystal lattice), for example caffeine and theophylline, cocrystallization provides an avenue to control the solid form and hence,

improve the physical stability. It is also an effective strategy for altering the mechanical properties of an API, thereby aiding manufacture into tablet dosage forms.^{22,23} Finally, cocrystallization has enabled oral bioavailability enhancement. This was demonstrated with carbamazepine-saccharine cocrystals, which exhibited superior biopharmaceutical properties compared to the marketed carbamazepine formulation containing anhydrous carbamazepine.³⁵⁰ Some of the cocrystal products in the market are Depakote® (valproic acid-sodium valproate)²⁴, Odomzo® (sonidegib diphosphate)³⁵¹, Lexapro® (escitalopram oxalate-oxalic acid)²⁵, Entresto® (valsartan-sacubitril)²⁶, Steglatro™ (ertugliflozin-L-pyroglutamic acid)²⁷ and Suglat® (iproglifozin-L-proline).²⁸

Over the past two decades, significant progress has been made in the design and synthesis of pharmaceutical cocrystals.^{23,345-347} However, the stability of cocrystals, specifically their potential to undergo dissociation, has not been extensively explored. The impact of temperature²⁹ and water vapor pressure^{30,31} on cocrystal stability was recently investigated. Caffeine³² and theophylline³³ cocrystals were prepared with different dicarboxylic acids, and the effect of water vapor pressure on cocrystal stability was studied. The aqueous solubility of the cofomer and the propensity of the API to form a hydrate were reported to be key determinants of dissociation. Cocrystal stability can also be influenced by temperature. Eddleston *et al*²⁹ studied the effect of high temperature on the dissociation behavior of a 1:1 cocrystal of caffeine with theophylline. Since pharmaceutical processing can entail elevated temperatures and water vapor pressures, stability testing under these conditions provide insight into potential instabilities during dosage form manufacture.

The formulation and manufacture of a cocrystal as a solid dosage form (for the purpose of this discussion, tablets) necessitates the use of excipients and often includes several unit operations. It is therefore important to evaluate the potential impact of both API-excipient interactions and processing conditions on cocrystal stability. Cocrystals are typically sustained by non-covalent interactions such as hydrogen bonds. They may be susceptible to dissociation in the presence of competing excipients.³⁵² Duggirala *et al*³⁴ evaluated the impact of a range of pharmaceutical excipients on the stability of CAFOXA cocrystals. The model cocrystal system, in the absence of excipients, was stable even at elevated water vapor pressures. The authors proposed the dissociation to be a result of the reaction between oxalic acid (the cofomer) and ionic excipients. Recently, Koranne *et al*³⁵ investigated the stability of another reportedly robust cocrystal, theophylline-glutaric acid, in multiple prototype formulation compositions. Pronounced dissociation occurred in the presence of excipients with a high water sorption propensity. In a continuation of this work, the role of cofomer and excipient properties on the solid-state stability of theophylline cocrystals was investigated.³⁵³ In both theophylline and caffeine cocrystal systems,^{34,35} the solution mediated dissociation was believed to be initiated at the interface of cocrystal and excipient particles,

specifically regions with lattice defects. Disorder can be introduced in the API and excipients during pharmaceutical unit operations steps such as milling, mixing, granulation and compression. The disorder introduced on the particle surface is expected to be more pronounced than in the bulk. However, the impact of processing, and specifically the role of lattice disorder, on cocrystal stability was not investigated by the authors. In light of the potential destabilizing effect of lattice disorder, it is important to evaluate the combined effects of lattice disorder and excipients on cocrystal stability.

We were interested in systematically understanding the impact of processing-induced lattice disorder on cocrystal stability. We therefore evaluated the impact of milling, a routinely employed unit operation, on the dissociation of CAFOXA cocrystals. In our earlier investigation, when binary mixtures of CAFOXA and dibasic calcium phosphate anhydrate (DCPA) were ground with 30% w/w water, cocrystal dissociation was immediately evident.³⁴ However, the role of lattice disorder on cocrystal stability was not investigated in detail. In this study, lattice disorder was introduced in CAFOXA and DCPA by milling. In an effort to reflect actual pharmaceutical processing, the milling times were short (≤ 2 min). *We hypothesize that even short milling times can induce adequate lattice disorder to render cocrystal system unstable.* The “higher energy” of the disordered regions, both in CAFOXA and DCPA, are believed to be the sites for preferential sorption of water, the medium for the dissociation reaction.

In an industrial setup, an API and an excipient may be ‘co-processed’ necessitating studies on how this may impact the product performance.^{354,355} When solid mixtures are milled, the extent of lattice disorder in each phase is expected to be influenced by its properties as well as the mixture composition.^{34,40} In order to study the impact of comilling on cocrystal dissociation, CAFOXA and DCPA were mixed first and then milled together (‘comilled mixture’). Milling together may result in an increase in the inter-particulate contact area amongst materials. In a separate set of experiments, the cocrystals and DCPA were milled separately and then mixed (‘physical mixtures’). Thus, two processing steps, i.e. milling and mixing, were interchanged to monitor their impact on cocrystal dissociation behavior.

The overall goal of this work was to systematically study the impact of processing-induced lattice disorder on the stability of the model cocrystal system. The specific objectives were (i) to quantify lattice disorder as a function of milling time, (ii) establish the relationship between degree of lattice disorder and extent of cocrystal dissociation, and (iii) understand the influence of co-processing (CAFOXA and DCPA) on lattice disorder and consequently, dissociation.

2.3 Experimental section

2.3.1 Materials.

Caffeine (CAF, Sigma Aldrich), oxalic acid (OXA, Sigma-Aldrich) and dicalcium phosphate anhydrous (DCPA, Rhodia Pharma Solutions) were used as received. Caffeine-oxalic acid cocrystal (CAFOXA) cocrystals were prepared using the aqueous slurry method³² and characterized by powder X-ray diffractometry (XRD). The experimental and calculated diffraction patterns are shown in Supporting Information (Figure 2.10).

2.3.2 Preparation of binary mixtures.

For determining the role of DCPA on CAFOXA cocrystal stability, the two components were used at a ratio of 1:1 w/w. The powders were processed in two different ways. For the ‘comilled samples’, the binary (CAFOXA-DCPA) mixture was first mixed and then milled. Hence, both the formulation components were milled together. For the second sample set, termed as ‘physical mixture’ for the purpose of this discussion, the individual components were first milled (separately) and then mixed.

2.3.3 Water sorption analysis.

Water sorption and desorption data was collected using an automated water sorption analyzer (DVS-1000 Advantage, Surface Measurement Systems, Middlesex, U.K.). Approximately 10 mg of the powder was placed in a quartz sample pan and equilibrated at 0% RH (25°C) for 1 h under a nitrogen flow rate of 200 mL/min. The RH was then increased at 10% increments to 90% RH. At each RH value, if the mass change (dm/dt) was less than 0.001% in 15 min, attainment of equilibrium was assumed. The maximum hold time at each RH value was 4 h.

2.3.4 Differential scanning calorimetry (DSC).

A differential scanning calorimeter (model Q2000, TA Instruments) equipped with a refrigerated cooling accessory was used. The instrument was calibrated with indium. Between 2 and 5 mg of sample was hermetically sealed in an aluminum pan. All measurements were performed at a heating rate of 10°C/min under nitrogen purge (50 mL/min).

2.3.5 Thermogravimetric analysis (TGA).

A thermogravimetric analyzer (model Q50 TGA, TA Instruments) was used. Approximately 5 mg of the powder sample was placed and heated in an aluminum pan from RT to 300°C at a rate of

10°C/min with a dry nitrogen purge (75 mL/min). The TGA data were analyzed using the commercial software (Universal Analysis 2000, TA Instruments, New Castle, DE).

2.3.6 Powder X-ray diffractometry (XRD).

The powder samples were exposed to Cu K α radiation (40 kV and 40 mA) using a diffractometer (D8 ADVANCE; Bruker AXS, Madison, WI, USA) over an angular range of 5 - 35° 2 θ with a step size of 0.0196° and a dwell time of 0.5 sec. Data analysis was performed using commercially available software (JADE Materials Data, Inc., Livermore, CA).

For percent crystallinity measurements, scans were performed over an angular range of 2 - 70° 2 θ with a step size of 0.0196° and a dwell time of 0.5 sec. The position of knife-edge was adjusted to obtain diffraction patterns at low angular values (high d-spacings). For all X-ray measurements, the sample weight was kept constant. The instrumental contribution to peak broadening in diffraction patterns was accounted for using lanthanum hexaboride (SRM 660c, NIST) as standard. For samples milled for different time durations, the total diffracted intensity remained constant, whereas the crystalline intensity dropped with increasing milling time. The unmilled samples were assumed to be 100% crystalline. The total diffracted intensity is the integrated intensity over the angular range of 2 to 70 °2 θ . The crystalline intensity is obtained by subtracting the background and amorphous contributions from the total diffracted intensity.

For the *in situ* dissociation measurements, the X-ray sample cell was maintained at 75% RH (RT) using an external humidifier (saturated sodium chloride solution). The relative humidity and temperature in the sample cell was monitored by sealing one end of a digital humidity sensor (EK-H4, Sensirion AG, Switzerland) into the X-ray sample cell, while the other end of the sensor was connected through an interface to a computer. This enabled us to continuously measure the headspace RH and temperature experienced by the sample. The intensity of the 10.6° 2 θ peak of caffeine hydrate (one of the decomposition products of cocrystal dissociation) was used to quantify cocrystal dissociation. A standard curve, relating 10.6° 2 θ peak of caffeine hydrate with its concentration in physical mixtures containing caffeine hydrate, calcium oxalate (another decomposition product) and CAFOXA (reactant) was generated, and used to quantify dissociation.

2.3.7 Cryomilling.

Cryomilling (or cryogenic milling) was performed using SPEX SamplePrep, Model 6750 freeze mill. A stainless steel impactor is driven back and forth against the end plugs of the cylindrical polycarbonate vial (SPEX SamplePrep #6751 vials) in the grinding chamber.³⁵⁶ The sample vial was submerged in liquid nitrogen throughout the milling process to circumvent thermal transitions.

A constant sample weight of one gram was loaded into the vial each time and milling was performed for predetermined time durations. The samples were milled for 10, 30, 60 and 120 sec at a constant milling rate of “10” (i.e. 20 impacts per sec). For milling times longer than one min, multiple cycles were used wherein the samples were milled for 1 min followed by cooling for 2 min. The pre-cooling time for all the samples was kept constant at 4 min. Following milling, the vials were equilibrated at room temperature in a desiccator containing anhydrous calcium sulphate.

2.3.8 Particle size distribution.

A laser diffraction particle analyzer (Microtrac Bluewave, with an in-line ultrasonicator) was used. The samples were suspended in Isopar-G and circulated through the optical cell. Data analysis was done using Microtrac Flex, which is based on algorithms utilizing Mie and modified Mie calculations for spherical and non-spherical materials, respectively. The results are represented as mean (volume-weighted) particle size with standard deviation (n=3).

2.3.9 Surface area.

BET surface area analysis was performed for the samples at -195.85°C with an equilibration interval of 10 sec. The ramp rate used for the study was 10°C/min and the duration of the run was 120 min.

2.4 Results and discussion

2.4.1 Baseline characterization.

Caffeine-oxalic acid (2:1) cocrystals (CAFOX). The X-ray diffraction (XRD) pattern of the cocrystal was superimposable on the calculated pattern from the Cambridge Structural Database (CSD; GANXUP). The thermal behavior, characterized by DSC and TGA, was in excellent agreement with literature.³⁴ TGA heating curve and its derivative plot exhibited no measurable weight loss up to 150°C (Supporting Information; Figure 2.11 and Figure 2.12). There was negligible water uptake (< 0.2% w/w) over the RH range of 0 to 90% (25°C). The sorption-desorption profiles are provided in Supporting Information; Figure 2.14.

Dibasic calcium phosphate, anhydrate (DCPA). The XRD pattern was in excellent agreement with literature reports.^{357,358} DCPA was characterized by intense peaks at 26.4 and 30.2° 2θ. Thermal analysis revealed degradation at elevated temperatures (> 400°C) with no evidence of melting.³⁵⁹ The water sorption and desorption profiles overlapped (Supporting Information; Figure 2.11, Figure 2.13 and Figure 2.14).³⁶⁰

2.4.2 Lattice disorder.

Lattice disorder refers to a disruption of the long range order of a crystalline solid or reduction in the crystallinity of a compound. Two types of disorders can be introduced into a perfectly crystalline solid i.e. thermodynamic disordering and kinetic disordering. A perfectly crystalline material possesses the three long range symmetry operators i.e. translational, orientational and conformational order. The loss of one or more of these symmetry operators leads to thermodynamic disordering in the material. On the other hand, kinetic disordering is the processing-induced disorder which refers to the gradual loss of sample crystallinity and generation of amorphous material.³⁶¹⁻³⁶⁵

Milling is known to cause lattice disorder, manifested as a decrease in the degree of crystallinity.^{366,367} However, in many previous investigations, milling was carried out for long time periods, sometimes extending to h.^{40,364} Since milling times tend to be quite short in actual pharmaceutical processing, our studies were restricted to very short processing times (≤ 120 sec). Moreover, high impact milling can increase the sample temperature.^{368,369} The surface of the particles which come in direct contact with the steel impactor can experience a rise in temperature.³⁷⁰⁻³⁷² This increase can be sufficient to cause physical as well as chemical transformations.⁴⁰ Cooling the samples with liquid nitrogen will minimize the risk of thermal effects.

Milling CAFOXA, for up to 2 min, did not cause a pronounced change in the XRD pattern (Figure 2.1A) except for a decrease in the intensity of the low angle peaks ($2\theta < 20^\circ$). In case of DCPA, no effect of milling could be discerned (Supporting Information; Figure 2.15). On the other hand, when a binary mixture of CAFOXA and DCPA (1:1 w/w) was milled (hereafter referred to as 'comilled' mixtures), even the shortest milling time (10 sec), resulted in a decrease in the intensity of the CAFOXA peaks. This decrease was measurable for the low angle peaks (Figure 2.1B and Supporting Information; Figure 2.16).

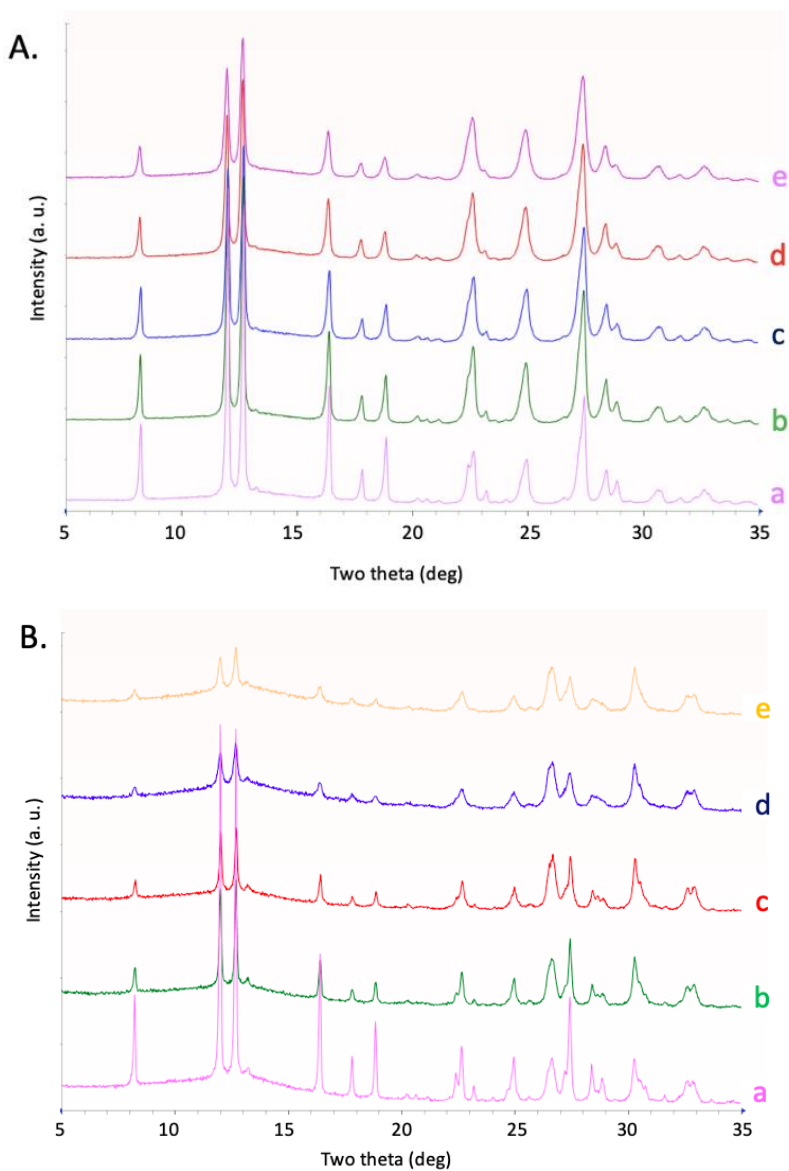


Figure 2.1. X-ray diffraction patterns of (A) milled CAFOXA and (B) comilled mixture of CAFOXA and DCPA (1:1 w/w). The milling times were: (a) 0, (b) 10, (c) 30, (d) 60, and (e) 120 sec.

The effect of milling on the crystallinity was determined by two approaches. The total diffracted intensity, i.e. the XRD pattern over the angular range of 3 to 70° 2 θ , provided a direct measure of the % crystallinity. The ‘as is’ cocrystals and DCPA were assumed to be 100% crystalline (reference standards). Therefore, the reported crystallinity values are with respect to the unmilled materials. Milling caused a measurable decrease in the crystallinity of CAFOXA. There appeared to be a linear decrease in crystallinity as a function of milling time for up to 60 sec. In contrast, the crystallinity of DCPA was unaffected by milling. The comilled systems were much more sensitive

to milling time. The decrease in crystallinity was most pronounced at the shorter milling times (Figure 2.2A). X-ray line broadening can be brought about, both by a reduction in crystallinity, and a decrease in crystallite size (typically < 1 micron). The particle size values are given in supporting information (Supporting Information; Figure 2.17). Milling for 10 sec caused a decrease in particle size of both CAFOXA and DCPA. However, longer milling times, caused a measurable but only a small change in the size of DCPA particles. In case of CAFOXA, the particle size seemed to be unaffected by milling times longer than 10 sec. The effect of milling time on particle size could also be discerned from surface area measurements. The comilled mixture milled for 120 sec, exhibited a very small (< 5%) increase in surface area (Supporting Information; Table 2.1). Therefore, the observed effects at longer milling times (milling time > 10 sec) could be attributed predominantly, if not completely, to lattice disorder.

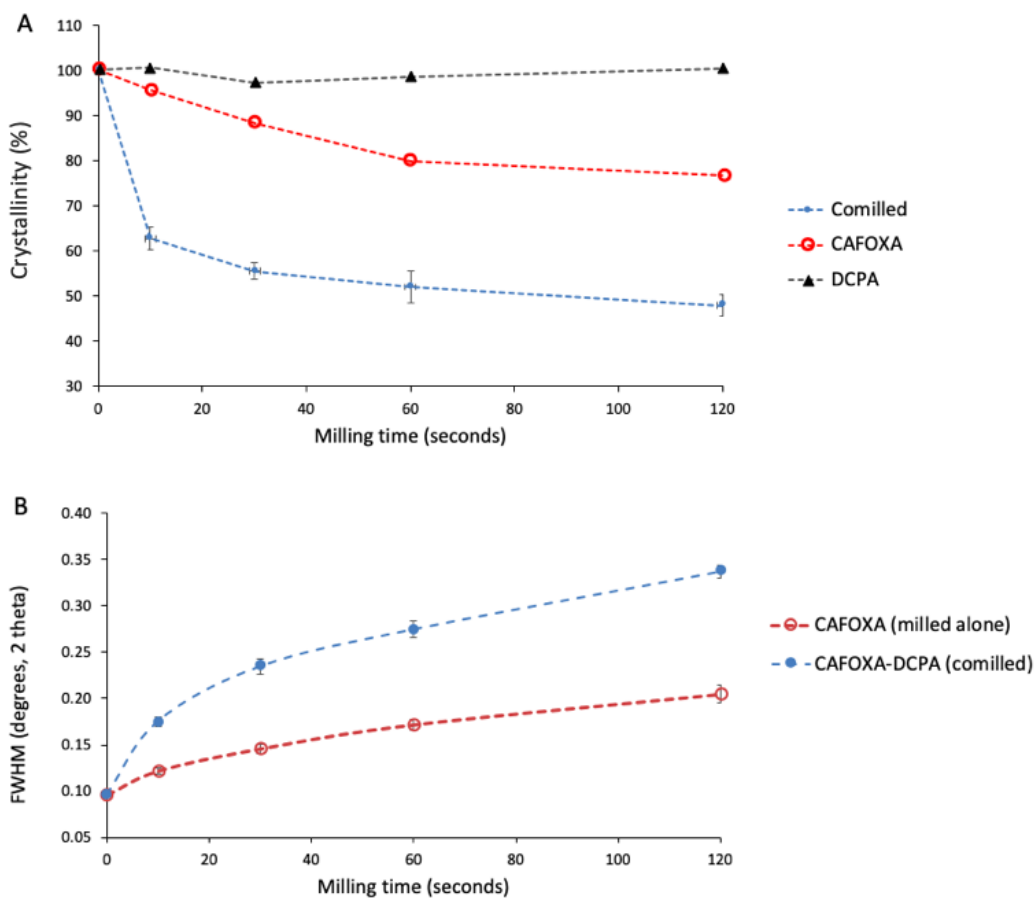


Figure 2.2. (A) Crystallinity (%) as a function of milling time of CAFOXA, DCPA and the comilled mixture of CAFOXA and DCPA. (B) The effect of milling time on the width of a representative diffraction peak of CAFOXA ($2\theta=16.4^\circ$) milled alone and with DCPA (comilled). The peak width is represented as full width at half maximum (FWHM in degrees,

20). The lines are drawn to assist in visualization of trends. Error bars represent standard deviation (n=3).

The width of the X-ray peaks, measured as full width at half maximum (FWHM), provided another measure of lattice disorder (Figure 2.2B). While the cocrystals milled alone exhibited an increase in FWHM as a function of milling time, this effect was more evident in the comilled mixtures. Thus, in the presence of DCPA, the effect of milling on the crystallinity of CAFOXA was amplified. No peak broadening was observed in the DCPA peaks, milled alone or comilled (Supporting Information; Figure 2.15).

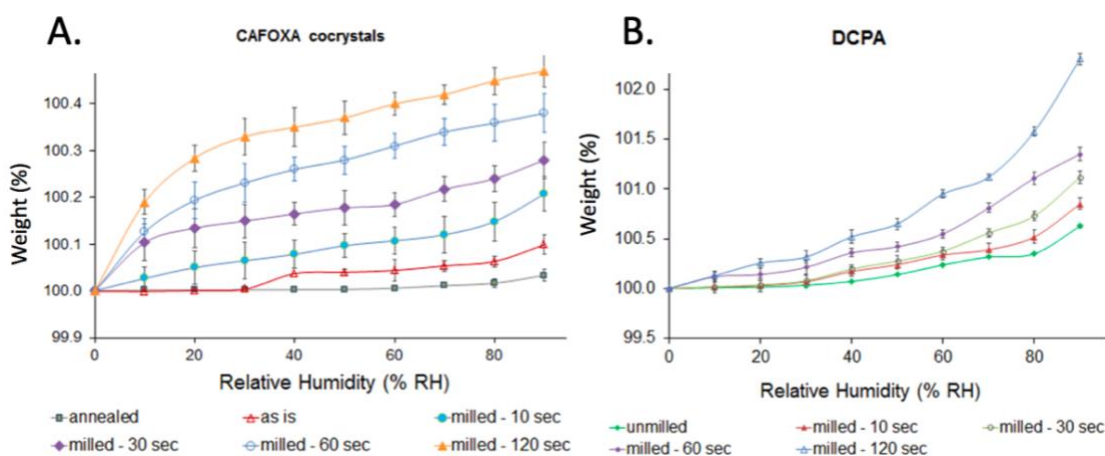


Figure 2.3. Gravimetric water sorption behavior of (a) CAFOXA cocrystals, and (b) DCPA (Mean \pm SD; n=3).

Water sorption behavior is an indirect but very sensitive indicator of lattice disorder. Crystalline solids will only adsorb water - a surface phenomenon and the amount adsorbed will be a function of the surface area of the solid. In case of partially crystalline materials, in addition to adsorption, there will also be sorption of water by the amorphous regions. The amount sorbed will be a function of the amorphous content of the sample and occurs principally via hydrogen bond interactions.³⁷³⁻³⁷⁵ As expected, the highly crystalline unmilled cocrystals exhibited a very small weight gain of 0.02% at 80% RH (Figure 2.3a). On the other hand, in the milled cocrystals, the weight gain increased as a function of milling time. Similar trends were observed in both DCPA (Figure 2.3b) and comilled mixtures (Figure 2.4).

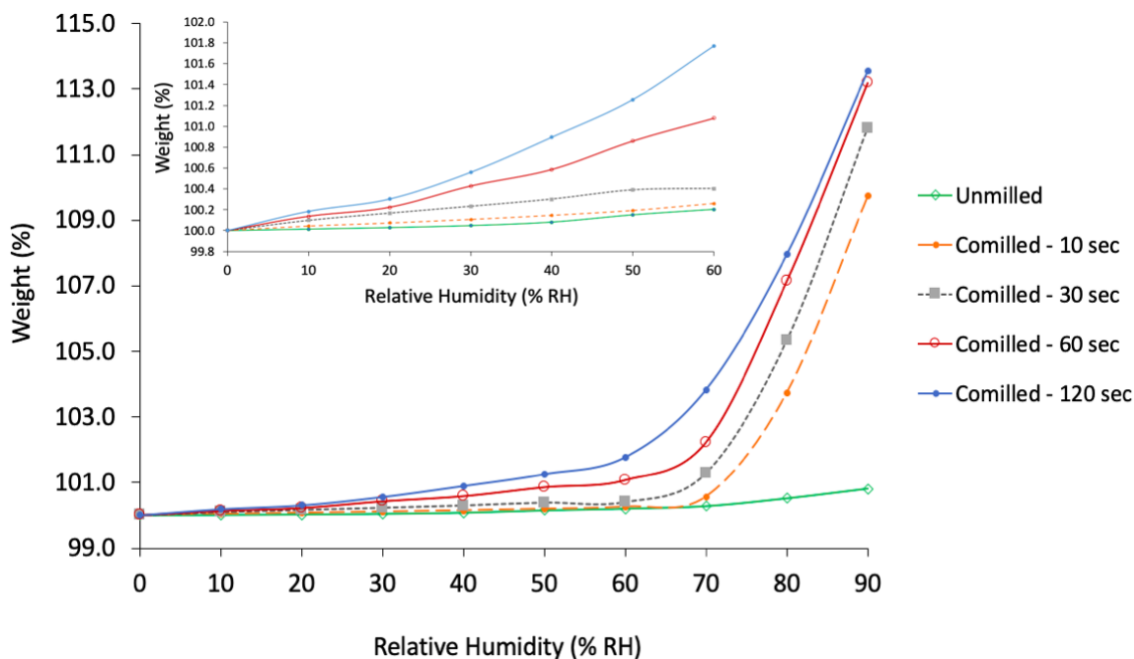


Figure 2.4. Gravimetric water sorption of comilled (CAFOXA-DCPA) mixtures (Mean \pm SD; n=3). The inset shows data at RH \leq 60%.

In case of DCPA, while there was no discernible reduction in crystallinity based on XRD measurements, the water sorption results suggested an increase in lattice disorder as a function of milling time. Water sorption is known to be a very sensitive indicator of lattice disorder and is particularly well suited to discern very early (first) evidence of disorder. For example, the disorder induced in completely crystalline sucrose by milling it for 5 sec became evident from water sorption data.^{376,377}

When CAFOXA and DCPA were comilled, the crystallinity of CAFOXA was influenced, both by the milling process and the presence of DCPA (Figure 2.2). The crystallinity of DCPA may also be affected similarly. The effect of milling in presence of the second component could be discerned from the difference in water sorption behavior between the comilled mixture and the individually milled components (CAFOXA and DCPA). At RH values up to 50%, the behavior of the comilled mixtures was comparable to the individual components (weighted average of the sorption behavior of CAFOXA and DCPA (Supporting Information, Figure 2.18). However, when the RH values were progressively increased (\geq 70%), the comilled mixtures exhibited an abrupt weight gain as a function of RH. These results suggest that factors other than crystallinity are likely to be responsible for the observed increase in water sorption. This was investigated in detail in the section dealing with co-processing.^{360,378}

2.4.3 Cocrystal dissociation.

As mentioned earlier, a major consequence of the lattice disorder induced by milling was the strong water sorption propensity of the system. Water sorption by the disordered lattice regions will lead to plasticization (i.e. T_g lowering), increase the molecular mobility and hence, the reactivity. When the binary mixture was milled for 10 sec and stored at RT/75% RH for 24 h, cocrystal dissociation was evident from XRD results (Figure 2.5a). Characteristic peaks of caffeine hydrate and calcium oxalate hydrates (monohydrate, dihydrate and trihydrate), all products of cocrystal dissociation, were observed^{373,374} (Figure 2.5a). The intensities of the product phases suggest substantial dissociation in 24 h.

Crystalline solids when stored at $RH > RH_0$ (water vapor pressure of its saturated solution) are known to dissolve in the sorbed water. The water vapor pressure of a saturated solution of CAFOXA (RH_0) at RT is not known. The RH_0 of DCPA, in light of its very low aqueous solubility, is expected to be close to 100%. However, the introduction of lattice disorder is known to facilitate water sorption at $RH < RH_0$.³⁷⁹ Therefore, at the surface of milled CAFOXA and DCPA particles, the sorbed water can “dissolve” in the disordered regions of both CAFOXA and DCPA. This water can now act as a medium and facilitate the reaction between CAFOXA and DCPA.^{37,38}

It is instructive to consider the “microenvironment” of disordered DCPA containing sorbed water. The “acidity” of excipients has been represented as either solution/suspension pH or pH_{eq} .^{380,381} The slurry pH of DCPA was reported to be ~ 5.5. Since the cocrystal is composed of a neutral API and an acidic cofomer (oxalic acid; pK_a values of 1.3 and 4.3 at 25°C),³⁴ only the ionization behavior of the latter would be pH dependent. Thus the microenvironment in the vicinity of DCPA would favor oxalic acid ionization and hence drive cocrystal dissociation. The water mediated transfer of protons from oxalic acid to hydrogen phosphate anion (HPO_4^-), is expected to result in the formation of calcium oxalate and phosphoric acid (Figure 2.5b). XRD provided evidence of all the phases except phosphoric acid (Figure 2.5a). The caffeine formed, following the dissociation of CAFOXA, existed as a hydrate. This is its expected physical form at RT/75% RH.^{34,382}

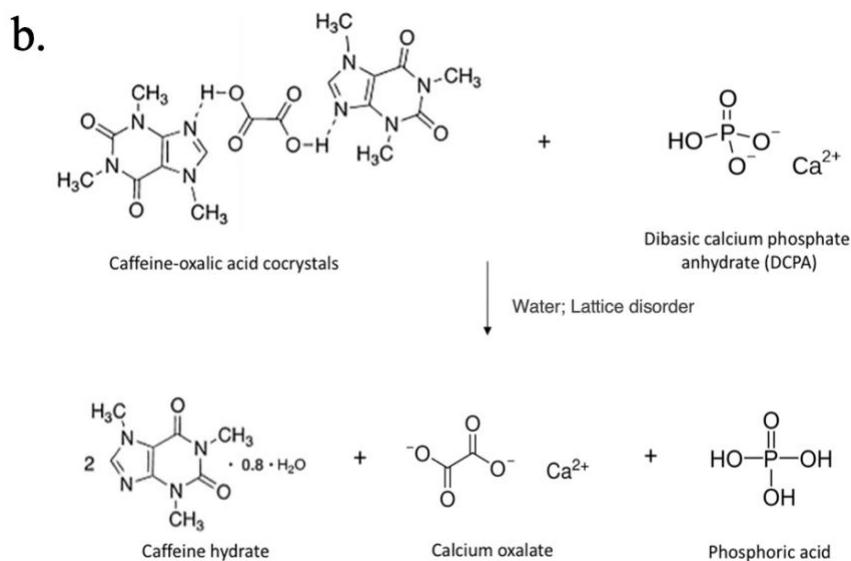
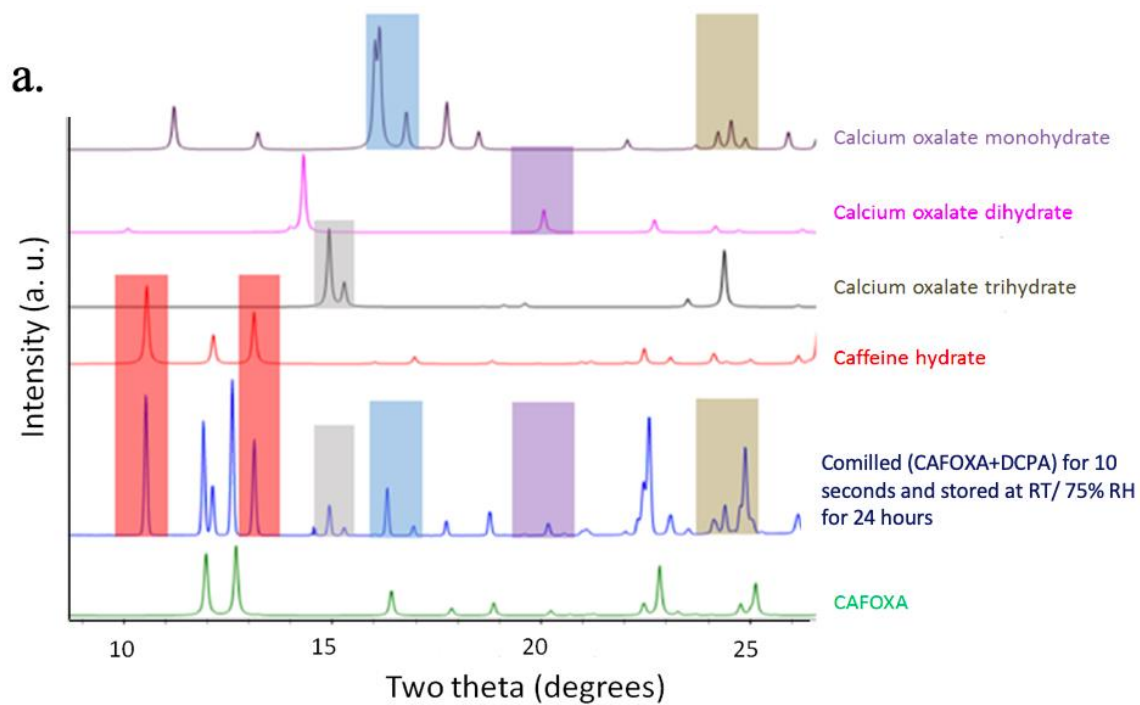


Figure 2.5. (a) X-ray diffraction patterns of a CAFOXA-DCPA (1:1 w/w) mixture comilled for 10 sec, and stored at RT/75% RH for 24 h. Characteristic peaks of possible decomposition products are highlighted. (b) Proposed mechanism of water mediated CAFOXA cocrystal dissociation in the presence of DCPA at RT/75% RH.

2.4.4 Experimental controls.

The roles of sorbed water, processing and excipient were evaluated using the following controls. (1) Comilled mixture (120 sec) stored at RT/0% RH. (2) ‘As is’ cocrystals milled for 120 sec and stored at RT/75% RH. (3) Physical mixture of ‘as is’ unmilled cocrystal and excipient stored at RT/75% RH. In all three systems, stored for up to a month, there was no evidence of cocrystal dissociation (no evidence of caffeine anhydrous/ hydrate formation).

The first control establishes the role of water in mediating the dissociation reaction. Milling (second control), as expected, caused a broadening of the XRD peaks of CAFOXA. However, on storage, there was a progressive decrease in peak width revealing recrystallization. The disordered surface regions are expected to sorb water. Water acts as a plasticizer, increases molecular mobility and facilitates recrystallization (Figure 2.6). This control established the role of DCPA in cocrystal dissociation. The lattice disorder caused by milling and the water sorption on storage at 75% RH are two conditions necessary for dissociation. However, the dissociation reaction could not proceed in the absence of the second reactant (DCPA). CAFOXA cocrystals were reported to be stable, even after slurring in water for 24 h.³⁰ The stability of the unmilled physical mixture (third control), highlighted the influence of milling induced lattice disorder on cocrystal dissociation. In the unmilled system, storage at 75% RH caused negligible water sorption. As pointed out earlier, highly crystalline CAFOXA and DCPA are not expected to sorb water at 75% RH. In the absence of sorbed water, the medium for the dissociation reaction is absent, and consequently the system is stable.

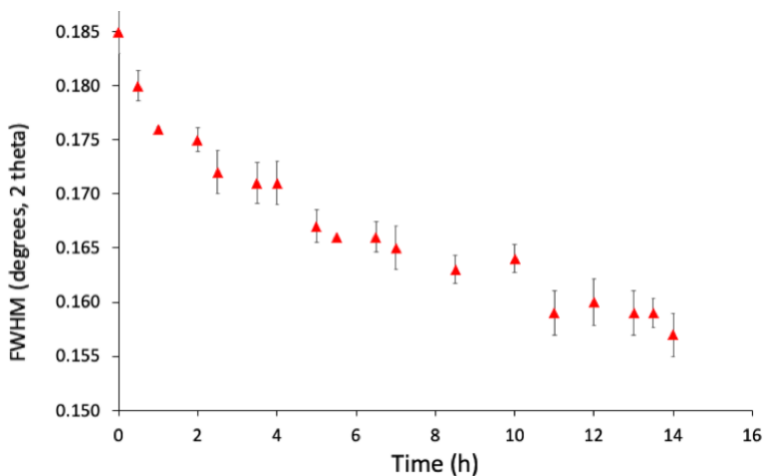


Figure 2.6. The effect of storage on the width of a representative diffraction peak of CAFOXA ($2\theta=16.4^\circ$). The peak width is represented as full width at half maximum (FWHM in degrees, 2θ). CAFOXA was milled for 120 sec and stored at RT/75% RH. Error bars represent standard deviation (n=3).

2.4.5 Impact of co-processing on cocrystal dissociation.

When the cocrystals and DCPA were milled separately (each for 120 sec) and then mixed ('physical mixture'), storage at RT/75% RH caused measurable dissociation in 10 h (Figure 2.7). However, when the comilled (the two components mixed and then milled for the same duration) sample was subjected to the same experiment, the dissociation observed was much more pronounced (Figure 2.9). The reduction in crystallinity following comilling was much higher than in the physical mixture (Figure 2.2). Moreover, milling together is expected to result in an increase in the inter-particulate contact area amongst materials.

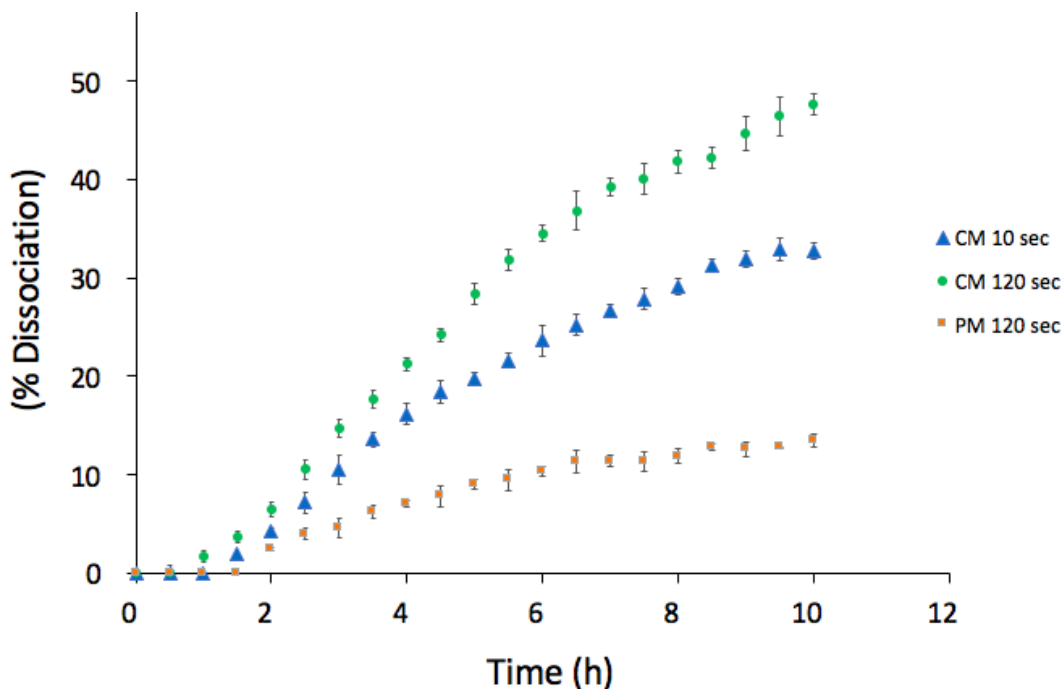


Figure 2.7. Dissociation (expressed in %) of CAFOXA following storage at RT/75% RH. A physical mixture of CAFOXA and DCPA (1:1 w/w) was comilled either for 10 (CM 10 sec) or 120 (CM 120 sec) sec. CAFOXA and DCPA were individually milled for 120 sec and mixed (PM 120 sec). Percent dissociation for comilled and physical mixtures maintained at RT/75% RH in an X-ray holder for 10 h. For details on the calculation of percent dissociation, refer to Supporting Information, Figure 2.19.

The water sorption behavior of the comilled and the physical mixtures was compared following storage under two conditions: RT/50% RH and RT/75% RH. As discussed in the section on lattice disorder, water sorption by the comilled mixtures at 50% RH resulted in a weight gain that was comparable to that of the separately milled components (Supporting Information, Figure 2.18). Though comilling resulted in higher lattice disorder than in the physical mixtures, this did not

translate to a substantial difference in the amount of sorbed water. At this RH, only a small amount of water was sorbed, which was insufficient to mediate cocrystal dissociation.

Upon exposure to 75% RH, the amount of water sorbed was adequate to mediate the dissociation reaction. Cocrystal dissociation could be inferred from the appearance of caffeine hydrate peak (Figure 2.8). Since comilling resulted in higher overall lattice disorder (discussed earlier, Figure 2.2), the amount of water sorbed is expected to be higher than in the physical mixtures. However, the difference in water sorption behavior between these differently processed samples, became very pronounced at $RH \geq 70\%$. Thus, factors other than lattice disorder likely play a role. The increased inter-particulate contact brought about by comilling, appears to facilitate the dissociation reaction. This is evident from the much higher peak intensity of caffeine hydrate in this system (Figure 2.8a), reflecting increased dissociation (Figure 2.7).

The dissociation reaction would be followed by additional water sorption. This is because the products of the dissociation reaction, caffeine hydrate and calcium oxalate hydrates, incorporate water in their lattices. The stoichiometric water content in the four hydrates- caffeine hydrate, calcium oxalate monohydrate, calcium oxalate dihydrate and calcium oxalate trihydrate are approximately 7, 12, 22 and 27% w/w respectively. The difference in the water sorption behavior between the comilled and physical mixture (milling for 120 sec) could therefore be attributed to the differences in the extent of cocrystal dissociation in these two systems.

2.4.6 Impact of lattice disorder on cocrystal dissociation.

The effect of comilling time on the dissociation behavior warranted detailed consideration. Comilling for only 10 sec brought about substantial instability (Figure 2.7). Milling for a much longer time period of 120 sec, caused only a marginal increase in cocrystal dissociation. We had earlier observed that a short milling time of 10 sec had the most pronounced impact on lattice disorder. These results have significant practical implications. It is evident that: (i) even very short processing times, can profoundly impact the lattice disorder, with implications on solid form stability, and (ii) highly ordered lattices (close to 100% crystalline; 'as is' CAFOXA and DCPA), appear to be most sensitive to processing. Once disorder is induced, further decrease in crystallinity appears to require longer processing times.

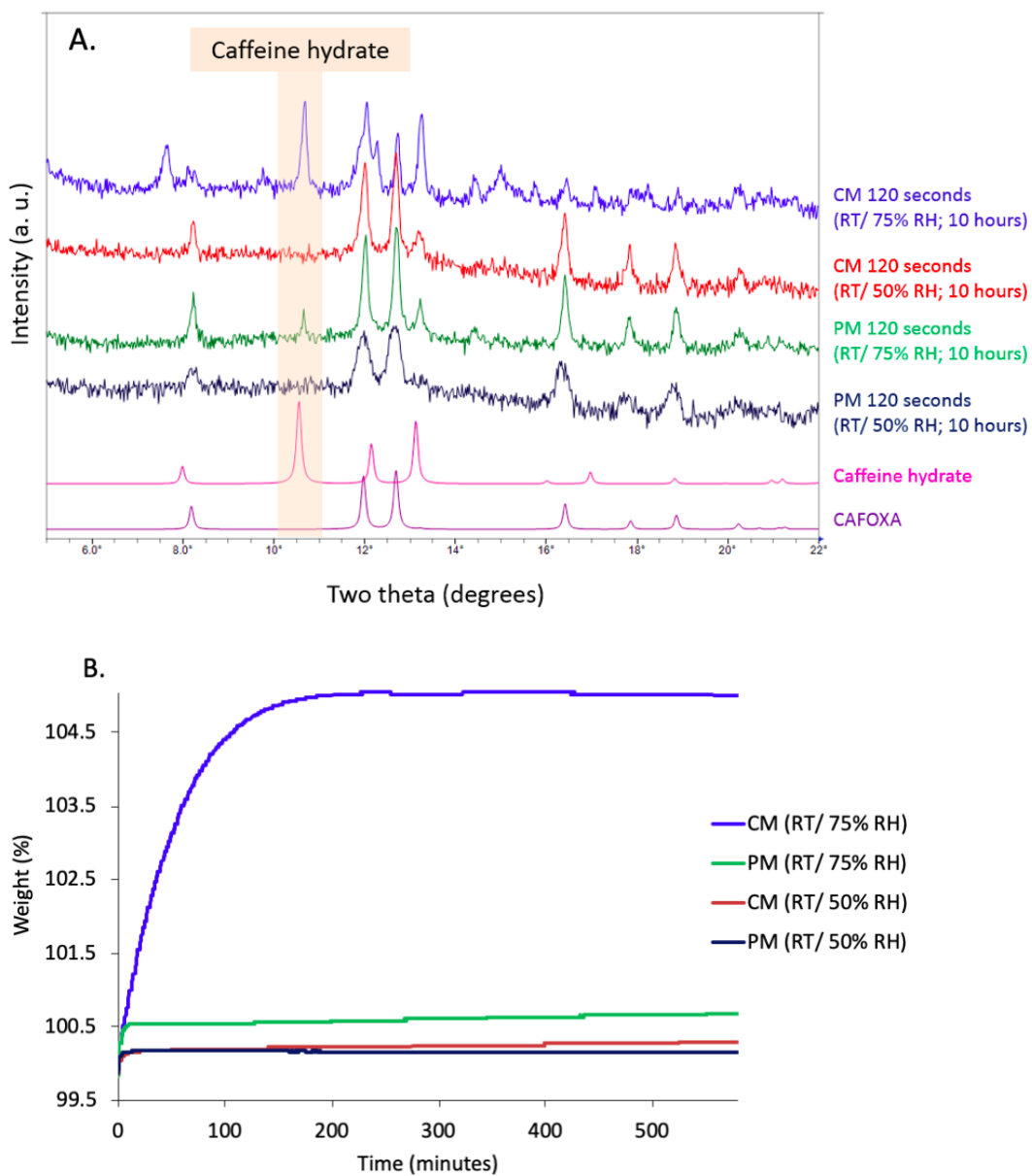


Figure 2.8. (A) X-ray diffraction patterns of CAFOXA and DCPA, individually milled and then mixed (PM), or comilled (mixed and milled together). The milling time was 120 sec and the mixtures were stored either at RT/50% RH or RT/75% RH for 10 h. The XRD patterns of CAFOXA (reactant) and caffeine hydrate (product) are also provided. (B) Water sorption kinetics of these mixtures at 50 or 75% RH (25°C).

2.5 Significance

In recent years, there have been significant advancements in the design and synthesis of pharmaceutical cocrystals, providing a new avenue to tailor the physicochemical, mechanical, and in several instances, the biopharmaceutical properties of drugs.³⁴⁹ Formulating a cocrystal into a dosage form (in this context, a solid formulation) will likely entail multiple unit operations such as milling, granulation and compaction. In many of these steps, the drug will be co-processed with one or more excipients. Mechanical stress, experienced during pharmaceutical processing, has resulted in physical transformations of the API.^{366,367,383-385} Such transitions can have an impact on the biopharmaceutical performance of the final dosage form.

We have evaluated the impact of realistic processing conditions (no longer than 2 min of milling) on crystallinity and subsequently, cocrystal stability. Even a very short milling time of 10 sec resulted in a measurable lattice disorder, and more importantly, rendered the system unstable leading to cocrystal dissociation. The disordered solids had a high propensity to sorb water, and we postulate that the drug-excipient interaction leading to cocrystal dissociation occurred in the sorbed water. The reaction was brought about by an interplay of three factors: (i) disorder (processing), (ii) water (ubiquitous) and (iii) excipient (formulation). Thus, this work highlights the potential for routine processing steps and a widely used excipient to facilitate the dissociation reaction. CAFOXA has been widely reported to be a robust cocrystal. However, transitioning this into a stable solid dosage form will require a careful consideration of the processing conditions and formulation composition.

It is also instructive to compare cocrystal dissociation with salt disproportionation. In cocrystals, since the API is non-covalently linked to the coformer, the presence of excipients with “competing” functional groups can lead to dissociation. Processing-induced lattice disorder can dramatically increase the reactivity and accelerate cocrystal dissociation. In case of salt formulations, the disproportionation propensity was influenced by the alterations in microenvironmental acidity brought about by the excipient.³⁸⁶ If we compare cocrystals to salts, one can argue that, cocrystals will pose formulation challenges (hydrogen bonds in cocrystals versus ionic bonds in salts).

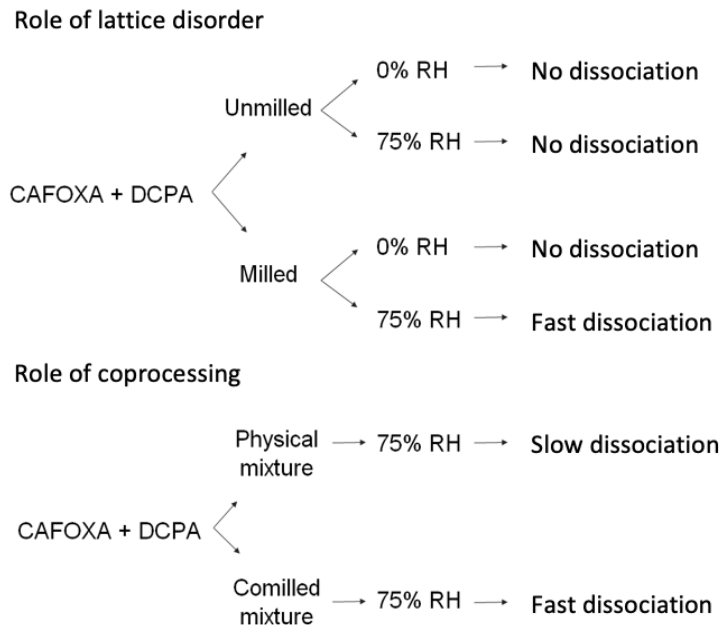


Figure 2.9. Flow chart highlighting the role of water, lattice disorder (induced by milling) and inter-particulate contact area on cocrystal dissociation.

Mitigation strategies. Lattice disorder, by enabling water sorption, sets the stage for the cocrystal-excipient interaction leading to dissociation. Thus, stability can likely be conferred by preventing lattice disorder. However, this is an unrealistic expectation, from the perspective of dosage form manufacture. If annealing is practically feasible, it can serve as a stabilization strategy. Careful control of the water vapor pressure may also prevent dissociation. The other mitigation strategies were discussed earlier.³⁵³ Hydrophobic excipients can potentially be used to coat, either the API or excipient particles, so as to serve as a barrier to water sorption.³⁸⁷ Alteration in microenvironmental pH, through the use of pH modifiers, has been observed to be effective. Similarly, the use of neutral excipients may also serve as a suitable strategy to mitigate cocrystal dissociation.³⁵³

2.6 Conclusions

Milling induced lattice disorder resulted in sufficient water sorption so as to mediate the cocrystal-excipient interaction, leading to dissociation of caffeine-oxalic acid (CAFOXA) cocrystals. In the absence of excipient (DCPA), the cocrystals were robust and withstood routine processing (milling) as well as exposure to elevated water vapor pressures. In the presence of excipient, while the unmilled powder mixtures were stable to elevated RH (75% at RT), lattice disorder induced by milling for just 10 sec resulted in a pronounced dissociation. Low levels of lattice disorder induced during routine processing steps in a drug product environment can lead to cocrystal instability.

2.7 Supporting information

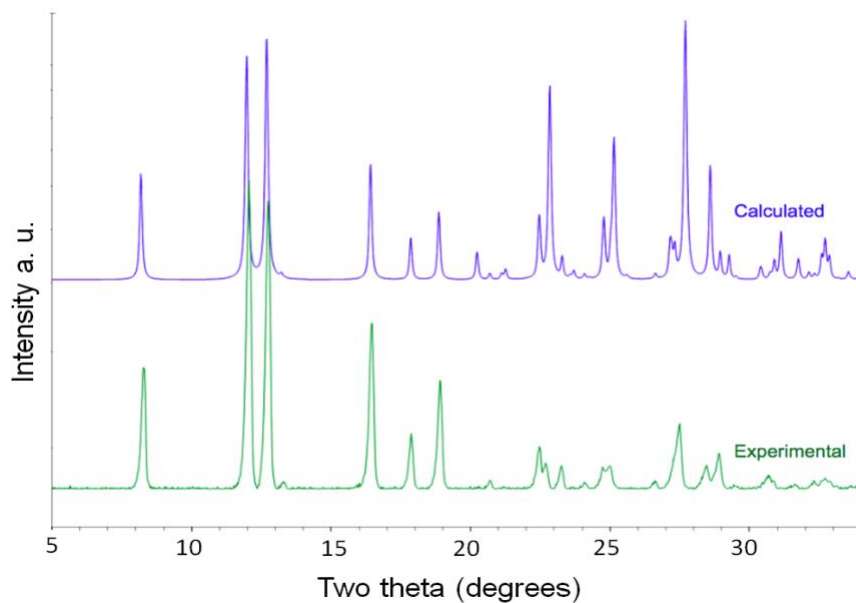


Figure 2.10. Experimental and calculated X-ray diffraction patterns of CAFOXA. The calculated pattern was obtained from the CSD database.

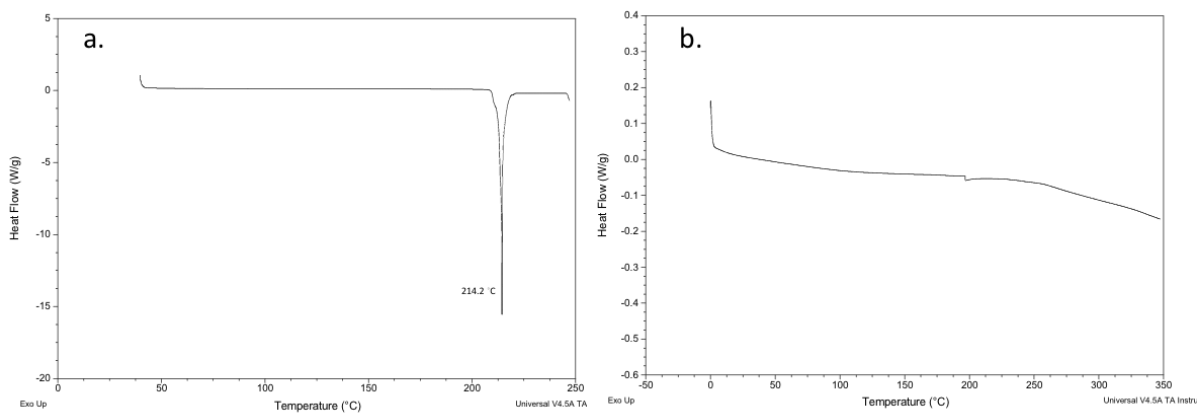


Figure 2.11. DSC heating curves of (a) CAFOXA and (b) DCPA. The samples were heated in hermetically sealed pans.

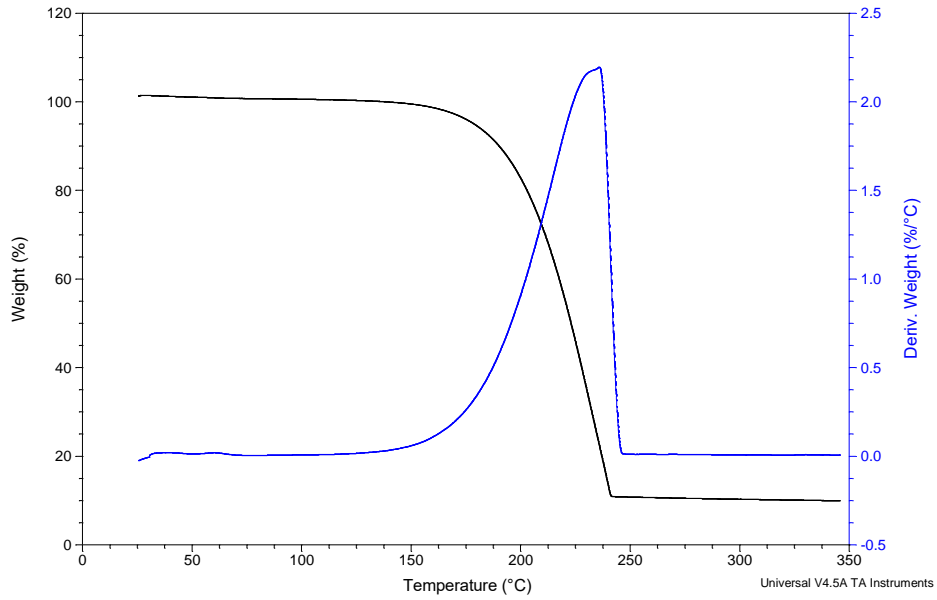


Figure 2.12. TGA and derivative (right y-axis) TGA heating curves of CAFOXA.

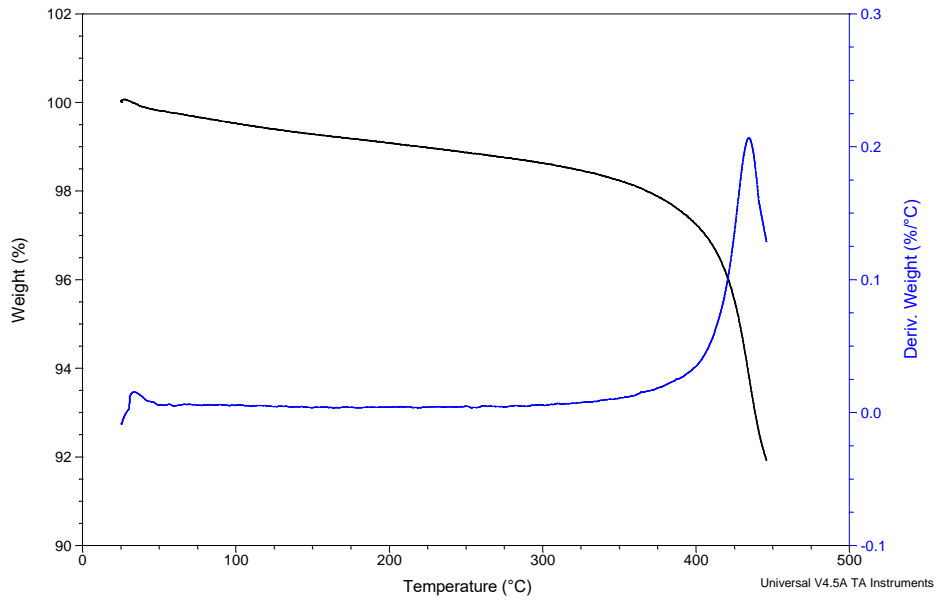


Figure 2.13. TGA and derivative (right y-axis) TGA heating curves of DCPA.

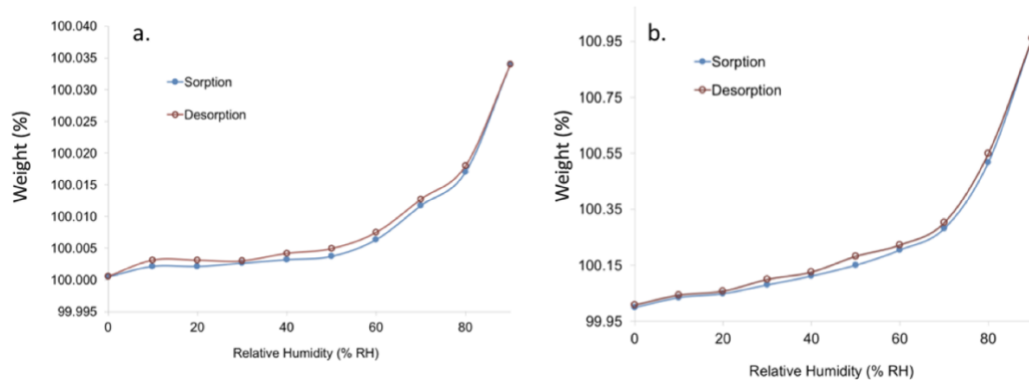


Figure 2.14. Water sorption and desorption curves of (a) CAFOXA and (b) DCPA at 25°C.

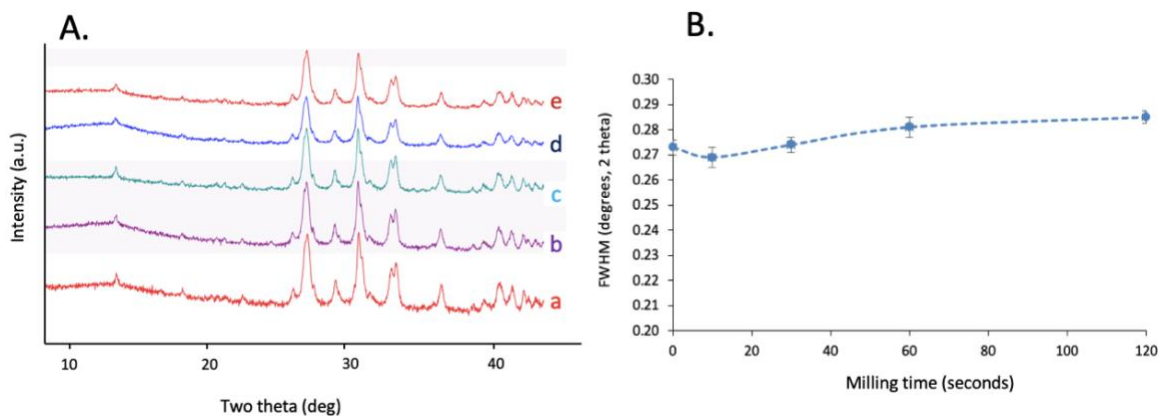


Figure 2.15. (A) X-ray diffraction patterns of DCPA samples milled for (a) 0, (b) 10, (c) 30, (d) 60 and (e) 120 sec. (B) The effect of milling time on the width of a representative diffraction peak of DCPA ($2\theta = 26.4^\circ$). The peak width is represented as full width at half maximum (FWHM in degrees, 2θ). Error bars represent standard deviation ($n=3$).

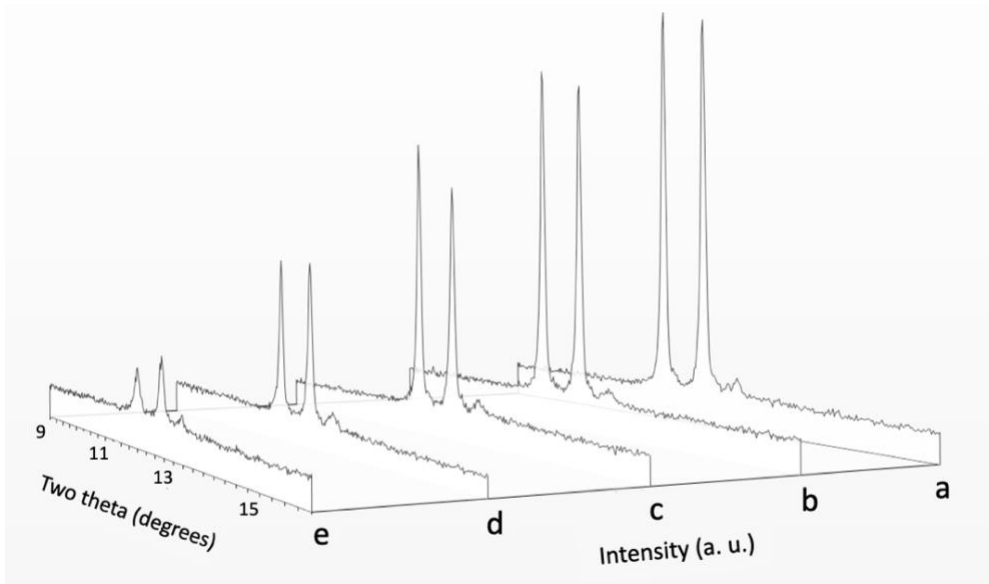


Figure 2.16. Overlay of X-ray diffraction patterns of comilled CAFOXA cocrystals. The milling times were (a) 0, (b) 10, (c) 30, (d) 60 and (e) 120 sec. The diffraction patterns were offset to assist in visualizing the peak intensities.

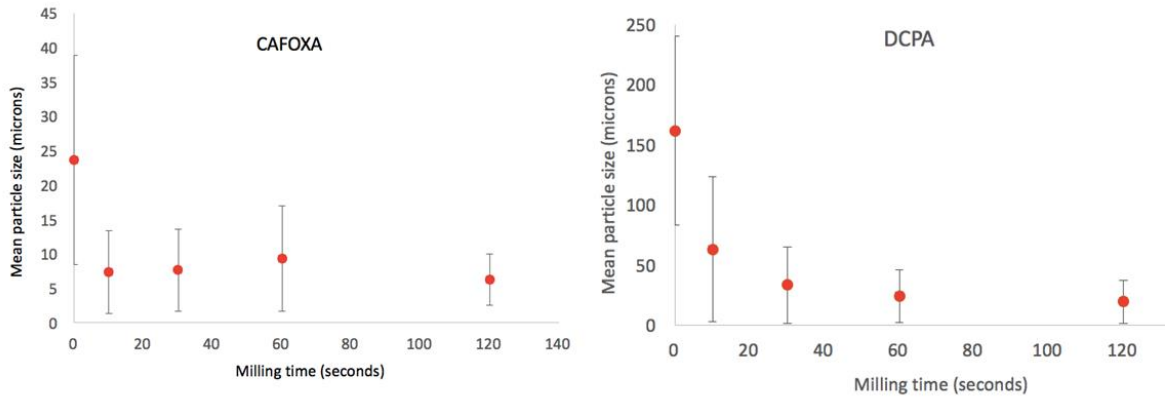


Figure 2.17. Mean particle size of unmilled and milled CAFOXA and DCPA (Mean \pm SD; n=3).

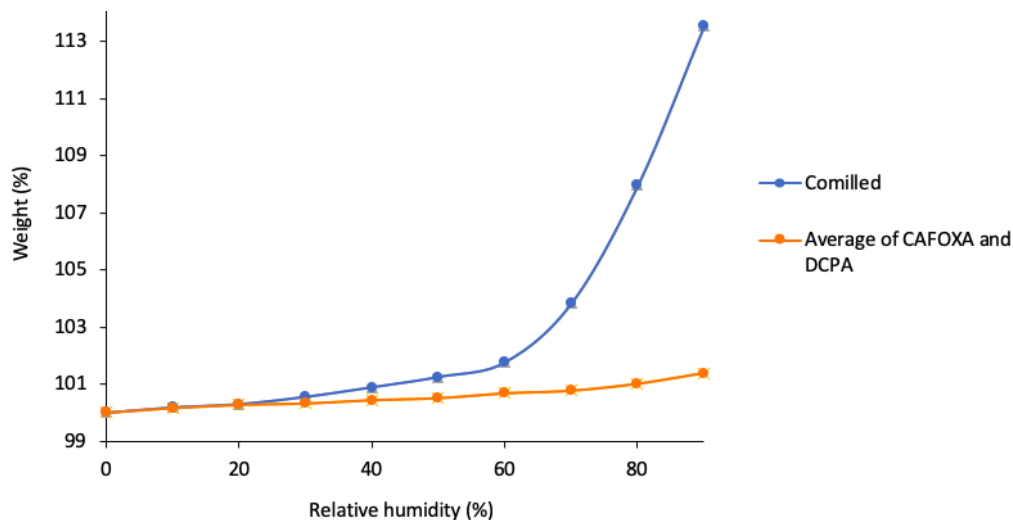


Figure 2.18. Water sorption data of comilled (CAFOXA-DCPA), and the average of separately milled CAFOXA and DCPA. All samples were milled for 120 sec.

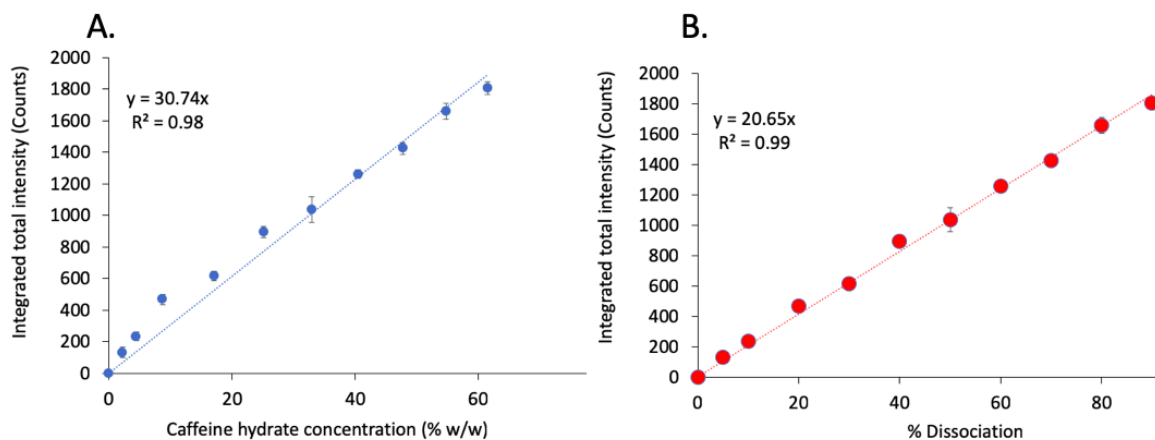


Figure 2.19. Plot of the caffeine hydrate peak intensity ($2\theta = 10.6^\circ$) versus its weight fraction in ternary mixtures of caffeine hydrate, CAFOXA and calcium oxalate. The dissociation of cocrystal will result in the formation of caffeine hydrate and calcium oxalate. Therefore, mixtures were prepared with CAFOXA concentration ranging from 97% to 9% w/w. The first sample is the cocrystal before it undergoes any dissociation (there caffeine hydrate content is 0.0% w/w). The last mixture represents 90% cocrystal dissociation (the caffeine hydrate content is 61.5% w/w). This data enabled us to generate a hypothetical “standard curve” of caffeine hydrate peak intensity as a function of % dissociation. Plot (b) was used to determine the % dissociation in the unknown samples (Figure 2.7 in the main manuscript). Error bars represent standard deviations (n=3).

Table 2.1. Surface area measurements of binary (CAFOXA-DCPA) powder mixtures.

Sample	BET Surface area (m²/ g)	% increase in surface area (compared to unmilled sample)
Unmilled physical mixture	6.82	-
Milled physical mixture (120 sec)	7.67	12.5%
Comilled mixture (120 sec)	7.03	3.1%

CHAPTER 3

Chapter 3. Use of Atomic Force Microscopy (AFM) to monitor surface crystallization of disordered caffeine-oxalic acid (CAFOXA) cocrystals in real time.

3.1 Synopsis

Our objective is to monitor surface crystallization of disordered caffeine-oxalic acid (CAFOXA) cocrystals under elevated water vapor pressure using AFM. Disorder was induced in the cocrystals using powder compaction and milling for 10 sec. The processes, reflective of realistic pharmaceutical processing steps, caused the surface reactivity to increase. The ‘active’ sites underwent rapid crystallization under elevated water vapor pressure. The disordered surface of the tablets had a high propensity to sorb water which led to a rise in the molecular mobility and consequently promoted crystallization. Using the technique, we were able to directly visualize crystal growth on the tablet surface. The work also revealed the important role played by the water vapor pressure in the atmosphere.

3.2 Introduction

Pharmaceutical cocrystals are becoming increasingly popular as an attractive strategy to modulate the physicochemical, mechanical and biopharmaceutical performance of active pharmaceutical ingredients.^{50,388,389} Cocrystals are defined as “*solids that are crystalline single phase materials composed of two or more different molecular and/or ionic compounds generally in a stoichiometric ratio which are neither solvates nor simple salts. If at least one of the cofomers is an active pharmaceutical ingredient (API) and the other is pharmaceutically acceptable, then it is recognized as a pharmaceutical cocrystal.*”^{390,391} Caffeine-oxalic acid (CAFOXA, 2:1) cocrystals have been extensively investigated. In contrast to caffeine, the cocrystal of caffeine with oxalic acid exhibited high resistance to hydrate formation under elevated vapor pressure (7 weeks at RT/98% RH). This enabled control of solid form and rendered CAFOXA suitable for development.^{30,31,50}

Recent work by Kaur *et al*³⁹² has highlighted the influence of processing induced lattice disorder on the stability of CAFOXA cocrystals in the presence of excipients. Disorder can be defined as a decrease in the long range order in crystalline lattices (also referred to as amorphization).^{240,361,393,394} Lattice disorder results in an increase in the free energy (mechanical activation), which in turn has implications on its physicochemical (for instance, solid-solid phase transitions) and mechanical properties. Owing to the critical impact of crystallinity on physicochemical and mechanical properties, it is imperative to detect and characterize lattice disorder.^{366,393-395}

Lattice disorder (i.e. loss in crystallinity) can be characterized using numerous techniques such as powder X-ray diffractometry (PXRD), Raman spectroscopy³⁹⁶⁻³⁹⁸, solid state nuclear magnetic resonance (ssNMR)^{399,400}, thermal analysis (calorimetry)^{401,402} and gravimetric water

sorption.⁴⁰³ These techniques provide average or bulk estimates of disorder.⁴⁰⁴ However, advancements in surface analysis techniques such as surface energy measurements (inverse gas chromatography, IGC)⁴⁰⁵ and atomic force microscopy (AFM)^{406,407} have allowed characterization of disorder localized on the sample surface. An understanding of the properties of the surface is important because they may be critical to the sample's physicochemical and mechanical performance.

AFM is a sensitive, non-destructive technique for direct imaging of surface structure. In AFM, imaging is performed by scanning the sample surface with a stylus or "tip" of nanoscale sharpness mounted near the end of a microcantilever. The forces experienced by the tip while interacting with a sample surface causes flexural cantilever motions which are measured by reflecting a laser beam off the cantilever and onto a split photodiode. These measurements in turn drive a feedback circuit to displace the cantilever base towards or away from the sample so as to keep the measurable approximately constant and thereby track (image) surface topography. Imaging can be performed in various "modes", traditionally including quasistatic contact or AC/"tapping", which differ in the feedback signal employed, i.e. either a cantilever's quasistatic deflection or its sinusoidally driven resonant amplitude, respectively. This topographic/structural imaging technique has been used to monitor phase changes on crystal surfaces and has found value in the surface evaluation of pharmaceuticals.⁴⁰⁸⁻⁴¹⁰ Recently, AFM was used to study the surfaces of CAFOXA and caffeine-malonic acid cocrystals following exposure to elevated water vapor pressure (RT/75% RH). While oxalic acid cocrystals exhibited surface restructuring to form "smoother" crystal surfaces, the malonic acid cocrystals sorbed water leading to cocrystal dissociation. Surface imaging captured the water sorption phenomenon.⁴¹¹

The surface restructuring, following storage at elevated RH, may be a consequence of a disordered surface. Low levels of lattice disorder induced during pharmaceutical processing can potentially go undetected when characterization is performed using techniques such as X-ray powder diffractometry (XRD) and differential scanning calorimetry (DSC), because these latter methods probe "bulk" or "average" disorder. The undesirable and disproportionate influence of surface disorder has previously been reported, thereby underlining the importance of its characterization.³⁹² We had earlier evaluated the impact of realistic processing conditions (milling for ≤ 2 minutes) on the crystallinity and subsequent stability of CAFOXA cocrystals.³⁹² Even a very short milling time of 10 sec caused measurable lattice disorder (measured by XRD and gravimetric water sorption), induced instability and led to cocrystal dissociation. This work highlighted the interplay of lattice disorder, water sorption and excipient on cocrystal dissociation. The results were particularly surprising because CAFOXA is considered a robust cocrystal.

As tablets are the most popular dosage forms, many pharmaceuticals will be subjected to compression. This raises an important question. What will be the effect of compression on the behavior of cocrystals, and more specifically, the behavior at cocrystal surfaces? Secondly, if the surfaces of crystals are disordered, will compression render these surfaces even more reactive? Thirdly, what role will ambient moisture (water vapor pressure in the atmosphere) play on the reactivity of the crystal surfaces?

Atomic force microscopy is a uniquely powerful technique to study the surfaces of particles. In this project, we wanted to evaluate the behavior of cocrystals following compression. Before compression, low levels of disorder were introduced in these crystals by cryomilling them for 10 sec. This enabled us to evaluate the combined effects of milling induced disorder and compression on the cocrystal behavior. AFM images of the compressed materials were obtained *while* they were exposed to 75% RH (at RT). This provided information on the surface behavior in real time.

Topography and phase imaging (the latter derived from the phase lag of tip motion relative to sinusoidal driving excitation, sensitive to tip-sample dissipation)⁴¹² were performed on the samples using AC/“tapping” mode of AFM. Using the technique, we were able to directly visualize crystal growth on the tablet surface. The process of compression caused the surface to become ‘active’ and recrystallize on storage. However, the introduction of additional low levels of lattice disorder, by milling the powder for 10 sec, caused a dramatic increase in surface reactivity and substantially accelerated the surface crystallization. The work also revealed the important role played by the water vapor pressure in the atmosphere. It is well known that disordered regions in lattice will have a strong tendency to sorb water.^{403,413,414} The attendant increase in molecular mobility drives the surface recrystallization. We believe that is the first report of the effects, in real time, of processing (compression) and lattice disorder (induced by milling) on the surface recrystallization behavior of particles on the tablet surface.

3.3 Experimental section

3.3.1 Materials.

Caffeine (CAF; Sigma-Aldrich) and oxalic acid (OXA; Sigma-Aldrich) were used as received. Caffeine-oxalic acid (CAFOXA) cocrystals were prepared using the aqueous slurry method.⁵⁰ The cocrystals were characterized using powder X-ray diffractometry (XRD). The experimental and calculated diffraction patterns were in agreement.

3.3.2 Differential scanning calorimetry (DSC).

A differential scanning calorimeter (model Q2000, TA Instruments) equipped with a refrigerated cooling accessory was used. The instrument was calibrated with indium. Approximately 2-5 mg of

powder sample was placed and sealed in a hermetic aluminum pan. All measurements were performed at a heating rate of 10 °C/minute under nitrogen purge (50 mL/min). The data was analyzed using TA Universal Analysis by TA Instruments, New Castle, DE.

3.3.3 Thermogravimetric analysis (TGA).

A thermogravimetric analyzer (model Q50 TGA, TA Instruments) was used. Approximately 4-5 mg of the powder sample was heated in an aluminum pan at a rate of 10 °C/min with a dry nitrogen purge (75 mL/min). The TGA data was analyzed using TA Universal Analysis by TA Instruments, New Castle, DE.

3.3.4 Preparation of tablets.

CAFOXA tablets were prepared by compressing 150 mg of the powder to 177 MPa in a hydraulic press (Carver model C laboratory press, Menomonee Falls, WI) using flat faced punches. The tablets, 8 mm in diameter and 1.5 mm thick, were annealed by storing at RT/75% RH for 3 weeks. In this case, annealing refers to crystallization of the disordered regions of the tablet by using elevated water vapor pressure to increase molecular mobility.

3.3.5 Water sorption analysis.

Water sorption analysis was performed for the annealed CAFOXA powder (starting material for preparing milled and tablet samples), the milled CAFOXA powder sample, the tablets freshly compacted and the annealed tablets. For data collection, a thin fragment of the tablets was used. Data were collected using an automated water sorption analyzer (DVS-1000 Advantage, Surface Measurement Systems, Middlesex, U.K.). Approximately 10 mg of the sample (powder or tablet) was placed in a quartz sample pan, and equilibrated at 0% RH (25°C) for 2 h under a nitrogen flow rate of 200 mL/min. The relative humidity (% RH) was raised in 10% increments to 90% RH and brought back to 0% RH, at 10% decrements. At each RH value, equilibrium was assumed if the mass change (dm/dt) was less than 0.001% in 15 min with maximum hold time set at 4 h for each RH value.

3.3.6 Cryogenic milling.

One gram of the powder sample was loaded into the cylindrical polycarbonate vial (SPEX SamplePrep #6751 vials) with stainless steel end plugs and an impactor (SPEX SamplePrep, model 6750). The vial was placed in the grinding chamber and remained submerged in liquid nitrogen throughout the milling experiment. The vials were pre-cooled for 20 minutes followed by milling for 10 sec at a milling rate of 10 (which refers to 20 impacts per sec). At the end of the milling process, the vials were equilibrated at RT in a desiccator containing anhydrous calcium sulphate prior to sample removal.

3.3.7 Atomic force microscopy (AFM).

Imaging was performed using a Keysight 5500 environmental scanning probe microscope running Picoview 1.20 software. The Keysight XYZ piezoscanner (model 9524A) was operated in closed loop X–Y (90 μm range) with a Z range of $\sim 8 \mu\text{m}$. The design of the instrument isolates the sample stage from the piezoelectric scanner and associated electronics, thus allowing for sample temperature and atmosphere control. The Keysight PicoAPEX sample chamber was customized by connecting a commercial humidity controller (ETS Electro-Tech Inc. model 514, with in-chamber hygrometer) to maintain 80 (± 5)% RH using an ultrasonic humidifier actuated by the controller. Data was collected in the dynamic mode, also referred to as “tapping” or AC mode. Under conventional amplitude-modulation feedback, with cantilever vibrated near its fundamental flexural resonance to provide height and phase along with error signal (amplitude) images. An aluminum-backside coated silicon cantilever (Mikromasch Europe; NSC 36) with a nominal force constant of 0.6 N/m, resonance frequency of 65 kHz and nominal radius of curvature of $\sim 8 \text{ nm}$ was used for all measurements at setpoint oscillation amplitudes in the 14 to 28 nm range, being $\sim 0.7\%$ of free oscillation amplitudes in the 20 to 40 nm range. Aided by the phase signal and amplitude and phase vs. Z curves, parameters were selected to place the oscillator in the net attractive regime to maintain a delicate tip-sample interaction. The resonant and drive frequencies were 98.50 and 98.85 kHz, respectively.⁴¹⁵ Image sizes ranged from 2 to 50 μm , and scan rates between 0.20 – 0.33 lines per sec at a resolution of 512x512 pixels. Data post-processing was performed using the freeware Gwyddion, version 2.53. Height and phase images were simultaneously acquired.

3.4 Results and discussion

3.4.1 Preliminary characterization. Baseline characterization of CAFOXA cocrystals was performed using thermal analysis (DSC and TGA), and XRD. The XRD pattern of CAFOXA cocrystals was superimposable on the pattern calculated from the Cambridge Structural Database (CSD; see Kaur *et al*³⁹², Figure S1). The thermal behavior, characterized by DSC and TGA (Supporting information; Figure 3.6), was in agreement with the literature.³⁴ The DSC heating curve exhibited a sharp endothermic event at 215°C reflecting the melting point of CAFOXA cocrystals.

There was a negligible weight change ($< 0.2\%$ w/w) over the RH range of 0 to 90% for the ‘as is’ powder sample (at 25°C; Figure 3.1). The very low water uptake by the CAFOXA sample at elevated RH is reflective of the highly crystalline nature of the material. For crystalline samples, the water uptake and consequent weight change is a function of the surface area of the sample available for adsorption – a surface phenomenon. On the other hand, for partially or completely

amorphous samples (in our case, compressed or milled samples), the weight gain will be due to both adsorption and bulk sorption (via hydrogen bond interactions) of water. The amorphous content in these sample will dictate the amount of water sorbed by the sample.

3.4.2 Lattice disorder and cocrystal instability.

In our previous work, the impact of realistic pharmaceutical processing (milling for 10 → 120 sec) on the crystallinity and consequent chemical stability of CAFOXA cocrystals was evaluated. The results indicated that even 10 sec of milling resulted in measurable disorder and a disproportionate increase in sample instability. The surface disorder induced by milling resulted in an attendant tendency of the sample to sorb water. The disorder translated to instability in the presence of DCPA at RT/75% RH.³⁹²

The diffraction patterns of unmilled and milled (for 10 sec) milled CAFOXA cocrystals seemed indistinguishable (Kaur *et al*³⁹², Figure 1a). Upon calculating percent crystallinity, a 4% drop in the diffraction pattern's AUC following milling (Kaur *et al*³⁹², Figure 2a) was observed for the milled samples. Gravimetric water sorption, an indirect but highly sensitive measure of lattice disorder, indicated a 10 fold increase (0.2% at RT/90% RH) in water uptake following milling (Figure 3.1). As discussed earlier, the amount of water sorbed by the sample is a function of the amorphous content of the sample. It is also instructive to recognize that milling also results in a decrease in the particle size of the sample, as has been reported in our previous work,³⁹² which may contribute to an increase in surface area and consequent weight gain under elevated RH. However, the weight gain due to particle size reduction is not expected to be pronounced.

As can be seen from Figure 3.1, measurable water sorption was also observed for the unmilled tablet compacts. At 25°C/90% RH, the freshly prepared tablet compact exhibited a weight gain of 0.09%. The weight gain was lower (0.05% under similar conditions) for the “annealed” tablets indicating crystallization of disordered regions of the tablet following storage at RT/75% RH for 3 weeks. Literature reports indicate that storage under elevated water vapor pressure promote recrystallization of CAFOXA.^{32,392} In our earlier work, we observed a pronounced decrease in the width (indicative of recrystallization) of a characteristic diffraction peak of CAFOXA cocrystal following storage of milled sample at RT/75% RH for 12 h (Figure 6 in Kaur *et al*³⁹²). This corroborated existing reports of CAFOXA crystallization upon exposure to elevated water vapor pressure.

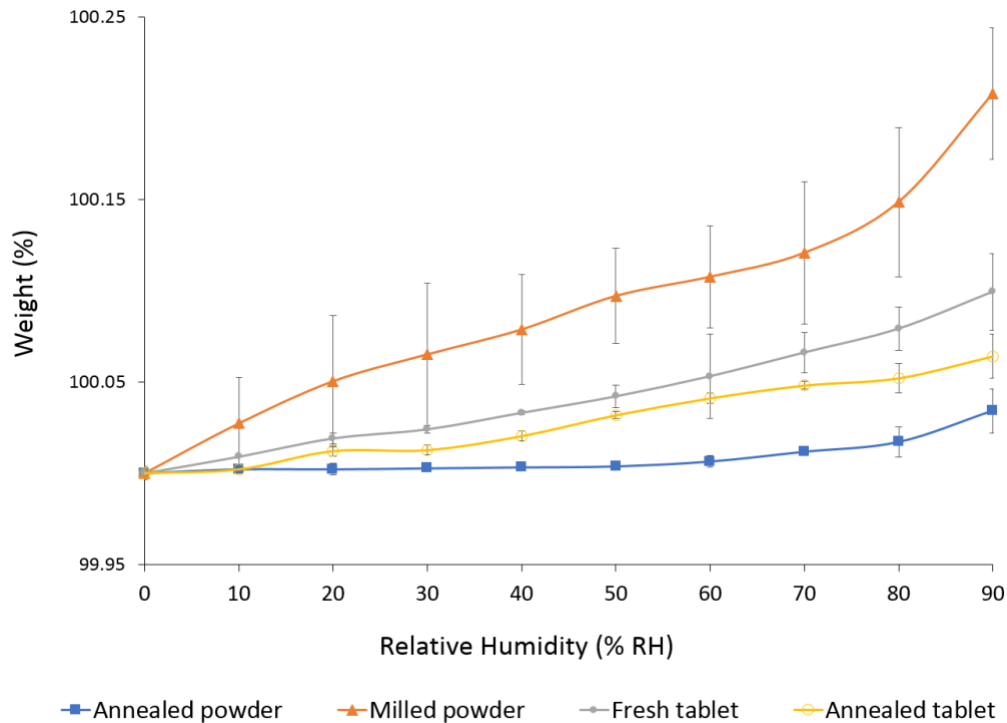


Figure 3.1. Water sorption data for CAFOXA powder and tablet samples at 25°C. The starting material (a highly crystalline powder sample of CAFOXA cocrystals) is referred to as the ‘annealed powder’. The powder was cryomilled for 10 sec and is referred to as the ‘milled sample’ in the figure legend. The behavior of a freshly prepared tablet as well as the tablet sample stored RT/75% RH for 3 weeks (‘annealed tablet’) are also shown.

3.4.3 Impact of tableting on the crystallinity of caffeine-oxalic acid (CAFOXA) cocrystals.

Compaction of a powder to form a tablet involves multiple stages. First, the applied pressure leads to a reduction in bulk volume (removal of air) and powder rearrangement to enable a close packing of the particles. Following dense packing, the high compression pressure leads to formulation of inter-particulate bonds and localized deformation of the crystals. The localized stresses can lead to either plastic deformation of the crystals or fracture. The tendency of the crystals to undergo brittle fracture is proportional to the compaction pressure.⁴¹⁶⁻⁴¹⁸ The high mechanical stresses experienced by the powder bed upon compression can also cause phase transformations. These transformations include amorphous \rightarrow crystalline⁴¹⁹, crystalline \rightarrow amorphous^{240,420} or a change in the polymorphic form.⁴²¹ In addition to the compression pressure, the tablet also experiences additional mechanical

stress on the surface owing to the die wall friction. Hence, the tablet surface is expected to exhibit a higher stress-induced phase transformation than the bulk (core).⁴¹⁹

CAFOXA cocrystals were plate shaped with smooth surface (Supporting information; Figure 3.8). These crystals are known to have a low elastic recovery and high fracture. The plate like habit renders it difficult for the crystals to orient themselves in different directions upon application of pressure, thereby resulting in fracture and poor compaction.⁴²²

Figure 3.2 shows the surface topography (XY plane) of a compressed tablet of CAFOXA cocrystals. Color scales are used to represent height as shown with the color bar at right. Topography imaging enables visualization of individual crystals that make up the tablet compact. It appears that while some crystals have void spaces (trenches) between them, others are pressed up against each other and show inward deformation at the interface. The 3D-rendered versions of the height images enable a better perception of these features.

Investigation of tablet surfaces have earlier been attempted using techniques (such as optical microscopy, SEM, laser profilometry and AFM) to determine compaction behavior, tablet porosity and to correlate crystal structure to mechanical properties.⁴²³⁻⁴²⁶

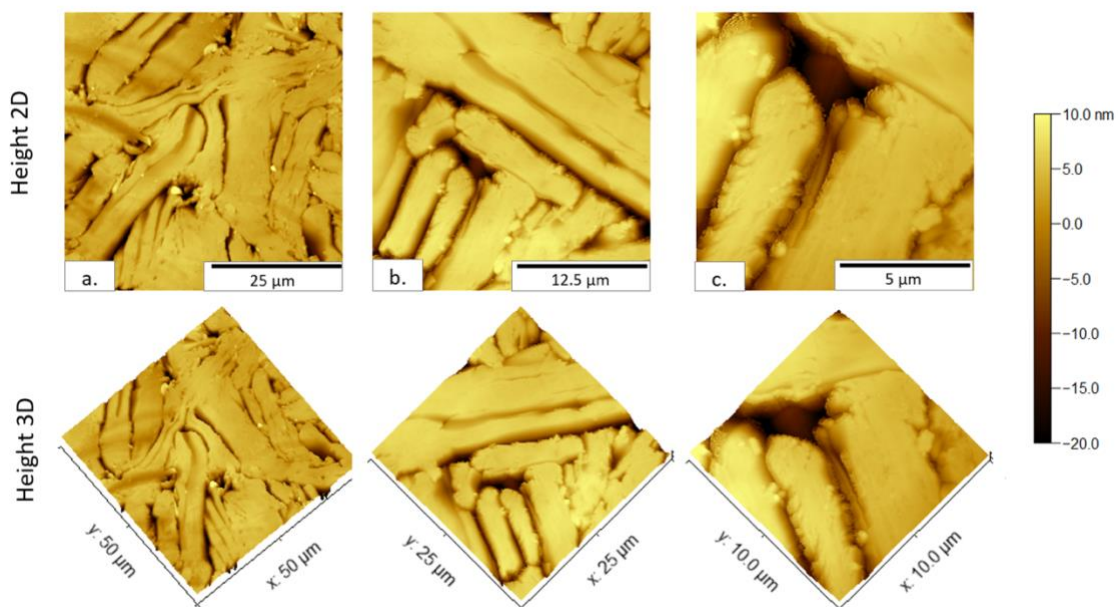


Figure 3.2. Representative 2D- (top) and 3D- (bottom) rendered AFM height images of a tablet surface prepared by compacting CAFOXA cocrystals. Acquired images decrease in size from left to right. (Vertical scale is stretched compared to lateral scale in the 3D renderings.)

3.4.4 Surface changes upon exposure to high humidity.

Figure 3.3 (left) compares representative 50x50- μm height images in 2D of (a) a freshly prepared compact of unmilled cocrystals and (b) the same sample following storage for 3 weeks at RT/75% RH, on a consistent color-rendering scale. The surfaces contain obvious “chasms”, dark in 2D rendering between crystals, as well as some apparent deformations at interfaces between abutting crystals (visible upon close inspection). Most notably, the freshly prepared tablet (a) exhibits a *relatively* smooth surface compared to the high-RH exposed tablet (b), qualitatively observed in the more uniform color rendering. Quantitative differences between (a) and (b) are extracted by Fourier analyzing (at right) the topography contained each 512x512 matrix dataset. Figure 3.3c overlays radial power spectral density functions extracted from each topography dataset. These curves display the lateral-scale-dependence of roughness, by plotting essentially the amplitude of Fourier components (i.e., sinusoidal decomposition of topography) versus their wavelength with log-log scaling. Large-amplitude, long-wavelength Fourier components are quantified in the left portion of the plots whereas small-amplitude, short-wavelength Fourier components are quantified in the right portion of the plots. Most importantly, one observes that the 75% RH annealed sample exhibits larger Fourier amplitudes (power spectral density) over essentially all wavelengths; that is, the annealed sample is rougher – varies more in height – over essentially all lateral scales evaluated. Thus this observation not only quantifies the presence of the obviously deep “chasms” separated by large lateral distances, but also a much less obvious presence of increased roughness over small scales. (We more closely examine such small-scale features in Figure 3.5.)

We attribute the decrease in surface smoothness following 75% RH exposure to crystal growth on the surface and resulting *heterogeneous* lateral displacement of molecules. As stated in the previous section, we postulate that compaction causes the creation of disorder. When stored at elevated RH, disordered regions on the surface of the sample can absorb water and the consequent increase in the molecular mobility facilitates crystallization. This proposed surface crystallization of disordered sites is qualitatively consistent with water sorption results in Figure 3.1: the “annealed tablets” sorb less water than freshly prepared compacts due to surface crystallization and reduction in disordered sites (that serve as major contributors to weight gain as humidity increases).

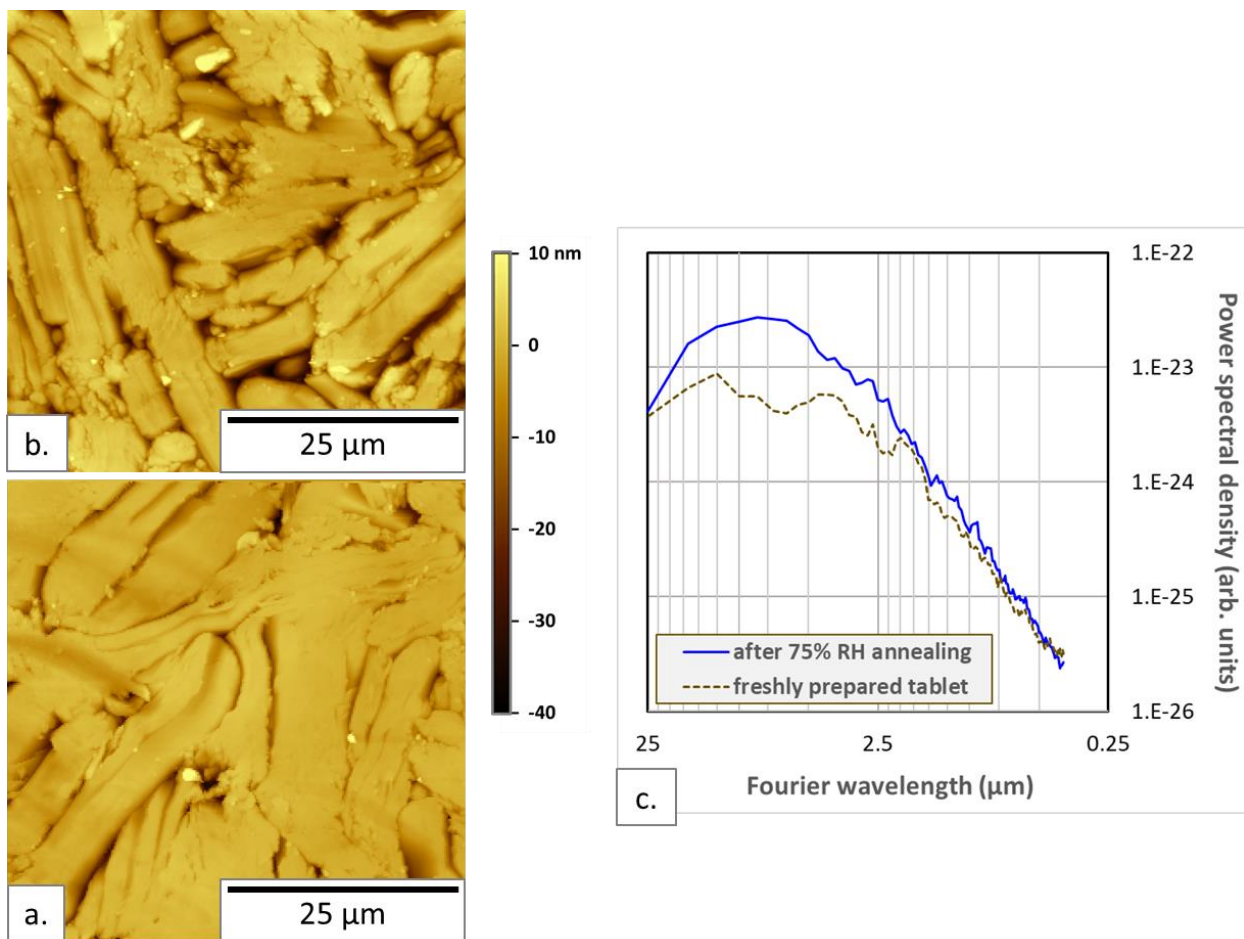


Figure 3.3. Representative 2D renderings of ambient AFM height images of (a) a freshly prepared tablet of CAFOXA cocrystals, and (b) the same tablet after storing at RT/75% RH for 3 weeks. (c) Radial power spectral density functions computed for images in (a,b).

3.4.5 Using *in situ* AFM to monitor surface crystallization on cocrystal tablets upon exposure to RT/75% RH.

In order to probe changes at disordered sample surface regions of CAFOXA cocrystals, cryomilling was employed to induce lattice disorder, then elevated-RH, *in situ* AFM imaging performed. Cryogenic milling, as opposed to milling at RT, was chosen to mitigate thermal effects. Processing-induced disorder is believed to be predominantly on the surface of the particles (at low levels of mechanical activation) as the surface of the particles experiences shear. Thus AFM is especially useful for imaging induced changes.

Figure 3.4 (t =0) contains exemplary 2D and 3D renderings of AFM height images of a 10 sec milled tablet compact. The sample was imaged in real time at 77 ($\pm 2\%$) RH (at RT). Crystal appearance and growth was observed on the surface of the sample as bright (in 2D case) needle-shaped objects. In 3D-rendering the corresponding crystal heights are quantified. While the 2D images are valuable to image crystal growth in the xy plane, 3D imaging provides quantification of vertical growth of these crystals above the principal surface plane (see two crystals highlighted within rectangles at 18 and 22 h).

Whereas various water vapor mediated changes have been observed over time scales of *weeks* for unmilled compacts, in Figure 3.4 pronounced changes in surface morphology are observed for milled samples within hours. We note that the growth of crystals is relatively faster over the first 10-12 h of exposure (seen over the course of many acquired images). Crystal growth is interpreted as a consequence of pronounced lattice disorder that is assumed to be prevalent on the sample surface. It is difficult, however, to interpret with confidence whether the growth of crystals over the surface is occurring as a consequence of molecular diffusion from the trenches.

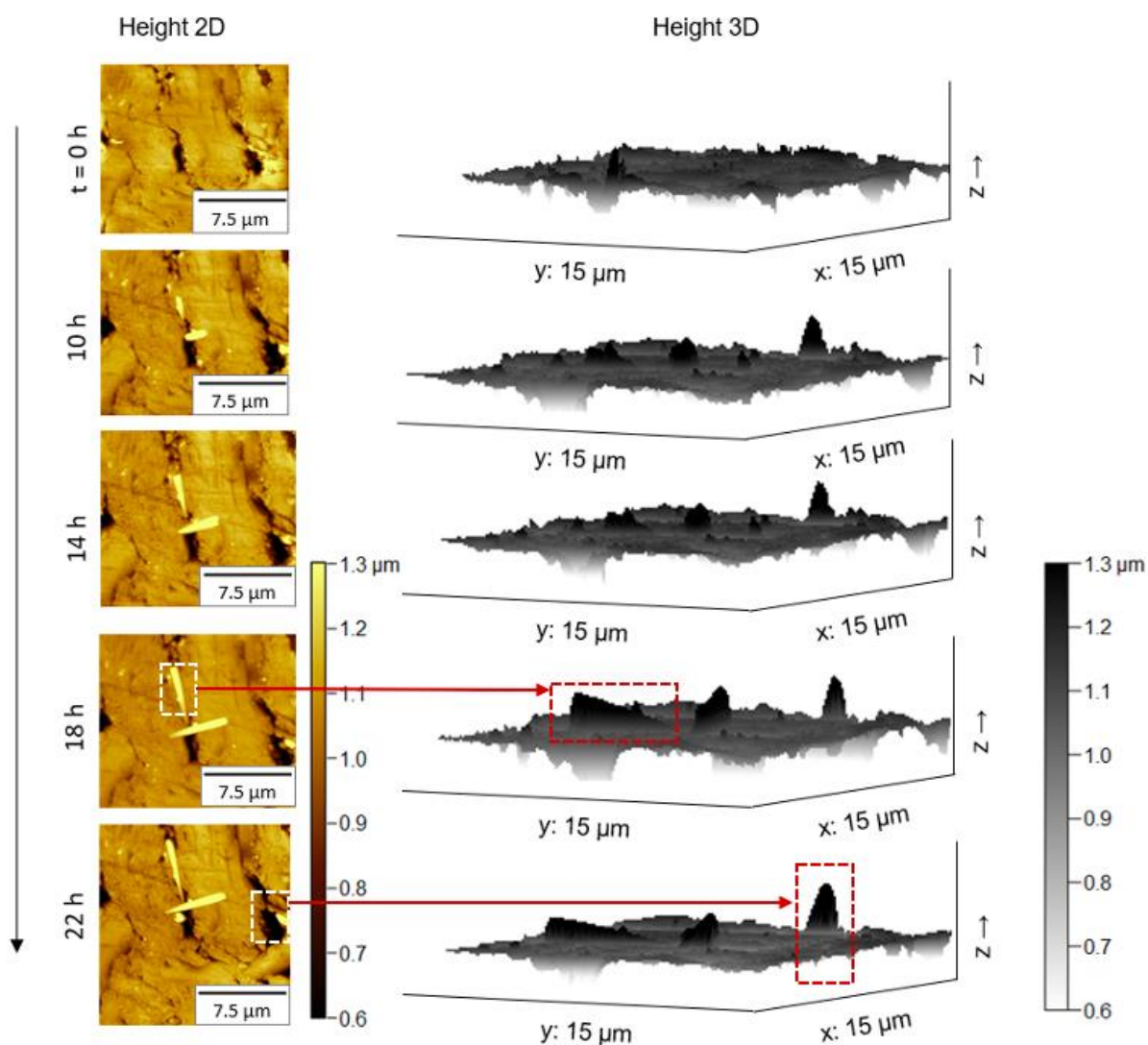


Figure 3.4. Representative 2D (left) and 3D (right) renderings of *in situ* AFM height images showing time-dependent surface topography transformation on a milled (10 sec) CAFOXA sample during exposure to RT/80% over 22 h. 2D and 3D renderings are explicitly designated with rectangles around two of the crystals. (Vertical scale is stretched compared to lateral scale in the 3D renderings.)

Figure 3.5 (i) exemplifies surface changes for a 10 sec milled compact following exposure to elevated vapor pressure, in real time. The larger effects of 8 h of exposure to 75% RH is seen by comparing 30x30- μm image (b) to that of (a): the appearance of elongated needle shaped crystals. Additional bright dots are also observed suggesting smaller crystals. Closer inspections of a subregion (dashed square) before and after the 8-hr exposure, as shown in (c,d), reveals clear evidence of surface coarsening and the appearance of rectilinear crystals on a smaller scale than the “needles” of (a,b). Imaging over an even smaller region, as shown in (e,f), to more closely examine such small-scale transformations, further revealed the coarsening of somewhat rounded, odd-shaped or polygonal “pebbles” into slightly larger and more squarish/rectilinear objects.

Figure 3.5 (ii-a) shows phase imaging of a 5x5- μm region of milled compact following exposure to 80% RH for 8 h. Phase imaging provides complementary information to surface topography and helps to distinguish regions with different mechanical properties. Dissipative interactions between tip and surface result in a modification of the phase shift between the base and tip ends of the AFM cantilever (physically 90 degrees at resonance when free from the surface but zeroed at this point in the Keysight AFM software).⁴¹⁵ Figure 3.5 (ii-a) reveals bright-phase crystallites embedded in a darker-phase matrix. Darker corresponds to higher energy dissipation (for the case of a net repulsive interaction, exploited here to maximize contrast) in regions away from obvious crystalline moieties. These darker regions of greater dissipation are postulated to be more amorphous/disordered sites. Thus one identifies crystals growing from more disordered regions on the surface following exposure to elevated water vapor pressure.

The crystals observed in Figure 3.5 (ii) had a different morphology than those seen in larger (20-50 μm) images. This morphology has not been previously reported in the literature. The probability of these crystals being a different polymorph or products of cocrystal dissociation was ruled out by XRD characterization. No change in the peak positions in the diffraction pattern of the milled samples was observed. The XRD results only showed sharpening of the peaks (decrease in peak broadening) and an increase in peak intensity following exposure of the milled sample to RT/75% RH (indicative of increase in sample crystallinity).

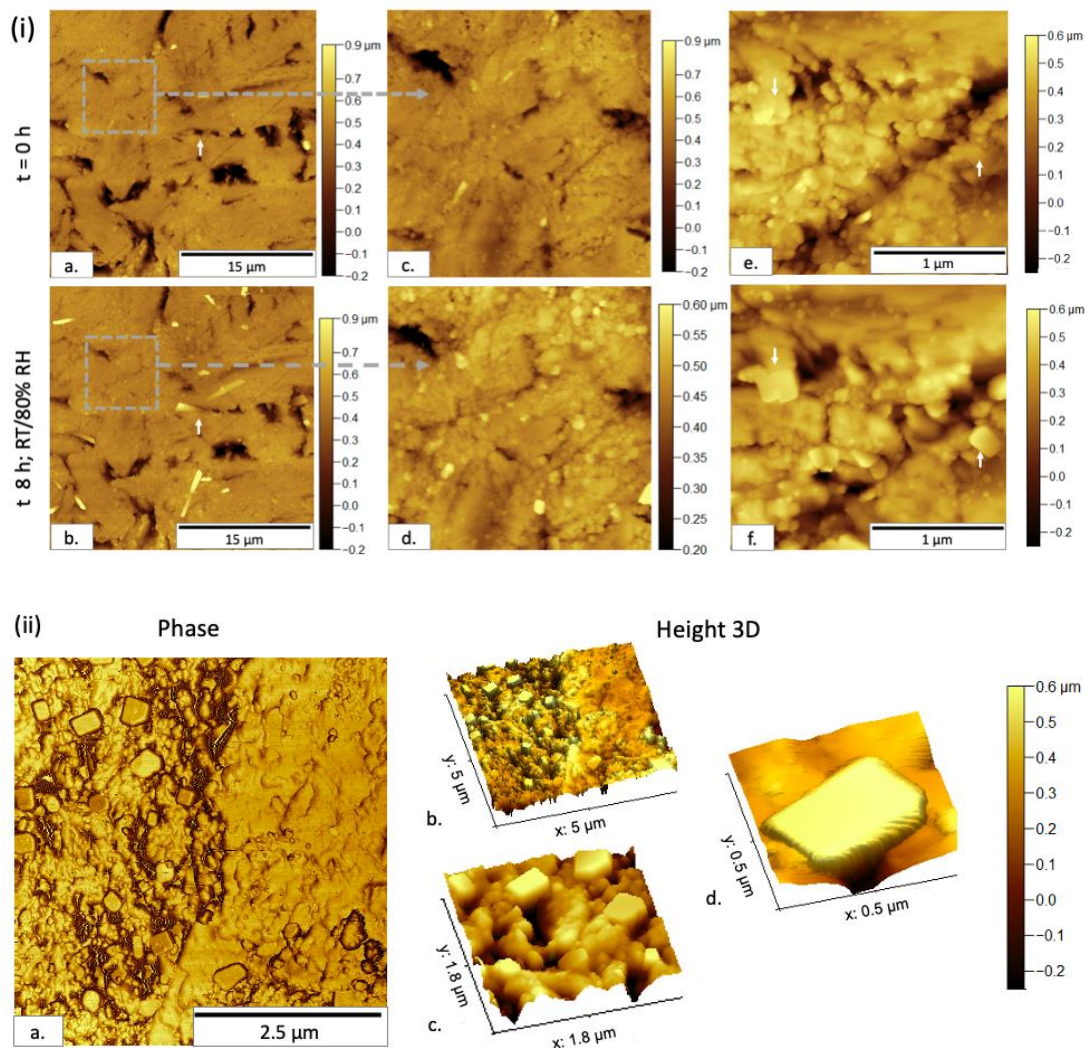


Figure 3.5. Representative AFM height and phase images showing recrystallization of milled (10 sec) CAFOXA sample upon exposure to RT/80% RH. (i) Comparison of the milled sample surface imaged *in situ* at RT/80%RH at $t = 0$ and 8 h. White arrows are used as reference markers. (ii) includes smaller, more highly resolved images of the recrystallized regions at 8 h. Crystals with a different morphology were observed in (ii).

3.5 Significance

Compression of crystalline materials is known to cause lattice disorder.⁴²⁷⁻⁴²⁹ The disordered regions, being metastable, would have a tendency to revert back to a crystalline state. Following compaction of several pharmaceuticals, including aspirin and sucrose, scanning electron microscopy revealed surface recrystallization.⁴³⁰ Interestingly, in some of the model compounds, crystallization was observed within 60 minutes of compression.

CAFOXA is directly compressible, and exhibits plastic deformation and brittle fracture upon consolidation. Tableting induced mechanical stresses led to crystalline defects, especially on the tablet surface. We postulate that the low levels of disorder induced as a consequence of pharmaceutical unit operations are predominant on the surface of the particles. This renders surface analysis highly valuable for imaging the induced disorder. The goal of this work is to characterize recrystallization of disordered tablet sample surfaces upon exposure to elevated vapor pressure.

The recrystallization is expected to be accelerated in the presence of water vapor. On exposure to water vapor, the disordered regions can sorb water, get plasticized and rapidly undergo recrystallization. Thus the “surface restructuring” can be accelerated when compacts are exposed to high RH. AFM provided a method for directly and selectively visualizing the compact surface. By performing the AFM studies under controlled RH conditions, the changes in compact surface were monitored in real time. These results provided the timescale for surface recrystallization as a function of processing as well as storage..

While pronounced changes were observed for the milled sample after 10 h, the surface of the compact continued to "evolve" up to 22 h (Figure 3.4). Thus the mobility on the compact surface is sustained for a prolonged time period. This behavior could be attributed to the combined effects of milling (for 10 sec) and compression. Please note that in the present work, milling is reflective of any/all unit operations that can potentially result in mechanical activation of the solids.

For the unmilled compacts, the structural changes were observed to occur at a slower pace (weeks following storage; Figure 3.3). The differences in time scales of structural transformations in Figure 3.3 and 3.4 is indicative of higher disorder (and consequently faster recrystallization) in the milled tablet samples.

It is instructive to recognize that during drug product manufacturing and storage, the presence of unbound water in the system can impact both the physicochemical stability of the API as well as excipient functionality, thereby rendering it undesirable. The recrystallization of the disordered regions observed in this work is a classic example of water mediated phase transformation in a drug

product environment. In our earlier work,³⁹² the presence of unbound water in the system resulted in rapid dissociation of CAFOXA cocrystals (milled for 10 sec) in the presence of excipient DCPA.

3.6 Conclusions

Lattice disorder is induced by routinely used pharmaceutical processing steps i.e. tablet compression and milling. The phase transformation of the disordered surface regions of CAFOXA cocrystals, upon exposure to elevated water vapor pressure, was studied using environmental AFM in real time. Topography and phase imaging indicate the appearance and growth of needle shaped crystals of CAFOXA at and above 75% RH (at RT). The crystallization was more discernable for the milled samples as compared to the unmilled tablet samples.

3.7 Supporting information

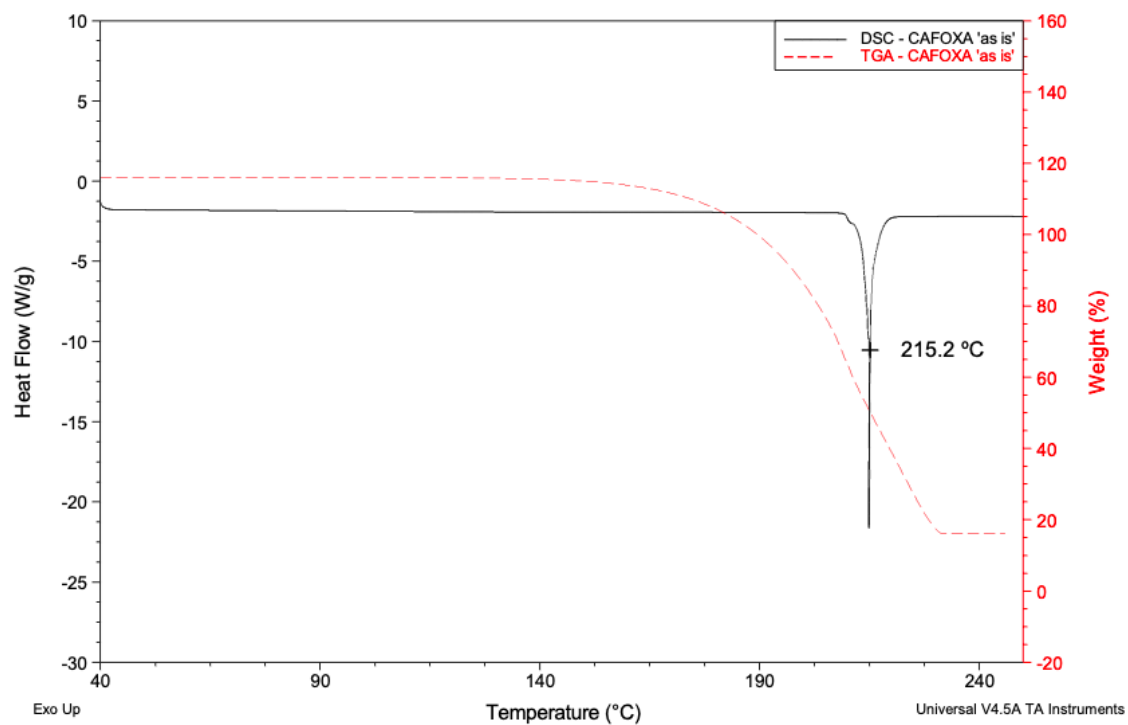


Figure 3.6. DSC and TGA heating curves of CAFOXA cocrystals.

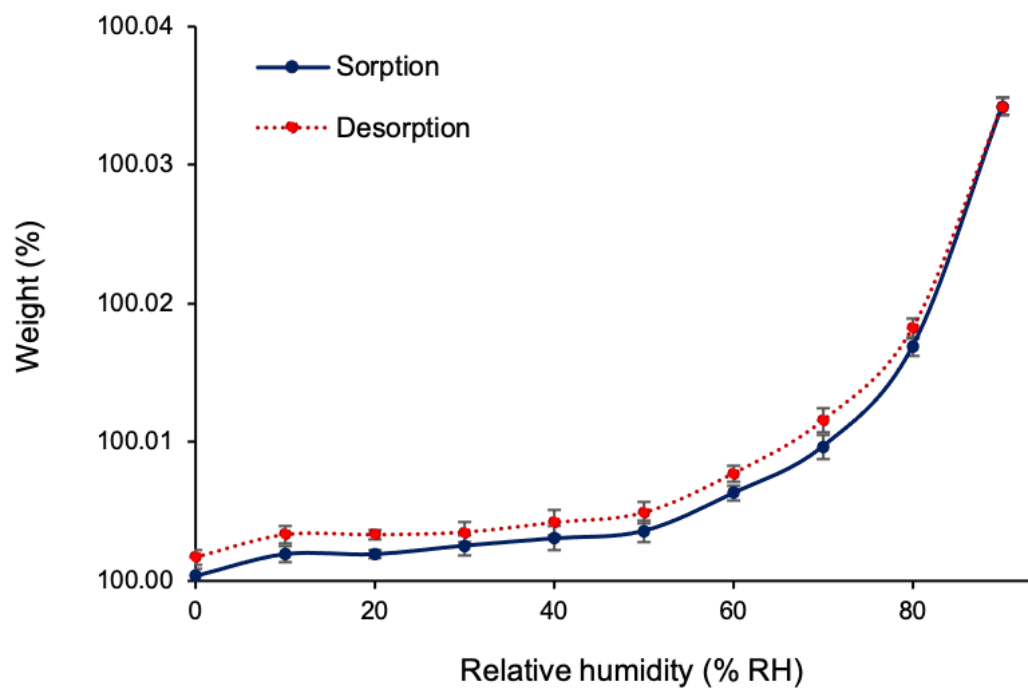


Figure 3.7. Gravimetric water-desorption behavior of CAFOXA cocrystals at 25°C.

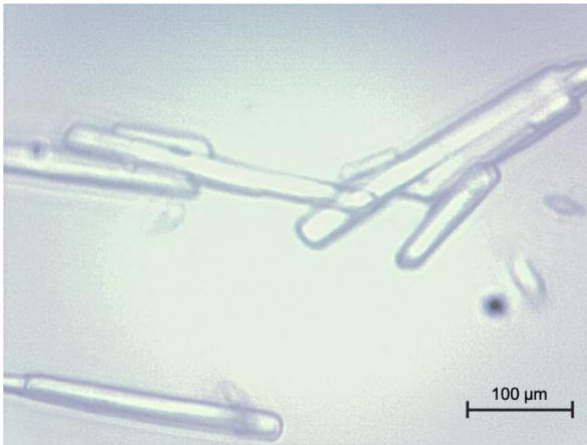


Figure 3.8. Optical microscopy of CAFOXA cocrystals.

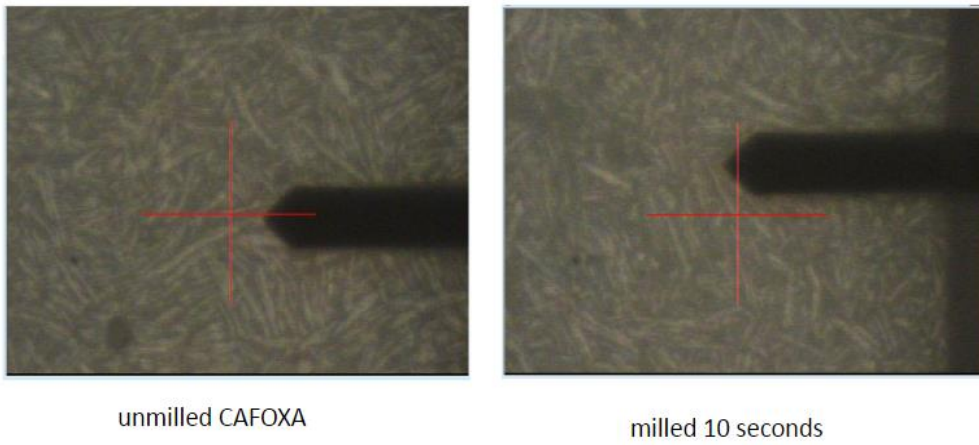


Figure 3.9. Optical images of the tablet sample and cantilever.

CHAPTER 4

Chapter 4. Partial dehydration of levothyroxine sodium pentahydrate in a drug product environment: structural insights into stability.*

*Reprinted with permission from Kaur, N., Young, V., Su Y., & Suryanarayanan, R. (2020). Partial dehydration of levothyroxine sodium pentahydrate in a drug product environment: structural insights into stability. *Mol Pharm*, 17 (10) 3915–3929. Copyright (2020) American Chemical Society.

4.1 Synopsis

Levothyroxine sodium pentahydrate (LSP; $C_{15}H_{10}I_4NNaO_4 \cdot 5H_2O$) gradually loses one molecule of water of crystallization as the water vapor pressure is decreased from 90 to 15% RH (40°C), a behavior characteristic of nonstoichiometric hydrates. LSP loses four molecules of water of crystallization to form levothyroxine sodium monohydrate (LSM; $C_{15}H_{10}I_4NNaO_4 \cdot H_2O$) under realistic storage conditions (40°C/0% RH for three hours). The crystal structure of LSP was determined following which the specimen was partially dehydrated *in situ* to form LSM. The crystal structure of LSM provided insight into its potential for high reactivity. Thus its presence in a drug product is undesirable. In LSP – oxalic acid mixtures stored in a hermetic container at 40°C, there was moisture transfer from drug to excipient. Synchrotron X-ray diffractometry revealed dehydration of LSP resulting in LSM, while anhydrous oxalic acid transformed to its dihydrate. In formulations of LSP, chemical degradation of levothyroxine sodium may be preceded by its partial dehydration.

4.2 Introduction

Levothyroxine sodium (3,3',5,5' tetraiodo-*l*-thyronine) is the sodium salt of the *levo* isomer of thyroxine (physiological thyroid hormone).^{242,431} It is the standard, and usually the only and life-long treatment option, for patients suffering from hypothyroidism, a chronic illness characterized by low thyroid hormone levels.^{300,432-434} Over 100 million levothyroxine prescriptions were dispensed in the United States in 2018.^{435,436}

Levothyroxine sodium formulations are available in the form of tablets, capsules and oral solutions.⁴³⁷⁻⁴³⁹ Solid dosage forms are formulated with the pentahydrate ($C_{15}H_{10}I_4NNaO_4 \cdot 5H_2O$). Precision in the amount of drug administered to the patient is necessitated by the narrow therapeutic index and is challenging because of its low dose (25-300 μ g/dose).^{433,440-444} Multiple studies have also revealed high patient sensitivity to the brand of the formulation and to minor alterations in formulation composition.^{285,289,292,445-448}

In addition to being one of the most prescribed drugs in the world, levothyroxine tablets continue to be one of the most recalled from the market, due to issues pertaining to the chemical instability of the active pharmaceutical ingredient (API).^{449,450} Levothyroxine sodium pentahydrate (LSP) is reported to undergo chemical decomposition through complex pathways.^{451,452} The chemical instability issue is exacerbated by its low dose. Considering the high excipient burden of the drug product, levothyroxine sodium formulations demand a rigorous control over additives, processing conditions and storage requirements in order to have an acceptable shelf life. In 2007, the FDA tightened the potency specification for levothyroxine sodium, from $100 \pm 10\%$ to $100 \pm 5\%$ (of the labelled amount) in marketed products. Soon after, in 2008, the US Pharmacopeial convention updated the product monograph to meet the new FDA specifications.^{453,454} This was done to control the quality of the marketed products and reduce variability in stability profile across manufacturers. However, there continue to be market recalls.⁴⁴⁹ Considering the critical need of this drug, the problem of chemical decomposition in levothyroxine sodium products needs to be urgently addressed and resolved.

The chemical stability of levothyroxine, both in the solid state and in solid dosage forms, has been the subject of several publications. In 2003, Patel *et al*⁴⁵⁵ reported that LSP was stable for 6 months even under accelerated stability conditions ($40^{\circ}\text{C}/75\% \text{ RH}$). However, the API exhibited pronounced chemical decomposition in the presence of excipients. The hygroscopicity and microenvironmental acidity of the excipients were critical determinants of API instability. Recently, the role of numerous excipients on the chemical stability of LSP was explored.^{247,456} There is incomplete understanding of the role of the physical form of levothyroxine sodium on its stability. Hamad *et al*⁴⁵⁷ attributed the chemical instability to oxidation of the dehydrated API. In this study, the impact of temperature, water vapor pressure and molecular oxygen on API stability was evaluated. The pentahydrate resisted oxidation under elevated temperature and water vapor pressure ($60^{\circ}\text{C}/75\% \text{ RH}$). However, when the water vapor pressure was reduced to $0\% \text{ RH}$, the API started losing its lattice water and the consequent dehydrated material underwent oxidative decomposition at RT. Thus, the chemical decomposition was preceded by partial dehydration. In another recent work, the high chemical reactivity of the dehydrated API was ascribed to amorphization of the crystalline (pentahydrate) lattice upon loss of bound water. The authors also indicated that the lattice water in levothyroxine sodium is present in channels and upon removal of water, oxygen occupies the vacated sites, leading to API oxidation.¹⁶⁴

While LSP is used in marketed formulations, the existence of the drug in other states of hydration has been suggested. However, these have not been comprehensively studied and characterized. Our preliminary studies suggested that the dehydration of the pentahydrate resulted in a crystalline

monohydrate with a different lattice structure and overall lattice “contraction” upon the loss of the four molecules of water. It is evident from the literature that the product phase formed by dehydration of a hydrate can be much more reactive than the parent compound.^{37,38,237,458-461} The potential for an increase in reactivity of levothyroxine, due to a change in its physical form, formed the motivation for this work.

Our work is driven by the following working hypotheses: (i) The crystal structure of levothyroxine sodium monohydrate (LSM), different from that of the pentahydrate, explains its high reactivity. (ii) In a drug product environment, LSP dehydrates to a lower hydrate, possibly LSM.

As a first step towards testing this hypothesis, we needed to comprehensively characterize the solid phases of levothyroxine. Specifically, the dehydration behavior of LSP, and the composition and properties of the product phases had to be understood. We had the following objectives. (i) Identify the conditions of formation and stability of the different hydrates of levothyroxine sodium. (ii) Understand the changes in crystal structure as the pentahydrate is dehydrated, first to the tetrahydrate and then to the monohydrate. (iii) Obtain the crystal structure of LSM. (iv) Use solid state nuclear magnetic resonance (ssNMR) to understand the changes in conformation during and following the solid state pentahydrate to monohydrate transition.

A battery of analytical techniques, specifically, differential scanning calorimetry (DSC), thermogravimetric analysis (TGA), gravimetric water sorption/desorption, powder X-ray diffractometry (XRD; both laboratory and synchrotron sources), and spectroscopy (IR and NMR) were used for the comprehensive characterization of the different solid phases of levothyroxine sodium. The dehydration phase behavior was monitored by XRD and ssNMR. The crystal structure of LSM provided insights into its chemical reactivity. The *in situ* monohydrate formation, by the pentahydrate dehydration, could potentially explain the observed chemical instability of levothyroxine sodium. It is instructive to recognize that this change in physical form can occur under realistic processing and storage conditions, and can impact the quality of marketed products.

4.3 Experimental section

4.3.1 Materials.

LSP ($C_{15}H_{10}I_4NNaO_4 \cdot 5H_2O$) was purchased from Biophore Pharma Inc and was used as received. The powder sample was stored in air-tight opaque polyethylene bags in a freezer at $-25^{\circ}C$. Drierite[®] (anhydrous calcium sulfate) was purchased from Sigma-Aldrich (St. Louis, MO).

4.3.2 Water sorption and desorption analysis.

Water sorption and desorption studies were performed using an automated water sorption analyzer (Q5000 SA, TA Instruments, New Castle, DE). Approximately 5 mg of the powder was placed in a quartz sample pan and equilibrated at 50% RH for 1 h at 40°C and a nitrogen flow rate of 200 mL/min. The RH was raised, at increments of 10%, up to 90%. The RH was then reduced, again in decrements of 10%, to 0%. At each RH value, if the mass change (dm/dt) was less than 0.005% in 15 min, attainment of equilibrium was assumed. The maximum hold time at each RH value was 4 h. Sorption and desorption studies were also performed at 20 and 25°C with all other parameters as discussed above. The data was analyzed using commercial software (Universal Analysis 2000, TA Instruments, New Castle, DE).

4.3.3 Differential scanning calorimetry (DSC).

A differential scanning calorimeter (model Q2000, TA Instruments, New Castle, DE) equipped with a refrigerated cooling accessory was used. The instrument was calibrated with indium. Approximately 5 mg sample was hermetically sealed in an aluminum pan with a pinhole. Measurements were performed at heating rates of 1, 5 10 and 20°C/min under a nitrogen purge (50 mL/min). The data was analyzed using commercial software (Universal Analysis 2000, TA Instruments).

4.3.4 Karl fischer titrimetry (KFT).

The water content in the powder samples was determined using a coulometric titration apparatus (Karl Fischer Coulometer C20, Mettler Toledo, Columbus, OH). Approximately 20 mg of the powder sample was introduced into the titration cell. The commercially available reagent, Hydranal, was used for the experiment. The reported results are the mean of three determinations.

4.3.5 Thermogravimetric analysis (TGA).

In a thermogravimetric analyzer (model Q50 TGA, TA Instruments, New Castle, DE), approximately 5 mg of the sample was heated in an aluminum pan from 25 to 300°C at 10°C/min under dry nitrogen purge (75 mL/min). The TGA data were analyzed using commercial software (Universal Analysis 2000, TA Instruments, New Castle, DE).

4.3.6 Powder X-ray diffractometry (PXRD).

Data was collected in a diffractometer (D8 Advance; Bruker AXS, Madison, WI) using Cu K α radiation (40 kV \times 40 mA) over an angular range of 5–35° 2 θ with a step size of 0.02° and a dwell

time of 0.5 sec. The instrument was equipped with a variable-temperature stage (TTK 450; Anton Paar, Graz- Straßgang, Austria) and a silicon strip one-dimensional detector (LynxEye, Bruker AXS, Madison, WI, USA). For the variable temperature experiment, the sample was heated at 10°C/min to 90°C. Commercially available software (Jade 2010, Materials Data, Livermore, CA) was used for data analysis.

4.3.7 Synchrotron X-ray diffractometry (SXRD).

Experiments were performed in transmission mode in the 17-BM-B beamline at Argonne National Laboratory (Argonne, IL, U.S.A.). A monochromatic circular X-ray beam (wavelength = 0.45256 Å; beam diameter = 300 µm) and a two-dimensional (2D) area detector (XRD-1621, PerkinElmer) were used. A triple-bounce channel-cut Si single-crystal monochromator with [111] faces polished was used, which limited the line broadening to its theoretical low limit (i.e., the Darwin width). The sample to detector distance was set at 900 mm. Calibration was performed using an Al₂O₃ standard (SRM 674a, NIST). Powder samples were hermetically sealed in aluminum pans and the diffraction pattern was collected in the transmission mode. Commercially available software (Jade 2010, Materials Data, Livermore, CA) was used for determining the integrated peak intensities.

4.3.8 SXRD of LSP tablet.

LSP powder (200 mg) was filled into a tablet die and held in place with a flat-faced lower punch. The powder bed was compressed in a hydraulic press (Carver model C laboratory press, Menomonee Falls, WI) to a compression pressure of 177 MPa. The tablet diameter was 8 mm, and the thickness was 1 mm. The tablet was placed in a sample chamber maintained at 40°C/0% RH. The chamber was made of aluminum, with a removable lid, and contained a sample holder with heaters and temperature/ humidity probes. The chamber also had a small air circulating muffin fan and glass beakers containing Drierite. Two circular windows were created in the chamber and sealed with Kapton tape to permit the entrance and exit of the X-ray beam. This setup allowed us to collect the diffraction data, in the transmission mode, while the tablets were stored under the desired condition. After 3 h, the chamber was returned to RT (~ 25°C) and the humidity of the chamber was increased to 75% RH. This was accomplished by placing a beaker containing saturated sodium chloride solution in the sample chamber. XRD patterns were collected over the next three hours.³⁸⁶

4.3.9 Dehydration of levothyroxine in a drug product environment.

A physical mixture of LSP and the excipient (1:1 w/w) was prepared, cryomilled for 5 sec and stored at 40°C in: (i) hermetically sealed DSC pans, (ii) chambers maintained at 75% RH and (iii) desiccators maintained at 0% RH. The chambers maintained at 0 and 75% RH also contained Oxyrase. Samples were collected at day 0, 14 and 28 and characterized using synchrotron XRD as previously discussed.

4.3.10 Single crystal X-ray diffraction.

A specimen of LSP (approximate dimensions 0.240 x 0.120 x 0.020 mm³) was placed into the center of a 200 µm MiTeGen Dual Thickness Microloop™ and mounted on a Bruker-AXS VENTURE PHOTON-III diffractometer (APEX3, Bruker Analytical X-ray Systems, Madison, WI) for data collection, first at 178 K for LSP and then at 268 K for LSM. The data collection was carried out using MoK α radiation (parabolic mirrors) with a frame time of 6 sec and a detector distance of 4.0 cm. A strategy program was used to assure complete coverage of all unique data in point group 1 symmetry to a high resolution limit of 0.70 Å. All frames were collected with 1.20° step widths. For LSP, a preliminary set of cell constants were calculated from reflections harvested from two sets of frames. These initial sets of frames were oriented such that orthogonal wedges of reciprocal space were surveyed. The intensity data were corrected for absorption and scaling (SADABS, Bruker Analytical X-ray Systems, Madison, WI). Final cell constants were calculated from 2739 strong reflections (SAINT Bruker Analytical X-ray Systems, Madison, WI). Once this experiment was completed the cryostat temperature was raised to 263 K while repeating the same data collection strategy. We hypothesized the specimen could be partially dehydrated *in situ* from LSP to LSM. The reflections became extremely streaky over the next 2 h of data collection. The appearance of the reflection data indicated an incomplete conversion to LSM or possibly this specimen was damaged beyond providing useful data. The 263 K data was not useful. The temperature of the cryostat was then raised to 268 K. While reflections that were streaky rapidly coalesced into point-shaped reflections, the high-resolution data were now limited to an approximate 0.80 Å resolution. A second unit cell determination using the same method as above found the unit cell volume for LSM based on previous XRD experimentation. The data collection was started using the same strategy as used above. The LSM crystal form appeared to be stable under these conditions for about 1.5 h when further dehydration to the presumed anhydrate turned the specimen to “dust”. Both LSP and LSM crystal structures were solved using SHELXT-2014 and refined using SHELXL-2018. The space group P1 was determined based on absence of reflection conditions and non-centrosymmetric intensity statistics. Direct-methods solutions were

calculated which provided most non-hydrogen atoms from the E-map. Full-matrix least squares / difference Fourier cycles were performed which located the remaining non-hydrogen atoms. All non-hydrogen atoms were refined with anisotropic displacement parameters except where indicated. All hydrogen atoms were placed in ideal positions and refined as riding atoms with relative isotropic displacement parameters unless otherwise stated.^{462,463} The crystal structure files have been submitted to CCDC (Deposition Number for LSP is 2011361 and LSM is 2011362).

4.3.11 Solid-state nuclear magnetic resonance spectroscopy.

ssNMR experiments were carried out on a 400 MHz Bruker HD Advance III spectrometer in the Biopharmaceutical NMR Laboratory, BNL, at Pharmaceutical Sciences, MRL (Merck & Co., Inc., West Point, PA, USA). An HFX magic angle spinning (MAS) probe was tuned to ^1H and ^{13}C double resonance modes for all one-dimensional (1D) and two dimensional (2D) ^{13}C experiments. Samples were packed into 4 mm zirconia rotors and spun at a MAS frequency of 12 kHz. Sample temperature was maintained at 294 K. 1D ^{13}C ramped-amplitude cross polarization (CP) MAS spectra were collected under SPINAL-64 heteronuclear decoupling with a ^1H decoupling field of 100 kHz during acquisition. 2D heteronuclear dipolar correlation (HETCOR) between ^1H and ^{13}C were obtained for chemical shift assignments, as described previously.⁴⁶⁴ Relatively short (50 ms) and long (2000 ms) contact time (τ_{CP}) were utilized to establish the ^{13}C and ^1H connectivity. 1D ^1H spectra were obtained from a direct polarization (zg) experiment. Typical pulses were 2.5 μs for ^1H and 4.0 μs for ^{13}C . A 2 ms of CP contact time and 24.6 ms acquisition time were used in each experiment. ^1H and ^{13}C chemical shifts were externally referenced to the ^1H intensity of water at 4.70 ppm and ^{13}C signal of α -Gly carbonyl signal at 176.49 ppm. All spectra were processed in TopSpin.

4.3.12 Scanning electron microscopy.

A field emission gun scanning electron microscope (FEG-SEM), JEOL 6500 equipped with an energy dispersive spectrometer (EDS) was used for morphological analyses. It has an operating range of 0.5 to 30 kV with an ultimate resolution of 1.5 nm. Secondary electron imaging was used for the mapping. The powder sample was sprinkled on an aluminum stub using a double-sided adhesive carbon tape (Ted Pella, PELCO Tabs, 12 mm OD, Prod No. 16084-1) and was coated with a thin layer (10 nm) of iridium.

4.3.13 High pressure liquid chromatography (HPLC).

To understand the chemical stability of levothyroxine sodium under different storage conditions and in the presence of excipients, HPLC analysis was performed. All chromatographic analyses were carried out using a Waters Alliance 2695 separations module equipped with degasser, quaternary pump, automatic injector, column oven and Waters 2996 Photo diode array detector. Separation was achieved using a Zorbax Eclipse XDB analytical column (150 mm x 4.6 mm id) with 5 μm particles and C18 stationary phase. The mobile phase was acetonitrile:water:trifluoroacetic acid (400:600:0.05) with a flow rate of 1 mL/min. The detector wavelength for UV absorption detection was set to 225 nm. The column was maintained at 25°C. Data was collected and analyzed using Empower 3 (Waters, PA). All samples were prepared using a solution of 0.01 M sodium hydroxide in methanol. The methanolic solution was prepared by diluting 1 mL of aqueous 1 M sodium hydroxide solution using methanol with a final volume of 100 mL.^{451,457,465} The calibration curve is presented in Supporting Information (Figure 4.11).

4.4 Results and discussion

4.4.1 Baseline characterization of LSP.

The X-ray diffraction pattern of LSP was superimposable on the diffraction pattern reported in the literature and the Powder Diffraction Files of the International Centre for Diffraction Data (QQQETG01; Supplementary Information, Figure 4.12).^{2,466} The thermal behavior, characterized using DSC and TGA, was in agreement with the literature (Figure 4.1).^{247,457} The DSC heating curve exhibited three endothermic events below 110°C all of them attributable to dehydration and vaporization of water. Based on the weight loss of 9.8% observed between RT and ~100°C, there is complete dehydration of the pentahydrate. The water content determined by KFT ($9.7 \pm 0.1\%$ w/w) was in agreement with the TGA results. The stoichiometric water content of the pentahydrate is 10.1% w/w. Based on the TGA profile, the loss of water appears to be gradual and continuous. This is supported by the DSC results, wherein overlapping endotherms were observed.

Complete dehydration of LSP appears to result in at least a partially amorphous phase. This conclusion is based on the appearance of a glass transition (T_g) event at ~156°C (Figure 4.1; inset). In a separate experiment, the sample was heated to 160°C, cooled to RT and reheated. While all the thermal events attributable to dehydration were absent, as expected, the T_g was observed. The overlapping exothermic events, observed at temperatures $\geq 200^\circ\text{C}$, could be attributed to decomposition of levothyroxine sodium.^{33,164}

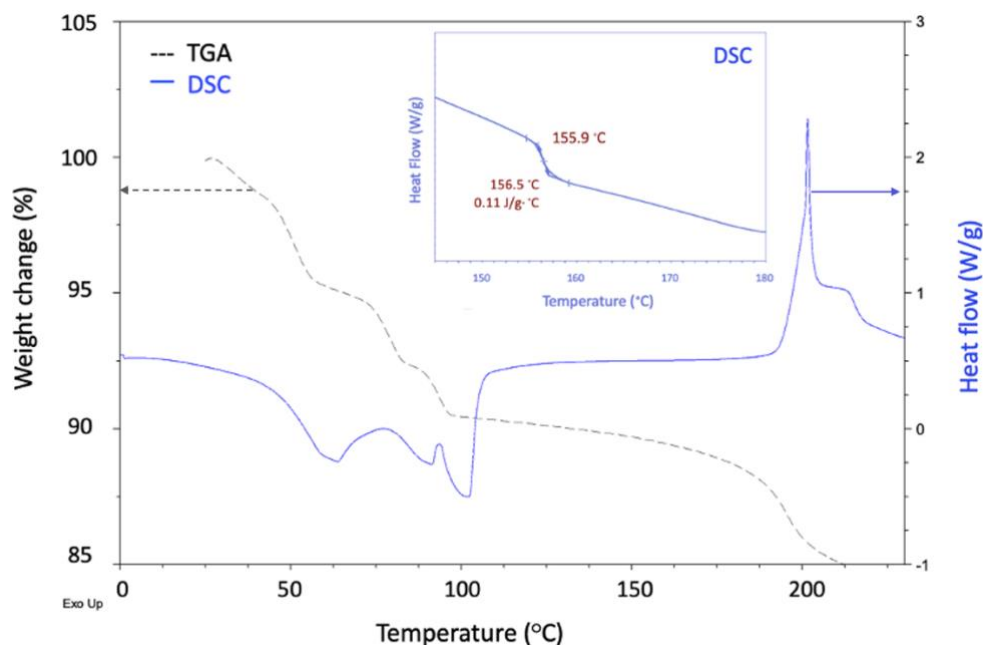


Figure 4.1. DSC and TGA heating curves of LSP. The DSC profile over the temperature range of 145 to 180 °C has been expanded in the inset.

4.4.2 Water sorption analysis.

The water sorption/desorption behavior of LSP was evaluated isothermally over the RH range of 90 to 0%, at 20, 25 and 40°C. The pentahydrate was equilibrated at 50% RH and the water vapor pressure was progressively increased. This RH was selected since LSP has been reported to undergo dehydration only below 50% RH.¹⁶⁴ After reaching 90% RH, the water vapor pressure was progressively decreased to 0%, and then increased back to 90%, and the weight was continuously monitored (Figure 4.2).

At all the three temperatures, there was no pronounced hysteresis. This becomes very clear when the desorption-sorption cycles were repeated several times at 40°C (Figure 4.2; inset). The desorption cycle aids in understanding the dehydration behavior of the pentahydrate. At 40°C, the total weight change between 90 and 0% RH was ~ 7.9% w/w with a progressive weight loss as the vapor pressure was decreased. Starting with the pentahydrate at 90% RH, when the water vapor pressure was lowered to 15% RH, the weight loss corresponds to loss of one molecule of water of crystallization (~2% w/w) indicating that levothyroxine sodium exists as a tetrahydrate at 40°C/15% RH. Below 15% RH, the sample exhibits a steep weight change and the total weight loss at 40°C/0% RH corresponds to removal of four molecules of water of crystallization (the calculated weight loss following dehydration of pentahydrate to monohydrate was 8.1%; the observed weight

loss was 7.9%). When the sample was held at 40°C/0% RH for 30 days, no further weight loss was observed indicating the resistance of the monohydrate to undergo further dehydration.

The water desorption/sorption behavior at 20 and 25°C were qualitatively similar to that at 40°C. At 20°C, a total weight change of 5.3% was observed between 90 and 0% RH. At 40°C, a much higher weight loss of 7.9% was observed. The effect of temperature became pronounced at RH < 20%. The tetrahydrate formation occurred at 20% RH at 40°C, but only at 10% RH at 20 and 25°C. The water desorption-sorption behavior is typical of a channel (or a non-stoichiometric) hydrate.^{164, 460} Levothyroxine sodium has been reported to have a ‘layered’ structure with hydrophobic sheets composed of levothyroxine and hydrophilic sheets of water along the 001 plane.²⁴² This is discussed in a subsequent section dealing with the crystal structures of levothyroxine sodium in different states of hydration.

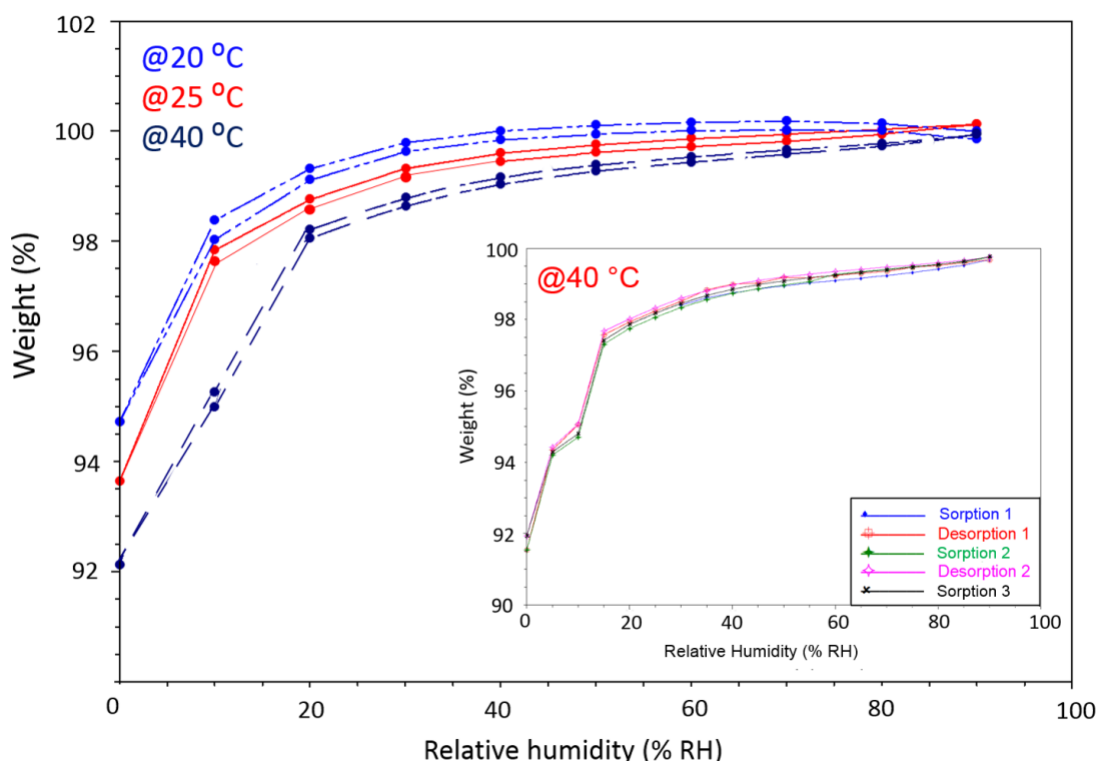


Figure 4.2. Water desorption and sorption behavior of LSP. The inset represents the isothermal water sorption/desorption at 40°C. For each cycle, the sample weight at 90% RH represents LSP (the starting material). The sample weight at other RH values were scaled accordingly. At each temperature, the lower profile was the sorption cycle.

4.4.3 Synchrotron XRD.

The diffraction patterns of the samples following storage under different conditions provided a detailed insight into the structural changes following dehydration of LSP. At 40°C/0% RH, we had earlier observed ~ 8% weight loss, leading to the formation of the monohydrate (Figure 4.2). The XRD pattern, reveals the change in lattice structure following partial dehydration (Figure 4.3). Peaks appeared at 9.2, 11.0, 12.0, 12.4 and 14.9° 2 θ . Thus, the pentahydrate to monohydrate transition is accompanied by a change in the crystal structure. The sharpness of the peaks indicates the highly crystalline nature of the monohydrate. However, when heated to 60°C/0% RH for 3 h, there was a pronounced change in the XRD pattern. There was also a loss in crystallinity, evident from the amorphous halo over the angular range of ~ 19 to 25° 2 θ . The water content of LSP, stored at 60°C/0% RH for 3 h, was ~ 1% w/w, suggesting that the sample was a mixture of LSM and anhydrous levothyroxine sodium. Heating to 85°C for 3 h caused complete dehydration. Based on our limited studies, complete water removal from the lattice by dehydration results in a partially crystalline anhydrous phase. This transition is also accompanied by a change in lattice structure. Preliminary indexing results of the sample heated to 60°C, revealed lattice contraction. The detailed characterization of anhydrous levothyroxine will be the subject of a future publication. Our DSC heating curve of the pentahydrate had revealed the appearance of a glass transition event at ~ 156°C (Figure 4.1). More comprehensive variable temperature XRD of levothyroxine sodium was conducted earlier.¹⁶⁴ When the pentahydrate was heated to 110°C, the residual crystallinity was low and at 120°C, the sample was X-ray amorphous. Interestingly, no chemical decomposition was observed, even in samples heated up to 130°C, revealing the thermal stability of this compound in the absence of molecular oxygen. This indicates that while dehydration of levothyroxine sodium is essential, it is not sufficient to induce chemical decomposition.

In another similar experiment performed at the synchrotron source *in situ*, LSP was compressed into a tablet, stored at 40°C/0% RH, and the diffraction patterns were continuously collected (Figure 4.4). In comparison to the powder patterns discussed previously, X-ray line broadening is observed for the tablets which is attributed to the compression induced loss in crystallinity. Following storage at 40°C/0% RH, pentahydrate to monohydrate transition was initiated within 30 mins and was complete in < 3 h. After 3 h, the chamber was returned to RT (~ 25°C) and the humidity of the chamber was increased to 75% RH. The transition back to the pentahydrate, initiated within the first hour of exposure to the elevated vapor pressure environment, was complete in < 3 h (Figure 4.5). Both the dehydration and rehydration kinetics under the test conditions appear

to be similar. Also, the crystallinity of the starting pentahydrate tablet to the rehydrated tablet seems comparable indicating no lattice disorder in the sample upon partial dehydration of LSP to LSM. In summary, while the monohydrate is crystalline, its complete dehydration results in a reduction in sample crystallinity. When the pentahydrate was dehydrated to the anhydrous form by heating to 85°C under nitrogen purge (in a powder diffractometer) and then exposed to 75% RH (at RT), it quickly regained moisture to convert to the stable pentahydrate but with a lower sample crystallinity (data not shown). Thus, the different hydration states are readily reversible. In another study, XRD data were collected, at 10°C intervals, when LSP was heated up to 130°C. Above 85°C, there was incremental lattice disorder with completely X-ray amorphous material observed at 120°C (Supporting information; Figure 4.13).¹⁶⁴

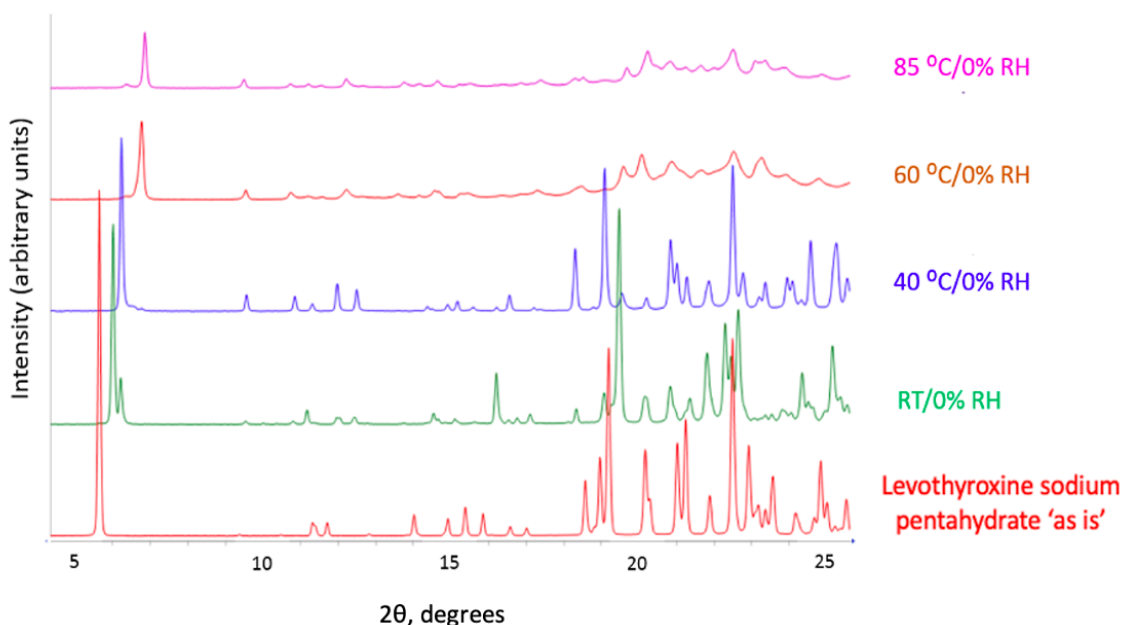


Figure 4.3. Diffraction patterns of LSP and samples analyzed following storage of LSP at different temperature/RH conditions for 3 h. The bottom pattern is that of ‘as is’ LSP. While the XRD patterns were obtained using synchrotron radiation (0.45256 Å), they were converted to Cu K α radiation (1.54 Å), so as to enable direct comparison with the reference patterns. The XRD patterns of LSP obtained following long term storage at 40°C/75% RH is presented in the supporting information (Figure 4.14).

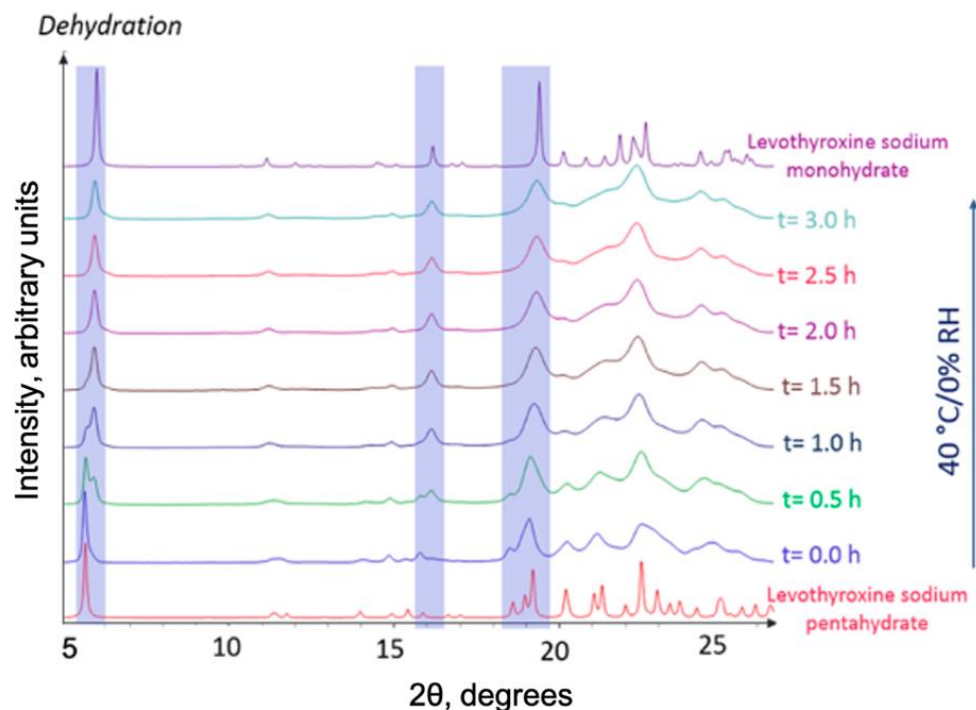


Figure 4.4. XRD patterns of an ‘as is’ LSP tablet stored at 40°C/0% RH for three hours. The experiment was performed using the temperature/humidity controlled chamber placed in the path of synchrotron beam. Selected angular ranges, where some of the characteristic peaks of LSP and LSM are observed, are highlighted. The topmost and bottommost diffraction patterns are the calculated diffraction patterns of LSM and LSP respectively. In an effort to maintain clarity, only diffraction patterns at selected time points are shown.

4.4.4 Single crystal XRD.

In order to elucidate the changes in the crystal lattice upon dehydration, the crystal structures of LSP and LSM were obtained. Crystals of LSP were grown by slow evaporation of a methanolic solution of levothyroxine sodium under ambient conditions. It is interesting that the salt crystallized as a pentahydrate, by incorporating water vapor from the atmosphere into the crystal lattice. The crystals were colorless, plate shaped and strongly birefringent (Supporting information; Figure 4.16, 4.17 and Figure 4.18).

LSP has a triclinic unit cell with the space group P1 and the unit cell parameters were in accordance with literature reports.^{242,466} The unit cell volume at 178 K was 1206.4(8) Å³. The LSP structure is perhaps better understood as the putative levothyroxine sodium tetrahydrate (LST) with two non-coordinated solvent water molecules within the hydrophilic region.²⁴² Figure 4.6 (a) depicts the

structural features of LSP. The central hexa-coordinated sodium cation and the aromatic portions of the thyroxine molecules have pseudo-inversion symmetry. The glycine fragments of the thyroxine molecules and the penta-coordinated sodium cation of Na₂ break this pseudo-symmetry. The carboxylic acid functional groups coordinate Na₁ at cis-positions while four water molecules fill the remainder of the coordination sphere. One water molecule OW₄ bridges Na₁ to Na₂. The second sodium cation is found penta-coordinated with four terminal water molecules. The present structure is in agreement with the previous reports,²⁴² with the exception of data collection temperature. At 178 K few N-H and O-H donor hydrogen atoms were located unambiguously in the difference Fourier map. Most were placed by inference based on these local hydrogen bond donor-acceptor environments. The N-H hydrogen atoms were refined positionally while maintaining a riding isotropic displacement relative to the host nitrogen atom. The water oxygen atoms exhibiting large anisotropic displacements were modelled in two disordered groups in the ratio of 0.69(3):0.31(3) with constrained isotropic displacements for the final model.

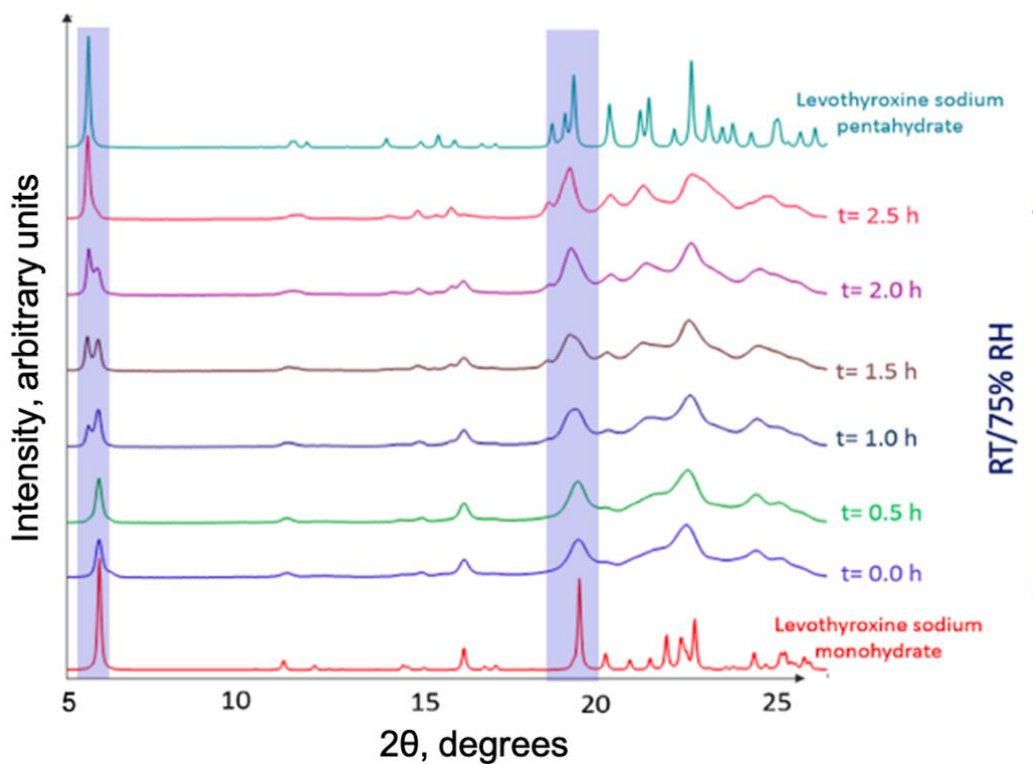


Figure 4.5. XRD patterns of levothyroxine sodium tablet stored at RT/75% RH for three hours. Before this experiment, LSP tablets had been stored at 40°C/0% RH for three hours. The results were presented in Figure 4.4. In a continuing experiment, the storage conditions were changed to RT/75% RH and the XRD patterns were collected. Selected angular ranges, where some of the characteristic peaks of LSP and LSM are observed, are highlighted. The

calculated diffraction patterns of LSP and LSM are also provided (Supporting information; Figure 4.15). The experiment was performed using the temperature/humidity controlled chamber placed in the path of synchrotron beam.

The loss of two solvent water molecules leads to the appearance of the putative LST at 40°C/15% RH in the water desorption curve. Since these water molecules are not coordinated with the sodium cations, their loss leads only to the collapse of water channels.²⁴² The water desorption curve appears to have a discontinuity whereby water loss accelerates in the continuum between LSP and LSM. We believe this water loss occurred while we monitored the diffraction experiment in the 263–268 K range resulting in the formation of LSM shown in Figure 4.6(b).

The thyroxine portions of the LSM crystal structure are similar to LSP with some flexing of torsional angles. Eight water molecules are lost as LSM forms with a reshuffling of some hydrogen bonds. There is a 64.1 Å³ decrease in the volume of the unit cell due to this phase transition (Table 4.1). The crystal structures of both LSP and LSM are uncommon in the coordination environments of the sodium cations to the carboxylate groups. In LSP, the alanine side chains on both molecules are coordinated to the same sodium cation, which in turn is bonded to the second sodium cations via a lone bridging water molecule. This structure isolates the -Na(H₂O)₅ cation fragment away from the thyroxine carboxylate groups. When water leaves the crystal lattice to form LSM, the two sodium cations and the thyroxine carboxylate groups transform to a bridged rhomboid-like assembly with each sodium cation coordinated directly to different water molecules. In LSP, the sodium cations were five- and six-fold coordinated. However, upon loss of water, the sodium cations, carboxylate groups and remaining coordinated water molecules reconstruct to form a coordinately unsaturated structure leaving the sodium cations three- and four-fold coordinated. An interesting feature of LSM is the disorder of one of the sodium cations (Na2/Na2') resulting in its partial occupancy in two different sites in the structure. This is illustrated in Figure 4.7 where the closest contacts to neighboring atoms for both Na2' are shown. The partial occupancies of Na2 and Na2' refine to a 0.69(3):0.31(3) ratio. Figure 4.7 illustrates these coordination environments. Na2' is within a void where the penta-coordinated Na2 was located in the LSP structure. As a test, if the partially-occupied Na2' atom is removed from the crystal structure, then PLATON/SOLV⁴⁶⁷ test finds the increase in void space is approximately 24.5 Å³ while Na2' makes no significant contacts with any oxygen atoms. This suggests it is disordered within this void space. A search of the CSD⁴⁶⁸ found no similar crystal structures containing two sodium cations, two carboxylic acid groups and only two water molecules in a similar arrangement comparable to LSM. This structure appears to

have unique coordination geometry not found elsewhere in the literature. These two disordered sodium positions are 1.629 Å apart.

An increase in the chemical reactivity was observed following storage of LSP at RT/0% RH.⁴⁵⁷ We had observed LSM formation under these conditions (Figure 4.2). By combining these two observations one can conclude that the monohydrate is chemically more reactive than the pentahydrate. The lattice structure, in these two hydration states, can explain the reactivity difference. In the asymmetric unit of LSP, the coordination number of one sodium cations is 5 and the second is 6. However, in LSM, the coordination numbers of the sodium cations are reduced to 3 and 4. The reduction in the coordination numbers of the sodium cations coupled with the conformational changes in the asymmetric unit, increase the risk for the sodium cations to be in close proximity to the oxidizable amino (NH₂) group, effectively activating the reaction of the amino group with atmospheric O₂. It is known that in sodium salts with easily oxidizable anions, the cation can activate this oxidation process, perhaps by initial weak coordination to the O₂ followed by rapid electron transfer to the anion.^{469,470}

The lattice modifications following the water loss can also explain the increased chemical reactivity. Following dehydration, oxygen can occupy “vacated channels” which were earlier occupied by water molecules in LSP. In other words, the water molecules in the LSP lattice exerted a “protective” effect and resisted interaction with oxygen. Following water loss and formation of LSM, the lattice is rendered “*porous and less protected*” thereby enabling interaction with oxygen. The crystal packing of LSP and LSM is provided in the supporting information (Figure 4.19). The vacated channel theory has been proposed recently.¹⁶⁴

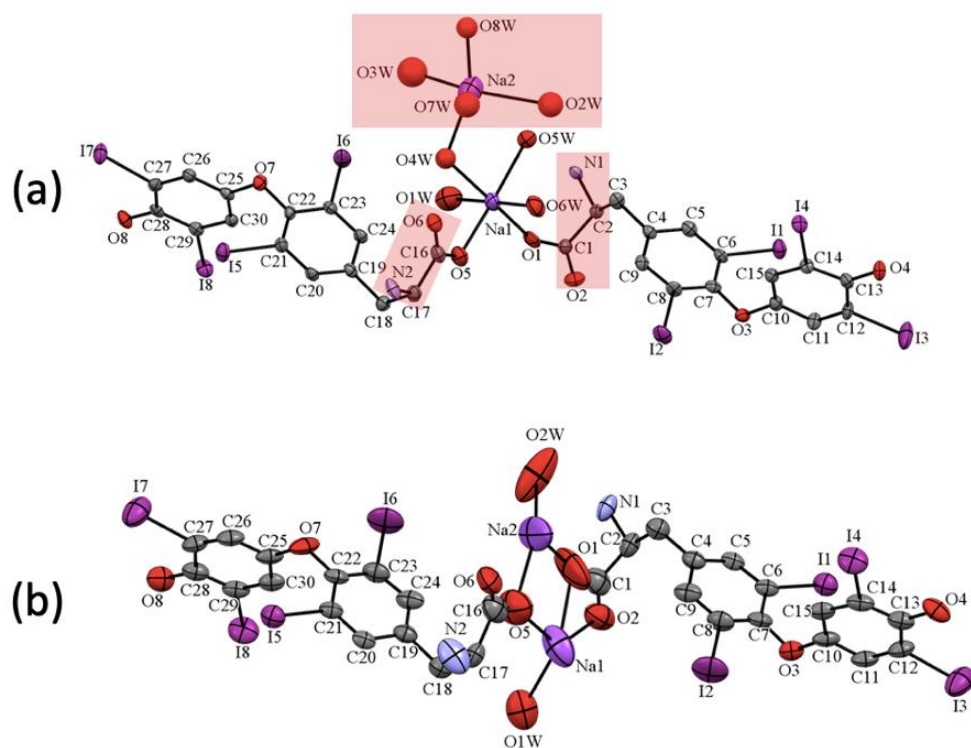


Figure 4.6. (a) LSP is displayed with anisotropic displacements drawn at 50% probability for all atoms except for water oxygens coordinated to Na2 which are drawn with isotropic displacements. The minor occupancy of these water molecules are omitted as well as all hydrogen atoms and both solvent water molecules. Atoms shaded in red break the pseudo-inversion symmetry of the two thyroxine molecules. (b) LSM is displayed with anisotropic displacements drawn at 50% probability for all atoms. The minor occupancy sites of the disordered sodium cation as well as all hydrogen atoms are omitted for clarity.²¹¹

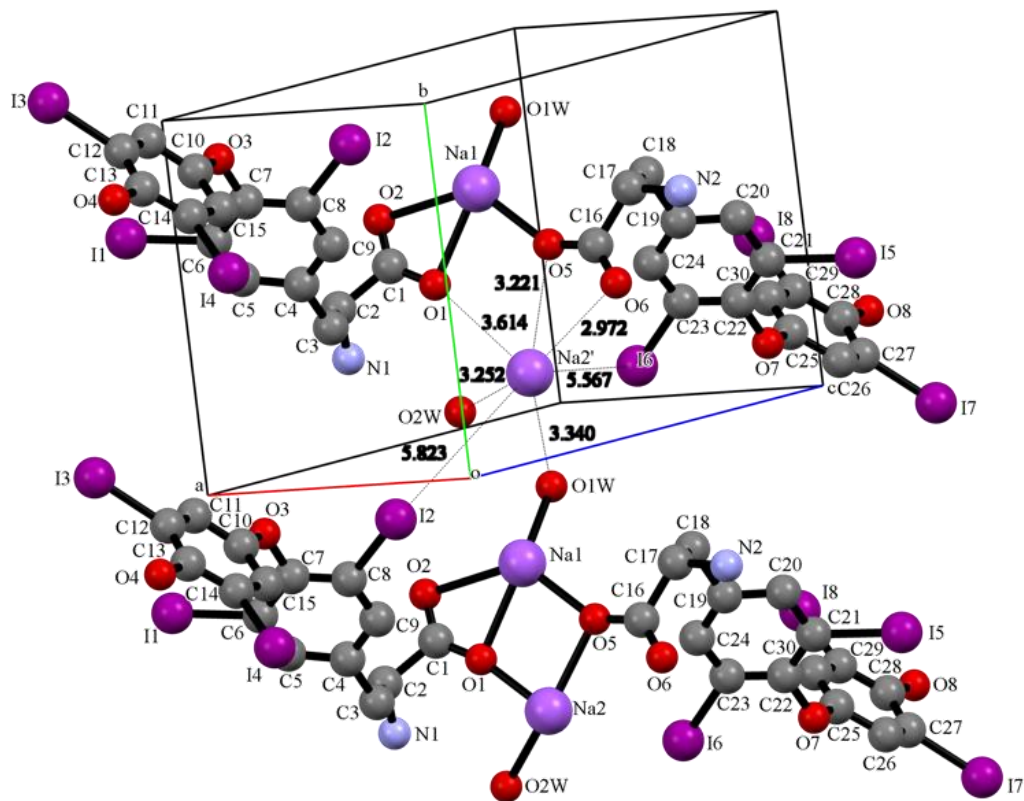


Figure 4.7. LSM is displayed in a ball and stick drawing to illustrate the non-bonded contacts (Å) found for Na2'. The non-bonding contacts between the two LSM residues above Na2' are also shown. One contact is omitted for clarity that overlaps in the foreground: Na2'... O8 (x, y, z-1) = 2.943 Å. The residue at the bottom illustrates the bonding for the major occupancy for Na2'.²¹¹

Table 4.1. Crystal data and structure refinement for LSP and LSM.

	Levothyroxine Sodium Pentahydrate	Levothyroxine Sodium Monohydrate
Identification code	LSP	LSM
Empirical formula	C ₃₀ H ₄₀ I ₈ N ₂ Na ₂ O ₁₈	C ₃₀ H ₂₄ I ₈ N ₂ Na ₂ O ₁₀
Formula weight	1777.82	1633.69
Temperature	178(2) K	268(2) K
Wavelength	0.71073 Å	0.71073 Å
Crystal system	Triclinic	Triclinic
Space group	P1	P1
Unit cell dimensions	$a = 8.151(3)$ Å $\alpha = 83.807(11)^\circ$ $b = 9.506(4)$ Å $\beta = 83.115(20)^\circ$ $c = 15.816(7)$ Å $\gamma = 85.228(12)^\circ$	$a = 8.692(4)$ Å $\alpha = 80.619(15)^\circ$ $b = 8.983(4)$ Å $\beta = 80.192(15)^\circ$ $c = 15.109(8)$ Å $\gamma = 83.420(13)^\circ$
Volume	1206.4(8) Å ³	1142.3(10) Å ³
Z	1	1
Density (calculated)	2.447 mg/m ³	2.375 mg/m ³
Absorption coefficient	5.228 mm ⁻¹	5.497 mm ⁻¹
$F(000)$	824	744
Crystal color, morphology	Colorless, Plate	Colourless, Plate
Crystal size	0.240 x 0.120 x 0.020 mm ³	0.240 x 0.120 x 0.020 mm ³
Theta range for data collection	2.161 to 30.638°	2.307 to 25.410°
Index ranges	-11 ≤ h ≤ 11, -13 ≤ k ≤ 13, -22 ≤ l ≤ 22	-10 ≤ h ≤ 10, -10 ≤ k ≤ 10, -18 ≤ l ≤ 18
Reflections collected	59915	23402
Independent reflections	14828 [$R(\text{int}) = 0.0443$]	8305 [$R(\text{int}) = 0.0609$]
Observed reflections	12984	5523
Completeness to theta = 25.242°	100.0%	100.0%
Absorption correction	Multi-scan	Multi-scan
Max. and min. transmission	0.6478 and 0.5406	0.6462 and 0.5062
Refinement method	Full-matrix least-squares on F^2	Full-matrix least-squares on F^2
Data / restraints / parameters	14828 / 380 / 546	8305 / 483 / 359
Goodness-of-fit on F^2	1.030	1.043
Final R indices [$>2\sigma(I)$]	$R1 = 0.0459$, $wR2 = 0.1021$	$R1 = 0.0713$, $wR2 = 0.1598$
R indices (all data)	$R1 = 0.0551$, $wR2 = 0.1078$	$R1 = 0.1132$, $wR2 = 0.1826$
Absolute structure parameter	-0.025(11)	0.12(3)
Largest diff. peak and hole	4.623 and -4.503 e.Å ⁻³	2.184 and -1.050 e.Å ⁻³

4.4.5 ssNMR of LSP and the dehydrated samples.

NMR chemical shifts are sensitive to the surrounding electronic environment and therefore are often utilized to probe structural changes of small organic molecules in both crystalline and amorphous forms.⁴⁷¹⁻⁴⁷⁴ XRD revealed structural differences between LSP and LSM. In this section, we utilize ^1H and ^{13}C ssNMR, as an orthogonal technique to X-ray, to investigate the dehydration induced structural perturbation of LSP from RT to 80°C at 0% RH. The chemical structure of LSP and its representative 2D ^{13}C - ^1H HETCOR spectra are shown in Figure 4.8(a) and Figure 4.20, respectively. In the 2D spectra, 1D ^{13}C and ^1H spectra are exhibited as projections in direct and indirect dimensions, respectively. The sample for 2D spectra (Supporting Information; Figure 4.20) is LSP powder stored at 40°C/0% RH for 3 h, the condition to cause LSP \rightarrow LSM transition. The 2D experiments facilitated the ^{13}C resonance assignments, which are critical for probing site-specific structural details.⁴⁷⁵ For example, the C1 shows correlations with aliphatic protons (H2/3) at a short mixing time at 50 ms and with aromatic protons at a relatively long contact time at 2000 ms.

Two sets of ^{13}C peaks are observed as expected since two LSP molecules in an asymmetric unit are non-identical and are known to exist in different conformations as shown in Figure 4.6.⁴⁷⁶⁻⁴⁷⁸ Tentative ^{13}C assignments are based on a solution NMR study⁴⁷⁹ and a combination of 1D ^{13}C and 2D ^{13}C - ^1H correlation experiments, as previously described.⁴⁶⁴ 2D spectra observe mostly one-bond correlations when utilizing a short CP transfer time (τ_{CP}) at 50 ms and demonstrate multi-bond connectivity at a relatively long 2000 ms transfer.

Table 4.2, in the supporting information, summarizes the chemical shifts of LSP stored at RT/0% RH and 85°C/0% RH. For example, the peaks at 175.9 and 173.5 ppm are attributed to the carboxylate carbons (C1). The peaks between 36.0 and 35.4 ppm are ascribed to the aliphatic side chain carbon (C2) directly bonded to the carboxylate and amine groups, while the peaks at 57.7 and 55.8 ppm are due to the aliphatic carbon (C3) attached to the tyrosine ring.

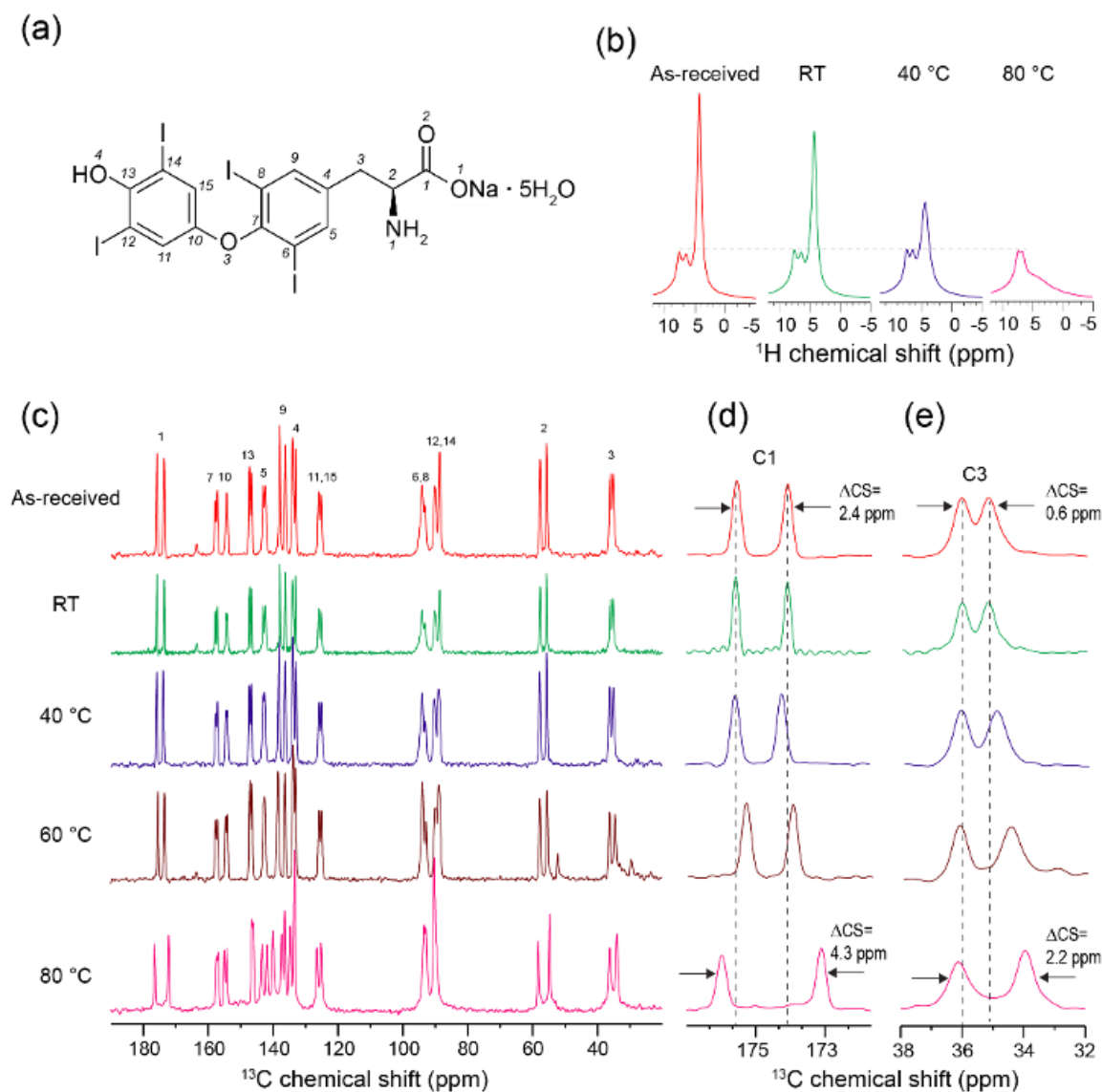


Figure 4.8. (a) Chemical structure of LSP. (b) 1D ^1H spectra of LSP powder and samples stored under different temperatures at 0% RH for 3 h. ^1H spectra are normalized by aromatic peaks of LSP at approximately 5-10 ppm. Note the gradually decreased intensity of the sharp water peak at ~ 4.55 ppm for samples stored at higher temperatures. (c) \rightarrow (e) 1D ^{13}C spectra of LSP powder and samples stored under different temperatures (0% RH) for 3 h. (c) Full spectra; and enlarged spectra of C1 (d) and C3 (e). Note the two sets of peaks from the two conformers in the crystalline lattice. The corresponding XRD patterns under these conditions are provided in Figure 4.3.

As-received LSP samples are stored at RT, 40°C, 60°C and 80°C in the desiccator (0% RH) for 3 hrs. The decreasing intensity of the water peak at approximately 4.39 ppm identifies the dehydration process, as shown in Figure 4.8(b). Specifically, the water peak gradually decreased when storing at higher temperatures and is significantly suppressed in the sample stressed at 80°C (i.e. a partially crystalline anhydrous phase). To elaborate the site-specific conformational change, we examine the ^{13}C chemical shift changes of these stressed samples in Figure 4.8 (c-e). The comparison indicates that the spectra of as-received LSP (red) and the one stored at RT (green) were very similar, despite the water loss. Discernible peak shifts start to appear, e.g. for C1 (b) and C3 (c), when dehydrating at 40°C and 60°C. Additional peaks are observed at 52.2 ppm and 29.6 ppm for the sample stored at 60°C (dark orange). Complete dehydration of LSP, observed following storage at 80°C (discussed earlier in the context of Figure 4.3), caused a more significant change in the ^{13}C NMR spectrum. This includes global chemical shift changes and additional peaks in the aromatic region. Moreover, samples stored up to 60°C show the relatively narrow peaks in ^{13}C spectra, suggesting high crystallinity. The spectrum of the fully dehydrated sample (80°C) exhibits observable broad baseline, e.g. in the aromatic region from 120 to 160 ppm, suggesting minor contents of conformational disorder. It is instructive to point out the similar pronounced changes in the XRD patterns when the LSP was heated to 80°C (Figure 4.3). We are currently using X-ray diffraction and ssNMR coupled with a simulated annealing approach to obtain the structure of anhydrous levothyroxine sodium.

The chemical shift differences (ΔCS), or peak splitting, of the two conformers of LSP samples stored at RT and 85°C are included in the supporting information (Table 4.3), and examples of ΔCS values, under all dehydration conditions, are plotted in Figure 4.9. First of all, the pentahydrate to monohydrate transition at 40°C has induced minor spectral changes, e.g. the Δ chemical shift of C2 and C3 in Figure 4.9. Moreover, the three aliphatic side chain carbons (C1, C2 and C3) and an aromatic carbon (C5) show pronounced changes in the chemical shift differences between the two conformers upon full dehydration at 80°C. For most other carbons, e.g. C7, C10, C13 and C12, C14, the peak splitting values are similar to that of the as-received samples. It is noteworthy that C1, C2 and C3 carbons are in close proximity to the bonded water molecules. Hence, it is not surprising that they are expected to experience pronounced changes in the chemical environment (and hence, chemical shifts) upon dehydration of the crystal lattice.

The changes in the peak positions for all carbon atoms can also be explained by the high conformational flexibility of the molecules.⁴⁸⁰⁻⁴⁸² For example, the conformational difference of dihydropyridine variants are observed by ^{13}C peak splitting in a combined X-ray and ssNMR study.⁴⁸³ Previous studies of levothyroxine have indicated the existence of two different

conformations for the biological “free” or unionized form.^{476,477} These conformations differ in the orientation of the diiodophenyl ring with respect to the amine group (cisoid and transoid conformers). In our study, examples of torsion angle differences between LSM and LSP are measured from the crystalline structures in Figure 4.6 and summarized in Table 4.2. The torsion angle χ [N1-C2-C1-O1] exhibits the largest change by 20.9°, confirming the conformational change as a result of the distinct proximity to sodium cations and water molecules. A future study, where LSP is subjected to controlled temperatures and humidity conditions in the NMR magnet, can provide insight into the conformational change under in situ conditions.^{484,485}

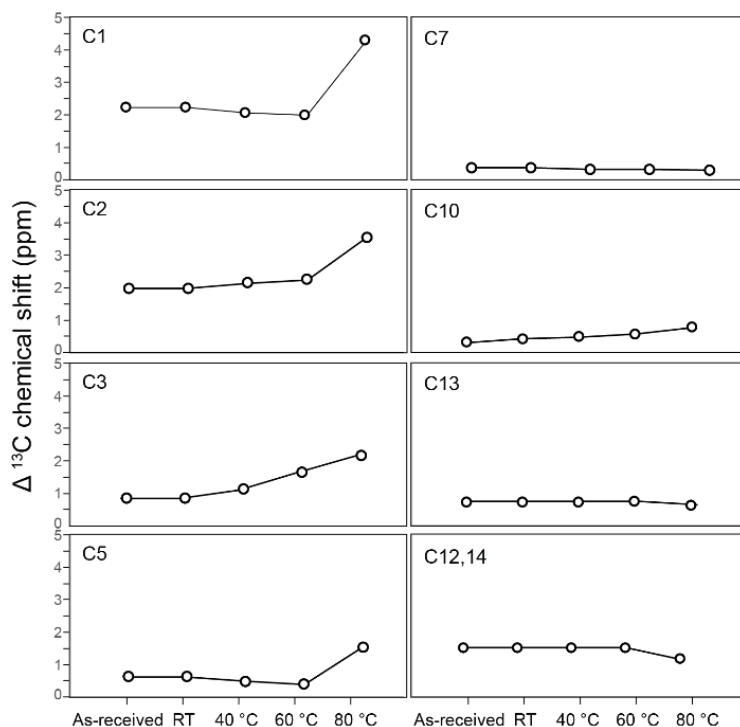


Figure 4.9. ^{13}C chemical shift differences (Δ) of the two conformers in the crystalline lattice for C1, C3, C5, C7, C10, C13, and C12, C14 in the spectra of LSP powder samples stored at different temperatures (at 0% RH) for 3 h.

Table 4.2. Conformational perturbations as observed from the different torsional angles (χ) between LSP and LSM.

Torsion angles (χ)	LSP (degrees)	LSM (degrees)	$\Delta \chi$ (degrees)
N1-C2-C1-O1	-49.4	-70.3	20.9
N1-C2-C3-C4	-161.9	-160.5	-1.4
C1-C2-C3-C4	75.8	77.7	-1.9
C2-C3-C4-C5	80.6	79.3	1.3
C6-C7-O3-C10	73.8	83.3	-9.5
C7-O3-C10-C11	-144.2	-149.2	5.0

4.4.6 Evaluating the physical stability of LSP in a “drug product” environment.

As discussed, LSP undergoes partial dehydration to the monohydrate under conditions that are realistic, and reflective of pharmaceutical processing and drug product storage (Figures 4.3-4.5). Previous studies have postulated that the formation of the monohydrate will precede chemical decomposition of the API in the formulated drug product.⁴⁵⁷

Recently, there have been reports of modifications in levothyroxine formulations including the addition of citric acid, an acidic excipient.^{258,486} Therefore, our interest was to study the influence of an acidic, highly crystalline and hygroscopic excipient on the phase behavior of LSP. We also wanted to check the possibility of moisture transfer from LSP to the excipient. Such a transfer could result in the formation of LSM in the drug product. The *in situ* formation of LSM could plausibly explain the chemical instability and product recall reported in commercial levothyroxine formulations.

The first excipient of interest was citric acid. Unfortunately, citric acid is characterized by a low deliquescence RH (75% RH at 25°C).⁴⁸⁷ Thus, its tendency for pronounced water sorption at RH \geq 75%, could pose problems in our experimental work. On the other hand oxalic acid had the attributes desired in an excipient. Oxalic acid, undergoes deliquescence at a much higher RH $>$ 98% (20°C).^{488,489} Oxalic acid, depending on the water vapor pressure in the atmosphere, exists either in the anhydrous form or as a dihydrate (at RT). Oxalic acid anhydrate is known to transition

to the dihydrate form at $RH \geq 12\%$ (20°C).^{488,490} Oxalic acid was therefore used as the model acidic excipient. Thus, in a LSP-oxalic acid mixture, there is potential for water transfer from the drug to the excipient.

In an effort to simulate a drug-excipient mixture in a tablet formulation, a physical mixture of LSP and oxalic acid (1:1 w/w) was prepared and stored at 40°C in a hermetically sealed pan. In this “closed” setup, any water released by the dehydration of LSP will not be able to leave the pan and will increase the RH of the headspace. The oxalic acid can sorb the water and transform to the dihydrate. If this process continues, there will be continuous moisture transfer from the drug to the excipient.

When LSP-oxalic acid mixture was stored in a hermetically sealed pan, LSP rapidly transformed to LSM within 14 days (Figure 4.10). It is evident from Figure 4.2 that if the headspace RH is $< 20\%$ (40°C), there will be rapid dehydration of LSP. We therefore postulate that, when the LSP – oxalic acid mixture was placed in a pan and sealed hermetically and stored at 40°C , the initial headspace RH was $< 20\%$. This low RH would have triggered the dehydration of LSP. The water released by the dehydration of LSP, would raise the headspace RH in the hermetic pan. The anhydrous oxalic acid is expected to sorb the water from the headspace. Oxalic acid anhydrate is known to transition to the dihydrate form at $RH \geq 20\%$ (5°C).⁴⁸⁸ Thus there would be a continuous transfer of water from levothyroxine to oxalic acid as is evident from Figure 4.10. The data indicates physical transformation in both the API (i.e. LSP \rightarrow LSM) and the excipient (oxalic acid to oxalic acid dihydrate). LSP is characterized by unique peak at $5.6^\circ 2\theta$. After 14 days, this peak disappeared and characteristic LSM peak appeared at $6.5^\circ 2\theta$. Oxalic acid anhydrate to dihydrate transition is evident from the disappearance of the peaks at 23.5 and $18.5^\circ 2\theta$, and appearance of peaks of 14.98 and $18.78^\circ 2\theta$. Thus, we observe partial dehydration of the API and hydrate formation in the excipient. It is noteworthy that this moisture transfer and incorporation of water in the lattice of the excipient occurs in a ‘static’ environment as the physical mixture was sealed hermetically in a DSC pan. The dehydration can be expected to be faster and more pronounced in an actual formulation due to the very low API concentration.

The conversion of LSP \rightarrow LSM cannot be identified using conventional solution based assays. The liquid chromatographic methods, conventionally used to assess the chemical stability of levothyroxine, cannot distinguish between the different physical forms of levothyroxine sodium. There was no detectable chemical decomposition following storage in a hermetically sealed pan after 28 days.

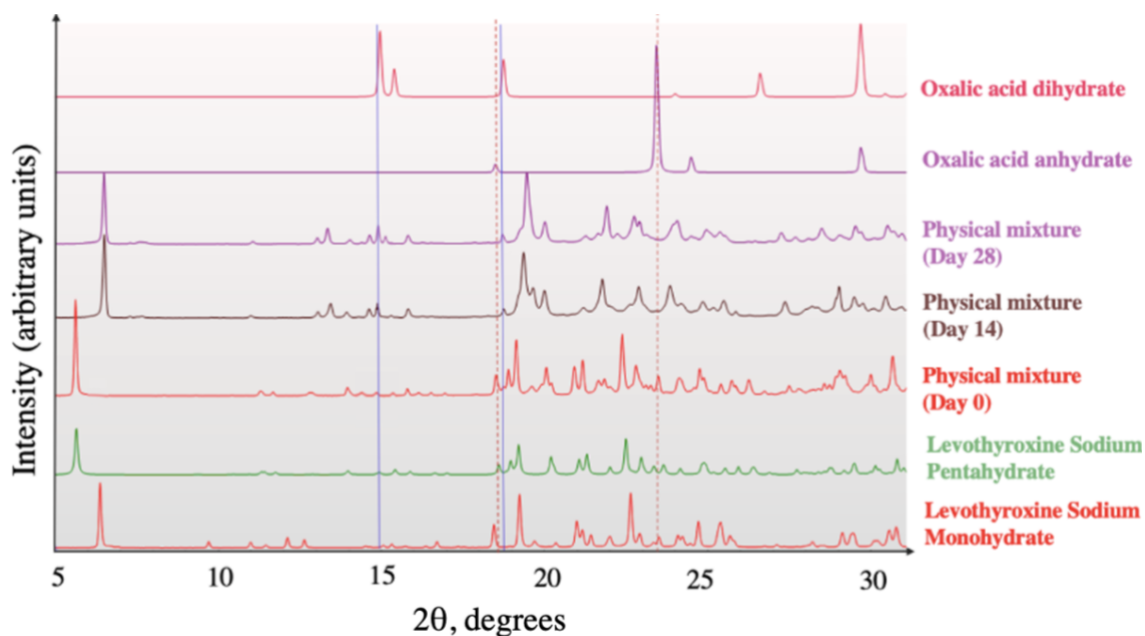


Figure 4.10. Overlay of XRD patterns of physical mixtures prepared using LSP and oxalic acid (1:1 w/w), and stored in hermetically sealed pans at 40°C. Dotted lines and solid lines represent characteristic peaks of oxalic acid and oxalic acid dihydrate, respectively.

4.5 Significance

As discussed in the Introduction section, the chemical stability of levothyroxine appears to be governed by its physical form.^{164,457} LSP resisted oxidation under elevated temperature and water vapor pressure (60°C/75% RH). However, when dehydrated, it underwent oxidative decomposition even at RT. These results suggest that the chemical decomposition is preceded by dehydration of LSP. Therefore, the goal of our work was to understand, at a structural and molecular level, the high reactivity of the dehydrated product of LSP and identify conditions of LSP dehydration.

In this work, we have characterized a new crystal form of levothyroxine sodium, levothyroxine sodium monohydrate (LSM). Under “modest” and realistic storage conditions of 40°C/0% RH, the pentahydrate to monohydrate transition occurred in < 3 h. It is noteworthy that the crystal structures of the two forms are different. The crystal structure of the monohydrate provides insights into its high chemical reactivity. The increased reactivity of LSM can be explained by one or more mechanisms: (i) oxygen occupying the sites previously held by water, (ii) a decrease in the coordination number of sodium cations, and (iii) dehydration-induced conformation changes in the molecule resulting in an increased propensity of the amino moiety to undergo oxidation.

It is clear from our studies that the LSP → LSM can occur in the final drug product (for example, tablets). In a drug product this may occur under two conditions: (i) If the LSP particles “perceive” a dry microenvironment. (ii) The LSP particles are in intimate contact with hygroscopic excipients. While we observed dehydration in presence of anhydrous oxalic acid, several other excipients are known to be hygroscopic. This includes superdisintegrants, diluents and binders.⁴⁹⁰

If LSM appears to be necessary for chemical decomposition, our efforts can be directed towards preventing dehydration of the active in drug products. It is well known that the concentration of levothyroxine sodium in drug products is low. This presents challenges but also provides opportunities for formulation modifications. The major challenge with formulating a low dose API is the high excipient burden which means that the excipients will govern the formulation properties. Hence, stable drug product design mandates diligence in excipient selection. Excipients promoting dehydration of the API must be avoided. Strategies such as surface coatings for API particles can also be explored to mitigate the risk of dehydration.

4.6 Conclusions

Levothyroxine sodium pentahydrate (LSP) is the standard treatment option for patients suffering from hypothyroidism. However, there is a limited understanding of the physical and chemical stability of LSP, leading to continued product recalls. The present work evaluated changes in the physical form of LSP under varying conditions of temperature and vapor pressure. Our X-ray diffraction results indicate a change in the crystal structure of levothyroxine sodium upon dehydration of the pentahydrate salt to the monohydrate form (LSM) at 40°C/0% RH. LSM has a higher chemical reactivity than LSP. The formation of LSM in a drug product is therefore detrimental to its chemical stability. This work underlines the importance of comprehensive physical form characterization in preformulation and formulation development.

4.7 Supporting information

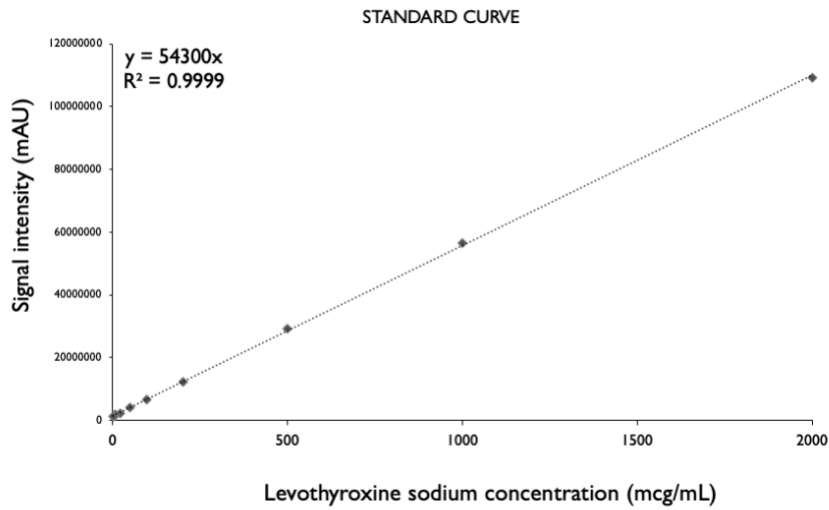


Figure 4.11. HPLC calibration curve for LSP prepared by dissolving LSP in an alkaline methanolic solution (discussed in depth in materials and methods).

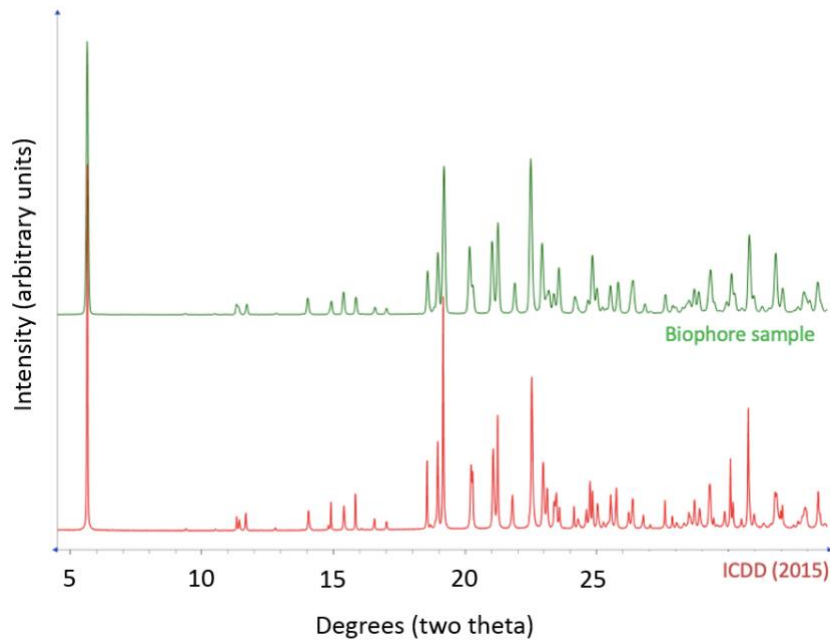


Figure 4.12. Reported and experimental X-ray diffraction pattern of levothyroxine sodium pentahydrate (LSP).⁴⁶⁶

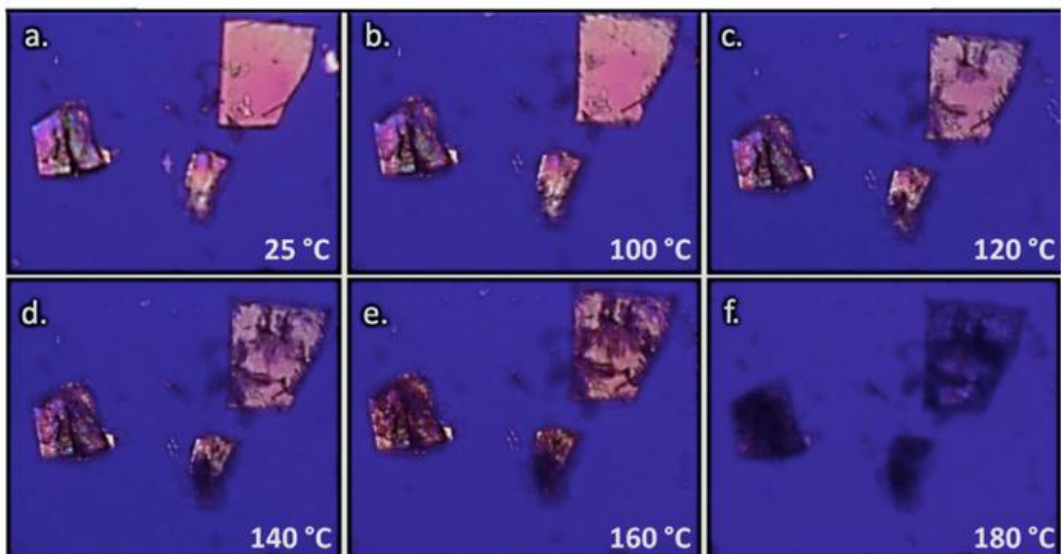


Figure 4.13. Hot stage microscopy of LSP crystals.

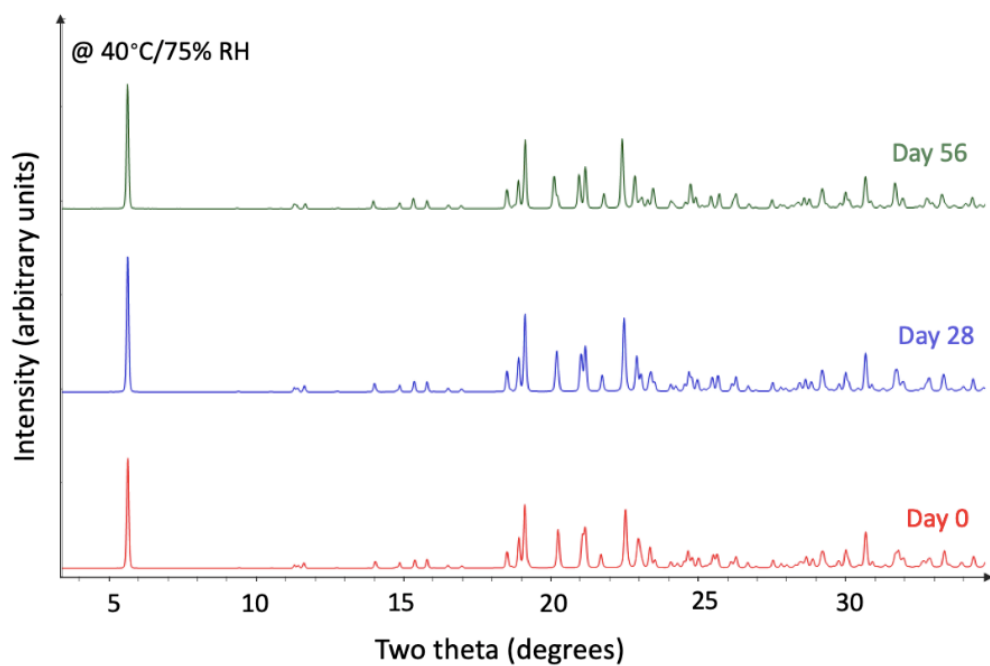


Figure 4.14. Overlay of the XRD patterns of LSP stored at 40°C/75% RH.

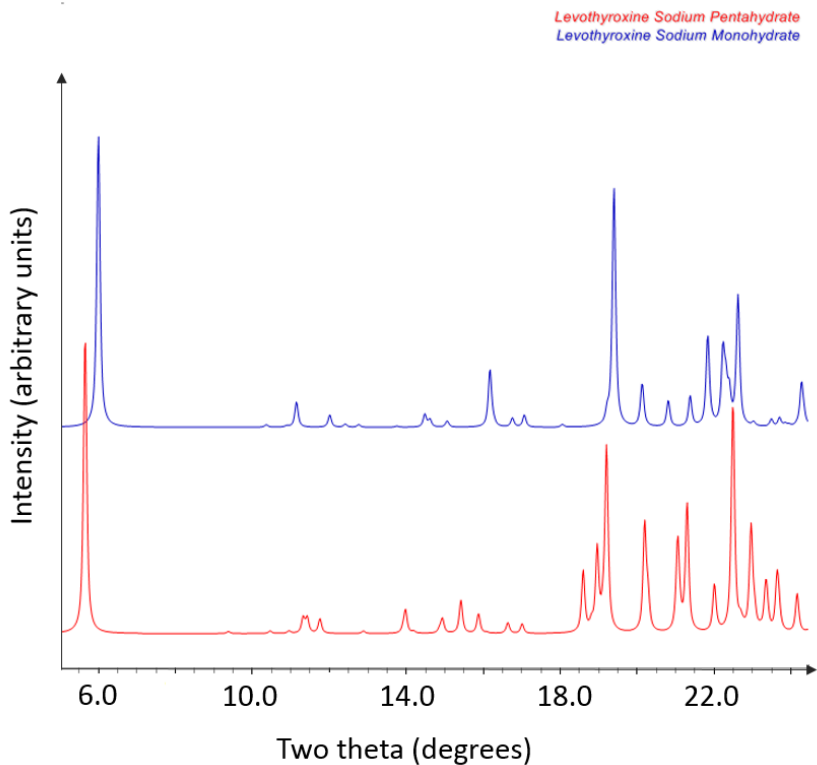


Figure 4.15. Calculated powder diffraction patterns for LSP and LSM. The powder patterns have been calculated in Mercury using the experimentally generated single crystal files. The pattern of LSP generated from the single crystal file shows an excellent overlap with the powder patterns (reported and experimental) shown in Figure 4.12.

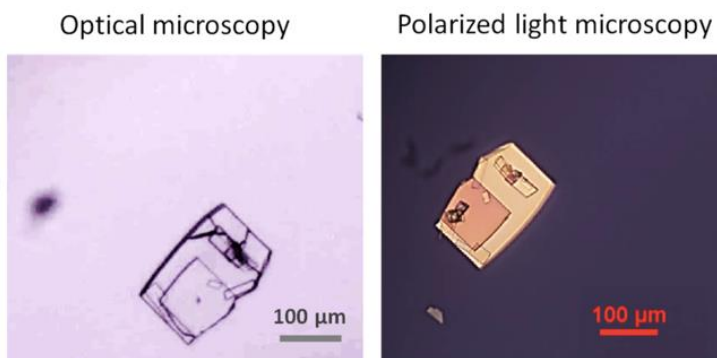


Figure 4.16. Optical and polarized light microscopic images of LSP.

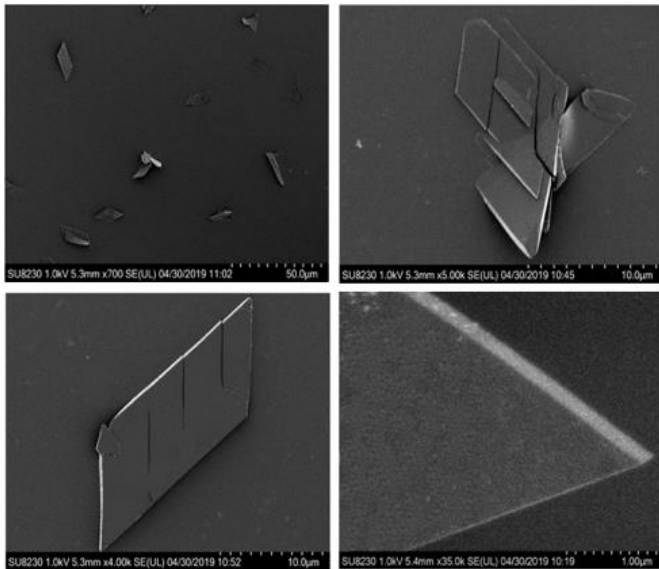


Figure 4.17. SEM images of LSP crystallized using methanol.

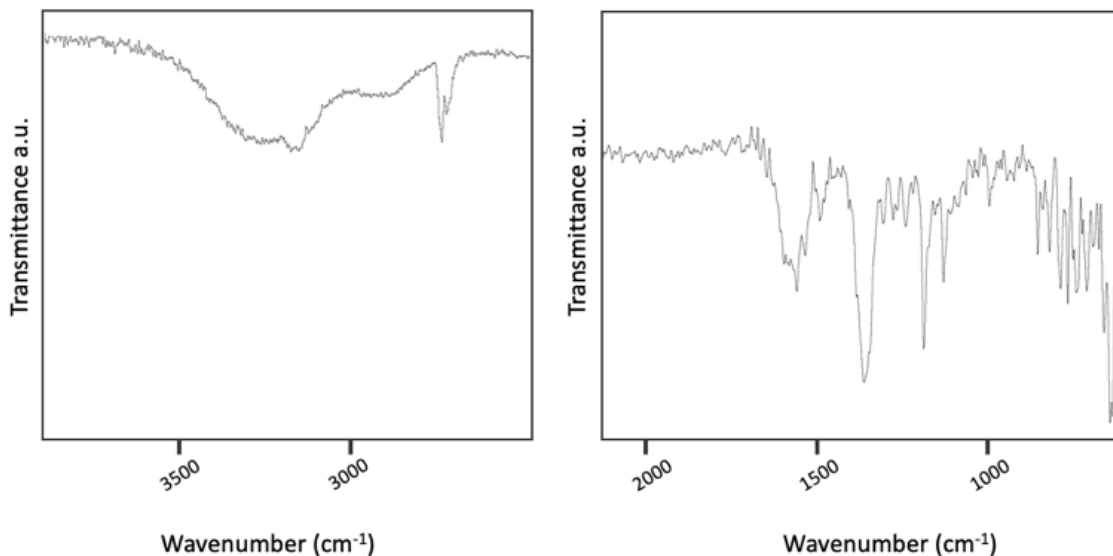


Figure 4.18. ATR-FTIR spectrum of LSP.

The broad band, in the 3200 and 3500 cm^{-1} region, represents the O-H stretching vibration due to the water of crystallization. The ether between the two aromatic rings is present at 1232 cm^{-1} . The stretching vibration for the C-O group appears between 1230-1140 cm^{-1} and the in plane deformation for the O-H group appear between 1410 and 1310 cm^{-1} . The characteristic asymmetric stretching and symmetric stretching vibration for the carboxylate anion appears around 1580 cm^{-1} and 1395 cm^{-1} respectively. Vibrations for the N-H and C-N group appear around 3400-3200 cm^{-1} and 1054 cm^{-1} , respectively. The N-H bending is observed at 1630 cm^{-1} .

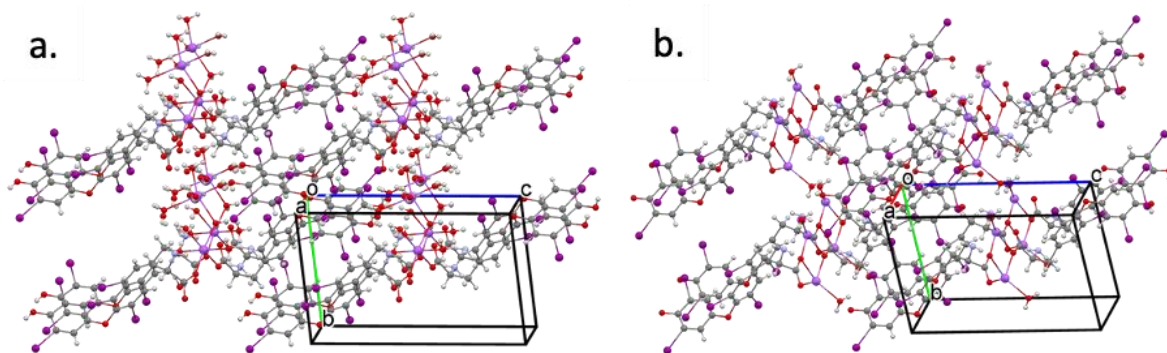


Figure 4.19. Crystal packing of LSP (a) and LSM (b).

In these multiple unit cell views, LSP has hydrophilic planes (010) separated by the hydrophobic regions made up of the aromatic groups along the *c*-axis. Water can easily be desorbed parallel to the *a*- and *b*-axes. LSM retains the same hydrophilic and hydrophobic regions, but it is noticeably less dense. Water can be readily sorbed to reform LSP or desorbed to form LSA.

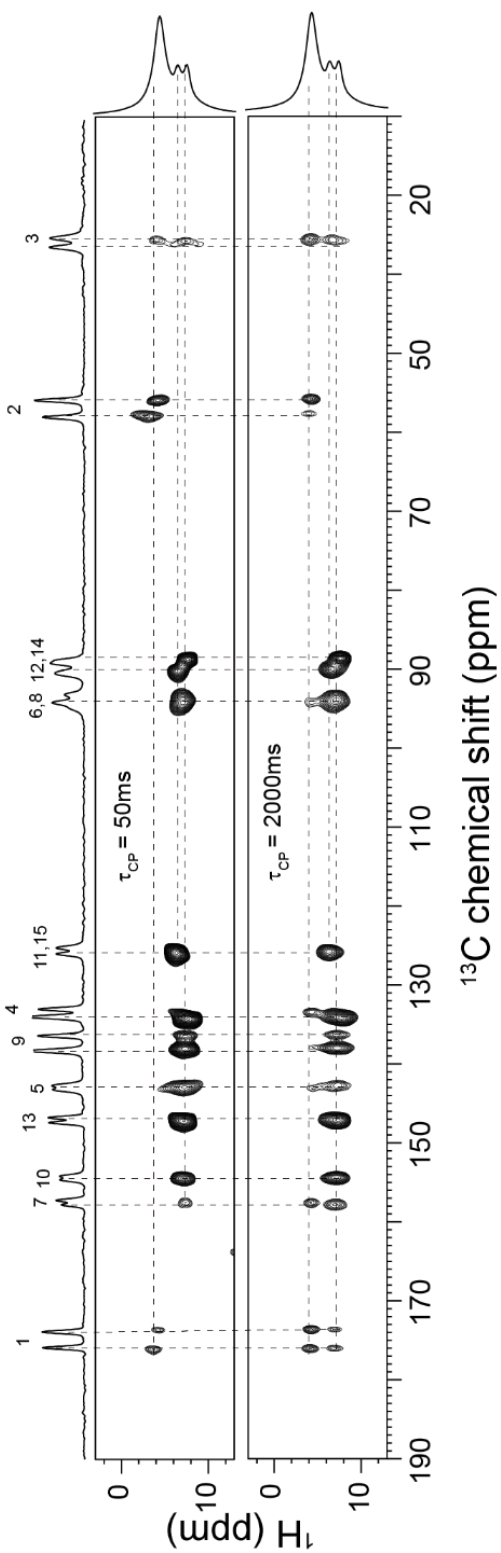


Figure 4.20. Representative 2D ^{13}C - ^1H HETCOR spectra of LSP, with 1D ^{13}C and ^1H spectra shown as projections in direct and indirect dimensions, respectively.

Table 4.3. ^{13}C chemical shifts (CS) of LSP samples stored at RT/0% RH and 85°C/0% RH, and the chemical shift differences (ΔCS) of the two conformers for each carbon.

Carbon No.	RT/0%RH		85°C /0%RH	
	CS (ppm)	ΔCS (ppm)	CS (ppm)	ΔCS (ppm)
1	175.9, 173.5	2.4	176.5, 172.2	4.3
2	57.7, 55.8	1.9	58.2, 54.7	3.5
3	36.0, 35.4	0.6	36.2, 34.0	2.2
4	134.1, 133.3	0.8	134.7, 133.4	1.3
5	143.1, 142.4	0.7	146.1, 143.4	2.7
6, 8	94.2, 93.4	0.8	93.4, 92.8	0.6
7	158.0, 157.3	0.7	157.4, 156.9	0.5
9	137.9, 136.3	1.6	137.3, 136.4	0.9
10	154.5, 154.1	0.4	155.0, 154.2	0.8
11, 15	126.1, 125.4	0.7	126.4, 125.2	1.2
12, 14	90.0, 88.5	1.5	90.3, 89.4	0.9
13	147.3, 146.7	0.6	146.5, 146.1	0.4

CHAPTER 5

Chapter 5. Investigating the influence of excipients on the stability of levothyroxine sodium pentahydrate.

*Reprinted with permission from Kaur, N., & Suryanarayanan, R. Investigating the Influence of Excipients on the Stability of Levothyroxine Sodium Pentahydrate. Mol Pharm. Copyright (2021) American Chemical Society.

5.1 Synopsis

A range of tablet excipients were evaluated for their influence on the physical form and chemical stability of levothyroxine sodium pentahydrate (LSP; $C_{15}H_{10}I_4NNaO_4 \cdot 5H_2O$). LSP-excipient binary powder blends were stored under two conditions – (a) in hermetically sealed containers at 40°C, and (b) at 40°C/75% RH. Using synchrotron X-ray diffractometry (XRD), the disappearance of LSP could be quantified and the appearance of crystalline levothyroxine (free acid) could be identified. Under hermetically sealed conditions (40°C), hygroscopic excipients such as povidone induced partial dehydration of LSP to form levothyroxine sodium monohydrate (LSM). When stored at 40°C/75% RH, acidic excipients induced measurable disproportionation of LSP resulting in the formation of levothyroxine (free acid). HPLC analyses of drug-excipient mixtures revealed that lactose monohydrate, microcrystalline cellulose and croscarmellose sodium caused pronounced chemical decomposition of LSP. On the other hand, magnesium stearate, sodium stearyl fumarate and alkaline pH modifiers did not affect the physical and chemical stability of the API following storage at 40°C/75% RH. HPLC, being a solution based technique, revealed chemical decomposition of the API but the technique was insensitive to physical transformations. Excipient properties such as hygroscopicity and microenvironmental acidity were identified to be critical determinants of both physical and chemical stability of LSP in a drug product. For drugs exhibiting both physical and chemical transformations, simultaneous solid-state and solution based analyses will enable comprehensive stability evaluation.

5.2 Introduction

Levothyroxine is the synthetic form of the endogenous hormone, thyroxine (T4), which regulates numerous physiological, metabolic, cardiovascular and neurological functions. In instances of hypothyroidism, patients require levothyroxine supplementation, often via oral administration.^{442,491,492} Levothyroxine is typically administered as immediate release tablets of levothyroxine sodium pentahydrate (LSP). It is a low dose drug with levothyroxine sodium content ranging from 25 to 300 µg per tablet.⁴⁹³⁻⁴⁹⁶ It is also a narrow therapeutic index drug, thereby

mandating precision and accuracy in the amount of drug administered to the patient.^{15,55,181,275,497-500}

Levothyroxine is one of most prescribed drugs in the United States.⁵⁰¹ However, the active pharmaceutical ingredient (API) can be unstable in drug products. Since its first introduction into the US market in 1955, there have been numerous instances of recalls of LSP tablets. These were predominantly due to chemical instability of the API and content non-uniformity in tablets.¹³⁴⁻¹⁴⁴ In an effort to reduce the variability in quality across manufacturers, in 2007, the FDA tightened the assay specifications for levothyroxine tablets from $100 \pm 10\%$ to $100 \pm 5\%$ of the labelled amount.^{156,158} There continue to be market recalls of the product due to unacceptable levels of chemical decomposition of the API in the formulation.^{131,502,503}

The physical and chemical stability of LSP ‘as is’ and in marketed drug products has been the subject of numerous publications.^{164-166,247,456,504} Levothyroxine is sensitive to chemical decomposition by light, pH, temperature, water and oxygen. The solution state chemical stability of LSP is influenced by pH and temperature with high levels of decomposition observed as the temperature is raised and the pH of the solution is decreased. The ability of lattice water to prevent oxidative decomposition of LSP in the solid-state has been the subject of multiple investigations.^{165,245} Loss of lattice water led to instability of the API in the drug product. A recent study by Kaur *et al*⁵⁰⁴ revealed changes in the crystal structure following partial dehydration of LSP to levothyroxine sodium monohydrate (LSM), and its consequent influence on chemical stability in the solid-state. LSP dehydrated under “modest” storage conditions. For example, when it was stored (‘as is’) at 40°C/0% RH, or as a physical mixture with hygroscopic excipients in hermetically sealed containers at 40°C.

In addition to formation of LSM, there is risk of disproportionation of the sodium salt to the free acid form of levothyroxine in the solid-state. Salt disproportionation is a solution mediated reaction and is expected to occur at the sorbed water interface between the drug and excipient particles in the formulation. As the microenvironmental acidity at the particle interface drops below the pH_{max} of LSP (9.05), there is potential for the sodium salt (anion) to convert to the free acid (unionized form).⁵⁰⁵ pH_{max} is defined as the pH of maximum solubility (in the solution state) and at pH_{max} , the salt and free acid coexist in equilibrium. For salts of weak acids (such as LSP), if the pH of the microenvironment drops below the pH_{max} , salt disproportionation will occur. In the presence of routinely used excipients, disproportionation of salts in the solid-state has been documented.⁵⁰⁶ The risk of excipient-induced salt disproportionation is especially high in the present case since excipients essentially constitute the entire dosage form. We believe that this is the first report of salt disproportionation in LSP tablets. There is abundant evidence of the detrimental effect of salt

disproportionation on drug product performance.^{9,11,381,507} Changes in the solid form during product development and storage also indicate a loss of regulatory process control.

It is well recognized that the excipients can have a significant impact on API stability in a drug product.⁵⁰⁸⁻⁵¹⁰ API-excipient incompatibility or interaction, during manufacture or shelf storage, can result in product failure. The potential for dehydration or disproportionation of LSP in a drug product mandates a detailed investigation. The USP assay of LSP is a solution based HPLC method wherein the drug is dissolved in a methanolic sodium hydroxide solution.²¹⁴ Dissolution of the API leads to complete loss of the solid-state information of interest. Additionally, dissolution in an alkaline medium will convert any free acid, which may have formed due to disproportionation of LSP, to the ionized form. Hence, both dehydration and salt disproportionation reactions will go undetected with the official HPLC method used for levothyroxine assay.

The chemical stability of LSP in solid dosage forms was studied in 2003 by Patel *et al.*¹⁶⁶ The API 'as is' was stable under accelerated stability testing conditions (40°C/75% RH) for 6 months. However, it exhibited pronounced chemical decomposition in the presence of numerous diluents (microcrystalline cellulose, dibasic calcium phosphate, lactose, mannitol and starch). Excipient hygroscopicity and microenvironmental acidity were reported to be critical determinants of API instability. In another work, API-excipient compatibility testing was performed using binary mixtures with an API to excipient weight ratio ranging between 1:1 and 1:100 w/w. The authors concluded that povidone, crospovidone and sodium lauryl sulfate (SLS), due to their hygroscopicity, induced pronounced API decomposition. While numerous excipients were studied, the work had some limitations which render its extrapolation to actual formulations challenging. The binary mixtures contained "excess" water and were stored at 60°C. Under the proposed test conditions, even the 'as is' API exhibited pronounced decomposition.²⁴⁷

There is a limited understanding of the influence of formulation composition, processing and storage conditions on the stability of LSP in a drug product. The goal of our work is to systematically investigate and understand the influence of excipients and storage conditions on the physical and chemical stability of LSP in solid oral dosage forms (tablets). Recent reports have indicated that physical form transformation (specifically dehydration) precedes oxidative decomposition of LSP.¹⁶⁵ Such a phase transformation of the API in a drug product can often reflect inappropriate formulation composition or poor process control, and will therefore warrant investigation. In this report, the physical stability is discussed in the context of the different hydration states of levothyroxine sodium and its disproportionation to form levothyroxine free acid. Our work is driven by the following working hypothesis: (i) In the presence of commonly used tableting excipients, LSP can undergo changes in its physical form, such as partial dehydration and

salt disproportionation. The physical instability of LSP is governed by excipient properties such as hygroscopicity and surface acidity. (ii) Physical transformation is the prelude to the chemical decomposition of levothyroxine.

To test the hypothesis, binary powder mixtures of LSP with a range of excipients were stored (i) at 40°C/75% RH and (ii) at 40°C in hermetically sealed pans. The storage in hermetically sealed pans simulates an actual drug product environment and enables an investigation of phase transformations such as moisture transfer from the API to the hygroscopic excipient. Storage under accelerated stability testing conditions provides an avenue to investigate salt disproportionation – a water mediated reaction. Storage of samples under these conditions also enable an accelerated evaluation of chemical stability of the API in presence of excipients.

The physical stability of the API in the powder blends was evaluated using synchrotron X-ray diffractometry (SXRD). Additionally, HPLC was performed to evaluate the chemical stability of LSP in binary mixtures. While SXRD provides information on the different physical forms of LSP (different hydration states) and the free acid form of levothyroxine, the HPLC method is designed to quantify the chemical decomposition of the active ingredient. We had the following objectives: (i) evaluate changes in the physical form of LSP when present as a mixture with excipients, (ii) quantify the chemical stability of LSP under accelerated stability testing conditions using both SXRD and HPLC and finally, (iii) assess the role of excipient properties (hygroscopicity and microenvironmental acidity) on the stability of LSP.

5.3 Experimental section

5.3.1 Materials.

Levothyroxine sodium pentahydrate (LSP; Figure 5.1) was used as received from Biophore Pharma Inc. Levothyroxine (free acid; C₁₅H₁₁I₄NO₄) was procured from Millipore Sigma. The powder samples were stored in air-tight and opaque containers in a freezer maintained at -25°C.

Levothyroxine has three ionizable moieties: carboxyl (pK_a 2.4) phenolic hydroxyl (pK_a 6.9) and amino group (pK_a 10.1).^{202,203} The experimentally determined aqueous solubility at 37°C of the free acid is 12 µg/mL, whereas that of LSP is 1.825 mg/mL. The calculated pH_{max} is 9.05.

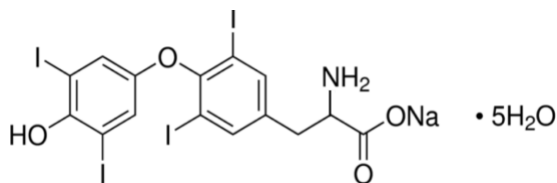


Figure 5.1. Chemical structure of LSP.

Microcrystalline cellulose (MCC) and croscarmellose sodium (CCS) were procured from FMC BioPolymer. USP grade dibasic calcium phosphate anhydrate was used as received from Rhodia Pharma Solutions. α - lactose monohydrate, maleic acid, sodium chloride (NaCl), Drierite® (anhydrous calcium sulfate) and sodium carbonate were purchased from Sigma Aldrich. Citric acid and stearic acid were procured from Fisher Scientific. Oxalic acid and tartaric acid were obtained from Pfaltz & Bauer. Sodium starch glycolate (SSG; Edward Mendell), magnesium stearate (MgSt; Mallinckrodt Laboratory Chemicals), povidone (Kollidon 30; BASF), sodium stearyl fumarate (SSF; JRS Pharma) and sodium bicarbonate (Mallinckrodt chemicals) were used as received.

5.3.2 Differential scanning calorimetry (DSC).

Thermal analysis of powder samples was performed using a differential scanning calorimeter (Q2000 by TA Instruments). The instrument is equipped with a refrigerated cooling accessory. The powder sample (2-5 mg) was hermetically sealed in an aluminum pan with a pinhole. Measurements were performed at a heating rate of 10°C/min, from 0 to 300°C, using a nitrogen purge rate of 50 mL/min. The data were analyzed using Universal Analysis 2000, a commercial software by TA Instruments.

5.3.3 Thermogravimetric analysis (TGA).

The powder sample (2-5 mg) was placed in an aluminum pan and heated in a thermogravimetric analyzer (Q50 TGA by TA Instruments), under a dry nitrogen purge, from 25 to 300°C at 10°C/min.

5.3.4 Powder X-ray diffractometry (PXRD).

Data collection and analyses were performed as previously discussed in Kaur *et al.*⁵¹¹

5.3.5 Synchrotron X-ray diffractometry (SXR).

Data collection and analyses were performed as previously discussed in Kaur *et al.*⁵¹¹

5.3.6 High performance liquid chromatography (HPLC).

The chemical stability of LSP, in the presence of excipients, was evaluated using HPLC analysis. All chromatographic analyses were carried out using a Shimadzu SPD-20A UV/VIS HPLC system equipped with Prominence series with a CBM-20A controller, dual LC-20AD XR pumps, DGU-20A 3R degasser, SIL-20AC XR autosampler, and CTO-20A column oven. Separation was achieved using a Zorbax Eclipse XDB analytical column (150 mm x 4.6 mm id) with 5 μ m particles and C18 stationary phase. The samples were extracted using a solution of 0.01 M sodium hydroxide

in methanol and diluted with the mobile phase. The mobile phase composed of acetonitrile :water:trifluoroacetic acid (400:600:0.05) and the flow rate was 1 mL/min. The detector wavelength for UV absorption was set to 225 nm and the column was maintained at 25°C. Given the alkaline nature of the extracting solution, the species being analyzed is the ionized (anion) form of levothyroxine. The data was collected and analyzed using Lab Solutions (Shimadzu).

5.3.7 Dehydration and salt disproportionation of LSP in hermetically sealed chambers.

Binary powder mixtures of LSP and each excipient (1:1 w/w; 10 mg) were cryomilled for 5 sec and stored at 40°C in hermetically sealed DSC pans. Cryomilling was done to facilitate intimate mixing of the API and the excipient. In order to minimize the risk of unintended transformations, the milling time was kept short. Cryomilling LSP for 5 sec did not bring about any discernible changes in its XRD pattern (obtained using synchrotron radiation). The sample was stable following storage in hermetic pans for one month (analyzed by XRD and HPLC). Milling of the samples and storage in hermetically sealed pans simulate pharmaceutical processing and product storage conditions, respectively. The excipients were (i) povidone (hygroscopic and neutral), (ii) oxalic acid (hygroscopic and acidic), and (iii) stearic acid (non-hygroscopic and acidic). Samples were characterized by SXRD after 2 and 4 weeks of storage.

5.3.8 Stability testing.

Unmilled binary powder blends of LSP with each excipient (1:5 w/w) were stored at 40°C in chambers maintained at 75% RH (saturated sodium chloride solution was used to generate 75% RH). The excipients are listed in Table 5.2. Samples were collected at day 0, 28, 56 and 84, stored at -20°C until analyzed by SXRD and HPLC. The unique peaks of levothyroxine free acid (d-spacing of 25.24 Å; $3.5^\circ 2\theta$ calculated for Cu K α radiation) and LSP (d-spacing of 15.65 Å ($5.6^\circ 2\theta$)), were used for characterization of both solid forms and for the quantification of LSP in binary mixtures (Figure 5.2C).

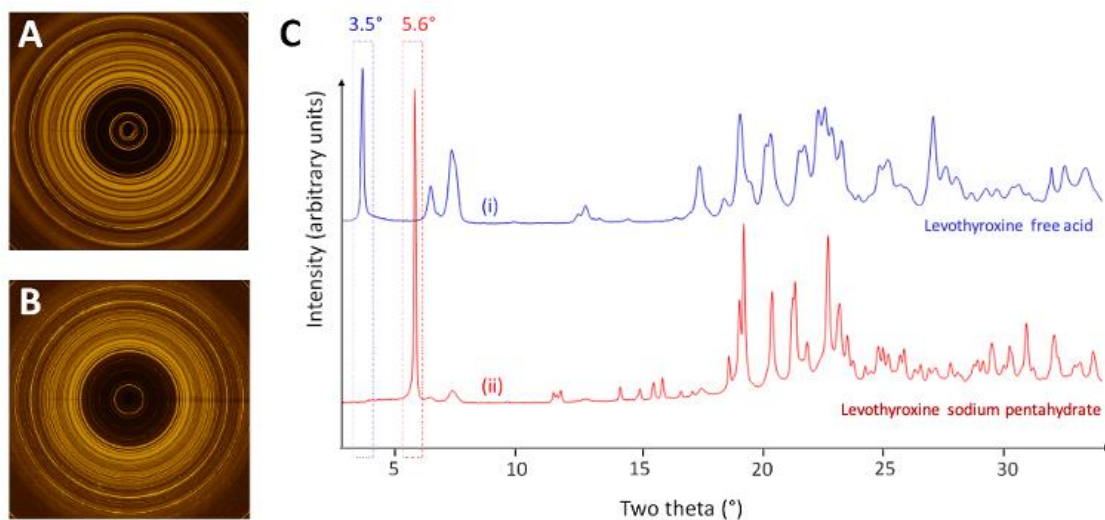


Figure 5.2. Two-dimensional XRD patterns of (A) levothyroxine (free acid; unionized levothyroxine) and (B) levothyroxine sodium pentahydrate obtained using synchrotron radiation ($\lambda = 0.45256 \text{ \AA}$). To facilitate visualization, the corresponding one-dimensional XRD patterns have been presented (C) as intensity versus 2θ plots (calculated for Cu $K\alpha$ radiation, $\lambda = 1.54 \text{ \AA}$). The “unique” peaks of levothyroxine free acid and LSP are seen at 3.5° and 5.6° 2θ , respectively.

5.4 Results and discussion

Baseline characterization of LSP was performed using DSC, TGA and XRD. The results were in agreement with earlier findings.^{165,243} These results have been reported in our previous work.⁵⁰⁴ The diffraction pattern of LSP was superimposable on the calculated powder pattern in the Cambridge Structural Database (CSD).⁵⁰⁴ Physical and chemical stability of ‘as is’ LSP was evaluated following 3 month storage under accelerated stability testing conditions ($40^\circ\text{C}/75\% \text{ RH}$). LSP exhibits high physical and chemical stability following storage under these conditions.

5.4.1 Physical stability.

5.4.1.1 Characterization of LSP-excipient binary mixtures in hermetically sealed pans.

Povidone is a component in numerous marketed oral levothyroxine tablets.⁵¹²⁻⁵¹⁶ Binary powder mixtures containing LSP and povidone (1:1 w/w) were stored at 40°C in hermetically sealed pans and analyzed by SXRD. The XRD pattern of the freshly prepared binary mixture was very similar to that of LSP (Figure 5.3). Following storage for 14 days, LSP exhibited dehydration to form LSM. Partial conversion to LSM is evident from the appearance of LSM diffraction peak at 6.5° 2θ and

retention of the reactant peak. Longer duration of storage (28 days) did not result in any appreciable change in the XRD pattern. In this “hermetically sealed” setup, any water released by the dehydration of LSP will not be able to leave the pan. If the released water remains “free”, it will raise the RH of the headspace and therefore prevent further dehydration of LSP. However, povidone is known to have a strong tendency to sorb water.⁵¹⁷ If any water released by the dehydration of LSP is immediately taken up by povidone, then the headspace RH will continue to remain low, promoting continued dehydration of LSP. Thus, there will be continuous moisture transfer from the LSP to povidone. The moisture transfer was confirmed by SXRD of the sealed pans at select time points.

The dehydration of LSP would potentially be faster and more pronounced in marketed levothyroxine formulations as the weight ratio of povidone to LSP is significantly higher in commercial drug products than in the test samples. LSM has a higher chemical reactivity than its pentahydrate counterpart.^{164,165,504,518} Hence, its appearance in hermetically stored samples could potentially explain chemical decomposition of levothyroxine sodium in marketed formulations containing hygroscopic excipients.

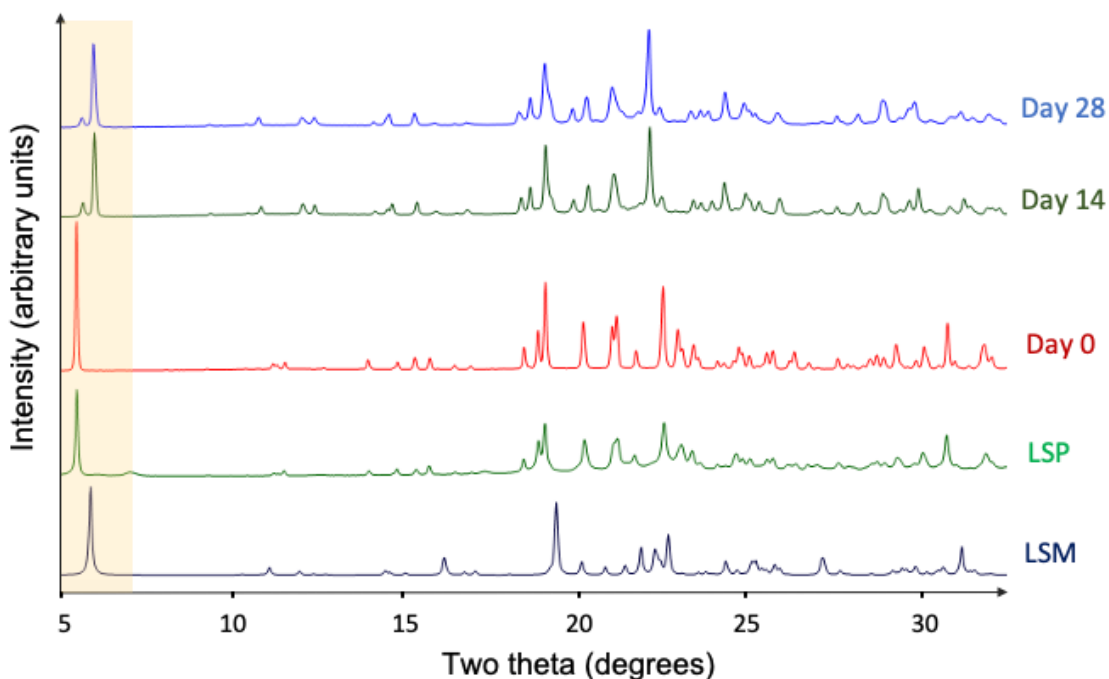


Figure 5.3. SXRD patterns of powder mixture of LSP and povidone (1:1 w/w) stored in hermetically sealed pans at 40°C. The highlighted region indicates partial dehydration of LSP to LSM during storage. The decrease in the intensity of the characteristic peak of LSP (peak

at 5.6° 2 θ) was accompanied by the appearance of the LSM peak at 6.5° 2 θ . The reference diffraction patterns of LSP and LSM are also provided.

Moisture transfer from LSP to excipient was also observed in LSP-anhydrous oxalic acid powder mixtures stored at 40°C. Following 14 days of storage in hermetic pans, unique peaks of LSM (due to partial dehydration of LSP) and oxalic acid dihydrate (due to hydration of oxalic acid) were observed. These results were reported and discussed comprehensively in our earlier work.⁵⁰⁴ The excipient of practical interest is citric acid, since it is used in a marketed levothyroxine tablet formulation.⁵¹⁹ Unfortunately, at RT, it deliquesces at 75% RH.^{487,520} Oxalic acid, on the other hand, has a strong tendency to sorb water – it transitions from the anhydrate to the dihydrate form at RH \geq 12% (RT).⁴⁸⁸ However, it does not deliquesce up to 97% RH (at RT). Oxalic acid was therefore an attractive alternative to study moisture transfer from LSP to crystalline hygroscopic excipients.^{488,489,521}

While LSP dehydration was observed following storage with hygroscopic excipients, when the same experiment was performed with stearic acid, the observations were quite different. Stearic acid is widely used as a tablet lubricant and is hydrophobic.^{522,523} The water released by the dehydration of LSP is expected to cause a pronounced increase in the headspace RH. This rise in RH will prevent further dehydration of LSP. We had earlier observed that, at 40°C, LSP exhibited a pronounced dehydration tendency only at RH < 15%.⁵⁰⁴ It is instructive to recognize that dehydration of a very small fraction of LSP will cause the release of sufficient water to result in a pronounced increase in headspace RH. Even after storage for 28 days, the XRD pattern substantially matched with that of LSP (Figure 5.4). Interestingly, the additional peaks could be attributed to levothyroxine free acid, a product of LSP disproportionation.

Levothyroxine free acid is characterized by a diffraction peak at 3.5° 2 θ (Figure 5.2). The disproportionation reaction is believed to be brought about by stearic acid. These findings were surprising in light of the extremely low aqueous solubility of stearic acid. As mentioned in the Experimental section, a physical mixture of LSP and stearic acid was cryomilled for 5 sec. While the primary objective of cryomilling was to bring about intimate mixing of LSP and stearic acid, it is recognized that milling can also cause lattice disorder and an increase in surface area. In an earlier investigation, cryomilling for 10 sec resulted in measurable lattice disorder in caffeine-oxalic acid cocrystal.⁵¹⁸ While the effect of milling on the extent of lattice disorder is expected to be compound-specific, it is reasonable to expect some lattice disorder in both LSP and stearic acid particles. More importantly, the impact of milling is expected to be more pronounced on the surface of particles than in the interior regions.

Any water released by the dehydration of LSP would be preferentially sorbed by the disordered regions of LSP and stearic acid. It is well known that amorphous compounds sorb more water than their crystalline counterparts.^{376,524} The water sorption will lead to plasticization. The attendant decrease in the glass transition temperature will increase the molecular mobility and consequently, the reactivity of the system. Thus, at the surface of stearic acid particles, the sorbed water will yield a highly acidic microenvironment (pH_{eq} of stearic acid = 2.74). The proposed mechanism of salt disproportionation is “dissolution” of both stearic acid and LSP in the sorbed water (at the interface of particles), enabling the water mediated reaction. The acidic microenvironment created by dissolution of stearic acid is postulated to facilitate proton transfer from the acid to levothyroxine sodium, leading to the formation of levothyroxine free acid and sodium stearate as reaction products. The reaction products may rapidly crystallize once their “concentration in solution” rises above their saturation solubility values. While we have evidence of crystallization of levothyroxine, characteristic peaks of sodium stearate were not observed. Considering the low levels of disproportionation in this sample, it is possible that the second reaction product, sodium stearate, has not crystallized. Unlike levothyroxine free acid, the high aqueous solubility of sodium stearate (54 mg/mL at 25°C) may facilitate its retention in the solution state.⁵²⁵

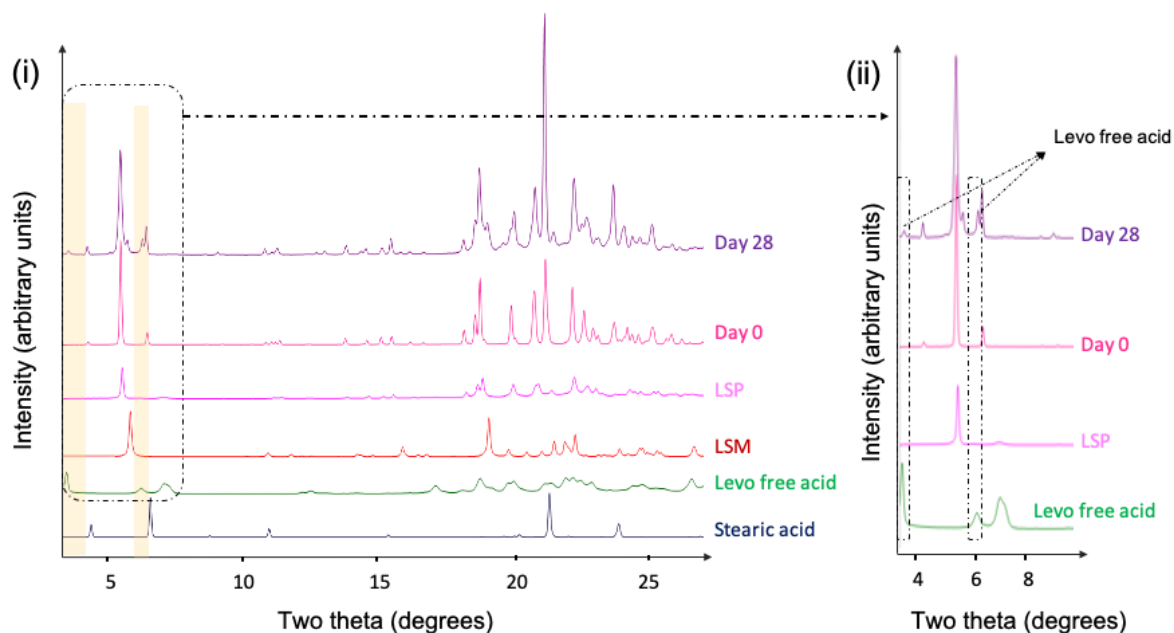


Figure 5.4. SXR D patterns of powder mixture of LSP and stearic acid (1:1 w/w) stored in hermetically sealed pans at 40°C. After 28 days of storage, salt disproportionation leading to the formation of levothyroxine free acid (peak at 3.5° 2θ) was observed.

5.4.1.2 Salt disproportionation.

Given the evidence of salt disproportionation, it is crucial to investigate the propensity of LSP to form the free acid in marketed formulations. As discussed in the previous section, while citric acid is used in the commercial formulation of levothyroxine, it is challenging to study it owing to its deliquescence under accelerated stability testing conditions. To circumvent this challenge, a range of organic acids with pK_a values above and below that of citric acid were used to study LSP disproportionation. These were oxalic, stearic, maleic and tartaric acids. These acids were also characterized by a high deliquescence RH. Their physical properties are listed in Table 5.1.

In physical mixtures of LSP-oxalic acid (1:5 w/w; Figure 5.5) and LSP-maleic acid (1:5 w/w; Figure 5.9), salt disproportionation with complete disappearance of the LSP peak was observed. In presence of stearic and tartaric acid, there was evidence of partial disproportionation of the salt to the free acid (Supporting information, Figure 5.10 and Figure 5.11). Based on the data collected after 28 days of storage, the extent of disproportionation induced by the organic acids can be rank ordered as: oxalic acid \approx maleic acid > tartaric acid > stearic acid. Salt disproportionation is a function of the pH_{max} of the salt (i.e. levothyroxine sodium) and the “pH” of the microenvironment. This is the pH of the microscopic sorbed water layer on the surface of the particles in which the solid has dissolved and formed a saturated solution.^{506,526} The propensity for disproportionation increased as function of the strength of the acid. Given the evidence of salt disproportionation even with stearic acid, it is reasonable to expect free acid formation with citric acid (pH_{eq} of citric acid < 1.6).³⁸¹

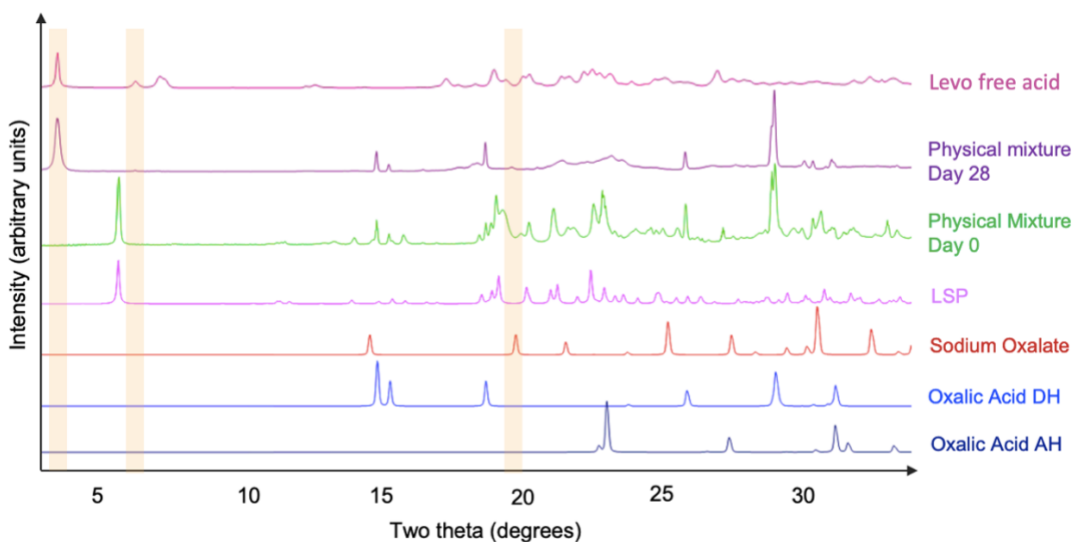
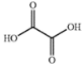
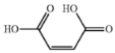
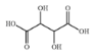
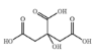
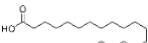


Figure 5.5. XRD patterns of a powder mixture of LSP and oxalic acid (1:5 w/w) stored at 40°C/75% RH. Following 28 days of storage, the characteristic peak of LSP at 5.6° 2 θ

completely disappeared. The appearance and the pronounced intensity of the characteristic diffraction peak of levothyroxine free acid at $3.5^\circ 2\theta$ indicates pronounced and possibly complete disproportionation during storage. The highlighted regions indicate the appearance of the characteristic diffractions peaks of levothyroxine free acid (3.5 and $6.1^\circ 2\theta$) and sodium oxalate ($19.9^\circ 2\theta$), the products of the disproportionation reaction.

Table 5.1. Physical properties of selected organic acids.

S.no.	Excipient	Structure	pK_a	Aqueous solubility at 25°C
1.	Oxalic acid		1.2, 4.2	0.14 g/mL
2.	Maleic acid		1.9, 6.2	0.78 g/mL
3.	Tartaric acid		3.0, 4.3	1.25 g/mL
4.	Citric acid		3.2, 4.8, 6.4	0.59 g/mL
5.	Stearic acid		4.9	Water insoluble

5.4.2 Chemical stability.

Our final interest was to comprehensively evaluate the stability of LSP in the presence of several excipients commonly used in its solid dosage forms. The excipients included a range of diluents, pH modifiers, lubricants and disintegrants (Table 5.2). In an effort to accelerate the drug-excipient interaction, the mixtures were stored at $40^\circ\text{C}/75\%$ RH, sampled periodically and subjected to SXRD. The intensity of the characteristic LSP diffraction peak ($5.6^\circ 2\theta$) was used as a preliminary indicator of LSP stability. A decrease in the peak intensity is indicative of the disappearance of the pentahydrate form of levothyroxine sodium. Additionally, a decrease in LSP peak intensity due to dehydration would be readily discerned by the appearance of diffraction peaks of LSM.⁵⁰⁴ However, dehydration is unlikely under accelerated stability testing conditions ($40^\circ\text{C}/75\%$ RH). Our earlier studies had revealed LSP \rightarrow LSM conversion only at a RH $< 15\%$ (40°C).⁵⁰⁴ Therefore, a decrease in LSP peak intensity, coupled with the absence of levothyroxine free acid peak, could be indicative of chemical decomposition. Therefore, powder blends were also subjected to HPLC so as to evaluate the chemical stability of LSP in these mixtures.

The SXRD results are presented in Figure 5.6 and Figure 5.7. Selected drug-excipient mixtures (the ones in Figure 5.6) were also subjected to HPLC analyses (Figure 5.8). In presence of several excipients, even after 3 months of storage at $40^\circ\text{C}/75\%$ RH, there was only a small ($\leq 2\%$) decrease

in the diffraction peak intensity of LSP. The excipients were magnesium stearate, mannitol, sodium carbonate, sodium bicarbonate, SSF and SSG. On the other hand, a pronounced decrease in LSP peak intensity (>10%) was observed in the presence of lactose, CCS and MCC (Figure 5.6). In the presence of DCPA, there was an intermediate level (between 5 and 10%) of decrease in peak intensity.

It is instructive to recognize that the solution based analytical methods are insensitive to the different physical forms of a compound in the solid state. Thus, the HPLC method will not distinguish between levothyroxine sodium in different hydration states (LSM and LSP). In the context of this discussion, it is also very important to recognize that the HPLC method (this is also the USP method) will not distinguish between levothyroxine sodium (salt) and levothyroxine (free acid). When the analyte is extracted using a methanolic solution of sodium hydroxide (details in the Experimental section), any levothyroxine (free acid) formed due to disproportionation of LSP will be converted to the ionized form. Thus, during the HPLC analysis, all the drug will be in the ionized state. The choice of 0.01 M NaOH as the extracting solution is based on the stability, solubility and molar absorptivity of the analyte, as well as the HPLC column stability.^{527,528} Thus, since the alkaline extracting solution used for the solution-based assay converts levothyroxine to its anionic form, the HPLC method is insensitive to salt disproportionation. Hence, while the SXRD method enabled the characterization of the physical form (quantification of LSP, appearance of crystalline levothyroxine free acid and LSM), the HPLC method provided a measure of the chemical stability.

Lactose is used in numerous LSP tablet formulations. However, the reducing sugar undergoes Maillard reaction with the primary amine group of LSP to form levothyroxine-2-ketolactose.⁴⁸⁶ Our results indicate roughly 15% decrease in the intensity of levothyroxine sodium peak in the API:excipient (1:5 w/w) powder blends [% remaining by SXRD is 85.7 (Figure 5.6) and by HPLC is 87.5 (Figure 5.8)]. Thus, under the accelerated stability testing conditions, in the presence of lactose, levothyroxine sodium can undergo decomposition.

In an effort to evaluate the role of sorbed water, three hygroscopic (moderately or very hygroscopic) excipients were selected (Table 5.2). The instability was most pronounced in the presence of MCC. Following 3 months of storage, the LSP peak intensity had decreased to ~ 81.0% of the initial value (Figure 5.6) while the HPLC assay revealed that 79.1% of levothyroxine sodium was remaining. MCC is a neutral and hydrophilic excipient. Water sorbed by MCC is considered to be “unbound/bulk” water.⁵²⁹ The water is believed to be sufficiently mobile and therefore available for the API to undergo solution mediated chemical decomposition.⁴⁵¹ A similar mechanism can explain the drug instability in the presence of CCS. While SXRD revealed the retention of ~82.7%

LSP, HPLC revealed 86.9% levothyroxine sodium. On the other hand, in the presence of SSG, there was a negligible change in LSP peak intensity reflecting the stability of LSP. Thus the availability of sorbed water alone is not sufficient to cause API decomposition. The maximum instability was observed in presence of MCC which has the lowest surface acidity (pH_{eq} of 3.6; Table 5.2). CCS, which is more hygroscopic than MCC, had a lower surface acidity (pH_{eq} of 5.3) and its destabilizing effect appeared to be slightly higher than that of MCC (Figure 5.6). Thus, the pH_{eq} of the excipient appears to be a powerful determinant of API stability. This was also evident from the fact that in the presence of SSG, which has lower surface acidity than CCS (pH_{eq} of 5.8 for SSG), the drug was stable with no evidence of decomposition (Figure 5.7).

In the presence of mannitol, while SXRD revealed < 2% decrease in LSP peak intensity, HPLC revealed ~ 5% decomposition. We do not have a satisfactory explanation for this seemingly anomalous result. In the presence of dicalcium phosphate anhydrate (DCPA), there was a modest but measurable decrease in LSP peak intensity (Figure 5.6). HPLC also revealed chemical decomposition (Figure 5.8). Mannitol and DCPA are only slightly hygroscopic. At the LSP-excipient particle interfaces, there might be only a limited amount of water available to serve as the reaction medium. While the low pH_{eq} value of these compounds ($\text{pH}_{\text{eq}} < 4$; Table 5.2) would be conducive to decomposition, the unavailability of water may decrease the extent of decomposition. These results suggest that in the absence of water to act as a reaction medium, the decomposition reaction may be prevented.

Finally, LSP exhibited an exceptionally high stability in the presence of magnesium stearate and SSF. This can be explained by both the alkaline microenvironment created by these lubricants (Table 5.2) and their non-hygroscopic nature.³⁸¹ LSP has been reported to be stable in the presence of 'alkaline' excipients.¹⁶⁶

Previous studies have documented the pronounced influence of pH modifiers on the chemical stability of LSP, both in the solid and solution states. Acidic pH modifiers were detrimental to API stability, whereas alkaline pH modifiers improve its solid-state stability.¹⁶⁶ To study the influence of excipient acidity on the solid state stability of LSP, binary blends were prepared with each oxalic acid, sodium carbonate and sodium bicarbonate. In the presence of alkaline pH modifiers, the API exhibited exceptional stability (Figure 5.7). On the other hand, in the presence of oxalic acid, we observed complete disappearance of the LSP peak and formation of levothyroxine free acid after 4 weeks of storage (Figure 5.5). The HPLC assay of the API in the presence of oxalic acid indicated gradual chemical decomposition of the API with > 25% decomposition following 3 months of storage at 40°C/75% RH (% API remaining by HPLC = 72.3%; Figure 5.8). Chemical

decomposition of the API in the presence of acidic pH modifiers (via deiodination)⁴¹⁵ is believed to be independent of its physical form (salt or free acid).

In our earlier investigation, we had stored a physical mixture of LSP and oxalic acid (1:1 w/w) in hermetically sealed pans at 40°C. Using SXR, we had observed partial dehydration of LSP (to LSM) and transition of oxalic acid to its dihydrate.⁵⁰⁴ Thus there was ‘transfer’ of water from the API to the excipient. However, in spite of the partial dehydration of LSP, we had not observed the decomposition of levothyroxine. There was also no evidence of the disproportionation of sodium levothyroxine. We postulate that in the sealed pan, all of the water was ‘bound’ in the oxalic acid crystal lattice (as dihydrate). This is a reasonable assumption in light of the strong propensity of anhydrous oxalic acid to form the dihydrate. The anhydrate → dihydrate transition in oxalic acid is known to occur at RH ≥ 12% (RT)⁴⁸⁸ Thus, in these sealed pans, at the LSM-excipient particle interfaces, adequate water might not be available to serve as the reaction medium. These results confirm the need for water to act as a reaction medium for the decomposition reaction.

5.4.3 Physical transition of LSP in drug products – potential impact on chemical stability

The results of all the stability testing have been comprehensively summarized (Scheme 5.1). The results can be divided into: (i) dehydration evaluated by SXR, (ii) disproportionation leading to free acid formation (qualitative analysis; by SXR), and (iii) chemical decomposition quantified by HPLC. It is evident that changes in the physical form have the potential to impact chemical stability of LSP in a drug product environment.

The chemical stability of levothyroxine sodium has been comprehensively investigated and has been the subject of numerous publications.^{163,165,166,247,451,456} However, the role of excipients, and specifically the combined effects of formulation components and processing conditions on the chemical stability, is not completely understood.^{166,247} Solution based methods such as HPLC, in light of their specificity and sensitivity, are used to assess the chemical stability of the API in dosage forms. Such an approach does not enable a comprehensive understanding of the stability behavior of LSP in tablet formulations. Dissolution of the API in the extracting phase leads to a loss of valuable solid form information. The active ingredient, LSP, can undergo dehydration in the drug product.^{164,504} The partially dehydrated phase, levothyroxine sodium monohydrate (LSM), has a propensity to undergo oxidative decomposition.¹⁶⁵ The high chemical reactivity of the dehydrated phase was explained by: (i) oxygen occupying the channels that were earlier occupied by lattice water, and (ii) conformational changes resulting in an increased propensity of the amino moiety to undergo oxidation.⁵⁰⁴ In the current work, for the first time, the propensity for LSP to undergo

disproportionation has been documented. The potential impact of disproportionation on chemical stability warrants further investigation.

As seen with LSP-organic acid blends, salt disproportionation was observed within weeks of storage under accelerated stability testing conditions (40°C/75% RH). This result is potentially significant since recently reformulated tablets of LSP contain citric acid.^{486,519} In light of the very low concentration of the API in drug products, even a small amount of citric acid in the formulation can induce pronounced salt disproportionation. The free acid form of levothyroxine has a 100 fold lower solubility than the sodium salt (LSP). While the influence of salt disproportionation on product performance is not known, the loss of solid form control is a cause of concern and mandates further investigation.

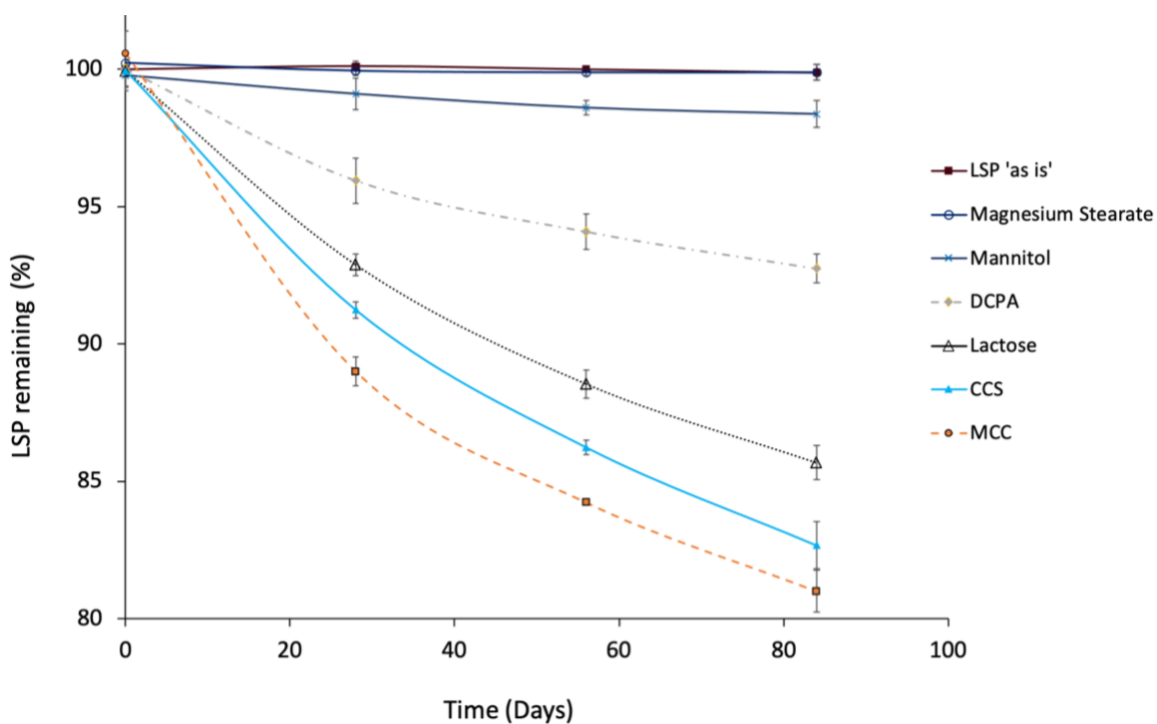


Figure 5.6. LSP remaining as a function of time following storage of binary powder blends of LSP and individual excipients (1:5 w/w). The samples were stored at 40°C/75% RH, and quantification of LSP was performed using SXRD. The integrated intensity of the diffraction peak at $5.6^\circ 2\theta$ (Cu $K\alpha$) was used for the quantification of LSP in powder blends. The calibration curve is available in the supporting information (Figure 5.12). Mean \pm SD (n=3).

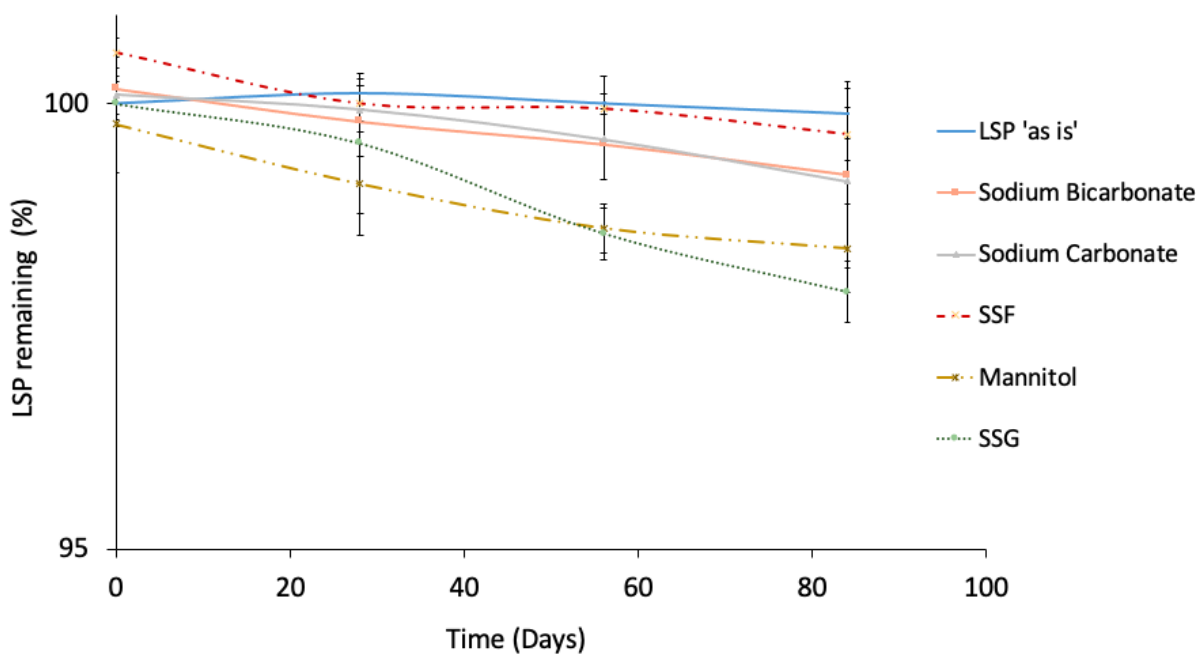


Figure 5.7. Concentration of LSP as a function of time following storage of binary powder blends of LSP and individual excipients (1:5 w/w). The samples were stored at 40°C/75% RH, and quantification of LSP was performed using SXRD. The integrated intensity of the diffraction peak at 5.6° 2θ (Cu Kα) was used for quantification of LSP in powder blends. The calibration curve is available in the supporting information (Figure 5.12). Results are reported as a mean of three measurements.

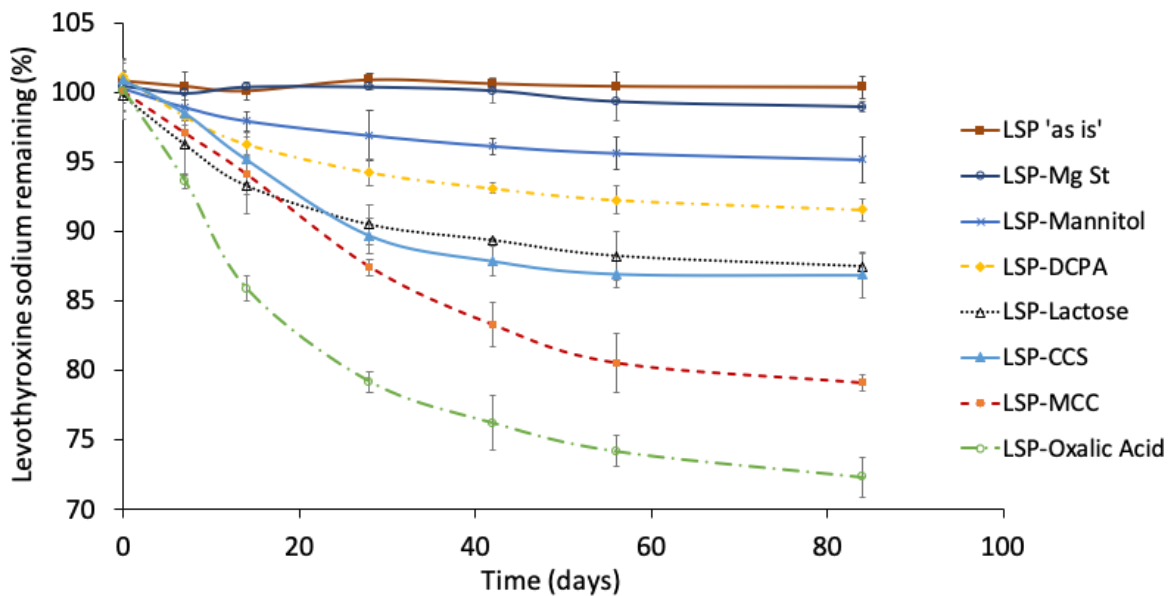


Figure 5.8. Concentration of levothyroxine sodium as a function of time following storage of binary powder blends of LSP and individual excipients (1:5 w/w). The samples were stored at 40°C/75% RH, and quantification of levothyroxine sodium was performed using HPLC. Results are reported as a mean of three measurements.

Table 5.2. Physical properties of excipients. ^{381,506}

S.no.	Excipient	Excipient type	pK _a	Surface acidity (pH _{eq})	Physical form	Water sorption behavior ⁵³⁰
1.	DCPA	Diluent	2.0, 7.1, 12.3	3.3	Crystalline	Slightly hygroscopic
2.	CCS	Disintegrant	4.3	5.3	Amorphous	Very hygroscopic
3.	SSG	Disintegrant	3.3	5.8	Amorphous	Very hygroscopic
4.	MCC	Diluent	11.9	3.6	Partially crystalline	Moderately hygroscopic
5.	Mannitol	Diluent	12.6	3.9	Crystalline	Slightly hygroscopic
6.	Lactose	Diluent	11.3	4.1	Crystalline	Slightly hygroscopic
7.	Mg St	Lubricant	4.9	7.3	Crystalline	Non hygroscopic
8.	SSF	Lubricant	3.6	8.3*	Crystalline	Non hygroscopic
9.	Sodium carbonate	pH modifier	10.3	8.6	Crystalline	Very hygroscopic
10.	Sodium bicarbonate	pH modifier	6.4, 10.3	8.3	Crystalline	Very hygroscopic

*Since the pH_{eq} is not known, the slurry pH value is provided.

5.5 Significance

As was pointed out earlier, the pharmacopeial (USP) assay method (HPLC) is insensitive to the state of hydration of levothyroxine sodium and also cannot distinguish between the unionized (acid) and ionized (salt) forms of levothyroxine in the solid state. Our studies strongly suggest that the physical form of levothyroxine will influence its chemical stability. Therefore, monitoring and controlling the physical form of levothyroxine in solid dosage forms may serve as an effective approach for preventing its chemical decomposition.

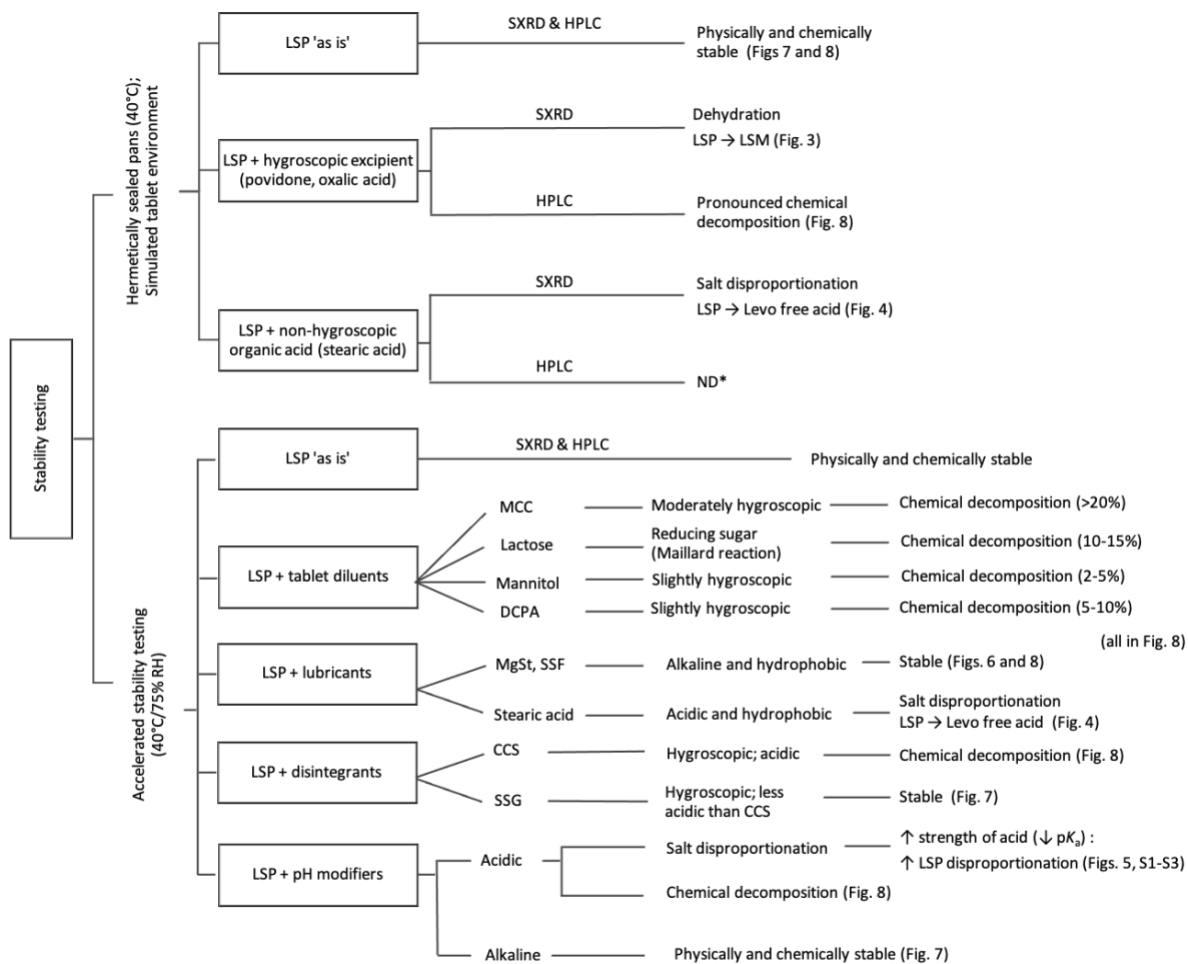
X-ray diffractometry provides a quick and ready approach to evaluate drug stability. By quantifying the LSP in the dosage form, one can readily assess the API stability. LSP quantification can be readily accomplished based on the intensities of one or more of its characteristic peaks. Interestingly, a decrease in the LSP peak intensity does not imply chemical decomposition. The disappearance of LSP could be attributed to its dehydration or disproportionation. Chemical decomposition can then be confirmed using a technique such as HPLC. Unfortunately, the API content in tablet dosage forms is so low that the conventional XRD methods and the laboratory diffractometers will not have the sensitivity to characterize the drug substance in the dosage form. In order to overcome the challenge posed by the sensitivity of the XRD technique, the API content was $\geq 20\%$ w/w in all the mixtures. However, in an actual drug product, the API to excipient weight ratio will typically be in the range of 1:1000 to 1:10,000. Hence, the influence of the excipient is expected to be much more pronounced in levothyroxine drug products than in our model mixtures. The instability could be further exacerbated by lattice disorder (or mechanical activation of the solids) induced during drug product manufacture.⁵¹⁸

It is important to recognize that the study was performed under accelerated stability testing conditions (40°C/75% RH). The powder samples were directly exposed to the elevated temperature and water vapor pressure. While this approach aids in identifying “problem” excipients, it does not necessarily reflect the effects which will be observed in ‘packaged’ containers. The influence of pharmaceutical processing on drug product stability mandates further investigation. In a literature report, tablets prepared by direct compression exhibited higher stability than those by wet granulation.²⁴⁶

A major challenge with formulating LSP, a low dose API, is the high excipient burden. Hence, excipients properties will be key to formulation performance and stability. To mitigate the risk of LSP dehydration and disproportionation, hygroscopic excipients (such as povidone and MCC) must be avoided. Dehydration of LSP can be prevented by coating the API particles.³⁸⁷ Coating will also prevent the API from perceiving the acidic microenvironment created by excipients. Alkaline pH

modifiers also provide an avenue to mitigate the risk of disproportionation in the drug product. Considering the risk of Maillard reaction with lactose, it will be prudent to avoid its use in LSP formulations. Recent studies have proposed the use of mannitol in lieu of lactose, to improve the API chemical stability in dosage forms.⁴⁸⁶

It is important to recognize that while evaluating the chemical stability of levothyroxine in the presence of excipients, only the disappearance of the reactant, was measured. Investigations into the exact mechanism of chemical decomposition of the API have been the subject of numerous publications^{490,531,532} but were outside the scope of this work.



*ND – not done; however, in light of the acidic microenvironment, decomposition is expected (as was observed with oxalic acid)

Scheme 5.1. Influence of excipients on the stability of LSP. SXR was used to monitor dehydration and disproportionation (both in the solid state), while the chemical decomposition was monitored by HPLC (solution based).

5.6 Conclusions

The physical and chemical stability of LSP was evaluated in presence of a range of pharmaceutical tablet excipients. LSP exhibited partial dehydration and disproportionation in the presence of hygroscopic and acidic excipients, respectively. LSP was susceptible to chemical decomposition in the presence of lactose monohydrate, microcrystalline cellulose and croscarmellose sodium. Alkaline and hydrophobic excipients provide an avenue to design stable solid oral dosage form of the API.

5.7 Supporting information

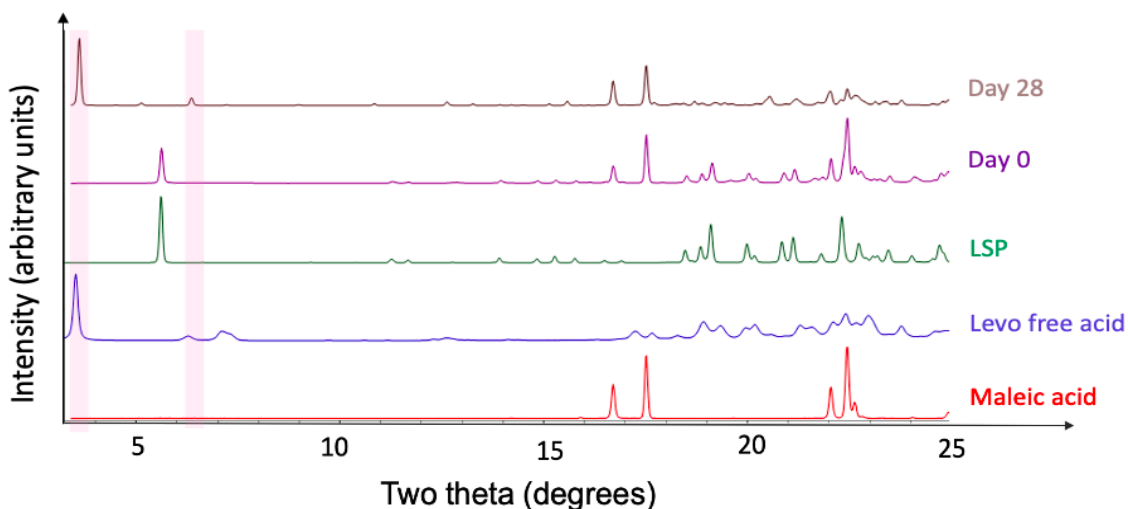


Figure 5.9. XRD patterns of physical mixtures of LSP and maleic acid (1:5 w/w) following storage at 40°C/75% RH for 28 days.

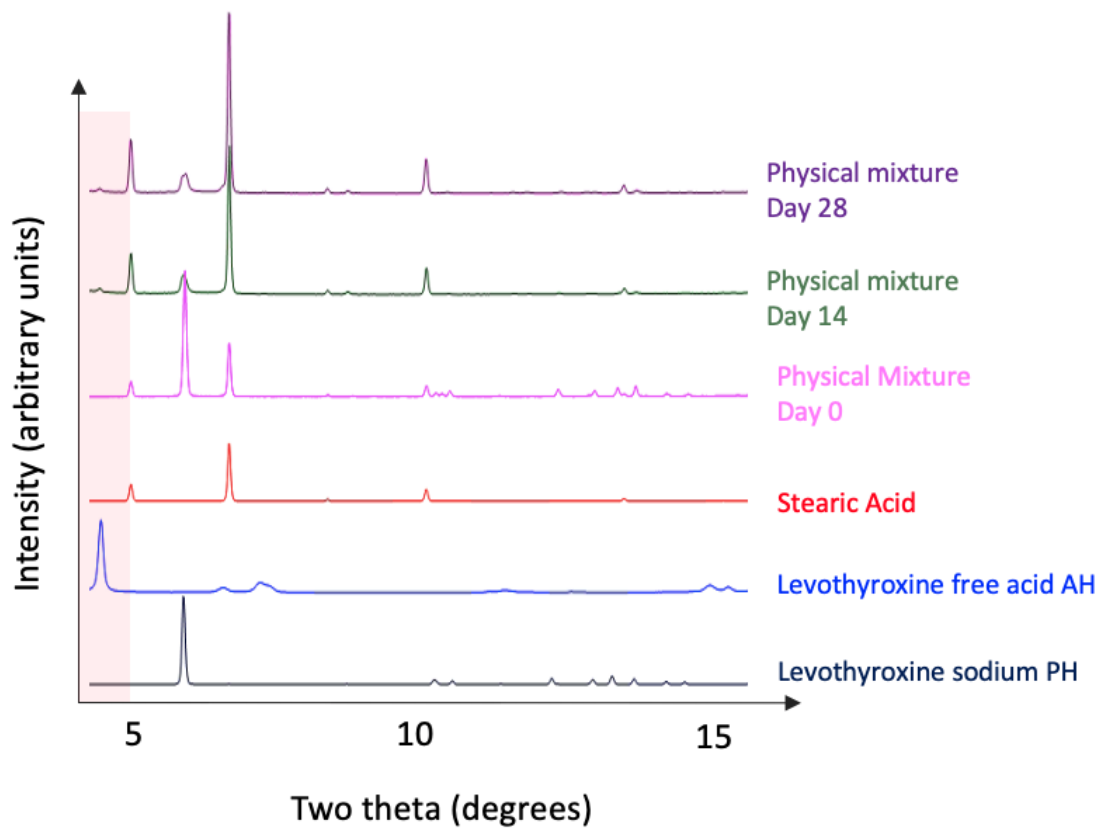


Figure 5.10. XRD patterns of physical mixtures of LSP and stearic acid (1:5 w/w) following storage at 40°C/75% RH for 28 days.

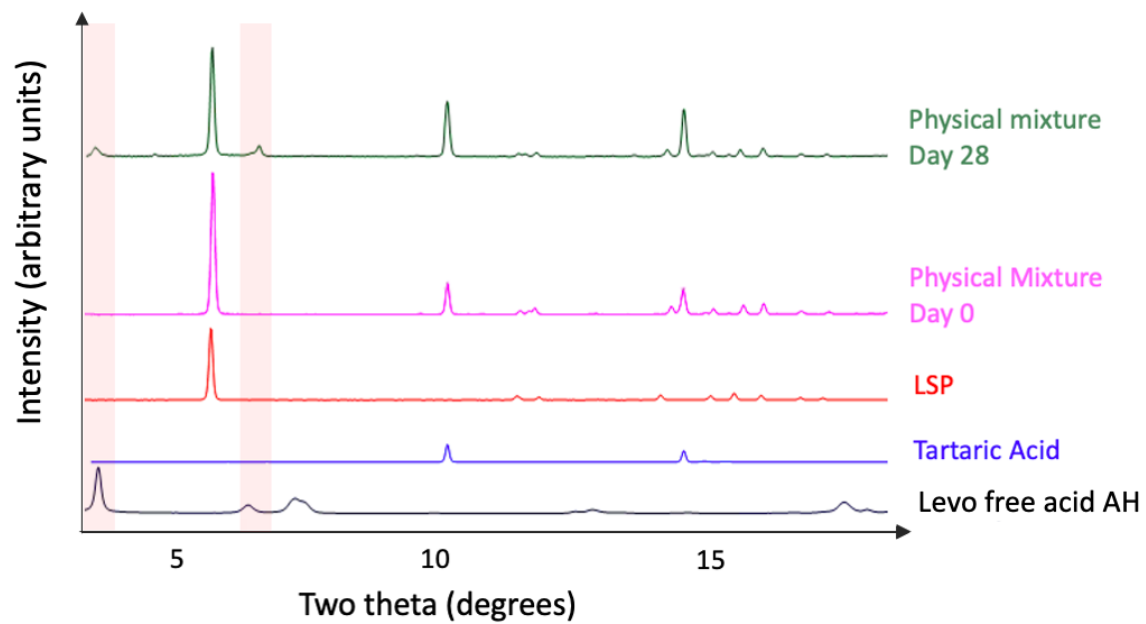


Figure 5.11. XRD patterns of physical mixtures of LSP and tartaric acid (1:5 w/w) following storage at 40°C/75% RH for 28 days.

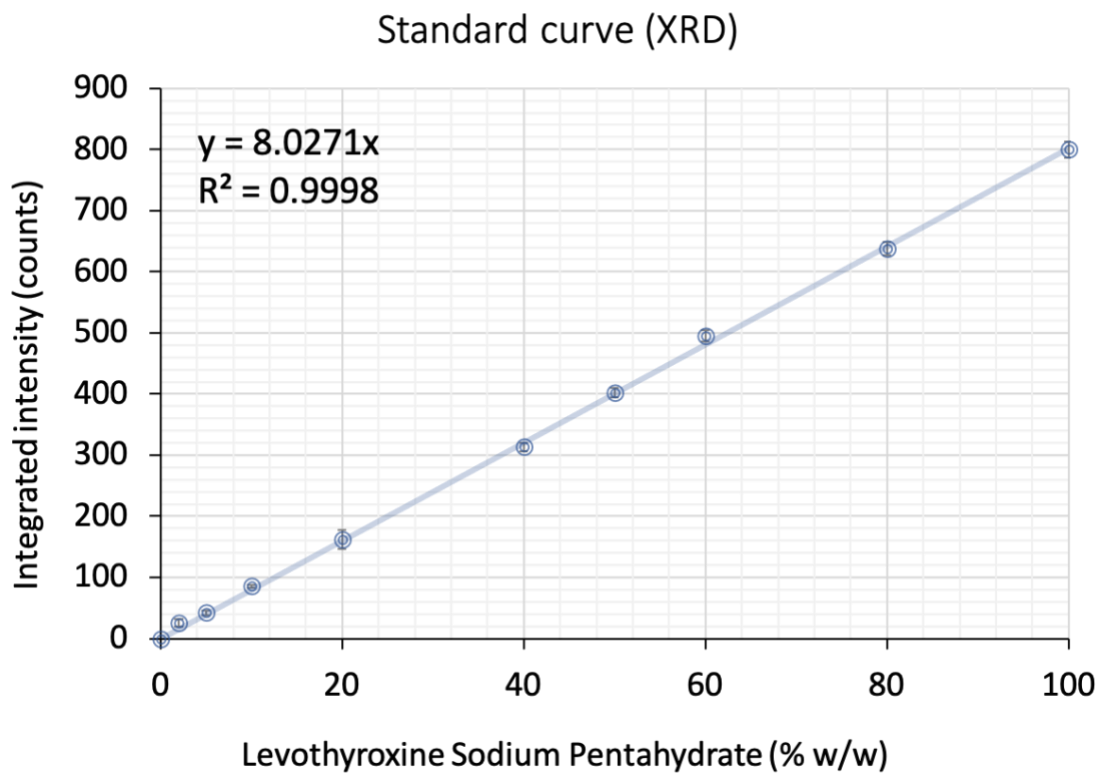


Figure 5.12. Plot of the integrated intensity of the 15.65 Å (peak at 5.6° 2θ for CuKα radiation) line of LSP as a function of LSP content in binary mixtures of LSP and stearic acid. Similar plots were observed for physical mixtures of LS

CHAPTER 6

Chapter 6. Summary

While salts and cocrystals provide an avenue to alter the physicochemical and mechanical properties of drugs, their success hinges on them retaining their physical form stability during pharmaceutical processing and product storage. The overarching goal of this thesis was to understand the factors affecting the physical and chemical stability of salts and cocrystals in a drug product environment. In order to develop mechanistic insights, the influence of pharmaceutical processing, excipient properties and storage conditions on the physical and chemical stability of the model compounds in oral solid dosage forms (specifically tablets) were investigated. A battery of complementary analytical techniques, such as single crystal and powder X-ray diffractometry (laboratory and synchrotron source), thermal analysis (DSC, TGA, HSM and VT-XRD), surface imaging using AFM and spectroscopy (ATR-FTIR, ssNMR and confocal Raman spectroscopy), were used. For both salts and cocrystals, the critical determinants of physical stability in a dosage form were excipient properties, especially hygroscopicity and microenvironmental acidity.

In Chapter 2, the influence of processing induced lattice disorder on the stability of caffeine-oxalic acid cocrystals (CAFOXA) was investigated (Figure 6.1). In a drug product environment, routine pharmaceutical processing steps, such as milling and compaction, have the potential to induce disorder in an otherwise crystalline system. Our working hypothesis was that even short milling times can induce sufficient lattice disorder to render the cocrystal system unstable. While the unmilled CAFOXA cocrystals were robust, the cocrystals dissociated to form free caffeine hydrate when low levels of disorder were introduced in the powder samples. Milling for even 10 sec resulted in a measurable disorder and an attendant tendency of the solid to sorb water. This was followed by cocrystal-excipient interaction leading to dissociation. The proposed mechanism of cocrystal dissociation entails the following sequence: sorption of water by disordered regions, dissolution of CAFOXA and dibasic calcium phosphate anhydrate (DCPA) in the sorbed water, followed by proton transfer from cofomer (oxalic acid) to DCPA, and the formation of hydrates of caffeine and calcium oxalate. In this work, the disproportionate influence of low levels of disorder on the stability of a model cocrystal system was demonstrated.

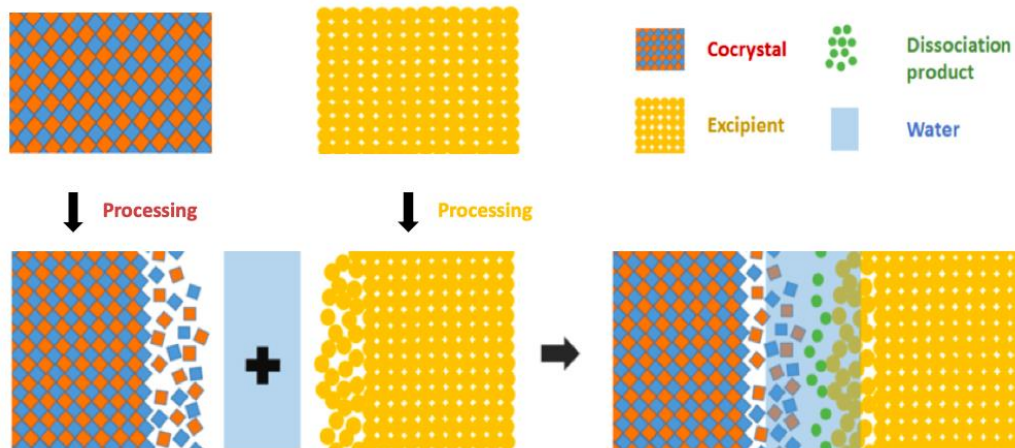


Figure 6.1. Schematic of lattice disorder introduced in crystalline materials during pharmaceutical processing, and the impact of lattice disorder on the water mediated dissociation of cocrystals in the presence of excipients.

In our earlier work (Chapter 2), the processing induced lattice disorder was proposed to be predominant on the surface of the solids. In Chapter 3, we aimed to characterize the surface disorder induced during milling and powder compaction for CAFOXA cocrystals using atomic force microscopy (AFM). The ‘as is’ cocrystals were plate shaped with a smooth surface. Pharmaceutical processing (compaction and short milling, in this case) resulted in low levels of disorder. AFM height and phase imaging was used to characterize surface crystallization of the disordered regions on the tablet surface. Crystallization of the disordered regions was induced by exposing the tablet surface to elevated water vapor pressure at RT (Figure 6.2). Water sorption by the disordered regions led to an attendant increase in molecular mobility thereby driving surface recrystallization. Real time AFM imaging of the disordered samples under elevated water vapor pressure enabled close monitoring of structural changes in the sample.

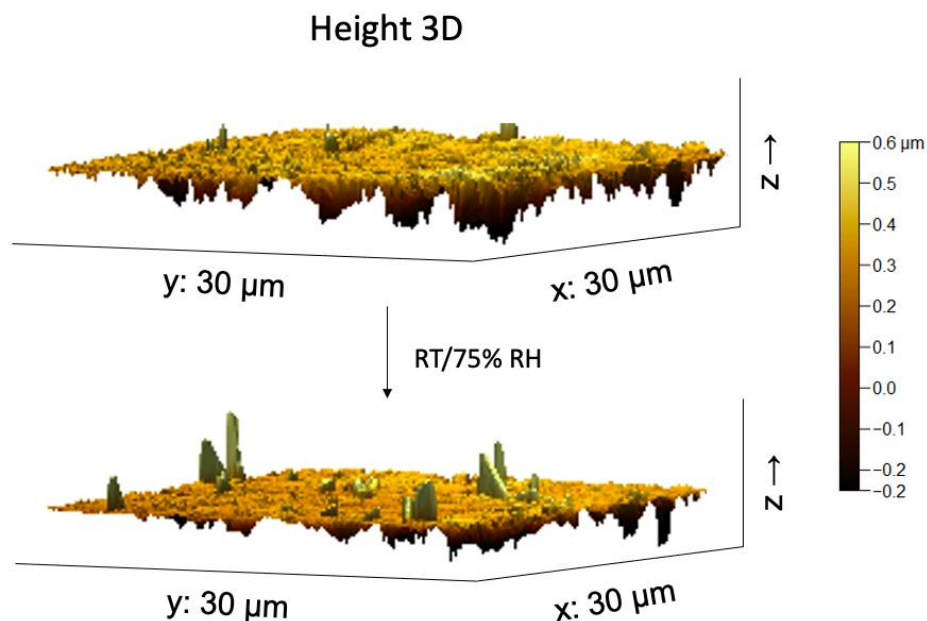


Figure 6.2. Representative AFM height images (3D) showing surface recrystallization of milled CAFOXA cocrystals upon exposure to RT/80% RH for 10 h.

In Chapter 4, dehydration induced structural change in a crystalline salt hydrate (levothyroxine sodium pentahydrate; LSP) and its consequent influence on the chemical stability of the API were the subject of investigation. Levothyroxine sodium is the synthetic form of thyroxine (physiological thyroid hormone). Levothyroxine sodium is the standard, and usually the only treatment option, for patients suffering from hypothyroidism. Solid dosage forms are formulated with the pentahydrate. LSP is reported to undergo chemical decomposition through complex pathways. The chemical instability issue is exacerbated by its low dose. While LSP is used in marketed formulations, our preliminary studies suggested that the dehydration of LSP occurred readily under modest processing and storage conditions, and resulted in a crystalline monohydrate (LSM) with a different lattice structure. The partially dehydrated form, LSM, has been reported to be more chemically reactive than LSP. The potential for an increase in reactivity of levothyroxine sodium, due to a change in its physical form, formed the motivation for this work. Our work was driven by the following working hypotheses: (i) The crystal structure of levothyroxine sodium monohydrate (LSM), different from that of the pentahydrate, explains its high reactivity. (ii) In a drug product environment, LSP dehydrates to a lower hydrate, possibly LSM.

Our results show that LSP gradually loses four molecules of water of crystallization to readily form LSM following storage under 40°C/0% RH for 3 h (Figure 6.3). The crystal structure of LSM provided insights into its high reactivity. In LSP – excipient mixtures stored in a hermetic container at 40°C, there was moisture transfer from drug to excipient. In formulations of LSP, chemical degradation of levothyroxine sodium may be preceded by its partial dehydration.

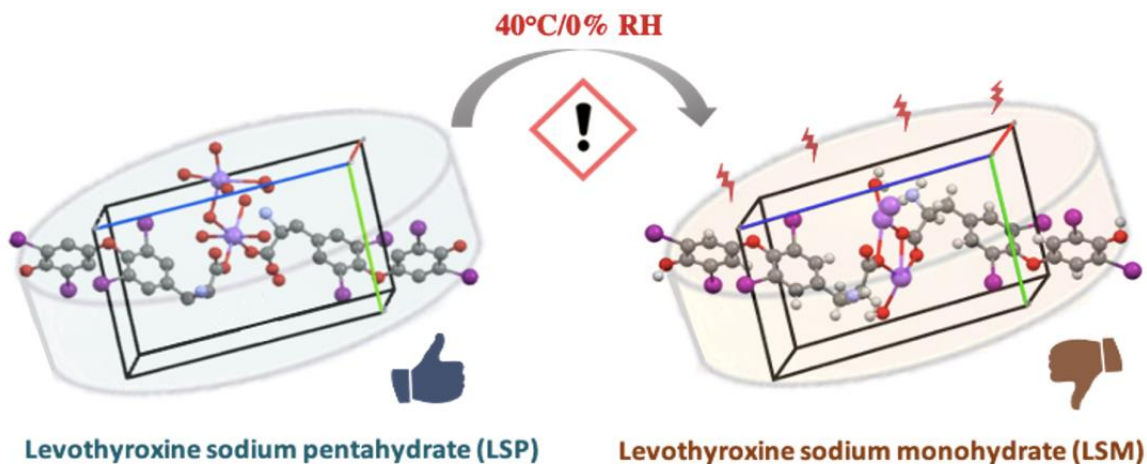


Figure 6.3. Schematic for partial dehydration of LSP under “modest” and realistic processing and storage conditions to form the more reactive form, LSM.

In Chapter 5, the physical and chemical stability of LSP, in presence of a range of tableting excipients, was investigated using SXRD and HPLC (Figure 6.4). Our work is driven by the following working hypotheses: (i) In presence of commonly used tableting excipients, LSP can undergo changes in its physical form, such as partial dehydration and salt disproportionation. The physical instability of LSP is governed by excipient properties such as hygroscopicity and surface acidity. (ii) Physical transformation is the prelude to the chemical decomposition of levothyroxine. The stability testing was performed under two conditions, (i) 40°C/75% RH and (ii) in hermetically sealed containers at 40°C.

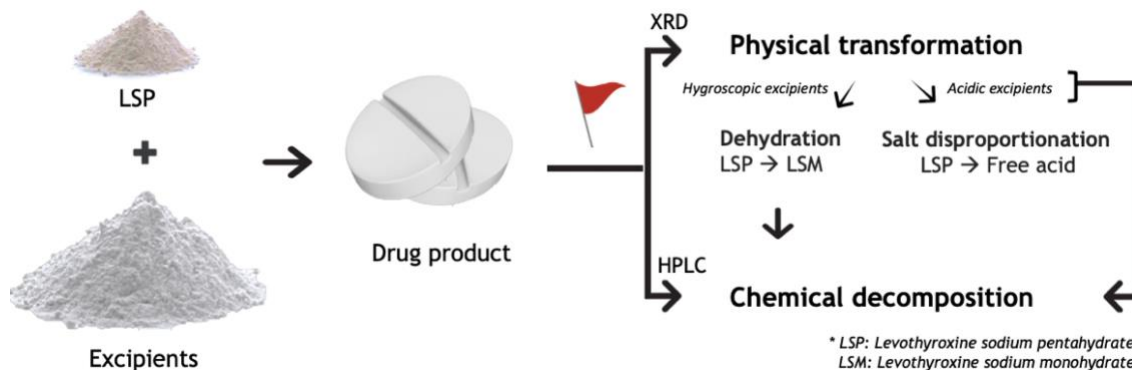


Figure 6.4. Schematic of the potential physical and chemical instability that may be induced in LSP when combined with a range of pharmaceutical tablet excipients.

LSP exhibited partial dehydration and disproportionation in the presence of hygroscopic and acidic excipients, respectively. Being a solution based technique, HPLC revealed chemical decomposition of the API but the technique was insensitive to physical transformations. LSP was susceptible to chemical decomposition in the presence of lactose monohydrate, microcrystalline cellulose and croscarmellose sodium. Excipient properties such as hygroscopicity and microenvironmental acidity were identified to be critical determinants of both physical and chemical stability of LSP in a drug product. Alkaline and hydrophobic excipients provide an avenue to design stable solid oral dosage form of the API.

CHAPTER 7

Chapter 7. Future work

This thesis focused on establishing a comprehensive understanding of the factors underlying the physical and chemical instability of salts and cocrystals in a drug product. The ultimate goal is design and develop stable solid oral dosage forms for the model system.

In **Chapter 2**, we demonstrated that pharmaceutical processing can induce lattice disorder in crystalline pharmaceutical solids. The work also highlighted that lattice disorder (in an otherwise crystalline sample) can have a disproportionate influence on the chemical reactivity of the system. The disorder is proposed to be higher on the surface of powder particles (experiencing the shear) as compared to the bulk. Based on the assumption that the lattice disorder is predominant on the surface, it can be hypothesized that cocrystal dissociation is initiated at the disordered interfaces of the cocrystal and excipient particles. Furthermore, it would also be interesting to compare the crystallinity of the surface and bulk of individual particles. Surface imaging using AFM provides an avenue to evaluate the crystallinity of individual particles. Our results also indicated that CAFOXA-DCPA coprocessing leads to a higher lattice disorder in CAFOXA cocrystals than when cocrystals were milled alone. It would be of value to investigate the influence of other excipients on the crystallinity of the API upon comilling. While “hard” excipients may increase disorder in the active, coprocessing with soft and plastically deforming excipients, such as glidants, would minimize lattice disorder.⁵¹¹ The magnitude of the processing induced disorder in the active will be a function of the mechanical properties of other excipients in the drug product, thereby necessitating an in-depth, systematic investigation. Furthermore, the influence of pharmaceutical processing on the crystallinity and functionality of the excipients also mandates consideration.

It is instructive to consider that microenvironment in the vicinity of DCPA (slurry pH 5.5) would favor oxalic acid ionization and hence, drive CAFOXA dissociation. Hence, the “acidity” of excipients would play a critical role in dictating the stability of CAFOXA cocrystals. It would be interesting to assess the influence of pH modifier on cocrystal stability (in presence of DCPA). Furthermore, formulation approaches, such as coating of the API particles, to minimize the direct contact between API and excipient particles would be of great value. Work on these aspects would aid informed decision for a formulator when selecting manufacturing processes.

In **Chapter 3**, AFM under controlled humidity conditions was used to evaluate the influence of water vapor pressure on the surface crystallization of disordered CAFOXA tablets. Since tablets are the most popular dosage forms, many pharmaceuticals will be subjected to processing steps such as milling and compression. It would be of value to study changes in the surface energy of the solids in response to mechanical activation by these processing steps. It would also be interesting

to develop a method to directly characterize and quantify disorder on the sample surface using AFM Peak Force QNM. Advances are being made to split micron-sized particles using a laser beam and consequently mount them on AFM for evaluation. This could enable deeper insights into structural disorder on the surface and bulk of milled particles. The application of terahertz pulsed imaging (TPI) can also be explored to achieve this objective.

In **Chapter 4**, we documented partial dehydration of LSP to form LSM (chemically more reactive than LSP). LSM readily forms in presence of hygroscopic tableting excipients such as povidone. Further studies examining the chemical stability of LSM in presence of tableting excipients would be valuable to advance the formulation development of stable solid oral dosage forms of the API. The instability of LSM in the solid state is attributed to its oxidative decomposition. Addition of an anti-oxidant to the formulation, as a stabilizing strategy, should be explored. The determination of the exact products of oxidative decomposition of LSM were outside the scope of this work. Further investigation into the mechanism and consequent products of oxidative decomposition would be of interest. Our studies indicate a continuum of crystal structures between LSP and LSM (including levothyroxine sodium tetrahydrate (LST)), and between LSM and LSA. While our work indicates a change in crystal structure from LSM→ LSA, the metastable nature of the anhydrous form and its consequent propensity to amorphize renders it challenging to elucidate the crystal structure of the completely dehydrated phase. It would be valuable to determine the crystal structure of the anhydrate as it can provide further insights into the structure - function relationship for this model system. A valuable addition to this work would be deeper insights into the location of water in the crystal structures of LSP and LSM. While ssNMR and single crystal XRD provided useful information, the exact location of water, and its interactions with the phenolic and amino moieties need further investigation. This information would enable a better understanding of the influence of crystal structure on the thermodynamic stability of the molecule.

In **Chapter 5**, the physical and chemical stability of LSP were evaluated in the presence of a range of tableting excipients. The work yielded vital insights into the factors influencing the chemical stability of LSP in a drug product environment. Under accelerated stability testing conditions, excipient hygroscopicity and microenvironmental acidity were recognized to be critical determinants of chemical stability. Acidic microenvironment promoted chemical decomposition whereas an alkaline microenvironment conferred stability to the API. It would be valuable to test the stability of LSP in prototype formulations containing acidic and alkaline pH modifiers. This would enable a comprehensive understanding of the different interplaying factors and their influence on the stability of LSP. In addition to chemical decomposition, LSP also exhibited salt

disproportionation to form the free acid form of levothyroxine in presence of “acidic” excipients. While the free acid form has a lower solubility than the sodium salt, its stability is incompletely understood. It would be interesting to the stability of the free acid form of levothyroxine, and the implications of its appearance in solid oral dosage forms. Another challenging aspect of this work was understanding the exact mechanism of chemical decomposition of LSP in presence of excipients. Levothyroxine is known to undergo chemical decomposition via multiple complex pathways: oxidation, deamination and deiodination. While we have been able to identify some excipient specific properties promoting instability, a valuable addition to this work would be characterization of the products of chemical decomposition. Investigations of this nature have previously been performed using advanced techniques such as LS-MS.

While outside the scope of this work, the photostability of LSP, especially in marketed formulations, mandates further investigation. The next logical step to ensuring solid form control in marketed formulations would be to develop validated methods for physical form characterization of levothyroxine. XRD was heavily used in the present work to evaluate physical and chemical stability of LSP in a drug product environment. It would be of value to perform similar investigations using spectroscopic techniques such as FTIR. Collaborative analysis using multiple techniques would enable deeper insights into the exact mechanism of instability of LSP with excipients used in the dosage form.

BIBLIOGRAPHY

Bibliography

1. Lawrence XY 2008. Pharmaceutical quality by design: product and process development, understanding, and control. *Pharm Res* 25(4):781-791.
2. Kalepu S, Nekkanti V 2015. Insoluble drug delivery strategies: review of recent advances and business prospects. *Acta Pharm Sin B* 5(5):442-453.
3. Serajuddin AT 2007. Salt formation to improve drug solubility. *Adv Drug Deliv Rev* 59(7):603-616.
4. Elder DP, Holm R, de Diego HL 2013. Use of pharmaceutical salts and cocrystals to address the issue of poor solubility. *Int J Pharm* 453(1):88-100.
5. Hancock BC, Parks M 2000. What is the true solubility advantage for amorphous pharmaceuticals? *Pharm Res* 17(4):397-404.
6. Fukuoka E, Makita M, Yamamura S 1989. Glassy state of pharmaceuticals. III.: Thermal properties and stability of glassy pharmaceuticals and their binary glass systems. *Chem Pharm Bull* 37(4):1047-1050.
7. Griesser UJ, Stowell JG. 2003. *Solid-state analysis and polymorphism*. ed.: Blackwell, Oxford.
8. Stahl PH, Wermuth CG. 2002. *Pharmaceutical salts: Properties, selection and use*. ed.: John Wiley & sons.
9. Christensen NPA, Rantanen J, Cornett C, Taylor LS 2012. Disproportionation of the calcium salt of atorvastatin in the presence of acidic excipients. *Eur J Pharm Biopharm* 82(2):410-416.
10. Unger EF 2009. Weighing benefits and risks—the FDA's review of prasugrel. *N Engl J Med* 361(10):942-945.
11. Thakral NK, Kelly RC 2017. Salt disproportionation: A material science perspective. *Int J Pharm* 520(1-2):228-240.
12. Williams AC, Cooper VB, Thomas L, Griffith LJ, Petts CR, Booth SW 2004. Evaluation of drug physical form during granulation, tableting and storage. *Int J Pharm* 275(1-2):29-39.
13. Stephenson GA, Aburub A, Woods TA 2011. Physical stability of salts of weak bases in the solid-state. *J Pharm Sci* 100(5):1607-1617.
14. Hsieh Y-L, Taylor LS 2015. Salt stability-effect of particle size, relative humidity, temperature and composition on salt to free base conversion. *Pharm Res* 32(2):549-561.
15. Guerrieri P, Taylor LS 2009. Role of salt and excipient properties on disproportionation in the solid-state. *Pharm Res* 26(8):2015-2026.
16. Hilfiker R. 2006. *Polymorphism in the pharmaceutical industry*. ed.: Wiley Online Library.
17. Vishweshwar P, McMahon JA, Bis JA, Zaworotko MJ 2006. Pharmaceutical co-crystals. *J Pharm Sci* 95(3):499-516.
18. Aitipamula S, Banerjee R, Bansal AK, Biradha K, Cheney ML, Choudhury AR, Desiraju GR, Dikundwar AG, Dubey R, Duggirala N 2012. Polymorphs, salts, and cocrystals: what's in a name? *Cryst Growth Des* 12(5):2147-2152.
19. Childs SL, Chyall LJ, Dunlap JT, Smolenskaya VN, Stahly BC, Stahly GP 2004. Crystal engineering approach to forming cocrystals of amine hydrochlorides with organic acids. Molecular complexes of fluoxetine hydrochloride with benzoic, succinic, and fumaric acids. *J Am Chem Soc* 126(41):13335-13342.
20. Caira MR, Bourne SA, Samsodien H, Engel E, Liebenberg W, Stieger N, Aucamp M 2012. Co-crystals of the antiretroviral nevirapine: crystal structures, thermal analysis and dissolution behaviour. *Cryst Eng Comm* 14(7):2541-2551.
21. Childs SL, Kandi P, Lingireddy SR 2013. Formulation of a danazol cocrystal with controlled supersaturation plays an essential role in improving bioavailability. *Mol Pharm* 10(8):3112-3127.
22. Chow SF, Chen M, Shi L, Chow AH, Sun CC 2012. Simultaneously improving the mechanical properties, dissolution performance, and hygroscopicity of ibuprofen and flurbiprofen by cocrystallization with nicotinamide. *Pharm Res* 29(7):1854-1865.

23. Karki S, Frišćić T, Fabian L, Laity PR, Day GM, Jones W 2009. Improving mechanical properties of crystalline solids by cocrystal formation: new compressible forms of paracetamol. *Adv Mater* 21(38-39):3905-3909.
24. https://www.accessdata.fda.gov/drugsatfda_docs/label/2011/018723s037lbl.pdf (accessed on 28 July 2018).
25. Harrison WT, Yathirajan H, Bindya S, Anilkumar H 2007. Escitalopram oxalate: co-existence of oxalate dianions and oxalic acid molecules in the same crystal. *Acta Crystallogr* 63(2):o129-o131.
26. <https://www.fda.gov/Drugs/InformationOnDrugs/ucm457521.htm> (accessed on July 28, 2018).
27. Bowles P, Brenek SJ, Caron Sp, Do NM, Drexler MT, Duan S, Dubé P, Hansen EC, Jones BP, Jones KN 2014. Commercial route research and development for SGLT2 inhibitor candidate ertugliflozin. *Org Process Res Dev* 18(1):66-81.
28. <https://www.astellas.com/en/corporate/news/detail/approval-of-suglat-tablets-a-s.html> (accessed 28 July 2018).
29. Eddleston MD, Lloyd GO, Jones W 2012. Cocrystal dissociation and molecular demixing in the solid state. *Chem Comm* 48(65):8075-8077.
30. Eddleston MD, Madusanka N, Jones W 2014. Cocrystal dissociation in the presence of water: A general approach for identifying stable cocrystal forms. *J Pharm Sci* 103(9):2865-2870.
31. Eddleston MD, Thakuria R, Aldous BJ, Jones W 2014. An investigation of the causes of cocrystal dissociation at high humidity. *J Pharm Sci* 103(9):2859-2864.
32. Trask AV, Motherwell WS, Jones W 2005. Pharmaceutical cocrystallization: engineering a remedy for caffeine hydration. *Cryst Growth Des* 5(3):1013-1021.
33. Trask AV, Motherwell WS, Jones W 2006. Physical stability enhancement of theophylline via cocrystallization. *Int J Pharm* 320(1):114-123.
34. Duggirala NK, Vyas A, Krzyzaniak JF, Arora KK, Suryanarayanan R 2017. Mechanistic Insight into Caffeine–Oxalic Cocrystal Dissociation in Formulations: Role of Excipients. *Mol Pharm* 14(11):3879-3887.
35. Koranne SA, Sahoo A, Krzyzaniak JF, Luthra S, Arora KK, Suryanarayanan R 2018. Challenges in transitioning cocrystals from bench to bedside: Dissociation in prototype drug product environment. *Mol Pharm* 15(8):3297-3307.
36. Byrn SR, Zografi G, Chen S. 2017. Solid state properties of pharmaceutical materials. ed.: Wiley Online Library.
37. Khankari RK, Grant DJ 1995. Pharmaceutical hydrates. *Thermochim Acta* 248:61-79.
38. Bates S, Kelly RC, Ivanisevic I, Schields P, Zografi G, Newman AW 2007. Assessment of defects and amorphous structure produced in raffinose pentahydrate upon dehydration. *J Pharm Sci* 96(5):1418-1433.
39. 2019. NifHaCaE. Thyroid Disease: assessment and Management. Available at <http://www.nice.org.uk/guidance/ng145> (accessed June 10, 2020).
40. Descamps M, Willart J, Dudognon E, Caron V 2007. Transformation of pharmaceutical compounds upon milling and comilling: the role of Tg. *J Pharm Sci* 96(5):1398-1407.
41. Lieberman HA, Lachman L. 1980. *Pharmaceutical Dosage Forms: Tablets*. ed.: Marcel Dekker.
42. Zhang GG, Law D, Schmitt EA, Qiu Y 2004. Phase transformation considerations during process development and manufacture of solid oral dosage forms. *Adv Drug Deliv Rev* 56(3):371-390.
43. Chieng N, Zujovic Z, Bowmaker G, Rades T, Saville D 2006. Effect of milling conditions on the solid-state conversion of ranitidine hydrochloride form 1. *Int J Pharm* 327(1-2):36-44.
44. Chieng N, Rades T, Saville D 2008. Formation and physical stability of the amorphous phase of ranitidine hydrochloride polymorphs prepared by cryo-milling. *Eur J Pharm Biopharm* 68(3):771-780.

45. Lin S-Y, Hsu C-H, Ke W-T 2010. Solid-state transformation of different gabapentin polymorphs upon milling and co-milling. *Int J Pharm* 396(1-2):83-90.
46. Griesser UJ. 2006. The importance of solvates. ed.
47. Bates S, Kelly RC, Ivanisevic I, Schields P, Zografi G, Newman AW 2007. Assessment of defects and amorphous structure produced in raffinose pentahydrate upon dehydration. *J Pharm Sci* 96(5):1418-1433.
48. Griesser U, Burger A 1995. The effect of water vapor pressure on desolvation kinetics of caffeine 4/5-hydrate. *Int J Pharm* 120(1):83-93.
49. Edwards HG, Lawson E, de Matas M, Shields L, York P 1997. Metamorphosis of caffeine hydrate and anhydrous caffeine. *J Chem Soc, Perkin Trans (10)*:1985-1990.
50. Trask AV, Motherwell WS, Jones W 2005. Pharmaceutical cocrystallization: engineering a remedy for caffeine hydration. *Cryst Growth Des* 5(3):1013-1021.
51. Chen Y, Tai H-Y 2020. Levothyroxine in the treatment of overt or subclinical hypothyroidism: a systematic review and meta-analysis. *Endocr J*:EJ19-0583.
52. Mateo RCI, Hennessey JV 2019. Thyroxine and treatment of hypothyroidism: seven decades of experience. *Endocrine* 66(1):10-17.
53. Duntas LH 2019. Seven Decades of Levothyroxine: A Comprehensive Profile. *Adv Ther* 36:27–29.
54. 2019. NifHaCaE. Thyroid Disease: assessment and Management. Available at www.nice.org.uk/guidance/ng145 (accessed June 10, 2020).
55. Niazi AK, Kalra S, Irfan A, Islam A 2011. Thyroidology over the ages. *Indian J Endocr Metab* 15(Suppl2):S121.
56. Mitchell AL, Hickey B, Hickey JL, Pearce SH 2009. Trends in thyroid hormone prescribing and consumption in the UK. *BMC public health* 9(1):132.
57. Virta LJ, Eskelinen SI 2011. Prevalence of hypothyroidism in Finland—a nationwide prescription study. *Eur J Clin Pharmacol* 67(1):73-77.
58. Tehrani FR, Tohidi M, Dovom MR, Azizi F 2011. A population based study on the association of thyroid status with components of the metabolic syndrome. *J Diabetes Metab* 2(8):1-6.
59. Escribano-Serrano J, Mancera-Romero J, Santos-Sanchez V, Paya-Giner C, Méndez-Esteban M, Garcia-Bonilla A, Marquez-Ferrando M, Hormigo-Pozo A, Michan-Dona A 2016. Prevalence of Hypothyroidism in Andalusia, Spain, Determined by Thyroid Hormone Consumption. *Rev Esp Salud Publica* 90:e1-12.
60. Leese G, Flynn R, Jung R, Macdonald T, Murphy M, Morris A 2008. Increasing prevalence and incidence of thyroid disease in Tayside, Scotland: the Thyroid Epidemiology Audit and Research Study (TEARS). *Clin Endocr* 68(2):311-316.
61. Ingoe L, Phipps N, Armstrong G, Rajagopal A, Kamali F, Razvi S 2017. Prevalence of treated hypothyroidism in the community: Analysis from general practices in North-East England with implications for the United Kingdom. *Clin Endocrinol* 87(6):860-864.
62. Jannini EA, Ullisse S, D'Armiento M 1995. Thyroid hormone and male gonadal function. *Endocr Rev* 16(4):443-459.
63. Bernal J 2007. Thyroid hormone receptors in brain development and function. *Nat Clin Pract Endocrinol Metab* 3(3):249-259.
64. Forrest D, Erway LC, Ng L, Altschuler R, Curran T 1996. Thyroid hormone receptor β is essential for development of auditory function. *Nat Genet* 13(3):354-357.
65. Bernal J, Guadaño-Ferraz A, Morte B 2003. Perspectives in the study of thyroid hormone action on brain development and function. *Thyroid* 13(11):1005-1012.
66. Arthur JR, Beckett GJ 1999. Thyroid function. *Br Med Bull* 55(3):658-668.
67. Katz AI, Emmanouel DS, Lindheimer MD 1975. Thyroid hormone and the kidney. *Nephron* 15(3-5):223-249.

68. Pillar TM, Seitz HJ 1997. Thyroid hormone and gene expression in the regulation of mitochondrial respiratory function. *Eur J Endocr* 136(3):231-239.
69. Fazio S, Palmieri EA, Lombardi G, Biondi B 2004. Effects of thyroid hormone on the cardiovascular system. *Recent Prog Horm Res* 59(1):31-50.
70. Klein I, Ojamaa K 2001. Thyroid hormone and the cardiovascular system. *N Engl J Med* 344(7):501-509.
71. Harvey CB, O'Shea PJ, Scott AJ, Robson H, Siebler T, Shalet SM, Samarut J, Chassande O, Williams GR 2002. Molecular mechanisms of thyroid hormone effects on bone growth and function. *Mol Genet Metab* 75(1):17-30.
72. Rajendran A, Bhavani N, Nair V, Pavithran PV, Menon VU, Kumar H 2021. Oral Levothyroxine is an Effective Option for Myxedema Coma: A Single-Centre Experience. *Eur Thyroid J* 10(1):23-29.
73. Mandel SJ, Brent GA, Larsen PR 1993. Levothyroxine therapy in patients with thyroid disease. *Ann Intern Med* 119(6):492-502.
74. Bandeira-Echtler E, Bergerhoff K, Richter B 2014. Levothyroxine or minimally invasive therapies for benign thyroid nodules. *Cochrane Database Syst Rev* (6):1465-1858.
75. Güllü S, Gürses MA, Baskal N, Uysal AR, Kamel AN, Erdogan G 1999. Suppressive therapy with levothyroxine for euthyroid diffuse and nodular goiter. *Endocr J* 46(1):221-226.
76. Burmeister LA, Goumaz M, Mariash C, Oppenheimer JH 1992. Levothyroxine dose requirements for thyrotropin suppression in the treatment of differentiated thyroid cancer. *J Clin Endocrinol Metab* 75(2):344-350.
77. Farwell A, Braverman L 2001. Thyroid and antithyroid drugs. *Goodman and Gilman's The Pharmacological Basis of Therapeutics Tenth edition McGraw-Hill:1563-1596.*
78. Murray GR 1891. Note on the treatment of myxoedema by hypodermic injections of an extract of the thyroid gland of a sheep. *Br Med J* 2(1606):796.
79. Fox E 1892. A case of myxoedema treated by taking extract of thyroid by the mouth. *Br Med J* 2(1661):941.
80. Mackenzie HW 1892. A case of myxoedema treated with great benefit by feeding with fresh thyroid glands. *Br Med J* 2(1661):940.
81. Jackson IM, Cobb WE 1978. Why does anyone still use desiccated thyroid USP? *Am J Med* 64(2):284-288.
82. Slater S 2011. The discovery of thyroid replacement therapy. Part 3: A complete transformation. *J R Soc Med* 104(3):100-106.
83. McAninch EA, Bianco AC 2016. The history and future of treatment of hypothyroidism. *Ann Intern Med* 164(1):50-56.
84. Bryan J 2019. Levothyroxine: from sheep thyroid injections to synthetic formulations. *Pharm J* 291:90.
85. Kendall EC 1915. The isolation in crystalline form of the compound containing iodine, which occurs in the thyroid: its chemical nature and physiologic activity. *J Am Med Assoc* 64(25):2042-2043.
86. Kendall E 1917. The thyroid hormone. *Collect Pap Mayo Clin Mayo Found* 9:309.
87. Harington CR 1926. Chemistry of thyroxine: constitution and synthesis of desiodo-thyroxine. *Biochem J* 20(2):300.
88. Harington CR 1926. Chemistry of thyroxine: isolation of thyroxine from the thyroid gland. *Biochem J* 20(2):293.
89. Harington CR, Barger G 1927. Chemistry of thyroxine: constitution and synthesis of thyroxine. *Biochem J* 21(1):169.
90. Kendall E. *Mayo Clinic Proceedings*, 1964, pp 548.
91. Nusynowitz ML 1983. The isolation of thyroxine. *JAMA* 250(15):2047-2048.
92. Lindholm J, Laurberg P 2011. Hypothyroidism and thyroid substitution: historical aspects. *J Thyroid Res* 2011.

109. Paul TL, Kerrigan J, Kelly AM, Braverman LE, Baran DT 1988. Long-term L-thyroxine therapy is associated with decreased hip bone density in premenopausal women. *JAMA* 259(21):3137-3141.
110. Gammage M, Parle J, Holder R, Roberts L, Hobbs F, Wilson S, Sheppard M, Franklyn J 2007. Association between serum free thyroxine concentration and atrial fibrillation. *JAMA Internal Medicine* 167(9):928-934.
111. Heeringa J, Hoogendoorn E, Van der Deure W, Hofman A, Peeters R, Hop W, den Heijer M, Visser TJ, Witteman JC 2008. High-normal thyroid function and risk of atrial fibrillation: the Rotterdam study. *JAMA Internal Medicine* 168(20):2219-2224.
112. Ettinger B, Wingerd J 1982. Thyroid supplements: effect on bone mass. *West J Med* 136(6):473.
113. Hak AE, Pols HA, Visser TJ, Drexhage HA, Hofman A, Witteman JC 2000. Subclinical hypothyroidism is an independent risk factor for atherosclerosis and myocardial infarction in elderly women: the Rotterdam Study. *Ann Intern Med* 132(4):270-278.
114. Tunbridge W, Evered D, Hall R, Appleton D, Brewis M, Clark F, Evans JG, Young E, Bird T, Smith P 1977. Lipid profiles and cardiovascular disease in the Wickham area with particular reference to thyroid failure. *Clin Endocrinol* 7(6):495-508.
115. Carr D, McLeod D, Parry G, Thornes H 1988. Fine adjustment of thyroxine replacement dosage: comparison of the thyrotrophin releasing hormone test using a sensitive thyrotrophin assay with measurement of free thyroid hormones and clinical assessment. *Clin Endocrinol* 28(3):325-333.
116. Klein I, Danzi S 2003. Evaluation of the therapeutic efficacy of different levothyroxine preparations in the treatment of human thyroid disease. *Thyroid* 13(12):1127-1132.
117. Health UDo, Food HS, Evaluation DACfD, Research. 2000. Guidance for Industry: Levothyroxine Sodium Tablets—In Vivo Pharmacokinetic and Bioavailability Studies and In Vitro Dissolution Testing. ed.: CDER.
118. Fish LH, Schwartz HL, Cavanaugh J, Steffes MW, Bantle JP, Oppenheimer JH 1987. Replacement dose, metabolism, and bioavailability of levothyroxine in the treatment of hypothyroidism. *N Engl J Med* 316(13):764-770.
119. Wartofsky L 2005. Levothyroxine therapy for hypothyroidism: should we abandon conservative dosage titration? *JAMA Internal Medicine* 165(15):1683-1684.
120. Wenzel K 1986. Optimization of levothyroxine treatment. Dosage dependence on the existing parenchymal mass, age, body weight and fasting intake. *Dtsch Med Wochenschr* 111(36):1356-1362.
121. Dietrich JW, Leow MK, Goede SL, Midgley JE, Landgrafe G, Hoermann R 2013. Do thyroid-stimulating hormone, body weight, or body mass index serve as adequate markers to guide levothyroxine dose titration? *J Am Coll Surg* 217(4):752-753.
122. Eligar V, Taylor PN, Okosieme O, Leese G, Dayan CM 2016. Thyroxine replacement: a clinical endocrinologist's viewpoint. *Ann Clin Biochem* 53(4):421-433.
123. Lage MJ, Vora J, Hepp Z, Espaillet R 2020. Levothyroxine Treatment of Pregnant Women with Hypothyroidism: Retrospective Analysis of a US Claims Database. *Adv Ther* 37(2):933-945.
124. 2012. Synthroid (levothyroxine sodium). Full prescribing information. ed.: AbbVie, North Chicago.
125. Colucci P, Yue CS, Ducharme M, Benvenga S 2013. A review of the pharmacokinetics of levothyroxine for the treatment of hypothyroidism. *Eur Endocrinol* 9(1):40.
126. Sawin CT, Surks MI, London M, Ranganathan C, Larsen PR 1984. Oral thyroxine: variation in biologic action and tablet content. *Ann Intern Med* 100(5):641-645.
127. LeBoff MS, Kaplan MM, Silva JE, Larsen PR 1982. Bioavailability of thyroid hormones from oral replacement preparations. *Metabolism* 31(9):900-905.

128. Shah RB, Collier JS, Sayeed VA, Bryant A, Habib MJ, Khan MA 2010. Tablet splitting of a narrow therapeutic index drug: a case with levothyroxine sodium. *AAPS PharmSciTech* 11(3):1359-1367.
129. Abou-Taleb BA, Nounou MI, Khalafallah N, Khalil S 2018. Effect of batch age on potency and dissolution of levothyroxine sodium tablets: impact of BP and USP monograph differences on dissolution results. *Drug Dev Ind Pharm* 44(11):1762-1769.
130. Wockhardt UK recalls Levothyroxine Oral Solution from pharmacies. *Pharmacy business*. 2020. <https://www.pharmacy.biz/wockhardt-uk-recalls-levothyroxine-oral-solution-from-pharmacies/> Accessed on August 10, 2020.
131. Specific batches of levothyroxine recalled as precautionary measure. *European Pharmaceutical Review - News*. 2020. <https://www.europeanpharmaceuticalreview.com/news/111777/specific-batches-of-levothyroxine-recalled-as-precautionary-measure/> Accessed on August 10, 2020.
132. USFDA. Levothyroxine recalls. <https://www.archive-it.org/collections/7993?q=levothyroxine+recall&show=ArchivedPages&hitsPerDupe=0&go=Search+the+Archive> Accessed on August 10, 2020.
133. FDA alert archive. April 2007. Available at https://www.drugs.com/fda_alerts_archive/april-2007.html Accessed August 10, 2020.
134. Recalls, Market Withdrawals, & Safety Alerts. Enforcement Reports. <https://wayback.archive-it.org/7993/20170722062203/https://www.fda.gov/Safety/Recalls/EnforcementReports/ucm272014.htm> Accessed on August 10, 2020.
135. Recalls, Market Withdrawals, & Safety Alerts. Enforcement Reports. <https://wayback.archive-it.org/7993/20170404195817/https://www.fda.gov/Safety/Recalls/EnforcementReports/ucm269605.htm> Accessed on August 10, 2020.
136. Recalls, Market Withdrawals, & Safety Alerts. Enforcement Reports. <https://wayback.archive-it.org/7993/20180126102747/https://www.fda.gov/downloads/Safety/Recalls/EnforcementReports/UCM167873.pdf> Accessed on August 10, 2020.
137. Recalls, Market Withdrawals, & Safety Alerts. Enforcement Reports. <https://wayback.archive-it.org/7993/20170404195824/https://www.fda.gov/Safety/Recalls/EnforcementReports/ucm262819.htm> Accessed on August 10, 2020.
138. Recalls, Market Withdrawals, & Safety Alerts. Enforcement Reports. <https://wayback.archive-it.org/7993/20170403231827/https://www.fda.gov/Safety/Recalls/EnforcementReports/ucm310739.htm> Accessed on August 10, 2020.
139. Recalls, Market Withdrawals, & Safety Alerts. Enforcement Reports. <https://wayback.archive-it.org/7993/20170722062146/https://www.fda.gov/Safety/Recalls/EnforcementReports/ucm283761.htm> Accessed on August 10, 2020.
140. Recalls, Market Withdrawals, & Safety Alerts. Enforcement Reports. Available at <https://wayback.archive-it.org/7993/20170722062245/https://www.fda.gov/Safety/Recalls/EnforcementReports/ucm242808.htm> Accessed on August 10, 2020.
141. Recalls, Market Withdrawals, & Safety Alerts. Enforcement Reports. Available at <https://wayback.archive-it.org/7993/20170404195823/https://www.fda.gov/Safety/Recalls/EnforcementReports/ucm264002.htm> Accessed on August 10, 2020.

142. Recalls, Market Withdrawals, & Safety Alerts. Enforcement Reports. Available at <https://wayback.archive-it.org/7993/20170404195845/https://www.fda.gov/Safety/Recalls/EnforcementReports/ucm247463.htm> Accessed on August 10, 2020.
143. Recalls, Market Withdrawals, & Safety Alerts. Enforcement Reports. Available at <https://wayback.archive-it.org/7993/20170722062149/https://www.fda.gov/Safety/Recalls/EnforcementReports/ucm282335.htm> Accessed on August 10, 2020.
144. Recalls, Market Withdrawals, & Safety Alerts. Enforcement Reports. Available at <https://wayback.archive-it.org/7993/20170722062208/https://www.fda.gov/Safety/Recalls/EnforcementReports/ucm268464.htm> Accessed on August 10, 2020.
145. Schreder S, Nischwitz M. 2002. Pharmaceutical levothyroxine preparation. ed.: Google Patents.
146. Food, Administration D 1997. Food and Drug Administration Notice Regarding Levothyroxine Sodium. Federal Register 62:157.
147. Kulig K, Golightly LK, Rumack BH 1985. Levothyroxine overdose associated with seizures in a young child. JAMA 254(15):2109-2110.
148. Gorman RL, Chamberlain JM, Rose SR, Oderda GM 1988. Massive levothyroxine overdose: high anxiety—low toxicity. Pediatrics 82(4):666-669.
149. Ho J, Jackson R, Johnson D 2011. Massive levothyroxine ingestion in a pediatric patient: case report and discussion. CJEM 13(3):165-168.
150. Kawakami T, Tanaka A, Negoro S, Morisawa Y, Mikami M, Hojo M, Yamamoto T, Uegaki S, Aiso M, Kawasaki T 2007. Liver injury induced by levothyroxine in a patient with primary hypothyroidism. Intern Med 46(14):1105-1108.
151. Lotan Shilo M, Susy Kovatz M, Ruth Hadari M, Eli Weiss PhD DN, Louis Shenkman M 2002. Massive Thyroid Hormone Overdose: Kinetics, Clinical Manifestations and Management. Isr Med Assoc J 4(4):298.
152. 2006. Guidance for Industry. Q8 Pharmaceutical Development. In Administration USDoHaHSFaD, editor, ed., Rockville, MD: FDA.
153. 1997. US FDA. Notice of proposed rulemaking. levothyroxine sodium. Docket No. 97N-0314. In Prescription Drug products UFaDA, editor, ed., U.S. Government Publishing Office: Washington, D.C. : Fed Regist. p 43535-43538.
154. After 46 years of sales, thyroid drug needs FDA approval. New York Times. Available at <https://www.nytimes.com/2001/07/24/science/after-46-years-of-sales-thyroid-drug-needs-fda-approval.html>. Accessed May 2020.
155. 1997. Fedral Register, Prescription Drug Products; Levothyroxine Sodium (Docket Number 97N-0314). In U.S. Government Publishing Office: Washington DC, editor, ed. p 43535-43538.
156. Burman K, Hennessey J, McDermott M, Wartofsky L, Emerson C 2008. The FDA revises requirements for levothyroxine products. Thyroid 18(5):487-490.
157. FDA Acts to Ensure Thyroid Drugs Don't Lose Potency Before Expiration Date. Available at <https://www.fda.gov/drugs/postmarket-drug-safety-information-patients-and-providers/fda-acts-ensure-thyroid-drugs-dont-lose-potency-expiration-date>. Accessed April 2020.
158. Mechcatie E 2006. FDA Panel Scrutinizes Thyroid Drug Stability. Family Practice News 36(22):19-19.
159. 2004. Thyroid experts warn of clinically important differences in potency of FDA-approved levothyroxine products. . Thyroid Experts Warning, ed.: The American Thyroid Association. USA. .
160. Levothyroxine sodium - list of product recalls. Available at <https://www.medprodisposal.com/recalls/levothyroxine-recall/>. Accessed April 2020.

161. Han DH. 2018. FDA: Thyroid Medications Recalled Due to Inconsistent Potency. <https://www.empr.com/uncategorized/fda-thyroid-medications-recalled-due-to-inconsistent-potency/>. Accessed in May 2020. MPR articles, ed.: Haymarket Media, Inc.
162. Abdallah S, Mohamed I 2016. Factor affecting photo and thermal stability of levothyroxine sodium. *J Pharm Res Int* 10(2):1-11.
163. Ledeti I, Romanescu M, Cîrcioban D, Ledeti A, Vlase G, Vlase T, Suciuc O, Murariu M, Olariu S, Matusz P 2020. Stability and Compatibility Studies of Levothyroxine Sodium in Solid Binary Systems—Instrumental Screening. *Pharmaceutics* 12(1):58.
164. Shah HS, Chaturvedi K, Hamad M, Bates S, Hussain A, Morris K 2019. New insights on solid-state changes in the levothyroxine sodium pentahydrate during dehydration and its relationship to chemical instability. *AAPS PharmSciTech* 20(1):39.
165. Hamad ML, Engen W, Morris KR 2015. Impact of hydration state and molecular oxygen on the chemical stability of levothyroxine sodium. *Pharm Dev Technol* 20(3):314-319.
166. Patel H, Stalcup A, Dansereau R, Sakr A 2003. The effect of excipients on the stability of levothyroxine sodium pentahydrate tablets. *Int J Pharm* 264(1-2):35-43.
167. Parizi MPS, Acosta AML, Ishiki HM, Rossi RC, Mafra RC, Teixeira ACSC 2019. Environmental photochemical fate and UVC degradation of sodium levothyroxine in aqueous medium. *Environ Sci Pollut Res* 26(5):4393-4403.
168. Saha S, Shahiwala AF 2009. Multifunctional coprocessed excipients for improved tableting performance. *Expert Opin Drug Deliv* 6(2):197-208.
169. Zarmpi P, Flanagan T, Meehan E, Mann J, Fotaki N 2017. Biopharmaceutical aspects and implications of excipient variability in drug product performance. *Eur J Pharm Biopharm* 111:1-15.
170. Jivraj M, Martini LG, Thomson CM 2000. An overview of the different excipients useful for the direct compression of tablets. *Pharma Sci Technol Today* 3(2):58-63.
171. Airaksinen S. 2005. Role of excipients in moisture sorption and physical stability of solid pharmaceutical formulations. ed.
172. Cooper DS, Duntas LH 2019. Thyroid hormone therapy: past, present, and future. *Endocrine* 66(1):1-2.
173. McAninch E 2016. History and Future of Treatment of Hypothyroidism *Ann Intern Med* 164(5):376-376.
174. Lev-Ran A 1983. Part-of-the-day hypertriiodothyroninemia caused by desiccated thyroid. *JAMA* 250(20):2790-2791.
175. Tessnow A 2019. It's not your thyroid...(probably).
176. Braverman LE, Ingbar SH 1964. Anomalous effects of certain preparations of desiccated thyroid on serum protein-bound iodine. *N Engl J Med* 270(9):439-442.
177. Mangieri C, Lund M 1970. Potency of United States Pharmacopeia desiccated thyroid tablets as determined by the antigoiatrogenic assay in rats. *J Clin Endocrinol Metab* 30(1):102-104.
178. Kaufman SC, Gross TP, Kennedy DL 1991. Thyroid hormone use: trends in the United States from 1960 through 1988. *Thyroid* 1(4):285-291.
179. Hennessey JV, Burman KD, Wartofsky L 1985. The equivalency of two L-thyroxine preparations. *Ann Intern Med* 102(6):770-773.
180. Hennessey JV, Evaul JE, Tseng Y-C, Burman KD, Wartofsky L 1986. L-thyroxine dosage: a reevaluation of therapy with contemporary preparations. *Ann Intern Med* 105(1):11-15.
181. Escalante DA, Arem N, Arem R 1995. Assessment of interchangeability of two brands of levothyroxine preparations with a third-generation TSH assay. *Am J Med* 98(4):374-378.
182. Gross J, R P-R 1952. The identification of 3, 5, 3'-L-triiodo-thyronine in human plasma. *The Lancet* 259(6705):439-441.
183. Gross J, Pitt-Rivers R 1953. 3: 5: 3'-Triiodothyronine. 2. Physiological activity. *Biochem J* 53(4):652.

184. Gross J, Pitt-Rivers R 1953. 3: 5: 3'-triiodothyronine. 1. Isolation from thyroid gland and synthesis. *Biochem J* 53(4):645.
185. Pitt-Rivers R, Stanbury JB, Rapp B 1955. Conversion of thyroxine to 3-5-3'-triiodothyronine in vivo. *J Clin Endocrinol Metab* 15(5):616-620.
186. Dorairajan N, Pradeep P 2013. Vignette thyroid surgery: a glimpse into its history. *Int Surg* 98(1):70-75.
187. Biondi B, Wartofsky L 2014. Treatment with thyroid hormone. *Endocr Rev* 35(3):433-512.
188. Hennessey JV 2015. Historical and current perspective in the use of thyroid extracts for the treatment of hypothyroidism. *Endocr Pract* 21(10):1161-1170.
189. Cooper DS, Duntas LH. 2019. *Thyroid hormone therapy: past, present, and future*. ed.: Springer.
190. Formenti AM, Mazziotti G, Giubbini R, Giustina A. 2016. Treatment of hypothyroidism: all that glitters is gold? , ed.: Springer. p 411-413.
191. Chaker L, Cappola AR, Mooijaart SP, Peeters RP 2018. Clinical aspects of thyroid function during ageing. *Lancet Diabetes Endocrinol* 6(9):733-742.
192. Santini F, Pinchera A, Marsili A, Ceccarini G, Castagna MG, Valeriano R, Giannetti M, Taddei D, Centoni R, Scartabelli G 2005. Lean body mass is a major determinant of levothyroxine dosage in the treatment of thyroid diseases. *J Clin Endocrinol Metab* 90(1):124-127.
193. Alexander EK, Pearce EN, Brent GA, Brown RS, Chen H, Dosiou C, Grobman WA, Laurberg P, Lazarus JH, Mandel SJ 2017. 2017 Guidelines of the American Thyroid Association for the diagnosis and management of thyroid disease during pregnancy and the postpartum. *Thyroid* 27(3):315-389.
194. Bao GW, Weinberg ME, Kwan C 2020. SUN-007 Elevated Levothyroxine Requirements Post-Partum as Initial Presentation of Placenta Accreta. *J Endocr Soc* 4(Supplement_1):SUN-007.
195. Walter-Sack I, Clanget C, Ding R, Goeggelmann C, Hinke V, Lang M, Pfeilschifter J, Tayrouz Y, Wegscheider K 2004. Assessment of levothyroxine sodium bioavailability. *Clin Pharmacokinet* 43(14):1037-1053.
196. Ain KB, Refetoff S, Fein HG, Weintraub BD 1991. Pseudomalabsorption of levothyroxine. *JAMA* 266(15):2118-2120.
197. Eligar P, Eligar V 2011. Levothyroxine: factors affecting its intestinal absorption and metabolism. *WLMJ* 3(4):9-14.
198. Benvenega S, Bartolone L, Squadrito S, GIUDICE FL, Trimarchi F 1995. Delayed intestinal absorption of levothyroxine. *Thyroid* 5(4):249-253.
199. Cooper DS 1984. Antithyroid drugs. *N Engl J Med* 311(21):1353-1362.
200. Tanguay M, Girard J, Scarsi C, Mautone G, Larouche R 2019. Pharmacokinetics and comparative bioavailability of a levothyroxine sodium oral solution and soft capsule. *Clin Pharm Drug Dev* 8(4):521-528.
201. Virili C, Antonelli A, Santaguida MG, Benvenega S, Centanni M 2019. Gastrointestinal malabsorption of thyroxine. . *Endocr Rev* 40(1):118-136.
202. Post A, Warren RJ. 1976. Sodium levothyroxine. *Analytical profiles of drug substances*, ed.: Elsevier. p 225-281.
203. Won CM 1992. Kinetics of degradation of levothyroxine in aqueous solution and in solid state. *Pharm Res* 9(1):131-137.
204. Kocic I, Homsek I, Dacevic M, Parojcic J, Miljkovic B 2011. An investigation into the influence of experimental conditions on in vitro drug release from immediate-release tablets of levothyroxine sodium and its relation to oral bioavailability. *AAPS PharmSciTech* 12(3):938.
205. Ivana K. 2013. *Biopharmaceutical characterization of levothyroxine sodium immediate-release tablets*. ed.: University of Belgrade.

206. (MHRA) MaHpRA. 2013. Levothyroxine: a review of clinical and quality considerations. Medicines and Healthcare products Regulatory Agency, ed.
207. Kasim NA, Whitehouse M, Ramachandran C, Bermejo M, Lennernäs H, Hussain AS, Junginger HE, Stavchansky SA, Midha KK, Shah VP 2004. Molecular properties of WHO essential drugs and provisional biopharmaceutical classification. *Mol Pharm* 1(1):85-96.
208. Pabla D, Akhlaghi F, Zia H 2009. A comparative pH-dissolution profile study of selected commercial levothyroxine products using inductively coupled plasma mass spectrometry. *Eur J Pharm Sci* 72(1):105-110.
209. Pabla D, Akhlaghi F, Zia H 2010. Intestinal permeability enhancement of levothyroxine sodium by straight chain fatty acids studied in MDCK epithelial cell line. *Eur J Pharm Sci* 40(5):466-472.
210. Lindenberg M, Kopp S, Dressman JB 2004. Classification of orally administered drugs on the World Health Organization Model list of Essential Medicines according to the biopharmaceutics classification system. *Eur J Pharm Biopharm* 58(2):265-278.
211. Macrae CF, Sovago I, Cottrell SJ, Galek PT, McCabe P, Pidcock E, Platings M, Shields GP, Stevens JS, Towler M 2020. Mercury 4.0: from visualization to analysis, design and prediction. *J Appl Crystallogr* 53(1):226-235.
212. Azran C, Porat D, Fine-Shamir N, Hanhan N, Dahan A 2019. Oral levothyroxine therapy postbariatric surgery: Biopharmaceutical aspects and clinical effects. *Surg Obes Relat Dis* 15(2):333-341.
213. Azran C, Porat D, Fine-Shamir N, Hanhan N, Dahan A 2019. Oral levothyroxine therapy postbariatric surgery: Biopharmaceutical aspects and clinical effects. *Surgery for Obesity and Related Diseases* 15(2):333-341.
214. Pharmacopoeia US. 2020. USP-NF Levothyroxine Sodium Tablets. https://online.uspnf.com/uspnf/document/1_GUID-023F9323-5475-4068-8E0C-452E09520242_5_en-US on Sept 11, 2020. USP 43–NF 38, ed.
215. Pharmacopoeia B. 2014. Dissolution of solid oral dosage forms. BPC, ed., London, UK. p 725-726.
216. Shaban K. 2018. Development, Characterisation and Assessment of Chemical Stability of Fast Dissolving Oral Levothyroxine Films. ed.: University of Brighton.
217. Administration AgDoHTGo. 2014. Australian Public Assessment Report for Thyroxine Sodium. , in AusPAR Eltroxin, Aspen Thyroxine, Thyroxine Aspen Thyroxine Sodium Aspen Pharma Pty Ltd PM-2012-04477-1-5. (TGA). Available at: <https://www.tga.gov.au/sites/default/files/auspar-thyroxine-sodium-140612.pdf>. ed.
218. Williams R, Phillips J, Mysels K 1955. The critical micelle concentration of sodium lauryl sulphate at 25 C. *Trans Faraday Soc* 51:728-737.
219. Bahr MN, Modi D, Patel S, Campbell G, Stockdale G 2019. Understanding the Role of Sodium Lauryl Sulfate on the Biorelevant Solubility of a Combination of Poorly Water-Soluble Drugs Using High Throughput Experimentation and Mechanistic Absorption Modeling. *J Pharm Pharm Sci* 22:221-246.
220. Boulton DW, Paul Fawcett J, Woods DJ 1996. Stability of an extemporaneously compounded levothyroxine sodium oral liquid. *Am J Health-Syst Pharm* 53(10):1157-1161.
221. Formenti AM, Daffini L, Pirola I, Gandossi E, Cristiano A, Cappelli C 2015. Liquid levothyroxine and its potential use. *Hormones* 14(2):183-189.
222. Usayapant A, Ibrahim BM. 2017. Levothyroxine liquid formulations. ed.: Google Patents.
223. Chandrashekhar K, Nagaraju B. 2018. Stabilized liquid formulation of levothyroxine. ed.: Google Patents.
224. Negro R, Valcavi R, Agrimi D, Toulis K 2014. Levothyroxine liquid solution versus tablet for replacement treatment in hypothyroid patients. *Endocr Pract* 20(9):901-906.

225. Cappelli C, Negro R, Pirola I, Gandossi E, Agosti B, Castellano M 2016. Levothyroxine liquid solution versus tablet form for replacement treatment in pregnant women. *Gynecol Endocrinol* 32(4):290-292.
226. Vita R, Di Bari F, Benvenga S 2017. Oral liquid levothyroxine solves the problem of tablet levothyroxine malabsorption due to concomitant intake of multiple drugs. *Expert Opin Drug Deliv* 14(4):467-472.
227. Benvenga S, Di Bari F 2017. Intestinal absorption and buccal absorption of liquid levothyroxine. *Endocrine* 58(3):591-594.
228. Peirce C, Ippolito S, Lanas A, Pesce M, Pontieri G, Arpaia D, Sarnelli G, Biondi B 2018. Treatment of refractory and severe hypothyroidism with sublingual levothyroxine in liquid formulation. *Endocrine* 60(1):193-196.
229. Yue C, Scarsi C, Ducharme M 2012. Pharmacokinetics and potential advantages of a new oral solution of levothyroxine vs. other available dosage forms. *Drug Res* 62(12):631-636.
230. Kazemifard AG, Moore DE, Aghazadeh A 2001. Identification and quantitation of sodium-thyroxine and its degradation products by LC using electrochemical and MS detection. *J Pharm Biomed Anal* 25(5-6):697-711.
231. Wortsman J, Papadimitriou D, Borges M, Defesche C 1989. Thermal inactivation of L-thyroxin. *Clin Chem* 35(1):90-92.
232. Neu V, Bielow C, Reinert K, Huber CG 2014. Ultrahigh-performance liquid chromatography-ultraviolet absorbance detection-high-resolution-mass spectrometry combined with automated data processing for studying the kinetics of oxidative thermal degradation of thyroxine in the solid state. *J Chromatogr A* 1371:196-203.
233. Neu V, Bielow C, Schneider P, Reinert K, Stuppner H, Huber CG 2013. Investigation of reaction mechanisms of drug degradation in the solid state: a kinetic study implementing ultrahigh-performance liquid chromatography and high-resolution mass spectrometry for thermally stressed thyroxine. *Anal Chem* 85(4):2385-2390.
234. Kannamkumarath SS, Wuilloud RG, Stalcup A, Caruso JA, Patel H, Sakr A 2004. Determination of levothyroxine and its degradation products in pharmaceutical tablets by HPLC-UV-ICP-MS. *J Anal Atom Spectrom* 19(1):107-113.
235. Kogermann K 2008. Understanding solid-state transformations during dehydration: new insights using vibrational spectroscopy and multivariate modelling.
236. Griesser UJ 2006. The importance of solvates. *Polymorphism in the pharmaceutical industry*:211-233.
237. Kitamura S, Koda S, Miyamae A, Yasuda T, Morimoto Y 1990. Dehydration effect on the stability of cefixime trihydrate. *Int J Pharm* 59(3):217-224.
238. Yoshioka S, Aso Y 2007. Correlations between molecular mobility and chemical stability during storage of amorphous pharmaceuticals. *J Pharm Sci* 96(5):960-981.
239. Byrn SR, Xu W, Newman AW 2001. Chemical reactivity in solid-state pharmaceuticals: formulation implications. *Adv Drug Deliv Rev* 48(1):115-136.
240. Newman AW, Byrn SR 2003. Solid-state analysis of the active pharmaceutical ingredient in drug products. *Drug Discov today* 8(19):898-905.
241. Joel N, Canepa F 1951. On the crystal structure of thyroxine. *Acta Crystallographica* 4(3):283-283.
242. Katrusiak A, Katrusiak A 2004. Thyroxine revisited. *J Pharm Sci* 93(12):3066-3075.
243. Kaduk J, Zhong K, Blanton T, Gates S, Fawcett T 2015. Powder X-ray diffraction of levothyroxine sodium pentahydrate, C₁₅H₁₀I₄NNaO₄(H₂O)₅. *Powder Diffr* 30(4):370-371.
244. Hamad ML, Engen W, Morris KR 2015. Impact of hydration state and molecular oxygen on the chemical stability of levothyroxine sodium. *Pharmaceutical development and technology* 20(3):314-319.

245. Law D, Gerhardt A, Toh C 2009. Physicochemical basis for the performance of oral solid dosage forms of levothyroxine sodium. *AAPS J* 11(S2).
246. 2014. Australian Public Assessment Report for Thyroxine Sodium. In Department of Health TGA, Australian Government, editor, ed. p 10-11.
247. Collier JW, Shah RB, Gupta A, Sayeed V, Habib MJ, Khan MA 2010. Influence of formulation and processing factors on stability of levothyroxine sodium pentahydrate. *AAPS PharmSciTech* 11(2):818-825.
248. Gupta VD, Odom C, Bethea C, Plattenburg J 1990. Effect of excipients on the stability of levothyroxine sodium tablets. *J Clin Pharm Ther* 15(5):331-336.
249. Thakral NK, Behme RJ, Aburub A, Peterson JA, Woods TA, Diserod BA, Suryanarayanan R, Stephenson GA 2016. Salt disproportionation in the solid state: role of solubility and counterion volatility. *Mol Pharm* 13(12):4141-4151.
250. Thakral NK, Kelly RC 2017. Salt disproportionation: A material science perspective. *Int J Pharm* 520(1-2):228-240.
251. Hsieh Y-L, Merritt JM, Yu W, Taylor LS 2015. Salt stability—the effect of pH max on salt to free base conversion. *Pharm Res* 32(9):3110-3118.
252. Castello RA, Mattocks AM 1962. Discoloration of tablets containing amines and lactose. *J Pharm Sci* 51(2):106-108.
253. Parikh N, Hite WC. 2018. Alditol-free, storage-stable thyroid hormone active drug formulations and methods for their production. ed.: Google Patents.
254. Mitra AK, Srinivas R, Thomas III CL. 1999. Stabilized thyroid hormone preparations and methods of making same. ed.: Google Patents.
255. Hanshew Jr DD, Wargo DJ. 2007. Storage stable thyroxine active drug formulations and methods for their production. ed.: Google Patents.
256. Hanshew Jr DD, Wargo DJ. 2006. Storage stable thyroxine active drug formulations and methods for their production. ed.: Google Patents.
257. Lipp H-P, Hostalek U 2019. A new formulation of levothyroxine engineered to meet new specification standards. *Curr Med Res Opin* 35(1):147-150.
258. Concordet D, Gandia P, Montastruc J-L, Bousquet-Mélou A, Lees P, Ferran A, Toutain P-L 2019. Levothyrox® new and old formulations: are they switchable for millions of patients? *Clin Pharmacokinet* 58(7):827-833.
259. Casassus B 2018. Risks of reformulation: French patients complain after Merck modifies levothyroxine pills. *BMJ* 360.
260. Fallahi P, Ferrari SM, Marchi S, De Bortoli N, Ruffilli I, Antonelli A 2017. Patients with lactose intolerance absorb liquid levothyroxine better than tablet levothyroxine. *Endocrine* 57(1):175-178.
261. Ruchała M, Szczepanek-Parulska E, Zybek A 2012. The influence of lactose intolerance and other gastro-intestinal tract disorders on L-thyroxine absorption. *Endokrynol Pol* 63(4):318-323.
262. Cellini M, Santaguida MG, Gatto I, Virili C, Del Duca SC, Brusca N, Capriello S, Gargano L, Centanni M 2014. Systematic appraisal of lactose intolerance as cause of increased need for oral thyroxine. *J Clin Endocrinol Metab* 99(8):E1454-E1458.
263. Muñoz-Torres M, Varsavsky M, Alonso G 2006. Lactose intolerance revealed by severe resistance to treatment with levothyroxine. *Thyroid* 16(11):1171-1173.
264. Ledeti I, Ledeti A, Vlase G, Vlase T, Matusz P, Bercean V, Şuta L-M, Piciu D 2016. Thermal stability of synthetic thyroid hormone l-thyroxine and l-thyroxine sodium salt hydrate both pure and in pharmaceutical formulations. *J Pharm Biomed Anal* 125:33-40.
265. Frontanes RA, Bruno MS, Garcia HL, Simamora P, Perez MA. 2002. Stable thyroid hormone preparations and method of making same. ed.: Google Patents.
266. Parikh N, Hite W. 2016. Liquid levothyroxine formulations. ed.: Google Patents.
267. Kirsch J, Nallamothe R, Polat BE. 2016. Levothyroxine formulation with acacia. ed.: Google Patents.

268. Uary N. 2012. Current challenges in the management of hypothyroidism. *US Pharmacist*, ed.
269. Vanderpump MP 2011. The epidemiology of thyroid disease. *Br Med Bull* 99(1).
270. Vita R, Benvenega S 2014. Tablet levothyroxine (L-T4) malabsorption induced by proton pump inhibitor; a problem that was solved by switching to L-T4 in soft gel capsule. *Endocr Pract* 20(3):e38-e41.
271. John-Kalarickal J, Pearlman G, Carlson HE 2007. New medications which decrease levothyroxine absorption. *Thyroid* 17(8):763-765.
272. Siraj ES, Gupta MK, Reddy SSK 2003. Raloxifene causing malabsorption of levothyroxine. *JAMA Internal Medicine* 163(11):1367-1370.
273. Csako G, McGriff NJ, Rotman-Pikielny P, Sarlis NJ, Pucino F 2001. Exaggerated levothyroxine malabsorption due to calcium carbonate supplementation in gastrointestinal disorders. *Ann Pharmacother* 35(12):1578-1583.
274. Bell M, FACE, David SH, Ovalle M, Fernando 2001. Use of soy protein supplement and resultant need for increased dose of levothyroxine. *Endocr Pract* 7(3):193-194.
275. Sherman SI, Malecha SE 1995. Absorption and malabsorption of levothyroxine sodium. *Am J Ther* 2(10):814-818.
276. Robertson SG, Glass BD 2019. Repackaging levothyroxine sodium tablets: storage conditions to maintain stability in a hot and humid environment. *J Pharm Pract Res* 49(5):414-420.
277. Chiovato L, Magri F, Carlé A 2019. Hypothyroidism in Context: Where We've Been and Where We're Going. *Adv Ther* 36:47-58.
278. Gaby AR 2004. "Sub-laboratory" Hypothyroidism and the Empirical use of Armour® Thyroid. *Altern Med Rev* 9(2):157-179.
279. Smith SR 1984. Desiccated Thyroid Preparations: Obsolete Therapy. *JAMA Internal Medicine* 144(5):926-927.
280. Hoang TD, Olsen CH, Mai VQ, Clyde PW, Shakir MK 2013. Desiccated thyroid extract compared with levothyroxine in the treatment of hypothyroidism: a randomized, double-blind, crossover study. *J Clin Endocrinol Metab* 98(5):1982-1990.
281. Pepper GM, Casanova-Romero PY 2014. Conversion to Armour thyroid from levothyroxine improved patient satisfaction in the treatment of hypothyroidism. *J Endocrinol Diabetes Obes* 2:1055-1060.
282. Benvenega S, Carlé A 2019. Levothyroxine Formulations: Pharmacological and Clinical Implications of Generic Substitution. *Adv Ther* 36:59-71.
283. Al-Jazairi AS, Blhareth S, Eqtefan IS, Al-Suwayeh SA 2008. Brand and generic medications: are they interchangeable? *Ann Saudi Med* 28(1):33-41.
284. Dong BJ, Brown CH 1991. Hypothyroidism resulting from generic levothyroxine failure. *J Am Board Fam Pract* 4(3):167-170.
285. Garber JR, Hennessey JV 2005. Generic levothyroxine: what is all the fuss about? *Endocr Pract* 11(3):205-207.
286. Pearce EN Generic and Branded Levothyroxine Preparations Are Not Bioequivalent in Children with Congenital Hypothyroidism. *Clin Thyroidol* 25(2):31-32.
287. Green WL 2005. New questions regarding bioequivalence of levothyroxine preparations: a clinician's response. *The AAPS journal* 7(1):E54-E58.
288. Association AT, Society E, Endocrinologists AAoC 2004. US Food and Drug Administration's Decision Regarding Bioequivalence of Levothyroxine Sodium. *Thyroid* 14(7):486-486.
289. Fliers E, Demeneix B, Bhaseen A, Brix TH 2018. European thyroid association (ETA) and thyroid federation international (TFI) joint position statement on the interchangeability of levothyroxine products in EU countries. *Eur Thyroid J* 7(5):238-242.

290. Sohail Siddiqui M, Shottliff K 2019. Levothyroxine-not all tablets are the same. *Prescriber* 30(7):31-34.
291. Toft A 2005. Which thyroxine? *Thyroid* 15(2):124-126.
292. Gibaldi M 2005. Bioequivalence of thyroid preparations: The final word? *The AAPS journal* 7(1):E59.
293. Toft DJ 2020. A Change in Levothyroxine Manufacturer Frequently Results in Abnormal Serum Thyroid Function Tests. *Clin Thyroidol* 32(5):211-213.
294. Abou-Taleb BA, Bondok M, Nounou MI, Khalafallah N, Khalil S. 2018. Are multisource levothyroxine sodium tablets marketed in Egypt interchangeable? *Ann Endocrinol*, ed.: Elsevier. p 23-29.
295. Copeland PM 1995. Two cases of therapeutic failure associated with levothyroxine brand interchange. *Ann Pharmacother* 29(5):482-485.
296. Di Girolamo G, Keller GA, Antonio R, Schere D, Gonzalez CD 2008. Bioequivalence of two levothyroxine tablet formulations without and with mathematical adjustment for basal thyroxine levels in healthy Argentinian volunteers: a single-dose, randomized, open-label, crossover study. *Clin Ther* 30(11):2015-2023.
297. 2020. *Approved Drug Products with Therapeutic Equivalence Evaluations*. . ed. p 21-22.
298. Emerson CH 2020. Understanding the Regulation of the Levothyroxine Market Has Implications for Managing Hypothyroidism. *Clin Thyroidol* 32(6):296–299.
299. Flinterman LE, Kuiper JG, Korevaar JC, Van Dijk L, Hek K, Houben E, Herings R, Franken AA, de Graaf JP, Horikx A 2020. Impact of a Forced Dose-Equivalent Levothyroxine Brand Switch on Plasma Thyrotropin: A Cohort Study. *Thyroid*.
300. Jonklaas J, Bianco AC, Bauer AJ, Burman KD, Cappola AR, Celi FS, Cooper DS, Kim BW, Peeters RP, Rosenthal MS 2014. Guidelines for the treatment of hypothyroidism: prepared by the american thyroid association task force on thyroid hormone replacement. *Thyroid* 24(12):1670-1751.
301. Blakesley V, Awni W, Locke C, Ludden T, Granneman GR, Braverman LE 2004. Are bioequivalence studies of levothyroxine sodium formulations in euthyroid volunteers reliable? *Thyroid* 14(3):191-200.
302. Castellana M, Castellana C, Giovanella L, Trimboli P 2020. Prevalence of gastrointestinal disorders having an impact on tablet levothyroxine absorption: should this formulation still be considered as the first-line therapy? *Endocrine* 67(2):281–290.
303. Trimboli P, Scappaticcio L, De Bellis A, Maiorino MI, Knappe L, Esposito K, Bellastella G, Giovanella L 2020. Different Formulations of Levothyroxine for Treating Hypothyroidism: A Real-Life Study. *Int J Endocrinol* 2020.
304. Al-Numani D, Scarsi C, Ducharme MP 2016. Levothyroxine soft capsules demonstrate bioequivalent pharmacokinetic exposure with the European reference tablets in healthy volunteers under fasting conditions. *Int J Clin Pharmacol Ther* 54(2):135.
305. Fiorini G, Ribichini D, Pasquali R, Vaira D 2016. In vivo dissolution of levothyroxine soft gel capsules. *Intern Emerg Med* 11(8):1151-1152.
306. Reardon DP, Yoo PS 2016. Levothyroxine tablet malabsorption associated with gastroparesis corrected with gelatin capsule formulation. *Case reports in endocrinology* 2016.
307. Boskovic O, Lazovic R, Smolovic B, Hasanbegovic M. 19th European Congress of Endocrinology, 2017.
308. Di DV, Paragliola RM, De WC, De RA, Papi G, Pontecorvi A, Corsello SM. 19th European Congress of Endocrinology, 2017.
309. Ernst FR, Sandulli W, Elmor R, Welstead J, Sterman AB, Lavan M 2017. Retrospective study of patients switched from tablet formulations to a gel cap formulation of levothyroxine: results of the CONTROL Switch study. *Drugs in R&D* 17(1):103-115.

310. Trimboli P, Virili C, Centanni M, Giovanella L 2018. Thyroxine treatment with softgel capsule formulation: usefulness in hypothyroid patients without malabsorption. *Front Endocrinol* 9:118.
311. Benvenga S 2019. Liquid and softgel capsules of l-thyroxine results lower serum thyrotropin levels more than tablet formulations in hypothyroid patients. *J Clin Transl Endocrinol* 18:100204.
312. Colucci P, D'Angelo P, Mautone G, Scarsi C, Ducharme MP 2011. Pharmacokinetic equivalence of a levothyroxine sodium soft capsule manufactured using the new food and drug administration potency guidelines in healthy volunteers under fasting conditions. *Ther Drug Monit* 33(3):355-361.
313. Virili C, Trimboli P, Romanelli F, Centanni M 2016. Liquid and softgel levothyroxine use in clinical practice: state of the art. *Endocrine* 54(1):3-14.
314. Vita R, Saraceno G, Trimarchi F, Benvenga S 2014. Switching levothyroxine from the tablet to the oral solution formulation corrects the impaired absorption of levothyroxine induced by proton-pump inhibitors. *J Clin Endocrinol Metab* 99(12):4481-4486.
315. Kucukler FK, Akbaba G, Arduc A, Simsek Y, Guler S 2014. Evaluation of the common mistakes made by patients in the use of Levothyroxine. *Eur J Intern Med* 25(9):e107-e108.
316. Peroni E, Vigone MC, Mora S, Bassi LA, Pozzi C, Passoni A, Weber G 2014. Congenital hypothyroidism treatment in infants: a comparative study between liquid and tablet formulations of levothyroxine. *Horm Res Paediatr* 81(1):50-54.
317. Vita R, Fallahi P, Antonelli A, Benvenga S 2014. The administration of L-thyroxine as soft gel capsule or liquid solution. *Expert Opin Drug Deliv* 11(7):1103-1111.
318. Kashanian S, Rostami E 2014. PEG-stearate coated solid lipid nanoparticles as levothyroxine carriers for oral administration. *J Nanopart Res* 16(3):2293.
319. SYNTHROID - levothyroxine sodium tablets for oral use. Highlights of prescribing information. Approval 2002. Available at https://www.accessdata.fda.gov/drugsatfda_docs/label/2017/021402s024s028lbl.pdf Accessed March 20, 2020.
320. Blouin R, Clifton G, Adams M, Foster T, Flueck J 1989. Biopharmaceutical comparison of two levothyroxine sodium products. *Clin Pharm* 8(8):588-592.
321. LEVOXYL® (levothyroxine sodium) tablets for oral use. Highlights of prescribing information. 2001. Available at https://www.accessdata.fda.gov/drugsatfda_docs/label/2018/021301s038lbl.pdf Accessed March 20, 2020.
322. UNITHROID tablets for oral use. Highlights of prescribing information. 2001. Available at https://www.accessdata.fda.gov/drugsatfda_docs/label/2018/021210s018lbl.pdf Accessed March 20, 2020.
323. Levo T. Available at <https://www.rxlist.com/levo-t-drug.htm>. Accessed March 20, 2020.
324. LEVO-T® (levothyroxine sodium) tablets, for oral use. Highlights of prescribing information. 2002. Available at https://www.accessdata.fda.gov/drugsatfda_docs/label/2017/021342s023lbl.pdf Accessed March 20, 2020.
325. EUTHYROX® (levothyroxine sodium) tablets for oral use. Highlights of prescribing information. Initial U.S. Approval: 2002. Available at https://www.accessdata.fda.gov/drugsatfda_docs/label/2018/021292s004%2c021292s005%2c021292s006lbl.pdf Accessed March 20, 2020.
326. Sept 2018. US FDA. Drug Approvals and Databases: Additions and Deletions for Prescription and OTC Drug Product Lists. Accessed in April 2020. In Administration USFaD, editor, ed.

327. October 2018. US FDA. Drug Approvals and Databases: Additions and Deletions for Prescription and OTC Drug Product Lists. Accessed in April 2020. In Administration USFaD, editor, ed.
328. Gardner J, Dew K 2011. The Eltroxin controversy: Risk and how actors construct their world. *Health Risk Soc* 13(5):397-411.
329. Dew K, Gardner J, Morrato EH, Norris P, Chamberlain K, Hodgetts D, Gabe J 2018. Public engagement and the role of the media in post-marketing drug safety: the case of Eltroxin®(levothyroxine) in New Zealand. *Crit Public Health* 28(4):388-401.
330. 2002. Levothyroxine sodium tablets USP. https://www.accessdata.fda.gov/drugsatfda_docs/label/2002/076187lbl.pdf. Accessed on March 20, 2020.
331. January 2019. US FDA. Drug Approvals and Databases: Additions and Deletions for Prescription and OTC Drug Product Lists. Accessed in April 2020. In Administration USFaD, editor, ed.
332. May 2019. US FDA. Drug Approvals and Databases: Additions and Deletions for Prescription and OTC Drug Product Lists. Accessed in April 2020. In Administration USFaD, editor, ed.
333. Home F 2013. Orange book: approved drug products with therapeutic equivalence evaluations. USA: US Food & Drug Administration.
334. Oroxine tablet. Available at <https://www.thyroidfoundation.org.au/resources/Documents/Oroxine%20CMI.pdf>. Accessed April 2020.
335. Tirosint capsules. Available at https://www.accessdata.fda.gov/drugsatfda_docs/label/2007/022121lbl.pdf. Accessed March 20, 2020.
336. Tirosint prescribing information. Available at <https://tirosint.com/what-makes-tirosint-different/dosages-directions/> Accessed March 20, 2020.
337. TIROSINT®-SOL (levothyroxine sodium) oral solution. Highlights of prescribing information. Available at https://www.accessdata.fda.gov/drugsatfda_docs/label/2016/206977s000lbl.pdf Accessed on March 20, 2020.
338. Oroxine powder for injection. Available at https://www.accessdata.fda.gov/drugsatfda_docs/label/2011/202231s000lbl.pdf. Accessed April 2020.
339. Thyreocomb N Sodium for Injection. Available at <https://www.sdrugs.com/?c=drug&s=thyreocomb%20nhttps://www.sdrugs.com/?c=drug&s=thyreocomb%20n>. Accessed May 2020.
340. Prescribing Information. Levothyroxine Sodium by Par Pharmaceuticals. Available at <http://www.parsterileproducts.com/products/assets/pdf/PI/2016/Levothyroxine-PI.pdf>. Accessed April 2020.
341. Levothyroxine Sodium for Injection. ANDA approval: 206163. Dept of health and human services. FDA. Available at https://www.accessdata.fda.gov/drugsatfda_docs/appletter/2016/206163Orig1s000ltr.pdf. Accessed April 2020.
342. March 2020. US FDA. Drug Approvals and Databases: Additions and Deletions for Prescription and OTC Drug Product Lists. Accessed in April 2020. In Administration USFaD, editor, ed.
343. January 2018. US FDA. Drug Approvals and Databases: Additions and Deletions for Prescription and OTC Drug Product Lists. Accessed in April 2020. In Administration USFaD, editor, ed.

344. December 2018. US FDA. Drug Approvals and Databases: Additions and Deletions for Prescription and OTC Drug Product Lists. Accessed in April 2020. In Administration USFaD, editor, ed.
345. Duggirala NK, Smith AJ, Wojtas Ł, Shytle RD, Zaworotko MJ 2014. Physical stability enhancement and pharmacokinetics of a lithium ionic cocrystal with glucose. *Cryst Growth Des* 14(11):6135-6142.
346. Vishweshwar P, McMahon JA, Peterson ML, Hickey MB, Shattock TR, Zaworotko MJ 2005. Crystal engineering of pharmaceutical co-crystals from polymorphic active pharmaceutical ingredients. *Chem Comm* 36:4601-4603.
347. Feng L, Karpinski PH, Sutton P, Liu Y, Hook DF, Hu B, Blacklock TJ, Fanwick PE, Prashad M, Godfredsen S 2012. LCZ696: a dual-acting sodium supramolecular complex. *Tetrahedron Lett* 53(3):275-276.
348. Almarsson Ö, Zaworotko MJ 2004. Crystal engineering of the composition of pharmaceutical phases. Do pharmaceutical co-crystals represent a new path to improved medicines? *Chem Comm* (17):1889-1896.
349. Duggirala NK, Perry ML, Almarsson Ö, Zaworotko MJ 2016. Pharmaceutical cocrystals: along the path to improved medicines. *Chem Comm* 52(4):640-655.
350. Hickey MB, Peterson ML, Scoppettuolo LA, Morrisette SL, Vetter A, Guzmán H, Remenar JF, Zhang Z, Tawa MD, Haley S 2007. Performance comparison of a co-crystal of carbamazepine with marketed product. *Eur J Pharm Biopharm* 67(1):112-119.
351. https://www.ema.europa.eu/documents/assessment-report/odomzo-epar-public-assessment-report_en.pdf.
352. Abourahma H, Urban JM, Morozowich N, Chan B 2012. Examining the robustness of a theophylline cocrystal during grinding with additives. *Cryst Eng Comm* 14(19):6163-6169.
353. Koranne S, Krzyzaniak JF, Luthra S, Arora KK, Suryanarayanan R 2019. Role of Coformer and Excipient Properties on the Solid-State Stability of Theophylline Cocrystals. *Cryst Growth Des* 2(19):868–875.
354. Curtin V, Amharar Y, Hu Y, Erxleben A, McArdle P, Caron V, Tajber L, Corrigan OI, Healy AM 2012. Investigation of the capacity of low glass transition temperature excipients to minimize amorphization of sulfadimidine on comilling. *Mol Pharm* 10(1):386-396.
355. Curtin V, Amharar Y, Gallagher KH, Corcoran S, Tajber L, Corrigan OI, Healy AM 2013. Reducing mechanical activation-induced amorphisation of salbutamol sulphate by co-processing with selected carboxylic acids. *Int J Pharm* 456(2):508-516.
356. <https://www.spexsampleprep.com/>.
357. Powder Diffraction File 01-077-0128 (Monetite), International Centre for Diffraction Data, Newtown Square, PA (1997).
358. Miyazaki T, Sivaprakasam K, Tantry J, Suryanarayanan R 2009. Physical characterization of dibasic calcium phosphate dihydrate and anhydrate. *J Pharm Sci* 98(3):905-916.
359. Rowe RC, Sheskey PJ, Owen SC. 2006. Handbook of pharmaceutical excipients. ed.: Pharmaceutical press London. p 94-96.
360. Schmidt P, Herzog R 1993. Calcium phosphates in pharmaceutical tableting. *Pharmacy World and Science* 15(3):116-122.
361. Newman A, Zografi G 2014. Critical Considerations for the Qualitative and Quantitative Determination of Process-Induced Disorder in Crystalline Solids. *J Pharm Sci* 103(9):2595-2604.
362. Bates S, Zografi G, Engers D, Morris K, Crowley K, Newman A 2006. Analysis of amorphous and nanocrystalline solids from their X-ray diffraction patterns. *Pharm Res* 23(10):2333-2349.
363. Angelo P, Subramanian R. 2008. Powder metallurgy: science, technology and applications. ed.: PHI Learning Pvt. Ltd. p 243-250.
364. Trasi NS, Boerrigter SX, Byrn SR 2010. Investigation of the milling-induced thermal behavior of crystalline and amorphous griseofulvin. *Pharm Res* 27(7):1377-1389.

365. Trasi NS, Byrn SR 2012. Mechanically induced amorphization of drugs: A study of the thermal behavior of cryomilled compounds. *AAPS PharmSciTech* 13(3):772-784.
366. Feng T, Pinal R, Carvajal MT 2008. Process induced disorder in crystalline materials: differentiating defective crystals from the amorphous form of griseofulvin. *J Pharm Sci* 97(8):3207-3221.
367. Feng T, Stanciu L, Carvajal M 2012. Making Sense of Milling: the Role of Water on the Micro-Structural Relaxation-Like of Cryo-Milled Griseofulvin. *Water* 4(1):18-36.
368. Suryanarayana C 2001. Mechanical alloying and milling. *Prog Mater Sci* 46(1-2):1-184.
369. Suryanarayana C, Ivanov E, Boldyrev V 2001. The science and technology of mechanical alloying. *Mater Sci Eng A* 304:151-158.
370. Takacs L, McHenry J 2006. Temperature of the milling balls in shaker and planetary mills. *J Mater Sci* 41(16):5246-5249.
371. Shah UV, Wang Z, Olusanmi D, Narang AS, Hussain MA, Tobyn MJ, Heng JY 2015. Effect of milling temperatures on surface area, surface energy and cohesion of pharmaceutical powders. *Int J Pharm* 495(1):234-240.
372. Chow PS, Lau G, Ng WK, Vangala VR 2017. Stability of Pharmaceutical Cocrystal During Milling: A Case Study of 1: 1 Caffeine–Glutaric Acid. *Cryst Growth Des* 17(8):4064-4071.
373. Newman A, Zografi G 2018. An Examination of Water Vapor Sorption by Multi-Component Crystalline and Amorphous Solids and Its Effects on their Solid-State Properties. *J Pharm Sci* 108(3):1061-1080.
374. Ahlneck C, Zografi G 1990. The molecular basis of moisture effects on the physical and chemical stability of drugs in the solid state. *Int J Pharm* 62(2-3):87-95.
375. Hancock BC, Zografi G 1993. The use of solution theories for predicting water vapor absorption by amorphous pharmaceutical solids: A test of the Flory–Huggins and Vrentas models. *Pharm Res* 10(9):1262-1267.
376. Saleki-Gerhardt A, Zografi G 1994. Non-isothermal and isothermal crystallization of sucrose from the amorphous state. *Pharm Res* 11(8):1166-1173.
377. Shamblin SL, Zografi G 1999. The effects of absorbed water on the properties of amorphous mixtures containing sucrose. *Pharm Res* 16(7):1119-1124.
378. Wu S-J, Sun CC 2007. Insensitivity of compaction properties of brittle granules to size enlargement by roller compaction. *J Pharm Sci* 96(5):1445-1450.
379. Kontny MJ, Grandolfi GP, Zografi G 1987. Water vapor sorption of water-soluble substances: studies of crystalline solids below their critical relative humidities. *Pharm Res* 4(2):104-112.
380. Govindarajan R, Zinchuk A, Hancock B, Shalaev E, Suryanarayanan R 2006. Ionization states in the microenvironment of solid dosage forms: effect of formulation variables and processing. *Pharm Res* 23(10):2454-2468.
381. Govindarajan R, Landis M, Hancock B, Gatlin LA, Suryanarayanan R, Shalaev EY 2015. Surface acidity and solid-state compatibility of excipients with an acid-sensitive API: case study of atorvastatin calcium. *AAPS PharmSciTech* 16(2):354-363.
382. Krzyzaniak JF, Williams GR, Ni N 2007. Identification of phase boundaries in anhydrate/hydrate systems. *J Pharm Sci* 96(5):1270-1281.
383. Feng T, Bates S, Carvajal MT 2009. Toward understanding the evolution of griseofulvin crystal structure to a mesophase after cryogenic milling. *Int J Pharm* 367(1-2):16-19.
384. Chamarthy SP, Pinal R 2008. The nature of crystal disorder in milled pharmaceutical materials. *Colloids Surf A* 331(1-2):68-75.
385. Otte A, Carvajal MT 2011. Assessment of milling-induced disorder of two pharmaceutical compounds. *J Pharm Sci* 100(5):1793-1804.
386. Koranne S, Govindarajan R, Suryanarayanan R 2017. Investigation of spatial heterogeneity of salt disproportionation in tablets by synchrotron X-ray diffractometry. *Mol Pharm* 14(4):1133-1144.

387. Thakral NK, Ragoonanan V, Suryanarayanan R 2013. Quantification, mechanism, and mitigation of active ingredient phase transformation in tablets. *Mol Pharm* 10(8):3128-3136.
388. Trask AV, Motherwell WS, Jones W 2006. Physical stability enhancement of theophylline via cocrystallization. *Int J Pharm* 320(1-2):114-123.
389. Vishweshwar P, McMahon JA, Bis JA, Zaworotko MJ 2006. Pharmaceutical co-crystals. *J Pharm Sci* 95(3):499-516.
390. Aitipamula S, Banerjee R, Bansal AK, Biradha K, Cheney ML, Choudhury AR, Desiraju GR, Dikundwar AG, Dubey R, Duggirala N 2012. Polymorphs, salts, and cocrystals: what's in a name? *Cryst Growth Des* 12(5):2147-2152.
391. Duggirala NK, Perry ML, Almarsson Ö, Zaworotko MJ 2016. Pharmaceutical cocrystals: along the path to improved medicines. *Chem Comm* 52(4):640-655.
392. Kaur N, Duggirala NK, Thakral S, Suryanarayanan R 2019. Role of lattice disorder in water-mediated dissociation of pharmaceutical cocrystal systems. *Mol Pharm* 16(7):3167-3177.
393. Saleki-Gerhardt A, Ahlneck C, Zografi G 1994. Assessment of disorder in crystalline solids. *Int J Pharm* 101(3):237-247.
394. Chamarthy SP, Pinal R 2008. The nature of crystal disorder in milled pharmaceutical materials. *Colloids Surf, A Physicochem Eng Asp* 331(1-2):68-75.
395. Salvador P, Garcia Gonzalez M, Munoz F 1992. Catalytic role of lattice defects in the photoassisted oxidation of water at (001) n-titanium (IV) oxide rutile. *J Phys Chem* 96(25):10349-10353.
396. Taylor LS, Zografi G 1998. The quantitative analysis of crystallinity using FT-Raman spectroscopy. *Pharm Res* 15(5):755-761.
397. Bai SJ, Rani M, Suryanarayanan R, Carpenter JF, Nayar R, Manning MC 2004. Quantification of glycine crystallinity by near-infrared (NIR) spectroscopy. *J Pharm Sci* 93(10):2439-2447.
398. Murphy BM, Prescott SW, Larson I 2005. Measurement of lactose crystallinity using Raman spectroscopy. *J Pharm Biomed* 38(1):186-190.
399. Auriemma F, Born R, Spiess HW, De Rosa C, Corradini P 1995. Solid-state ¹³C-NMR investigation of the disorder in crystalline syndiotactic polypropylene. *Macromolecules* 28(20):6902-6910.
400. Ek R, Wormald P, Iversen T, Nyström C 1995. Crystallinity index of microcrystalline cellulose particles compressed into tablets. *Int J Pharm* 125(2):257-264.
401. Hogan SE, Buckton G 2000. The quantification of small degrees of disorder in lactose using solution calorimetry. *Int J Pharm* 207(1-2):57-64.
402. Mackin L, Zanon R, Park JM, Foster K, Opalenik H, Demonte M 2002. Quantification of low levels (< 10%) of amorphous content in micronised active batches using dynamic vapour sorption and isothermal microcalorimetry. *Int J Pharm* 231(2):227-236.
403. Sheokand S, Modi SR, Bansal AK 2014. Dynamic vapor sorption as a tool for characterization and quantification of amorphous content in predominantly crystalline materials. *J Pharm Sci* 103(11):3364-3376.
404. Shah B, Kakumanu VK, Bansal AK 2006. Analytical techniques for quantification of amorphous/crystalline phases in pharmaceutical solids. *J Pharm Sci* 95(8):1641-1665.
405. Ticehurst M, York P, Rowe R, Dwivedi S 1996. Characterisation of the surface properties of α -lactose monohydrate with inverse gas chromatography, used to detect batch variation. *Int J Pharm* 141(1-2):93-99.
406. Begat P, Young PM, Edge S, Kaerger JS, Price R 2003. The effect of mechanical processing on surface stability of pharmaceutical powders: visualization by atomic force microscopy. *J Pharm Sci* 92(3):611-620.
407. Price R, Young PM 2005. On the physical transformations of processed pharmaceutical solids. *Micron* 36(6):519-524.

408. Chow EH, Bučar D-K, Jones W 2012. New opportunities in crystal engineering—the role of atomic force microscopy in studies of molecular crystals. *Chem Comm* 48(74):9210-9226.
409. Thakuria R, Eddleston MD, Chow EH, Lloyd GO, Aldous BJ, Krzyzaniak JF, Bond AD, Jones W 2013. Use of in situ atomic force microscopy to follow phase changes at crystal surfaces in real time. *Angew Chem Int Ed* 52(40):10541-10544.
410. Thakuria R, Eddleston MD, Chow EH, Taylor LJ, Aldous BJ, Krzyzaniak JF, Jones W 2016. Comparison of surface techniques for the discrimination of polymorphs. *Cryst Eng Comm* 18(28):5296-5301.
411. Cassidy A, Gardner C, Jones W 2009. Following the surface response of caffeine cocrystals to controlled humidity storage by atomic force microscopy. *Int J Pharm* 379(1):59-66.
412. Cleveland JP, Anczykowski B, Schmid AE, Elings VB 1998. Energy dissipation in tapping-mode atomic force microscopy. *Applied Physics Letters* 72(20):2613-2615.
413. Newman A, Zografi G 2019. An examination of water vapor sorption by multicomponent crystalline and amorphous solids and its effects on their solid-state properties. *J Pharm Sci* 108(3):1061-1080.
414. Zografi G 1988. States of water associated with solids. *Drug Dev Ind Pharm* 14(14):1905-1926.
415. Haugstad G. 2012. Atomic force microscopy: understanding basic modes and advanced applications. ed.: John Wiley & Sons.
416. Down GRB 1983. Localized particle fracture during compression of materials expected to undergo plastic deformation. *Powder Technol* 35(2):167-169.
417. Augsburger LL, Hoag SW. 2016. Pharmaceutical dosage forms-tablets. 3 ed.: CRC press.
418. Hiestand E, Wells J, Peot C, Ochs J 1977. Physical processes of tableting. *J Pharm Sci* 66(4):510-519.
419. Thakral NK, Yamada H, Stephenson GA, Suryanarayanan R 2015. Spatial distribution of trehalose dihydrate crystallization in tablets by x-ray diffractometry. *Mol Pharm* 12(10):3766-3775.
420. Pan X, Julian T, Augsburger L 2006. Quantitative measurement of indomethacin crystallinity in indomethacin-silica gel binary system using differential scanning calorimetry and X-ray powder diffractometry. *AAPS PharmSciTech* 7(1):E72-E78.
421. Chan H, Doelker E 1985. Polymorphic transformation of some drugs under compression. *Drug Dev Ind Pharm* 11(2-3):315-332.
422. Aher S, Dhumal R, Mahadik K, Ketolainen J, Paradkar A 2013. Effect of cocrystallization techniques on compressional properties of caffeine/oxalic acid 2: 1 cocrystal. *Pharm Dev Technol* 18(1):55-60.
423. Seitavuopio P, Rantanen J, Yliruusi J 2003. Tablet surface characterisation by various imaging techniques. *Int J Pharm* 254(2):281-286.
424. Seitavuopio P, Rantanen J, Yliruusi J 2005. Use of roughness maps in visualisation of surfaces. *Eur J Pharm Biopharm* 59(2):351-358.
425. Riippi M, Antikainen O, Niskanen T, Yliruusi J 1998. The effect of compression force on surface structure, crushing strength, friability and disintegration time of erythromycin acistrate tablets. *Eur J Pharm Biopharm* 46(3):339-345.
426. Joiris E, Di Martino P, Berneron C, Guyot-Hermann A-M, Guyot J-C 1998. Compression behavior of orthorhombic paracetamol. *Pharm Res* 15(7):1122-1130.
427. Koivisto M, Heinänen P, Tanninen VP, Lehto V-P 2006. Depth profiling of compression-induced disorders and polymorphic transition on tablet surfaces with grazing incidence X-ray diffraction. *Pharm Res* 23(4):813-820.
428. Fukuoka E, Makita M, Yamamura S 1993. Preferred Orientation of Crystallites in Tablets. III. Variations of Crystallinity and Crystallite Size of Pharmaceuticals with Compression. *Chem Pharm Bull* 41(3):595-598.

429. Leuenberger H, Rohera BD 1986. Fundamentals of powder compression. I. The compactibility and compressibility of pharmaceutical powders. *Pharm Res* 3(1):12-22.
430. Mitchell A, Down G 1984. Recrystallization after powder compaction. *Int J Pharm* 22(2-3):337-344.
431. Chemburkar SR, Deming KC, Reddy RE 2010. Chemistry of thyroxine: an historical perspective and recent progress on its synthesis. *Tetrahedron* 11(66):1955-1962.
432. Wartofsky L 2002. Levothyroxine: therapeutic use and regulatory issues related to bioequivalence. *Expert Opin Pharmacother* 3(6):727-732.
433. Wiersinga WM 2001. Thyroid hormone replacement therapy. *Horm Res Paediatr* 56(Suppl. 1):74-81.
434. Wang J, Sanchez-Rosello M, Acena JL, del Pozo C, Sorochinsky AE, Fustero S, Soloshonok VA, Liu H 2014. Fluorine in pharmaceutical industry: fluorine-containing drugs introduced to the market in the last decade (2001-2011). *Chemical reviews* 114(4):2432-2506.
435. Fuentes A, Pineda M, Venkata K 2018. Comprehension of top 200 prescribed drugs in the US as a resource for pharmacy teaching, training and practice. *Pharmacy* 6(2):43.
436. <https://www.statista.com/statistics/780284/levothyroxine-prescriptions-number-in-the-us/>.
437. Tanguay M, Girard J, Scarsi C, Mautone G, Larouche R 2019. Pharmacokinetics and Comparative Bioavailability of a Levothyroxine Sodium Oral Solution and Soft Capsule. *CPDD* 8(4):521-528.
438. Virili C, Antonelli A, Santaguida MG, Benvenga S, Centanni M 2018. Gastrointestinal malabsorption of thyroxine. *Endocr Rev* 40(1):118-136.
439. Hennessey JV 2017. The emergence of levothyroxine as a treatment for hypothyroidism. *Endocrine* 55(1):6-18.
440. Casassus B 2018. Risks of reformulation: French patients complain after Merck modifies levothyroxine pills. *Br Med J* 360:1-3.
441. Abou-Taleb BA, Bondok M, Nounou MI, Khalafallah N, Khalil S. *Ann Endocrinol*, 2018, pp 23-29.
442. Mandel SJ, Brent GA, Larsen PR 1993. Levothyroxine therapy in patients with thyroid disease. *Ann Intern Med* 119(6):492-502.
443. Helfand M, Crapo LM 1990. Monitoring therapy in patients taking levothyroxine. *Ann Intern Med* 113(6):450-454.
444. Greenwood AI, Clay MC, Rienstra CM 2017. 31P-dephased, 13C-detected REDOR for NMR crystallography at natural isotopic abundance. *Journal of magnetic resonance* 278:8-17.
445. Benvenga S, Carlé A 2019. Levothyroxine Formulations: Pharmacological and Clinical Implications of Generic Substitution. *Adv Ther* 36:59-71.
446. Hennessey JV 2013. Generic vs name brand L-thyroxine products: interchangeable or still not? *J Clin Endocrinol Metab* 98(2):511-514.
447. Green WL 2005. New questions regarding bioequivalence of levothyroxine preparations: a clinician's response. *The AAPS journal* 7(1):54-58.
448. https://www.endocrinesociety.org.au/documents/ESAsstatementonthyroxine_Walshv3.docx. Accessed 2019.
449. Harris RK, Hodgkinson P, Zorin V, Dumez JN, Elena-Herrmann B, Emsley L, Salager E, Stein RS 2010. Computation and NMR crystallography of terbutaline sulfate. *Magnetic resonance in chemistry : MRC* 48 Suppl 1:S103-112.
450. Adams C 2001. FDA Could Make Abbott Pull Synthroid, Popular Thyroid Drug, From the Market. *Wall Street Journal* 1.
451. Won CM 1992. Kinetics of degradation of levothyroxine in aqueous solution and in solid state. *Pharm Res* 9(1):131-137.
452. Post A, Warren RJ. 1976. Sodium levothyroxine. ed.: Elsevier.
453. Goudreau N, Lemke CT, Faucher AM, Grand-Maitre C, Goulet S, Lacoste JE, Rancourt J, Malenfant E, Mercier JF, Titolo S, Mason SW 2013. Novel inhibitor binding site discovery on

- HIV-1 capsid N-terminal domain by NMR and X-ray crystallography. *ACS chemical biology* 8(5):1074-1082.
454. Que C, Lou X, Zemlyanov DY, Mo H, Indulkar AS, Gao Y, Zhang GGZ, Taylor LS 2019. Insights into the Dissolution Behavior of Ledipasvir–Copovidone Amorphous Solid Dispersions: Role of Drug Loading and Intermolecular Interactions. *Mol Pharm* 16(12):5054-5067.
455. Patel H, Stalcup A, Dansereau R, Sakr A 2003. The effect of excipients on the stability of levothyroxine sodium pentahydrate tablets. *Int J Pharm* 264(1-2):35-43.
456. Gupta VD, Odom C, Bethea C, Plattenburg J 1990. Effect of excipients on the stability of levothyroxine sodium tablets. *J Clin Pharm Ther* 15(5):331-336.
457. Hamad ML, Engen W, Morris KR 2015. Impact of hydration state and molecular oxygen on the chemical stability of levothyroxine sodium. *Pharm Dev Technol* 20(3):314-319.
458. Sundaramurthi P, Suryanarayanan R 2014. Azithromycin Hydrates—Implications of Processing-Induced Phase Transformations. *J Pharm Sci* 103(10):3095-3106.
459. Kogermann K 2008. Understanding solid-state transformations during dehydration: new insights using vibrational spectroscopy and multivariate modelling. Dissertation, Faculty of Pharmacy of the University of Helsinki:150-156.
460. Griesser UJ. 2006. The importance of solvates. In Hilfiker R, editor *Polymorphism in the pharmaceutical industry*, ed.: Weinheim: Wiley-VCH. p 211-233.
461. Te RL, Griesser UJ, Morris KR, Byrn SR, Stowell JG 2003. X-ray diffraction and solid-state NMR investigation of the single-crystal to single-crystal dehydration of thiamine hydrochloride monohydrate. *Cryst Growth Des* 3(6):997-1004.
462. Sheldrick GM 2015. Crystal structure refinement with SHELXL. *Acta Crystallographica Section C: Structural Chemistry* 71(1):3-8.
463. Sheldrick GM 2015. SHELXT—Integrated space-group and crystal-structure determination. *Acta Crystallographica Section A: Foundations and Advances* 71(1):3-8.
464. Lu X, Xu W, Hanada M, Jermain SV, Williams RO, 3rd, Su Y 2019. Solid-state NMR analysis of crystalline and amorphous Indomethacin: An experimental protocol for full resonance assignments. *J Pharm Biomed Anal* 165:47-55.
465. 2011. Levothyroxine Sodium. United States Pharmacopeia USP34-NF29 Rockville The United States Pharmacopeial Convention:4980–4982.
466. Kaduk J, Zhong K, Blanton T, Gates S, Fawcett T 2015. Powder X-ray diffraction of levothyroxine sodium pentahydrate, C₁₅ H₁₀ I₄ NNaO₄ (H₂ O)₅. *Powder Diffr* 30(4):370-371.
467. Spek AL 2015. Platon Squeeze: a tool for the calculation of the disordered solvent contribution to the calculated structure factors. *Acta Crystallographica Section C: Structural Chemistry* 71(1):9-18.
468. Groom CR, Bruno IJ, Lightfoot MP, Ward SC 2016. The Cambridge structural database. *Acta Crystallographica Section B: Structural Science, Crystal Engineering and Materials* 72(2):171-179.
469. Remko M, Rode BM 2006. Effect of metal ions (Li⁺, Na⁺, K⁺, Mg²⁺, Ca²⁺, Ni²⁺, Cu²⁺, and Zn²⁺) and water coordination on the structure of glycine and zwitterionic glycine. *J Phys Chem A* 110(5):1960-1967.
470. Connor GP, Holland PL 2017. Coordination chemistry insights into the role of alkali metal promoters in dinitrogen reduction. *Catal* 286:21-40.
471. Harper JK, Doebbler JA, Jacques E, Grant DM, Von Dreele RB 2010. A Combined Solid-State NMR and Synchrotron X-ray Diffraction Powder Study on the Structure of the Antioxidant (+)-Catechin 4,5-hydrate. *J Am Chem Soc* 132(9):2928-2937.
472. Lu X, Tsutsumi Y, Huang C, Xu W, Byrn SR, Templeton AC, Buevich AV, Amoureux J-P, Su Y 2020. Molecular packing of pharmaceuticals analyzed with paramagnetic relaxation enhancement and ultrafast magic angle pinning NMR. *Physical Chemistry Chemical Physics* 22(23):13160-13170.

473. Lu X, Huang C, Li M, Skomski D, Xu W, Yu L, Byrn SR, Templeton AC, Su Y 2020. Molecular Mechanism of Crystalline-to-Amorphous Conversion of Pharmaceutical Solids from 19F Magic Angle Spinning NMR. *J Phys Chem B* 124(25):5271-5283.
474. Baias M, Dumez JN, Svensson PH, Schantz S, Day GM, Emsley L 2013. De novo determination of the crystal structure of a large drug molecule by crystal structure prediction-based powder NMR crystallography. *Journal of the American Chemical Society* 135(46):17501-17507.
475. Lu X, Huang C, Lowinger MB, Yang F, Xu W, Brown CD, Hesk D, Koynov A, Schenck L, Su Y 2019. Molecular interactions in posaconazole amorphous solid dispersions from two-dimensional solid-state NMR spectroscopy. *Mol Pharm* 16(6):2579-2589.
476. Cody V. Proceedings of the 1977 Laurentian Hormone Conference, 1978, pp 437-475.
477. Cody V 1979. Molecular conformation of thyroid hormones: Structure and binding interactions of thyroxine. *Endocr Res Comm* 6(2):123-134.
478. Craik D, Andrews P, Border C, Munro S 1990. Conformational studies of thyroid hormones. I. The diphenyl ether moiety. *Aust J Chem* 43(5):923-936.
479. Ruggenthaler M, Grass J, Schuh W, Huber CG, Reischl RJ 2017. Levothyroxine sodium revisited: A wholistic structural elucidation approach of new impurities via HPLC-HRMS/MS, on-line H/D exchange, NMR spectroscopy and chemical synthesis. *J Pharm Biomed Anal* 135:140-152.
480. Horii F, Hirai A, Kitamaru R 1987. CP/MAS carbon-13 NMR spectra of the crystalline components of native celluloses. *Macromolecules* 20(9):2117-2120.
481. Morales-Ríos MS, Martínez-Richa A, Hernández-Gallegos Z, Hernández-Barragán A, Vera-Graziano R, Joseph-Nathan P 2007. Studies of dihydropyridines by X-ray diffraction and solid state 13C NMR. *Z Naturforsch B* 62(4):549-555.
482. Khan M, Enkelmann V, Brunklaus G 2009. Solid-State NMR and X-ray Analysis of Structural Transformations in O–H···N Heterosynthons Formed by Hydrogen-Bond-Mediated Molecular Recognition. *J Org Chem* 74(6):2261-2270.
483. Morales-Ríos MS, Martínez-Richa A, Hernández-Gallegos Z, Hernández-Barragán A, Vera-Graziano R, Joseph-Nathan P 2007. Studies of dihydropyridines by X-ray diffraction and solid state 13C NMR. *Zeitschrift für Naturforschung B* 62(4):549-555.
484. Yin J, Huang C, Guan H, Pang Z, Su Y, Kong X 2019. In situ solid-state NMR characterization of pharmaceutical materials: An example of drug-polymer thermal mixing. *Magnetic resonance in chemistry : MRC*.
485. Yuan X, Sperger D, Munson EJ 2014. Investigating Miscibility and Molecular Mobility of Nifedipine-PVP Amorphous Solid Dispersions Using Solid-State NMR Spectroscopy. *Mol Pharm* 11(1):329-337.
486. Lipp H-P, Hostalek U 2019. A new formulation of levothyroxine engineered to meet new specification standards. *Curr Med Res Opin* 35(1):147-150.
487. Salameh AK, Taylor LS 2006. Deliquescence-induced caking in binary powder blends. *Pharm Dev Technol* 11(4):453-464.
488. Ma Q, He H, Liu C 2013. Hygroscopic properties of oxalic acid and atmospherically relevant oxalates. *Atmos Environ* 69:281-288.
489. Braban CF, Carroll MF, Styler SA, Abbatt JP 2003. Phase transitions of malonic and oxalic acid aerosols. *J Phys Chem A* 107(34):6594-6602.
490. Chemburkar SR, Deming KC, Reddy RE 2010. Chemistry of thyroxine: an historical perspective and recent progress on its synthesis. *Tetrahedron* 66(11).
491. Hart F, Maclagan N 1950. Synthetic thyroxine in the treatment of myxoedema. *J Endocrinol* 6(4):xxxiv.
492. Toft AD 1994. Thyroxine therapy. *N Engl J Med* 331(3):174-180.
493. Thyrolar tablets. Available at <https://media.allergan.com/actavis/actavis/media/allergan-pdf-documents/product-prescribing/2018-06-Thyrolar-Clean.pdf>. Accessed in April 2020. .

494. 2019. Levothyroxine sodium tablets by Alvogen, Inc. Highlights of prescribing information. In Administration USFaD, editor, ed.
495. Oroxine tablet. Available at <https://www.thyroidfoundation.org.au/resources/Documents/Oroxine%20CMI.pdf>. Accessed in April 2020.
496. Triostat. Available at <https://www.accessdata.fda.gov/scripts/cder/daf/index.cfm?event=overview.process&ApplNo=020105>. Accessed in April 2020.
497. Pabla D, Akhlaghi F, Zia H 2009. A comparative pH-dissolution profile study of selected commercial levothyroxine products using inductively coupled plasma mass spectrometry. *Eur J Pharm Biopharm* 72(1):105-110.
498. Uary N 2012. Current challenges in the management of hypothyroidism. *US Pharmacist*.
499. Wiersinga WM, Duntas L, Fadeyev V, Nygaard B, Vanderpump MP 2012. 2012 ETA guidelines: the use of L-T4+ L-T3 in the treatment of hypothyroidism. *Eur Thyroid J* 1(2):55-71.
500. (MHRA) MaHpRA 2013. Levothyroxine: a review of clinical and quality considerations. Medicines and Healthcare products Regulatory Agency.
501. The top 300 of 2019. Available at <https://clincalc.com/DrugStats/Top300Drugs.aspx> Accessed on June 10, 2020.
502. Wockhardt UK recalls Levothyroxine Oral Solution from pharmacies. Pharmacy business. 2020. Available at <https://www.pharmacy.biz/wockhardt-uk-recalls-levothyroxine-oral-solution-from-pharmacies/> Accessed on August 10, 2020.
503. USFDA. Levothyroxine recalls. Available at <https://www.archive-it.org/collections/7993?q=levothyroxine+recall&show=ArchivedPages&hitsPerDupe=0&go=Search+the+Archive> Accessed on August 10, 2020.
504. Kaur N, Young V, Su Y, Suryanarayanan R 2020. Partial dehydration of levothyroxine sodium pentahydrate in a drug product environment: structural insights into stability. *Mol Pharm* 17(10):3915–3929.
505. Lu X, Lee Y-M, Seo MS, Nam W 2020. Proton-promoted disproportionation of iron (V)-imido TAML to iron (V)-imido TAML cation radical and iron (IV) TAML. *Chem Comm* 56(76):11207-11210.
506. Koranne S, Lalge R, Suryanarayanan R 2020. Modulation of Microenvironmental Acidity: A Strategy to Mitigate Salt Disproportionation in Drug Product Environment. *Mol Pharm* 17(4):1324-1334.
507. John CT, Xu W, Lupton LK, Harmon PA 2013. Formulating weakly basic HCl salts: relative ability of common excipients to induce disproportionation and the unique deleterious effects of magnesium stearate. *Pharm Res* 30(6):1628-1641.
508. Du J, Hoag SW 2001. The influence of excipients on the stability of the moisture sensitive drugs aspirin and niacinamide: Comparison of tablets containing lactose monohydrate with tablets containing anhydrous lactose. *Pharm Dev Technol* 6(2):159-166.
509. Raijada D, Cornett C, Rantanen J 2013. A high throughput platform for understanding the influence of excipients on physical and chemical stability. *Int J Pharm* 453(1):285-292.
510. Shetty N, Park H, Zemlyanov D, Mangal S, Bhujbal S, Zhou QT 2018. Influence of excipients on physical and aerosolization stability of spray dried high-dose powder formulations for inhalation. *Int J Pharm* 544(1):222-234.
511. Chen S, Sheikh AY, Ho R 2014. Evaluation of effects of pharmaceutical processing on structural disorders of active pharmaceutical ingredient crystals using nanoindentation and high-resolution total scattering pair distribution function analysis. *J Pharm Sci* 103(12):3879-3890.
512. 2017. Synthroid. Highlights of prescribing information. Available at https://www.accessdata.fda.gov/drugsatfda_docs/label/2017/021402s024s028lbl.pdf Accessed March 20, 2020.
513. 2019. Levothyroxine sodium tablets by Alvogen, Inc. Highlights of prescribing information.

514. 2002. Levothyroxine sodium tablets USP. Available at https://www.accessdata.fda.gov/drugsatfda_docs/label/2002/076187lbl.pdf. Accessed March 20, 2020.
515. January 2019. US FDA. Drug Approvals and Databases: Additions and Deletions for Prescription and OTC Drug Product Lists. Accessed April 2020.
516. May 2019. US FDA. Drug Approvals and Databases: Additions and Deletions for Prescription and OTC Drug Product Lists. Accessed April 2020.
517. Fitzpatrick S, McCabe JF, Petts CR, Booth SW 2002. Effect of moisture on polyvinylpyrrolidone in accelerated stability testing. *Int J Pharm* 246(1-2):143-151.
518. Kaur N, Duggirala NK, Thakral S, Suryanarayanan R 2019. The Role of Lattice Disorder in Water Mediated Dissociation of Pharmaceutical Cocrystal Systems. *Mol Pharm* 16(7):3167-3177.
519. Euthyrox. 2018. Highlights of prescribing information. https://www.accessdata.fda.gov/drugsatfda_docs/label/2018/021292s004,021292s005,021292s006lbl.pdf. Accessed February 2021., ed.
520. Lafontaine A, Sanselme M, Cartigny Y, Cardinael P, Coquerel G 2013. Characterization of the transition between the monohydrate and the anhydrous citric acid. *J Therm Anal Calorim* 112(1):307-315.
521. Zamora IR, Tabazadeh A, Golden DM, Jacobson MZ 2011. Hygroscopic growth of common organic aerosol solutes, including humic substances, as derived from water activity measurements. *J Geophys Res Atmos* 116(D23):1-12.
522. Dubinskaya V, Polyakov N, Suponitskii YL, Dement'eva N, Bykov V 2010. Studies of moisture exchange between stearic acid, calcium stearate, and magnesium stearate. *Pharm Chem J* 44(2):89-93.
523. Wang J, Wen H, Desai D 2010. Lubrication in tablet formulations. *Eur J Pharm Biopharm* 75(1):1-15.
524. Saleki-Gerhardt A, Ahlneck C, Zografi G 1994. Assessment of disorder in crystalline solids. *Int J Pharm* 101(3):237-247.
525. 1976. The Merck Index. 9th ed. ed., Rahway, New Jersey: Merck & Co., Inc.
526. Badawy SIF 2001. Effect of salt form on chemical stability of an ester prodrug of a glycoprotein IIb/IIIa receptor antagonist in solid dosage forms. *Int J Pharm* 223(1-2):81-87.
527. Smith DJ, Biesemeyer M, Yaciw C 1981. The separation and determination of liothyronine and levothyroxine in tablets by reversed-phase high performance liquid chromatography. *J Chromatogr Sci* 19(2):72-78.
528. Rapaka RS, Roth J, Brine G, Prasad VK 1982. A simple HPLC method for the dissolution studies on levothyroxine sodium tablets. *Int J Pharm* 12(4):285-294.
529. Zografi G, Kontny MJ 1986. The interactions of water with cellulose-and starch-derived pharmaceutical excipients. *Pharm Res* 3(4):187-194.
530. Newman AW, Reutzel-Edens SM, Zografi G 2008. Characterization of the "hygroscopic" properties of active pharmaceutical ingredients. *J Pharm Sci* 97(3):1047-1059.
531. Harington CR, Barger G 1927. Chemistry of thyroxine: constitution and synthesis of thyroxine. *Biochemical Journal* 21(1):169.
532. Panmanad D, Joshi M, Patil R, Joshi P, Jadhav V 2016. Synthesis and Characterization of Potential Impurities in Levothyroxine. *Chemical Science* 5(4):1082-1089.